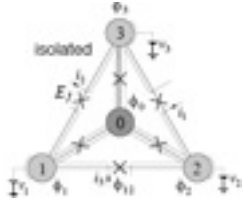


Tetrahedra, Dark Energy, and Cold Fusion

Frank Dodd (Tony) Smith, Jr. - 2010

Abstract (4 pages - Table of Contents on page 5)

1 - Start with a regular Tetrahedron in flat 3-dim space



Tetrahedron Josephson Junction Quantum Computer Qubit

2 - Add 4 + 12 Tetrahedra sharing faces to get 17 Tetrahedra



The 4 fit face-to-face exactly in 3-dim,

but



the 12 do not fit exactly in 3-dim,

However, all 17 do fit exactly in curved 3-dim space which is naturally embedded in 4-dim space described by Quaternions.

3 - Add 4 half-Icosahedra (10 Tetrahedra each) to form a 40-Tetrahedron Outer Shell around the 17 Tetrahedra and so form a 57-Tetrahedron TetraJJ Nucleus



Like the 12 of 17, the Outer 40 do not exactly fit together in flat 3-dim space.

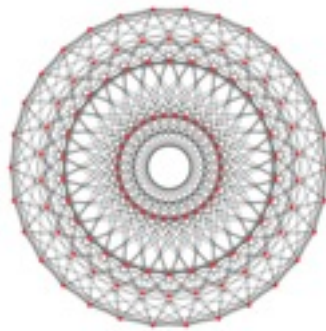
If you could force all 57 Tetrahedra to fit together exactly, you would be curving 3-dim space by a Dark Energy Conformal Transformation.

4 - The TetraJJ Nucleus can be combined with a Triangle of a Pearce D-Network



to form a 300-tetrahedron configuration TetraJJPearce

5 - Doubling the 300-cell TetraJJPearce produces a $\{3,3,5\}$ 600-cell polytope

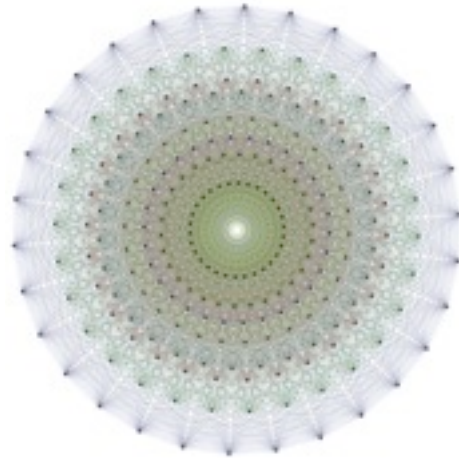


of 600 Tetrahedra and 120 vertices in 4-dim

6 - Adding a second $\{3,3,5\}$ 600-cell displaced by a Golden Ratio screw twist used 4 TetraJJ Nuclei to produce a 240 Polytope with 240 vertices in 4-dim

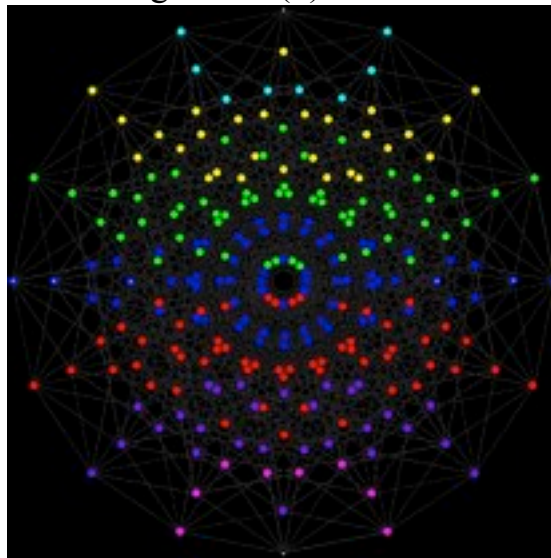


7 - Extend 4-dim space to $4+4 = 8$ -dim space by considering the Golden Ratio algebraic part of 4-dim space as 4 independent dimensions, thus transforming the 4-dim 240 Polytope into the 240-vertex 8-dim Gosset Polytope



that represents the Root Vectors of the E8 Lie Algebra and the first shell of an 8-dim E8 Lattice

8 - The 240 Root Vectors of 248-dimensional E8 have structure inherited from the 256-dimensional real Clifford Algebra $Cl(8)$



which structure allows construction of a E8 Physics Lagrangian from which realistic values of particle masses, force strengths, etc., can be calculated.

9 - Similar Tetrahedral Structures provide an understanding of
Palladium Cold Fusion

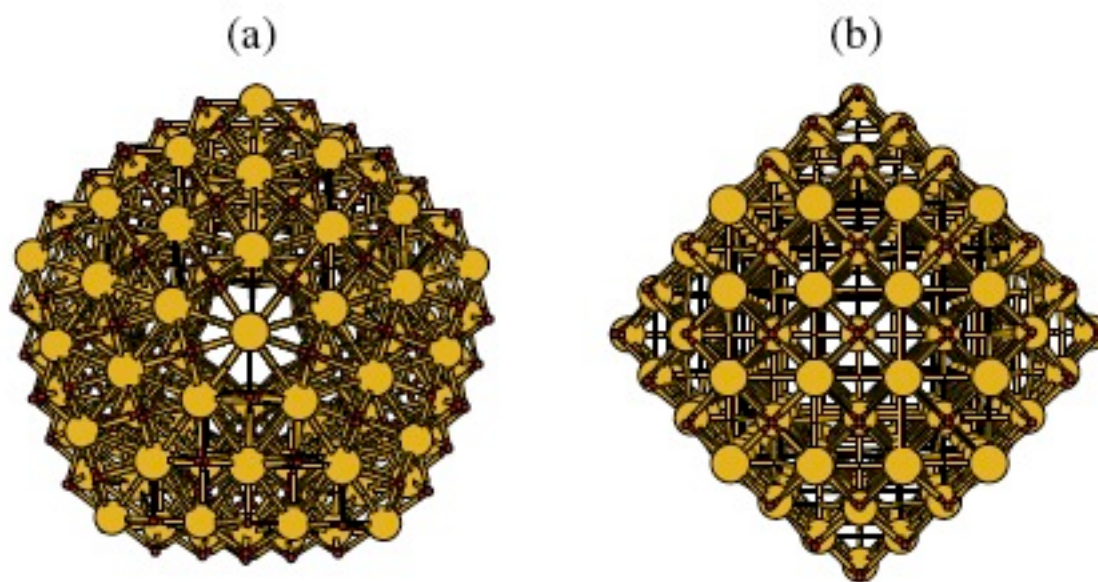


Figure 1. Palladium clusters fully loaded with hydrogen.
(a) $\text{Pd}_{147}\text{H}_{200}$, I_h symmetry; (b) $\text{Pd}_{147}\text{H}_{164}$, O_h symmetry.

in terms of the Fuller Jitterbug Transformation



Figure 4.13 Buckminster Fuller's 'jitterbug' transformation relating the cuboctahedron and the icosahedron.

Table of Contents

Dark Energy and Josephson Junctions - page 6 (some possibly relevant data - pages 8 and 9)
Tetrahedral Josephson Junctions - page 10
3-dimensional Diamond Lattice (packing) space for TetraJJ - page 12
TetraJJ Nucleus of 57 tetrahedra in 3-dim space - page 15
Symmetry of the TetraJJ Nucleus - page 19
Extension of a TetraJJ Nucleus to an Array in 3-dim space - page 24
Hopf Fibration, Clifford Algebras, AQFT, EPR Entanglement - page 36
Tetrahelix model of Fundamental Fermions - page 44
Geometry of the Four Fundamental Forces - page 50
Diamond Lattice space - page 56
4-dim Feynman Checkerboard SpaceTime - page 58
8-dim E8 SpaceTime - page 66
Quasicrystals and Tetrahedral Packing - page 88
TetraJJ Geometry: Nanometer to Planck Casimir-NearField-DarkEnergy - page 94
Gold Atom Clusters - page 100
Cold Fusion and Palladium Atom Clusters - page 109
Appendix - Tetrahedra, Faces, Edges and Vertices - page 130

Dark Energy and Josephson Junctions

In astro-ph/0512327 Christian Beck says: "... if dark energy is produced by vacuum fluctuations then

there is a chance to probe some ... dark energy ... properties by simple laboratory tests based on Josephson junctions.

These electronic devices can be used to perform 'vacuum fluctuation spectroscopy', by directly measuring a noise spectrum induced by vacuum fluctuations. One would expect to see a cutoff near 1.7 THz in the measured power spectrum, provided the new physics underlying dark energy couples to electric charge. The effect exploited by the Josephson junction is a subtle nonlinear mixing effect and has nothing to do with the Casimir effect or other effects based on van der Waals forces. A Josephson experiment of the suggested type will now be built, and we should know the result within the next 3 years. ...".

The Josephson experiment mentioned by Christian Beck is by P A Warburton of University College London, who says in EPSRC Grant Reference: EP/D029783/1: "... dark energy may be measured in the laboratory using resistively-shunted Josephson junctions (RS-JJ's). Vacuum fluctuations in the resistive shunt at low temperatures can be measured by non-linear mixing within the Josephson junction. If vacuum fluctuations are responsible for dark energy, the finite value of the dark energy density in the universe (as measured by astronomical observations) sets an upper frequency limit on the spectrum of the quantum fluctuations in this resistive shunt. Beck and Mackey calculated an upper bound on this cut-off frequency of 1.69 THz. ...

We therefore propose to perform measurements of the quantum noise in RS-JJ's fabricated using superconductors with sufficiently large gap energies that the full noise spectrum up to and beyond 1.69 THz can be measured. ... At higher frequencies tunnelling of quasiparticles dominates over all other electronic processes....

Nitride junctions have cut-off frequencies of around 2.5 THz, which should give sufficiently low quasiparticle current noise around 1.69 THz at accessible measurement temperatures.

Cuprate superconductors have an energy gap an order of magnitude higher than the nitrides, but here there is finite quasiparticle tunnelling at voltages less than the gap voltage, due to the d-wave pairing symmetry. ...".

HOW TO DESIGN A 10^{12} HZ JOSEPHSON JUNCTION ?

A PhysicsWeb article by Belle Dume at <http://physicsweb.org/article/news/8/6/17> describes the Beck and Mackey paper, saying "... In 1982, Roger Koch and colleagues, then at the University of California at Berkeley and the Lawrence Berkeley Laboratory, performed an experiment in which they measured the frequency spectrum of current fluctuations in Josephson junctions.

Their system was cooled to millikelvin temperatures so that thermal vibrations were reduced to a minimum, leaving only zero-point quantum fluctuations. ...".

So,

our junction must be cooled to a few millikelvin, which was done back in 1982, which means that the next question is how to find a junction sensitive to terahertz fluctuations.

Here are a couple of relevant references:

According to a paper by at <http://www.iop.org/EJ/abstract/0953-2048/15/12/309>

Terahertz frequency metrology based on high-Tc Josephson junctions

by J Chen¹, H Horiguchi, H B Wang, K Nakajima, T Yamashita and P H Wu

published 22 November 2002: "... Using YBa₂Cu₃O₇/MgO bicrystal Josephson junctions operating between 6-77 K, we have studied their responses to monochromatic electromagnetic radiation from 50 GHz to 4.25 THz.

We have obtained direct detections for radiation at 70 K from 50 GHz to 760 GHz and at 40 K from 300 GHz to 3.1 THz. ...".

Some details of how to make such things were outlined at

http://fy.chalmers.se/~tarasov/e1109m_draft.htm

by E. Stepantsov, M. Tarasov, A. Kalabukhov, T. Lindstroem, Z. Ivanov,

T. Claeson dated August 2001: "... Submicron YBCO bicrystal Josephson

junctions and devices for high frequency applications were designed, fabricated and experimentally studied. The key elements of these devices are bicrystal

sapphire substrates. ... A technological process based on deep ultraviolet

photolithography using a hard carbon mask was developed for the fabrication of

0.4-0.6 mm wide Josephson junctions. ... These junctions were used as Josephson detectors and spectrometers at frequencies up to 1.5 THz ...".

Some data that may be relevant are:

1 - the critical density in our universe now is about $5 \text{ GeV}/\text{m}^3$

2 - it is made up of Dark Energy : Dark Matter : Ordinary Matter
in a ratio DE : DM : OM = 73 : 23 : 4

3 - the density of the various types of stuff in our universe now is

DE = about $4 \text{ GeV} / \text{m}^3$

DM = about $1 \text{ GeV} / \text{m}^3$

OM = about $0.2 \text{ GeV} / \text{m}^3$

4 - the density of vacuum fluctuations already observed in Josephson Junctions is about $0.062 \text{ GeV}/\text{m}^3$ which is for frequencies up to about $6 \times 10^{11} \text{ Hz}$

5 - the radiation density (for photons) varies with frequency as the 4th power of the frequency, i.e., as $(\pi h / c^3) \nu^4$

6 - if Josephson Junction frequencies were to be experimentally realized up to $2 \times 10^{12} \text{ Hz}$, then, if the photon vacuum fluctuation energy density formula were to continue to hold, the vacuum energy density would be seen to be $0.062 \times (20/6)^4 =$ about $7 \text{ GeV}/\text{m}^3$ which exceeds the total critical density of our universe now

7 - to avoid such a divergence being physically realized, neutrinos should appear in the vacuum at frequencies high enough that $E = h \nu$ exceeds their mass of about $8 \times 10^{-3} \text{ eV}$, or at frequencies over about $1.7 \times 10^{12} \text{ Hz}$

8 - if Josephson Junctions could be developed to see vacuum fluctuation frequencies up to 10^{12} Hz , and if the photon equation were to hold there, then the observed vacuum fluctuation density would be about $0.5 \text{ GeV}/\text{m}^3$ which is well over the $0.2 \text{ GeV} / \text{m}^3$ Ordinary Matter energy density which means that DE and/or DM COMPONENTS WOULD BE SEEN IN VACUUM FLUCTUATIONS IN JOSEPHSON JUNCTIONS THAT GO UP TO 10^{12} HZ FREQUENCY

9 - $10^{28} \text{ cm} =$ present radius of our universe $= 10^{26} \text{ m}$

The radius of our universe at the time our solar system formed 5 by ago may have been about half its present radius,.

Uranus orbit = 19 AU = $19 \times 380,000 \text{ km} = 19 \times 3.8 \times 10^8 \text{ m} = 7 \times 10^9 \text{ m}$

Uranus orbit volume = $\frac{4}{3} \times \pi \times 7^3 \times 10^{27} \text{ m}^3 = 1.4 \times 10^{30} \text{ m}^3$
Earth Reserves Duration for 10^{10} people using energy at USA level for the period roughly around 2006 AD (Terawatt-years - years of reserves):

Gas 550 TWy -1 year

Oil (not including Thomas Gold deep oil) 850 TWy-1 year

Methane (not including Thomas Gold deep methane) 1,500 TWy - 2 year

Coal 7,000 TWy - 7 year

Uranium (using 1/1000 of total in ocean) 1.9×10^9 TWy - 2,000,000 years

Deuterium (using 1/1000 of total in ocean) 1.9×10^9 TWy - 2,000,000 years

Lithium (as source of tritium) 1.9×10^9 TWy - 2,000,000 years

Thorium (using 1/1000 of total in ocean) 7.9×10^9 TWy - 8,000,000 years

1 GeV = $10^{(-10)}$ J joule, 1 eV = $10^{(-19)}$ J joule,

A megaton of TNT is 4.184×10^{15} joules

Q the quad (short for quadrillion) is defined as 10^{15} BTUs,
which is about 1.055×10^{18} joules,

If 10^{10} people consumed enough energy to maintain a USA-type standard of living by using energy at the same rate as the USA around 2006 AD, that would be about 100 Q (quadrillion BTU, or 10^{15} BTU), or about 300×10^{11} kw-hours (kilowatt-hours), for each year, for about 3×10^8 (300 million) people, or about 10^5 kw-hours/year per person

for a total energy consumption for all 10^{10} people per year of about $10^5 \times 10^{10} = 10^{16}$ kw-hours/year = 3×10^4 Q/year.

Using about 10,000 hours in a year as an approximation to about 8,766 hours in a year: 1 Q = 3×10^{11} kw-hours = 3×10^{14} watt-hours = 300×10^{12} watt-hours = 300 Terawatt-hours = $300 \times 10^{(-4)}$ Terawatt-years = (1/30) Terawatt-years so that the total energy consumption for all 10^{10} people per year would be about 3×10^4 Q/year = 10^3 Terawatt-years/year.

To control Dark Energy, in addition to just observing it, Tetrahedral Josephson Junctions may be useful.

A very useful reference is the 2003 dissertation of Christopher Bell at St. John's College Cambridge entitled "Nanoscale Josephson devices", on the web at http://www.dspace.cam.ac.uk/bitstream/1810/34607/1/chris_bell_thesis.pdf

Feigelman, Ioffe, Geshkenbein, Dayal, and Blatter in cond-mat/0407663 say:
"... Superconducting tetrahedral quantum bits ...

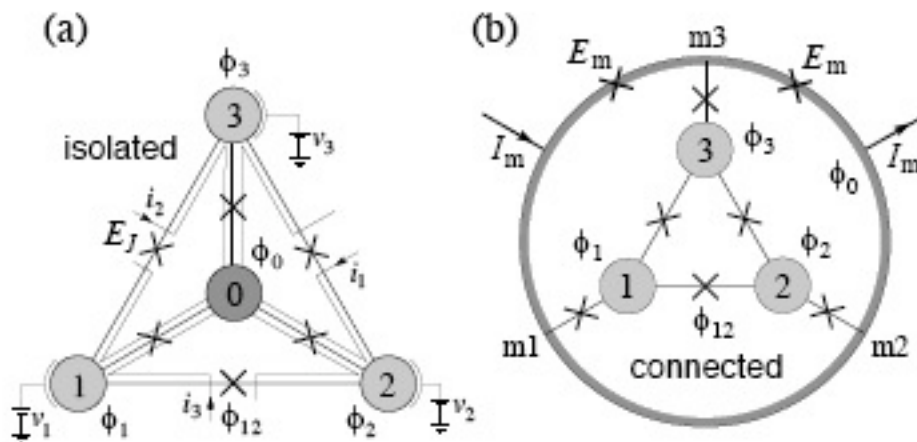


FIG. 1: (a) Tetrahedral superconducting qubit involving four islands and six junctions (with Josephson coupling E_J and charging energy E_C); all islands and junctions are assumed to be equal and arranged in a symmetric way. The islands are attributed phases ϕ_i , $i = 0, \dots, 3$. The qubit is manipulated via bias voltages v_i and bias currents i_i . In order to measure the qubit's state it is convenient to invert the tetrahedron as shown in (b) — we refer to this version as the 'connected' tetrahedron with the inner dark-grey island in (a) transformed into the outer ring in (b). The measurement involves additional measurement junctions with couplings $E_m \gg E_J$ on the outer ring which are driven by external currents I_m (schematic, see Fig. 6 for details); the large coupling E_m effectively binds the ring segments into one island.

... The novel tetrahedral qubit design we propose below operates in the phase-dominated regime and exhibits two remarkable physical properties:

first, its non-Abelian symmetry group (the tetrahedral group T_d) leads to the natural appearance of degenerate states and appropriate tuning of parameters provides us with a doubly degenerate groundstate. Our tetrahedral qubit then emulates a spin-1/2 system in a vanishing magnetic field, the ideal starting point for the construction of a qubit.

Manipulation of the tetrahedral qubit through external bias signals translates into application of magnetic fields on the spin; the application of the bias to different elements of the tetrahedral qubit corresponds to rotated operations in spin space.

Furthermore, geometric quantum computation via Berry phases ... might be implemented through adiabatic change of external variables.

Going one step further, one may hope to make use of this type of systems in the future physical realization of non-Abelian anyons, thereby aiming at a new generation of topological devices ... which keep their protection even during operation ...

The second property we wish to exploit is geometric frustration:

In our tetrahedral qubit ... it appears in an extreme way by rendering the classical minimal states continuously degenerate along a line in parameter space. Semi-classical states then appear only through a fluctuation-induced potential, reminiscent of the Casimir effect ... and the concept of inducing 'order from disorder' ...

The quantum-tunneling between these semi-classical states defines the operational energy scale of the qubit, which turns out to be unusually large due to the weakness of the fluctuation-induced potential. Hence the geometric frustration present in our tetrahedral qubit provides a natural boost for the quantum fluctuations without the stringent requirements on the smallness of the junction capacitances, thus avoiding the disadvantages of both the charge- and the phase- device:

The larger junctions reduce the demands on the fabrication process and the susceptibility to charge noise and mesoscopic effects, while the large operational energy scale due to the soft fluctuation-induced potential reduces the effects of flux noise. Both types of electromagnetic noise, charge- and flux noise, appear only in second order ...

in order to benefit from a protected degenerate ground state doublet, the qubit design requires a certain minimal complexity; it seems to us that the tetrahedron exhibits the minimal symmetry requirements necessary for this type of protection and thus the minimal complexity necessary for its implementation. ...”.

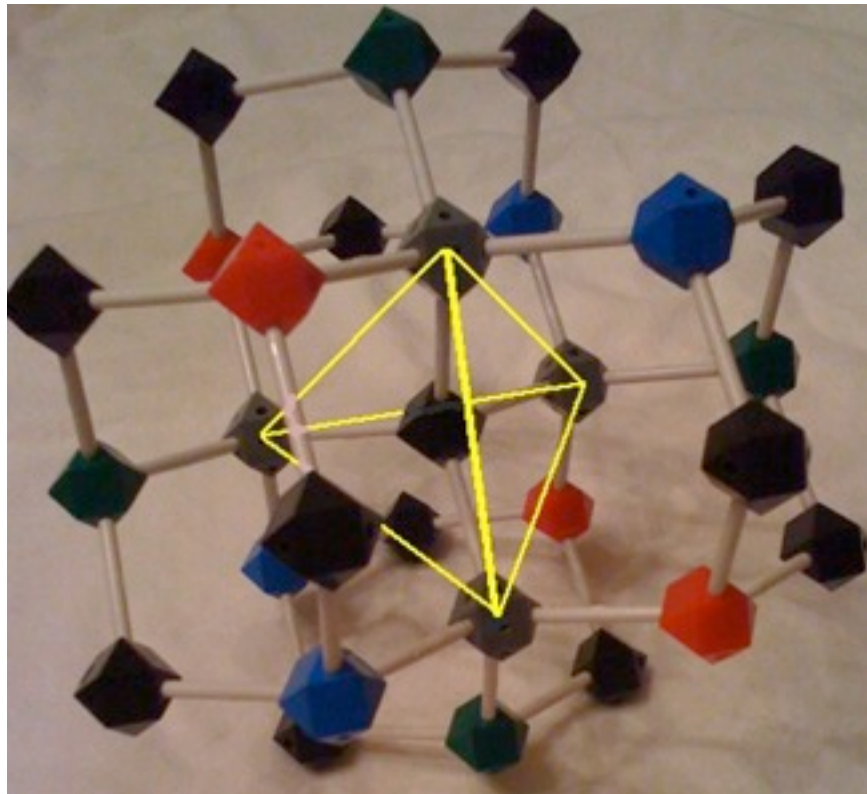
Given the basic tetrahedral structure of each individual Josephson Junction Qubit Node:

What should a Dark Energy Tetrahedral Josephson Junction Array look like ?

First, consider that fabrication should be in flat 3-dimensional space, which has a natural fundamental 3-dimensional Diamond Lattice (packing) structure.

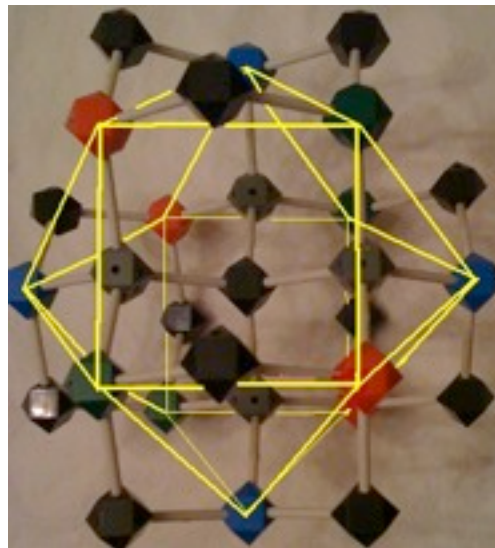
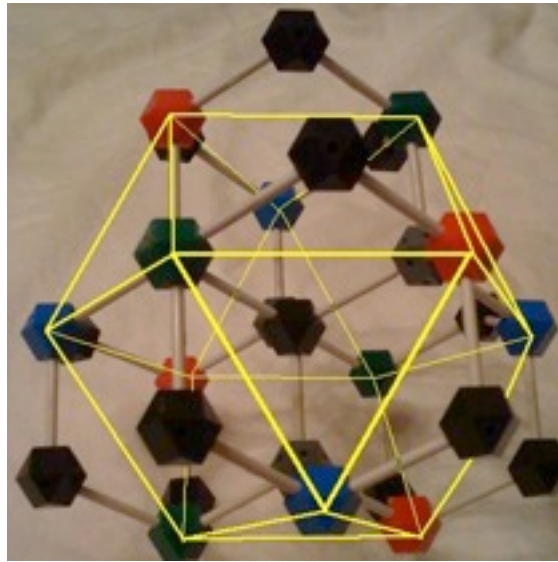
Starting with a central node, here is how to build up the first three shells of a 3-dimensional Diamond Lattice using a node-and-stick modelling system:

The center vertex is black and the 4 shell-1 vertices are gray.
The 4 shell-1 vertices form a tetrahedron (yellow lines)



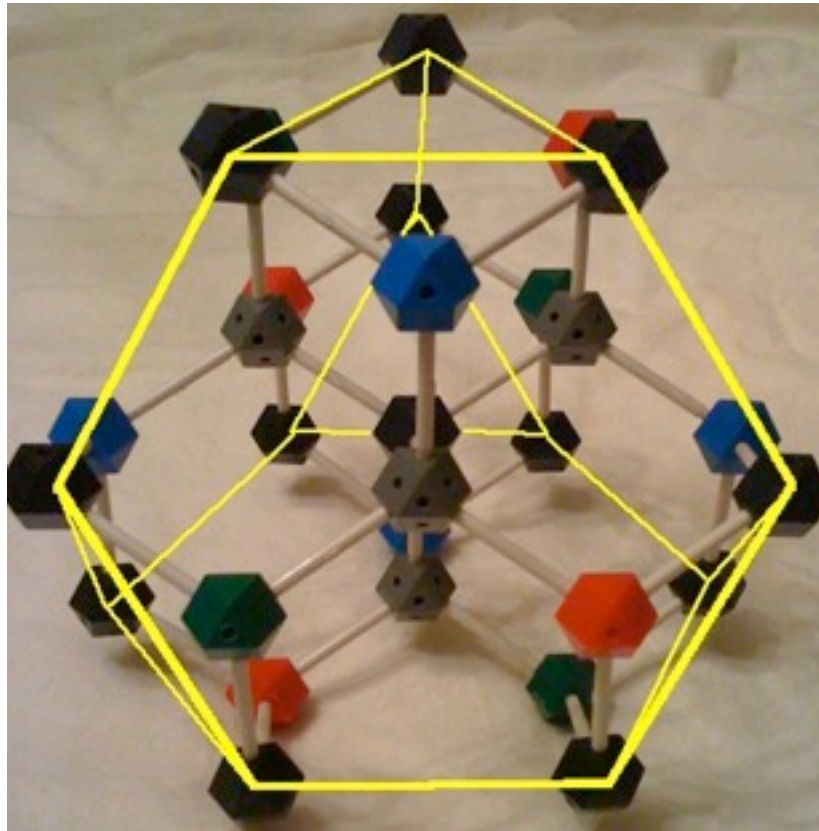
and can be considered to be at radius $\sqrt{0.75}$ from the central vertex.

The 12 shell-2 vertices (red, green, blue) form a (yellow) cuboctahedron



at radius $\sqrt{2}$ from the central vertex,
so that there within the first 2 shells of the Diamond Lattice
there are $1 + 4 + 12 = 1 + 16 = 17$ vertices.

The 12 shell-3 vertices (black) form a (yellow) truncated tetrahedron



are at radius $\sqrt{2.75}$ from the central vertex,
so that there within the first 3 shells of the Diamond Lattice
there are $1 + 4 + 12 + 12 = 1 + 28 = 29$ vertices.

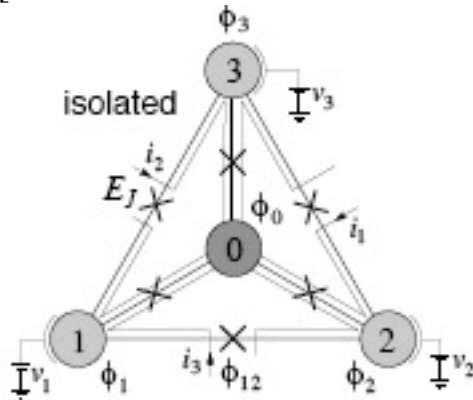
Jean-Francois Sadoc and Remy Mosseri
in their book “Geometric Frustration” (Cambridge 2006) said: “...
**the diamond crystalline structure can be obtained
by starting from an f.c.c. structure
and adding a second replica of the f.c.c. structure,
translated by $(1/4, 1/4, 1/4, 1/4)$ with respect to the first one. ...”.**

Construction of TetraJJ Nucleus in 3-dim space

Eric A. Lord, Alan L. Mackay, and S. Ranganathan in their book “New Geometries for New Materials” (Cambridge 2006) said:

“... The gamma-Brass cluster ... starts from a single tetrahedron

[all tetrahedra should be seen as

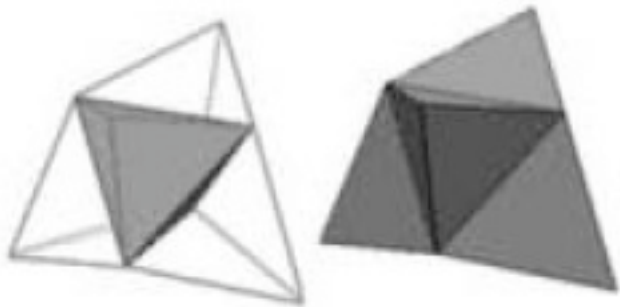


TetraJJ Quantum Computer Qubits]

Place four spheres in contact.

Then place a sphere over each face of the tetrahedral cluster.

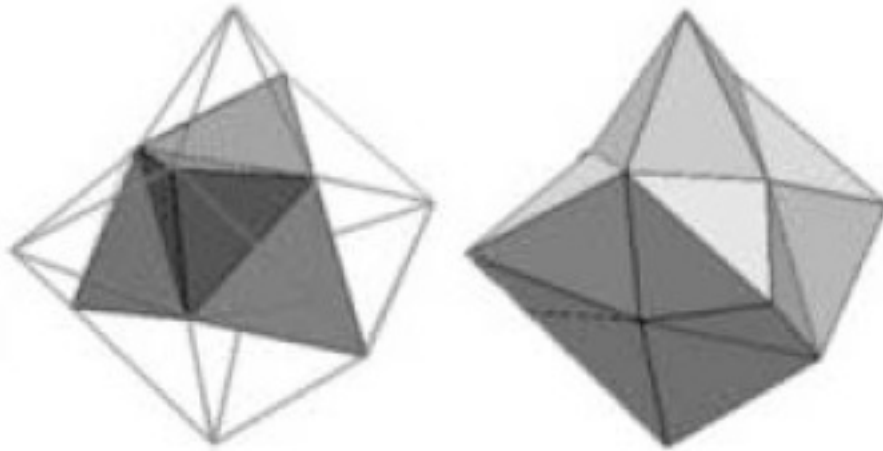
The centres and bonds then form a stella quadrangula



built from five regular tetrahedra ...[a total of $1+4 = 5$ tetrahedra]...

Six more spheres [vertices] placed over the edges of the original tetrahedron form an octagonal shell. In terms of the network of centres and bonds we now have added 12 [= 2×6] more tetrahedra ...

There are now five tetrahedra around each edge of the original tetrahedron. ...



...[we now have $1+4+12 = 17$ tetrahedra]...

[The 12 newly added tetrahedra]... are not quite regular ...[i.e., nonzero Fuller unzipping angles appear as described by Thomas Banchoff in his book “Beyond the Third Dimension” (Scientific American Library 1990) where he said:

“... in three-space we can fit five tetrahedra around an edge ...

[image from Conway and Torquato PNAS 103 (2006) 10612-10617

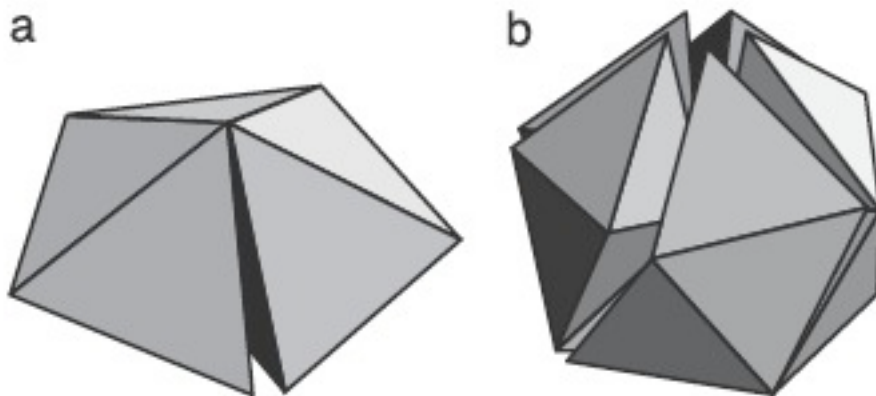


Fig. 1. Certain arrangements of tetrahedra. (a) Five regular tetrahedra about a shared edge. The angle of the gap is 7.36° . (b) Twenty regular tetrahedra about a shared vertex. The gaps amount to 1.54 steradians.]

... with a ... small amount of room to spare,
which allows folding into 4-space ...[where the fit can be made exact]...” .]

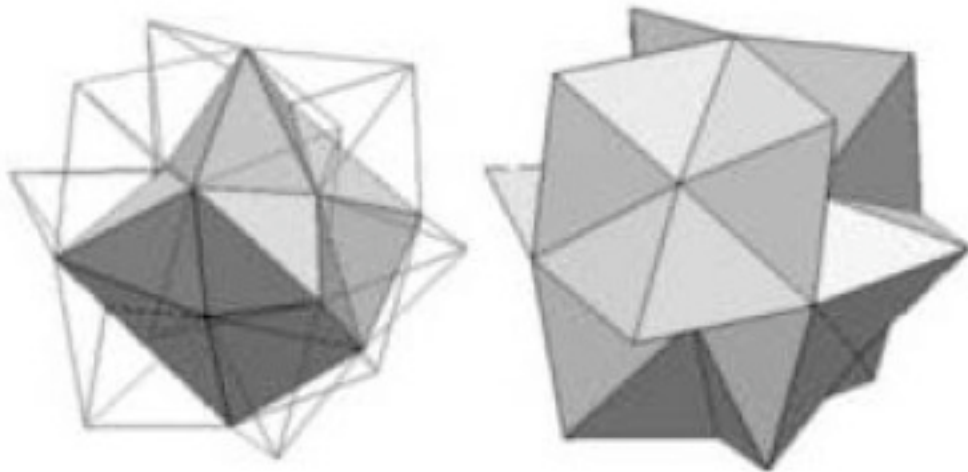
Note that all the subsequently added tetrahedra of layers and structures further out from the center are also “not quite regular”, or, in other words, leave gaps among tetrahedra that are related to the Fuller unzipping angle.

The irregularity, or Fuller unzipping angle, can be visualized as the amount of curvature in a collection of TetraJJ by which it deviates from the flatness of 3-dim space described by the 3-dim Diamond Lattice.

The irregularity goes away in curved 3-dim space, which, if it is to be realized in a flat space, must be realized in 4-dim space by adding a 4th dimension to 3-dim space.

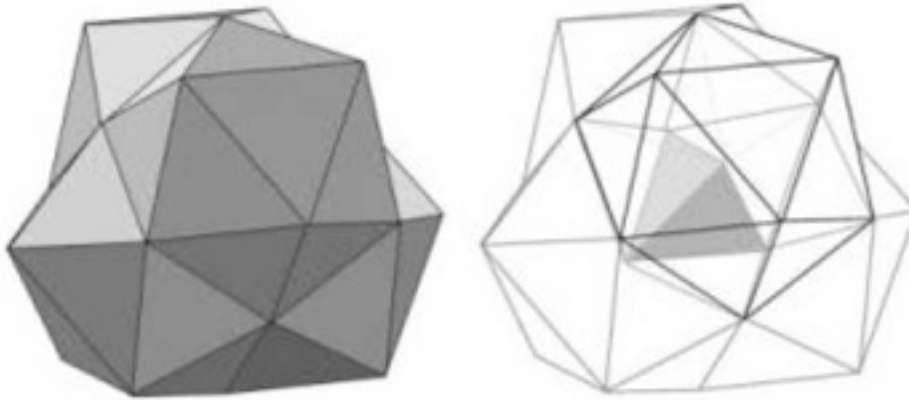
However, for now, we will continue with construction of the TetraJJ Nucleus and its Array in 3-dim space, and leave additional dimensions to later sections of this paper.]

... 12 more spheres [vertices in addition to the $1+4+12 = 17$] complete the rings of five tetrahedra around the edges of the four secondary tetrahedra ...[They add $2 \times 12 = 24$ more tetrahedra for a total of $1+4+12+24 = 41$ tetrahedra]...



... Without increasing the number of vertices [which is now 26],

inserting 16 more tetrahedra reveals the structure to be four interpenetrating icosahedra sharing a common tetrahedral building block ...



...[and gives a total of $41 + 16 = 57$ tetrahedra]... and 26 vertices ... the model of the 26-atom gamma-brass cluster as four interpenetrating icosahedral clusters

...

This cluster can be further augmented by placing [$4 \times 3 = 12$] extra spheres ... we then have 38 spheres ...”.

Note that each of the 4 interpenetrating icosahedra has:

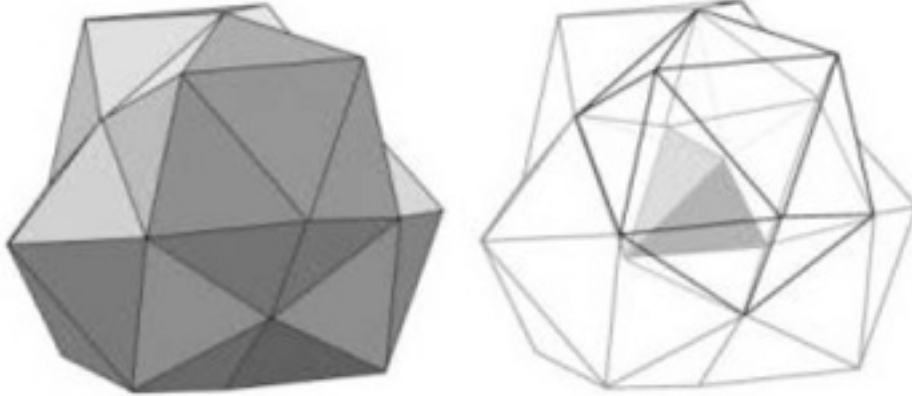
- 10 tetrahedra to itself (each belongs to only 1)
- 6 tetrahedra shared with one other (each belongs to 2)
- 3 tetrahedra shared with two others (each belongs to 3)
- 1 tetrahedron shared with all three others (belongs to 4)

so

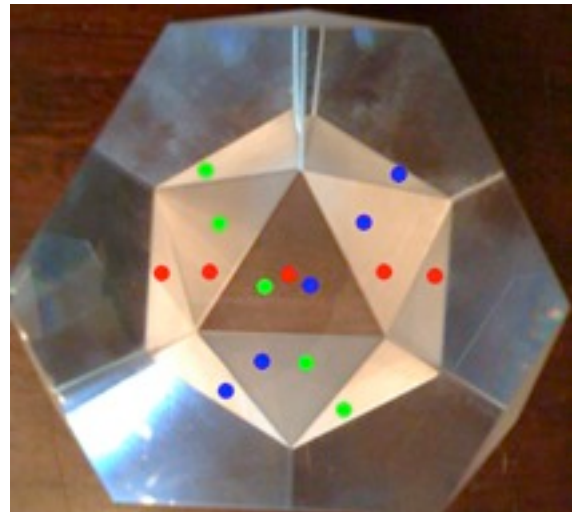
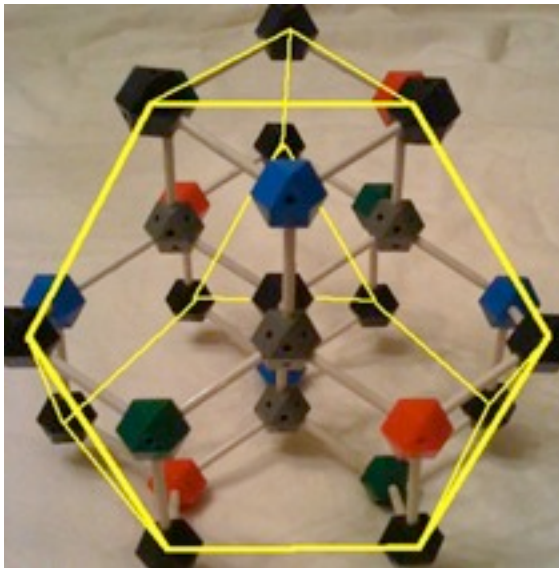
the total number of tetrahedra in a TetraJJ Nucleus
is $4 \times 10 + 4 \times 6/2 + 4 \times 3/3 + 4 \times 1/4 = 40 + 12 + 4 + 1 = 57$.

Symmetry of the TetraJJ Nucleus

The exterior of a 57-tetrahedron TetraJJ Nucleus



consists of 4 half-Icosahedra in a configuration that resembles



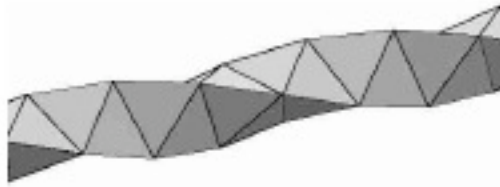
a truncated tetrahedron whose reflection view through each of its 4 large faces shows an image that appears to be a half-icosahedron that looks like the inner half of the Interpenetrating Icosahedron for which the Exterior half-Icosahedron that is opposite the large face is the exterior half.

The TetraJJ Nucleus central tetrahedron is marked by three (red, green, blue) dots. For each of the 4 large faces (and opposite truncations) of the TetraJJ Nucleus there are 6 ways (2 of each color) to start at the central tetrahedron and go out to the surface through face-sharing 3-chains of 3 tetrahedera.

Each of those 3-chains of tetrahedra can be fit together with another 3-chain going out in the opposite direction, so the $4 \times 6 = 24$ 3-chains become $24/2 = 12$ 5-chains, called Tetrahelices because they are helical chains of tetrahedra, that extend through the TetraJJ Nucleus.

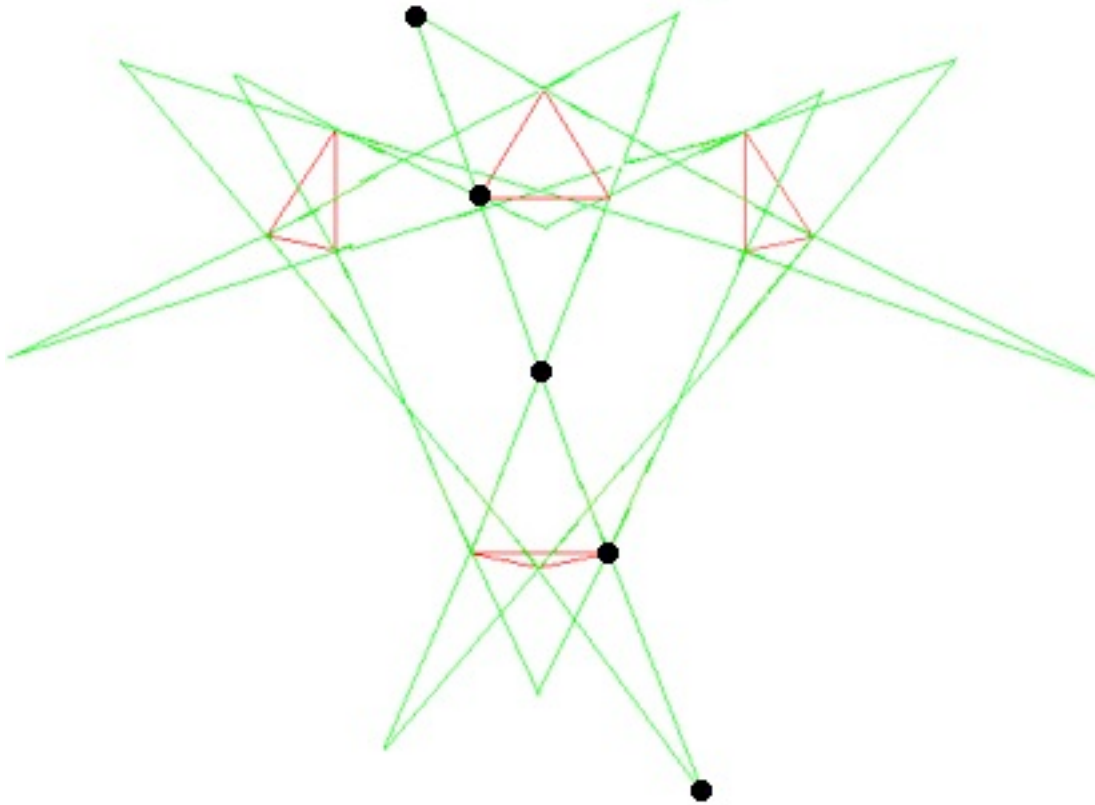
Lord and Ranganathan in Eur. Phys. J. D 15 (2001) 335-343 said:

“... A Coxeter helix is a polygonal helix such that every set of four consecutive vertices form a regular tetrahedron ... This produces a twisted rod of tetrahedra, the Boerdijk-Coxeter helix ...”



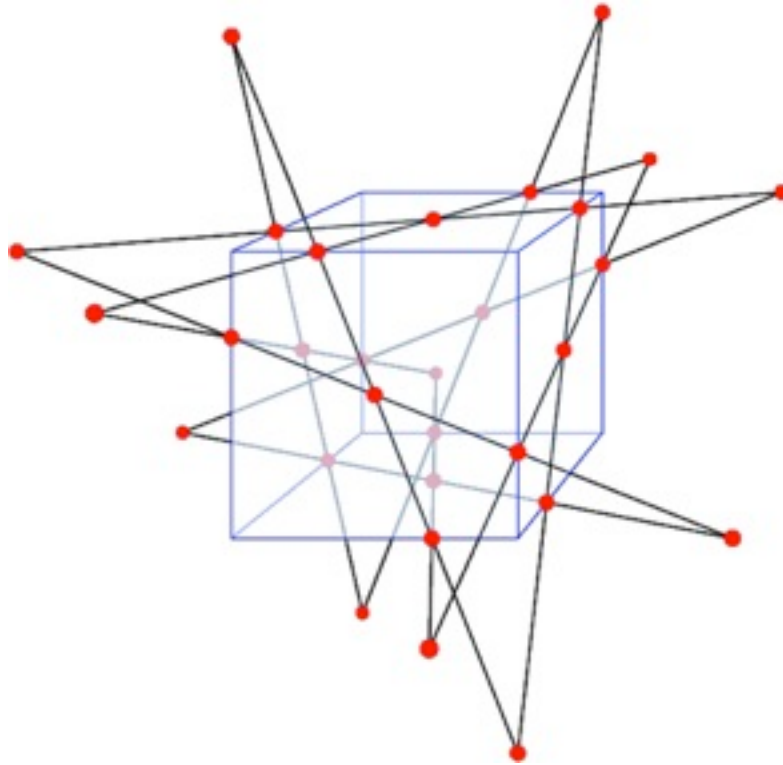
The B-C helix is generated from a single regular tetrahedron by repeated application of a screw transformation. ...”.

R. W. Gray on his web site at rwgrayprojects.com describes the configuration "... There are 12 possible Tetrahelix passing through a single Tetrahedron: 6 Clockwise and 6 Counter clockwise ... For ... the way 12 Tetrahelix pass through a single Tetrahedron [corresponding to the Truncated Tetrahedron large-scale structure of the TetraJJ Nucleus]... draw ... red ... triangles ...[in the modification below of the images by R. W. Gray they are the 4 truncations of the Truncated Tetrahedron large-scale structure of the TetraJJ Nucleus]... The lines which ... will be a symmetry axis for a Tetrahelix ... will be shown in green ...

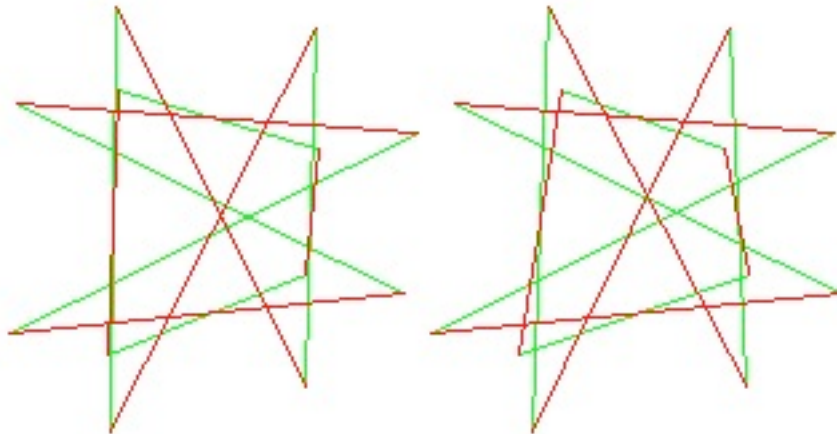


There are 12 green lines, so there are 12 Tetrahelix passing through ...[the TetraJJ Nucleus Truncated]... Tetrahedron. Six of these will have a Clockwise screw sense and 6 will have a Counter Clockwise screw sense. ... a Tetrahelix's symmetry axis will intersect 5 other Tetrahelix axis of symmetry and 2 of the intersection points are outside the Tetrahedron. ...[the intersection points for one of the Tetrahelix lines are shown above as black dots]... Note that the green lines come in crossing pairs. ...".

The 12 Tetrahelices, in 6 pairs, form the geometrical configuration of the Schläfli Double-6. With a lot of 3-dim lines projected down to 2-dim images, it may be hard to see which crossings are real in 3-dim and which are just look that way in 2-dim, so here is an image modified from wiki commons that shows the crossings as red dots and shows a cube to help perspective.

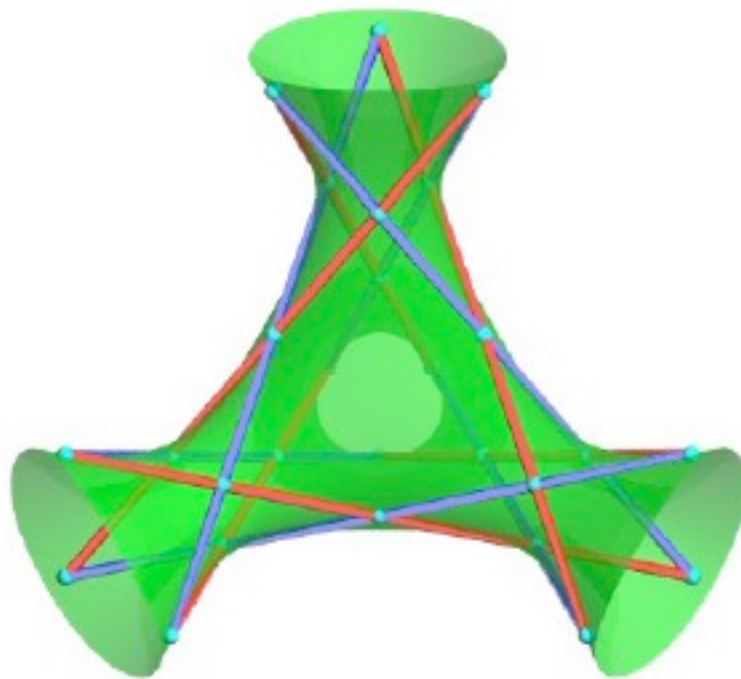


Crossings may be clearer in this stereo image

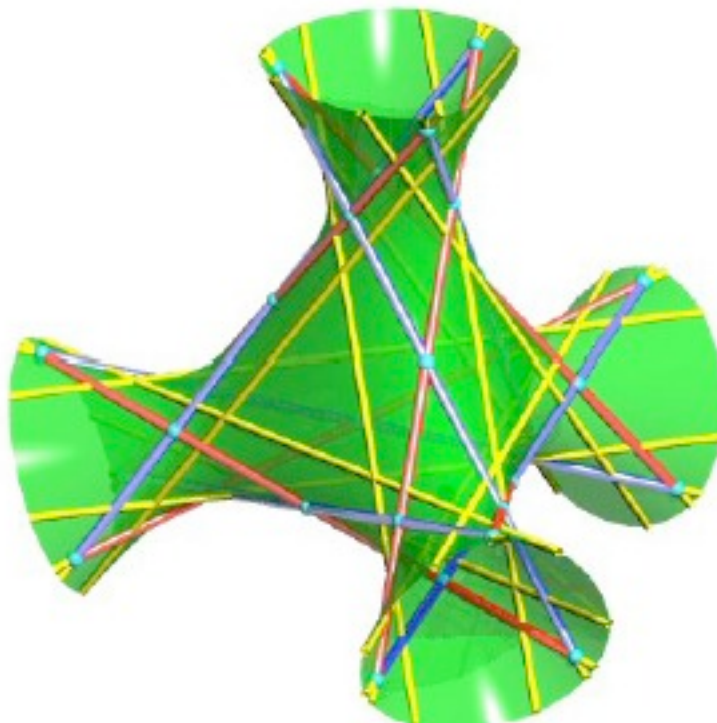


in which 6 of the Tetrahelix lines have been colored red to indicate their helicity being opposite to that of the 6 remaining as green.

Robert Ferreol and Alain Esculier on their mathcurve.com web site say: "... Il existe une unique surface cubique ... contenant les 12 droites du double-six ...



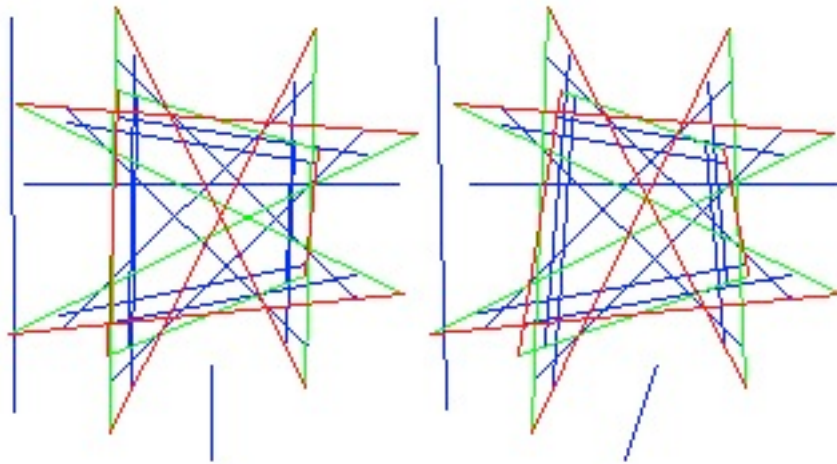
... Les 27 droites de cette surface sont ... les 12 ... plus les 15 droites ... (en jaune)



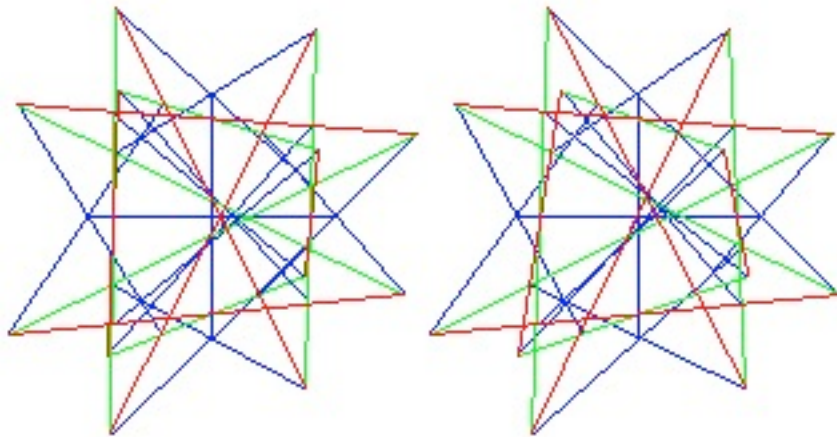
...

...”

The 12 lines of the Double-6 are 12 of the 27 lines on a general cubic surface with the other $27 - 12 = 15$ being closely related as can be seen above and also in this stereo image



in which the 12 Double-6 lines are red and green and the other 15 are blue. Since each of the $12+15 = 27$ lines have 5 points of crossing, the configuration has $27 \times 5 = 135$ points. In case it might help in visualization, here



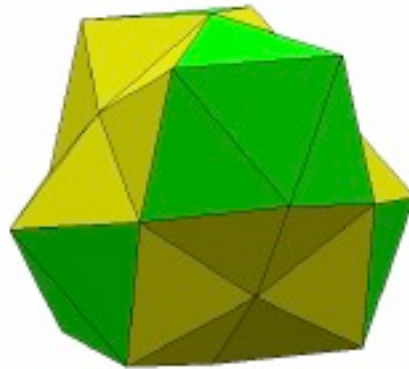
is a stereo image of the 27 line 45 point configuration that is dual to the 27 line 135 point configuration shown above.

The symmetry group of the 27 line configuration, and so of the Tetra JJ Nucleus, is of order $72 \times 6! = 51,840$ and is the Weyl Group of the Lie Algebra E_6 . (see Coxeter, Math. Z. 200 (1988) 3-45).

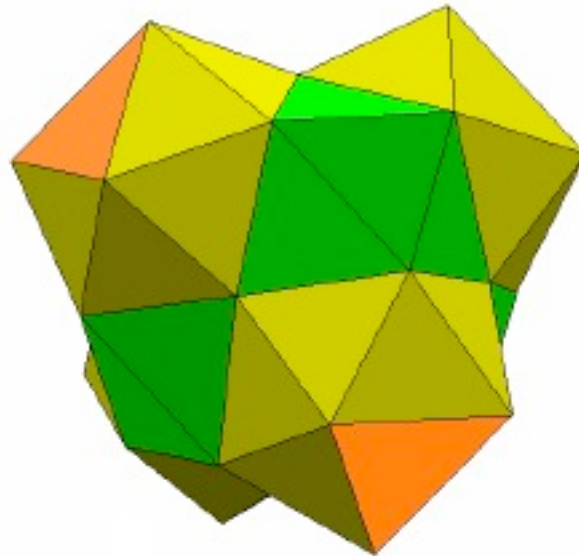
Extension of a TetraJJ Nucleus to an Array in 3-dim space

To extend a 57-tetrahedron 26-vertex TetraJJ Nucleus,
first construct some auxiliary structures,
the first of which is an 81-tetrahedron 38-vertex Pearce Cluster:

Begin with a 57-tetrahedron 26-vertex TetraJJ Nucleus



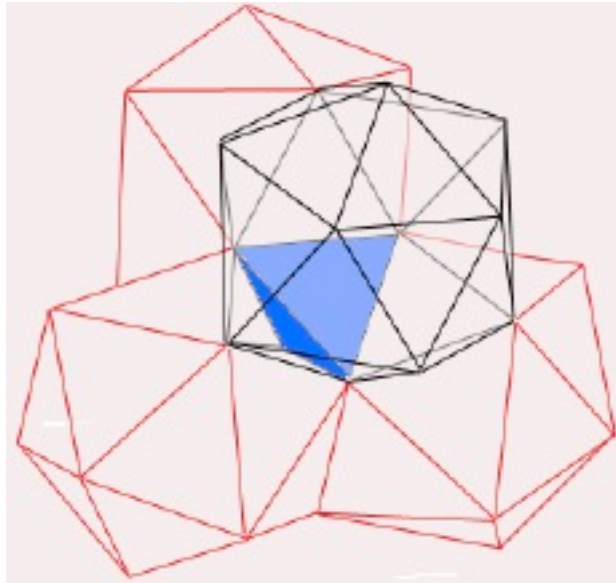
Then add 40 more tetrahedra and 12 more vertices to get



97 tetrahedra with 38 vertices.

Then remove the $4 \times 4 = 16$ tetrahedra of the type of those colored green
(note that this does not remove any vertices)

to get the 81-tetrahedron 38-vertex Pearce Cluster



which has the configuration of four icosahedra in face contact with a central tetrahedron and with each other.

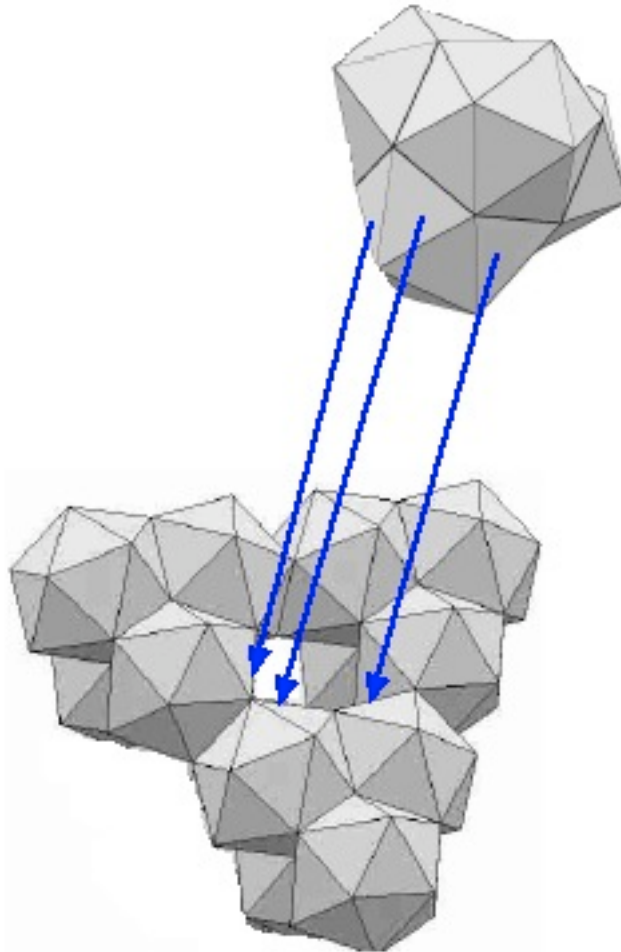
Then note that 4 Pearce Clusters can be put in face contact with each other to form the basis of what Lord and Ranganathan in Eur. Phys. J. D 15 (2001) 335-343 describe as “... a D [Diamond] network open packing in which a regular tetrahedron is centered at each node ...



... and is linked to neighboring nodes by oblate icosahedra. ...”.

Then, consider a Pearce Triangle formed by 3 Pearce Clusters

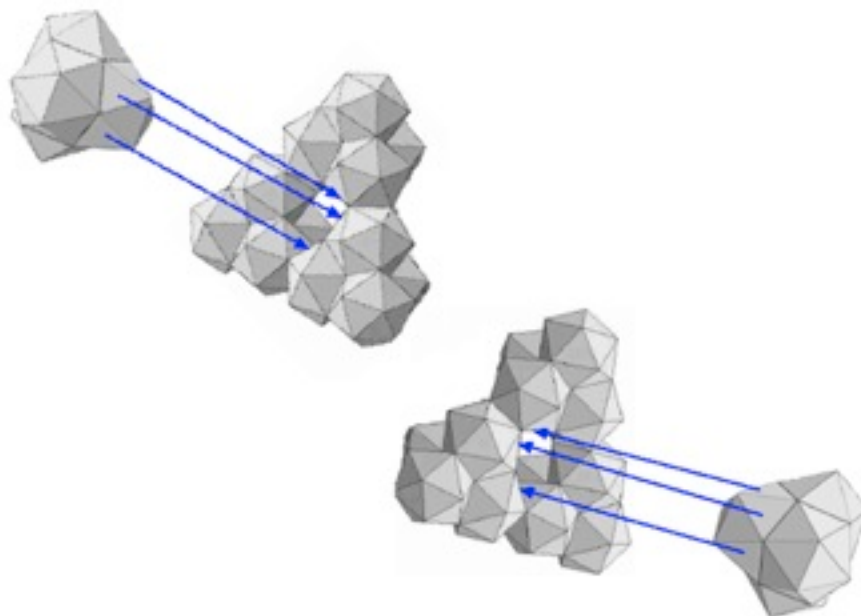
and note that a TetraJJ Nucleus can fit into the hole in the center of the Pearce Triangle:



Since the Pearce Triangle is made up of 3 Pearce Clusters each joined to the other 2 by a triangular face,
the Pearce Triangle has $3 \times 81 = 243$ tetrahedra and $3 \times 38 - 3 \times 3 = 105$ vertices.

Since the TetraJJ Nucleus has 57 tetrahedra and 26 vertices,
and since fitting it into the center of the Pearce Triangle effectively cancels 9
vertices in forming the combined TetraJJPearce configuration,
the TetraJJPearce has $243 + 57 = 300$ tetrahedra and $105 + 26 - 9 = 122$ vertices.

Then, to form a $\{3,3,5\}$ 600-cell, combine two TetraJJPearce to form



with $300 + 300 = 600$ tetrahedra and $122 + 122 = 244$ vertices .

Folding up the flat Pearce Triangles gives

(as I counted from pictures)

$244 - 22 - 22 = 200$ vertices.

Matching the two TetraJJPearce combinations gives

(I have not yet counted this explicitly from pictures, so this step is conjectural)

$200 - 80 = 120$ vertices.

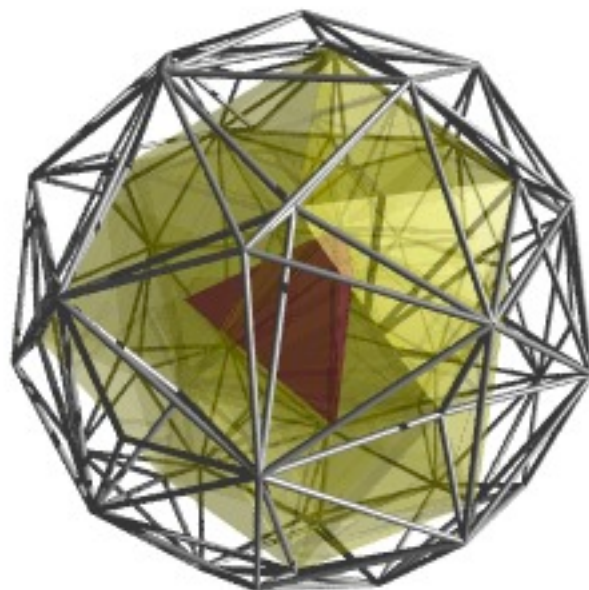
So, we have expanded two TetraJJ Nuclei to form a $\{3,3,5\}$ 600-cell.

In either curved 3-dimensional space (such as a 3-sphere S^3)

or in 4-dimensional space,

all the tetrahedra and icosahedra and TetraJJ Nuclei and Pearce Clusters
are exactly regular.

Here (from wikipedia) is an image of a 3-dim projection of a 4-dim 600-cell



with a central tetrahedron shown in red.

Two $\{3,3,5\}$ 600-cell sets of 20 vertices form a 240 Polytope in 4 dimensions and if 4-dimensional space is extended to 8-dimensional space by considering Golden Ratio Irrational Algebraic Coordinates to be independent, the 240 vertices of the 240 Polytope form the Root Vectors of the E8 Lie Algebra.

Jean-Francois Sadoc and Remy Mosseri in their book

“Geometric Frustration” (Cambridge 2006) said:

“... **The polytope 240** ...[is]... not a regular polytope in the Coxeter sense ... but ... **an ordered structure on a hypersphere ... S³ ...**

the diamond crystalline structure can be obtained by starting from an f.c.c. structure and adding a second replica of the f.c.c. structure, translated by $(1/4, 1/4, 1/4, 1/4)$ with respect to the first one.

Similarly,

polytope 240 is generated by adding two replicas of the $\{3,3,5\}$, displaced along a screw axis of S₃. ...

Each vertex of the first $\{3,3,5\}$ replica is surrounded by four vertices from the second replica. ... The local configuration is perfectly tetrahedral ...

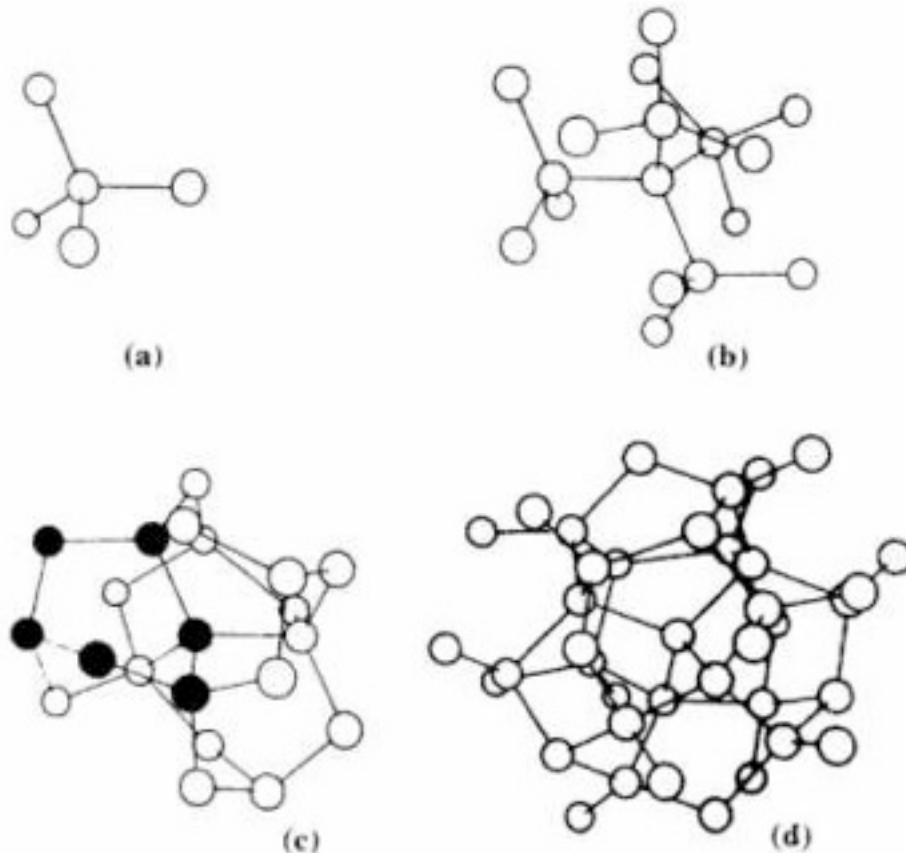


Fig. 2.10. Local view of the polytope '240'. (a) Five vertices, the tetrahedral symmetry is clearly visible; (b) 17 vertices; (c) 21 vertices, a six-fold ring is distinguished; (d) 39 vertices.

which shows orthogonal mapping of subsets of increasing size of the polytope. ... polytope 240 is locally denser than the diamond structure. This is exactly the corollary of what was said ... for the {3,3,5} compared to the f.c.c. dense structure ...

The direct symmetry group of ... polytope 240 ... is ... $G_{240} = Y' \times O' / Z_2$ where ... Y' ... is the binary icosahedral group ... [and] ...

O' ... is the binary ... octahedral group ...

Note ... The direct symmetry group of the {3,3,5} polytope is a sub-group of $SO(4)$ which reads $G' = Y' \times Y' / Z_2$... Since the order of Y' is 120, the quotient by Z_2 implies that the order of G' is 7200. ... The total symmetry group G also includes indirect orthogonal transformations, analogous to reflections ... This adds 7200 new elements and gives the full group G of order 14400. ...

O' is not a subgroup of Y' ... polytope 240, while sharing some of the {3,3,5} symmetries, also has new symmetries, in particular a 40-fold screw axis ...

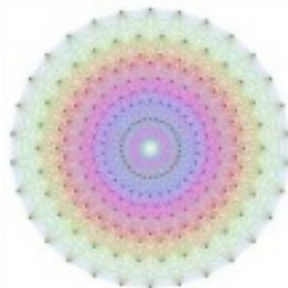
Another way to describe the 240 ... is to ... follow a building rule similar to that which leads to the diamond structure starting from the f.c.c. structure:

a new vertex is placed at the centre of some tetrahedral cells of the compact structure. In the f.c.c. case, one tetrahedron over two is centered, while in the present case, one tetrahedron over five will be centered, which has the consequence of breaking the five-fold symmetry of the polytope {3,3,5}, only a tenfold screw axis being preserved.

One gets a regular structure with 240 vertices, called polytope 240, which is chiral; it cannot be superimposed on its mirror image.

The polytope 240 with opposite chirality has ... $O' \times Y' / Z_2$ as its symmetry group. ...”.

If 4-dimensional space is extended to 8-dimensional space by considering Golden Ratio Irrational Algebraic Coordinates to be independent, the 240 vertices of the 240 Polytope form

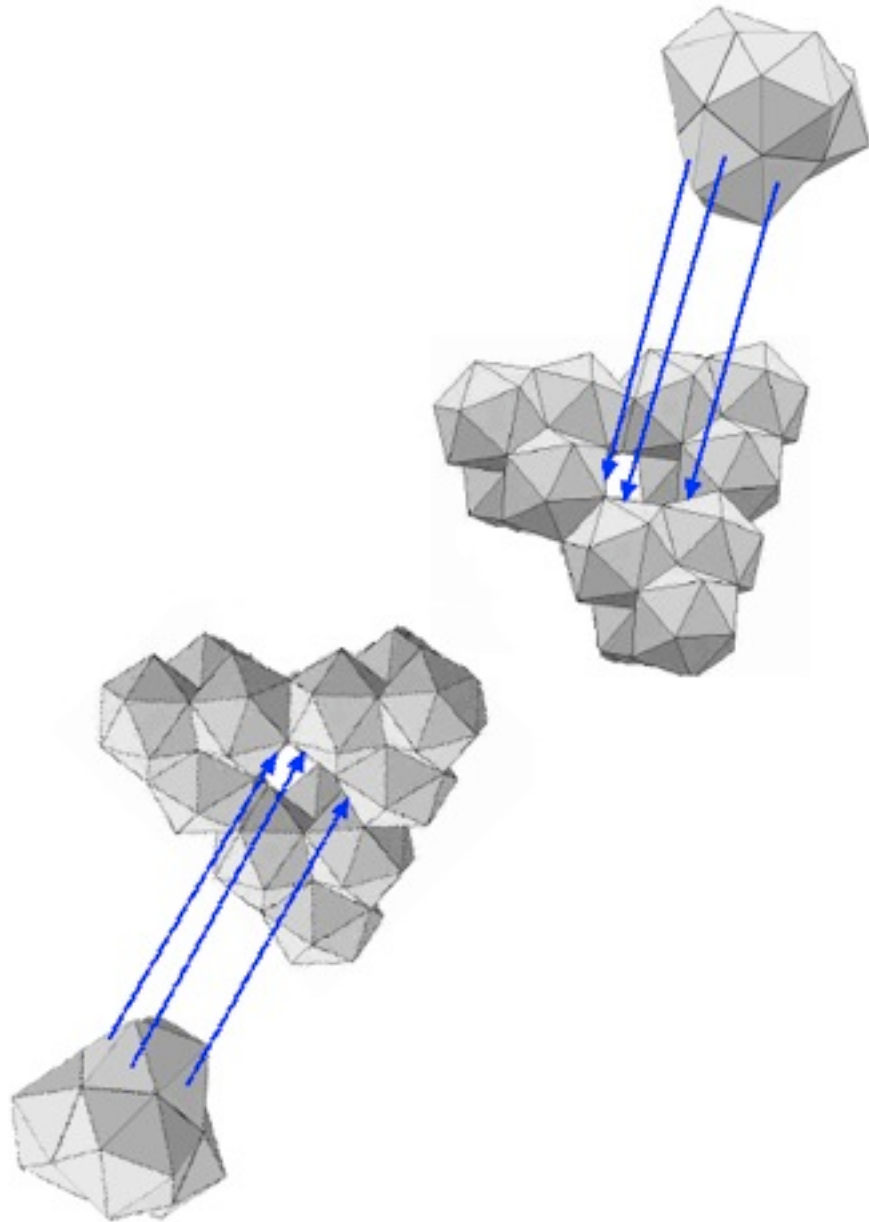


the 240 Root Vectors of the E8 Lie Algebra.

As to chirality, note that the Lie Algebra structure

248-dim E8 = 120-dim adjoint of D8 + 128-dim half-spinor of D8
does not include the other mirror image half-spinor of D8.

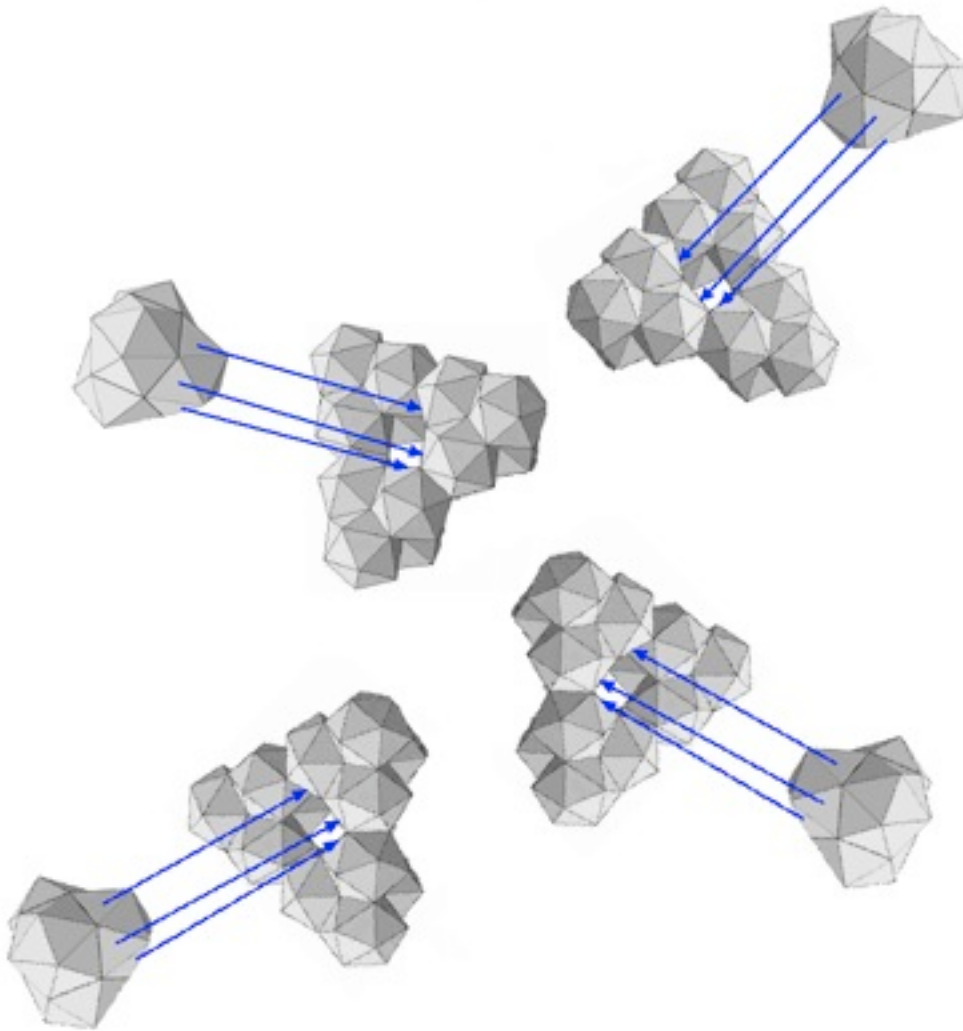
My guess is that if you want to build in our flat 3-dimensional space
a TetraJJ Array for exploring Dark Energy
it should be made of 600 Tetrahedral Josephson Junctions in the configuration
described above for the $\{3,3,5\}$ 600-cell (note that in the image that I assembled
perspective is not accurately portrayed):



Note that since the 600 tetrahedra will not fit together exactly in flat 3-dim space they will not share vertices as efficiently as the $\{3,3,5\}$ 600-cell the number of vertices will be much larger than 120.

Dark Energy phenomena might be seen between the two 300-cell sheets each of which has a TetraJJ Nucleus core.

Note also that since it takes two 600-cells to make a 240 Polytope it may be that a larger (1200 cells, 4 TetraJJ cores) array



would give better results with respect to experimenting with Dark Energy.

Matthew Bennett and Kurt Wiesenfeld in their paper entitled
“Averaged Equations for **Distributed Josephson Junction Arrays**”
at <http://www.physics.gatech.edu/mbennett/dist2003.pdf>

say:

"... The Kirchhoff limit is valid provided the size of the system is small compared to the wavelength of the electromagnetic radiation.

As it happens, the twin technological goals of generating higher operating frequencies ... and larger output powers (and thus more junctions) both work against this limit. ...

To take an example,

an array operating at 300 GHz - not a particularly high frequency for Josephson junctions - corresponds to a wavelength of 0.4 millimeters when the index of refraction is 2.5;

for a typical spacing of 10 micrometers, this is about the same size as an array of about 40 junctions - not a particularly large number for Josephson arrays ...

at higher frequencies the current in the wire is not necessarily spatially uniform, so the wire becomes a significant dynamical entity which couples the junctions along its length. ... we model the wire as a lossless transmission line ...

...

The resonant case is especially revealing, and leads to significant physical insight into achieving attracting synchronized dynamics.

The tighter the clusters, the more likely it is that phase locked solutions appear. ...

There are also hints that distributed arrays exhibit fundamentally different phenomena than their lumped counterparts.

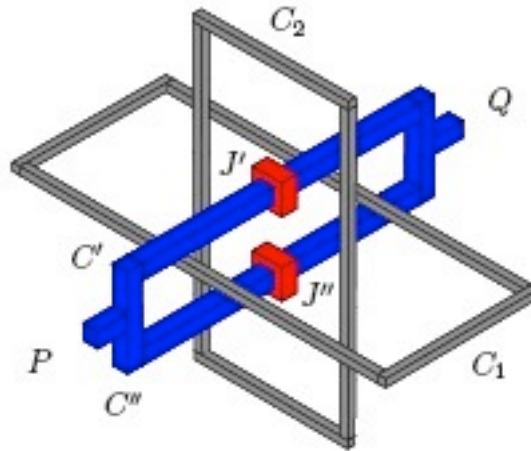
In one case, experiments on distributed Josephson arrays reported evidence of super-radiance ...".

Roman V. Buniy and Thomas W. Kephart in their paper

“Higher order Josephson effects”

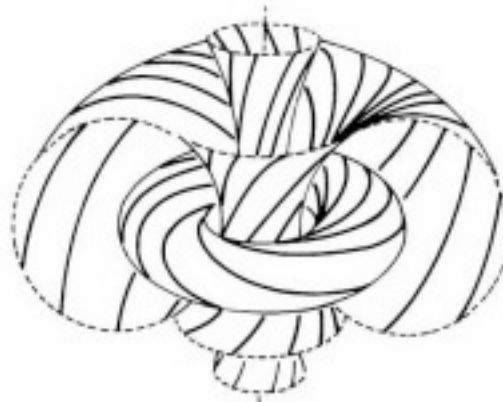
arXiv 0808.1892 said: "... Gaussian linking of superconducting loops containing Josephson junctions with enclosed magnetic fields give rise to interference shifts in the phase that modulates the current carried through the loop, proportional to the magnitude of the enclosed flux. We generalize these results to **higher order linking of a superconducting loop with several magnetic solenoids**, and show there may be **interference shifts proportional to the product of two or more fluxes**. ...

The simplest example is a Borromean ring arrangement ...



... where the semiclassical path corresponds to one ring, which has higher order linking with two flux tubes carrying fluxes Φ_1 and Φ_2 , which make up the other two rings. We found the phase shift in this system is ...[proportional to the product $\Phi_1 \Phi_2$]... Higher order cases were explored in ...[hep-th/0611335 and hep-th/0611336]... and shown to be related to commutator algebras of homotopy generators of the configuration space $R^3 \setminus \{ T_1 \cup T_2 \}$, where T_1 and T_2 are the tubes containing the fluxes. ... The same general logic can be applied to systems of superconductors, Josephson junctions, and magnetic fluxes where the Josephson effect can arise ...".

The Buniy and Kephart paper may be particularly relevant with respect to **the Hopf fibration geometry of the $\{3,3,5\}$ 600-cell** discussed in the next section, due to



the high level of linking of the Hopf circles in the $\{3,3,5\}$ 600-cell.

Hopf Fibration, Clifford Algebras, AQFT, EPR Entanglement

Lord and Ranganathan in Eur. Phys. J. D 15 (2001) 335-343 and J. Non-Crys. Solids 334&335 (2004) 121-125 said:

“... The polytope $\{3,3,5\}$ [600-cell] has 120 vertices, 720 edges, 1200 equilateral triangle faces and 600 regular tetrahedral cells.

Five cells surround each edge and twenty surround each vertex - forming a regular icosahedron.

Circuits of 30 face-sharing tetrahedra occur in $\{3,3,5\}$. They are metrically identical to the ...[Coxeter helix]... in three dimensional Euclidean space. ...



... every set of four ...[neighboring]... vertices is the set of vertices of a regular tetrahedron with ...[for a $\{3,3,5\}$ with radius 1]... edge length $1/T$... where T is the golden number, $T = (1+\sqrt{5})/2$ and $S = -T^{-1} = (1-\sqrt{5})/2$...

The 120 vertices of $\{3,3,5\}$ lie in tens on 12 great circles, which are twelve circles of a Hopf fibration.

... the vertices can be assigned in tens to twelve fibres ... in 24 different ways ... corresponding to 12 left and 12 right fibrations ... The twelve fibres are represented as the twelve vertices of an icosahedron ... base space of the fibre bundle ... and the icosahedron edges represent the nearest neighbor relationship ...

The special transformations of the form $x \rightarrow px$; and $x \rightarrow xq$... p and q ...[being]... quaternions p and q ... are called, respectively,

left and right Clifford translations. ...

For any given point x in S^3 ,

a transformation $x \rightarrow px$ generates a great circle in S^3 ...

we can generate a great circle through every point x of S^3 .

This set of circles constitute a left Hopf fibration. ...

Similarly,

right Hopf fibrations are defined in terms of the transformations $x \rightarrow xq$.

... no two of the circles can intersect ... every pair of circles is linked!

The circles are the fibres of the fibration. ...

To obtain realistic models of E^3 structures from the elegant geometry of $\{3,3,5\}$

the polytope has to be mapped in some way,

by unfolding it or by a projection method ...

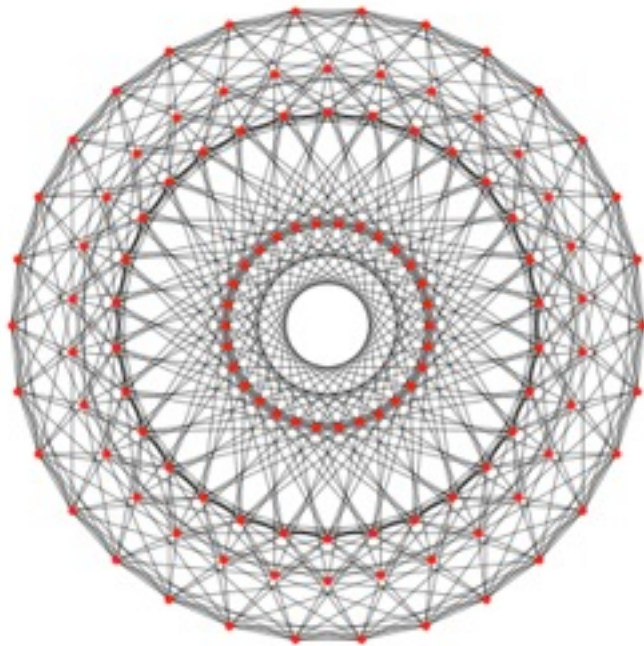
To obtain a realistic model ... from the corresponding structure in $\{3,3,5\}$

a mapping is required

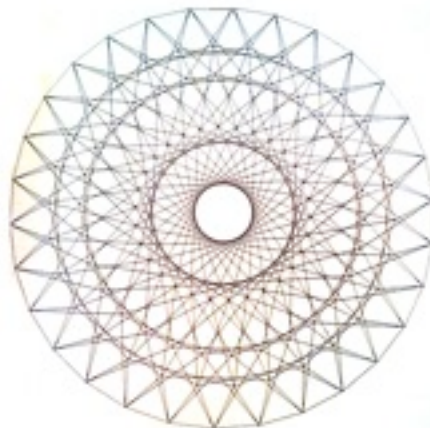
that maps great circles of a Hopf fibration of S^3 to helices in E^3

The central helix obtained by ... projection of $\{3,3,5\}$... is an almost exact Coxeter helix: the number of edges per turn is $30/11 = 2.727$, instead of 2.731 ...”.

H. S. M. Coxeter in his book “Regular Complex Polytopes” (Cambridge 2nd ed 1991) said: “... In 1931 Heinz Hopf ... described a representation of the 3-sphere ... whose points ... satisfy ... the 2-sphere ... Each point ...[of the 2-sphere]... represents ... a great circle ... two such great circles are disjoint, and the whole set of ... such circles is a Hopf fibration of the 3-sphere ... **A finite version of the Hopf fibration can be seen in the distribution of the 120 vertices of [the 600-cell] $\{3,3,5\}$ [with 120 vertices, 720 edges, 1200 faces (triangular), and 600 cells (tetrahedra)] ... into 12 decagons ...**



[or the $3\{5\}3$ complex polygon counterpart of the $\{3,3,5\}$...



... into twelve ‘parallel’ decagons ...”.

To visualize **the 12 circles of a Hopf fibration of {3,3,5}** note that they can be distributed as follows:

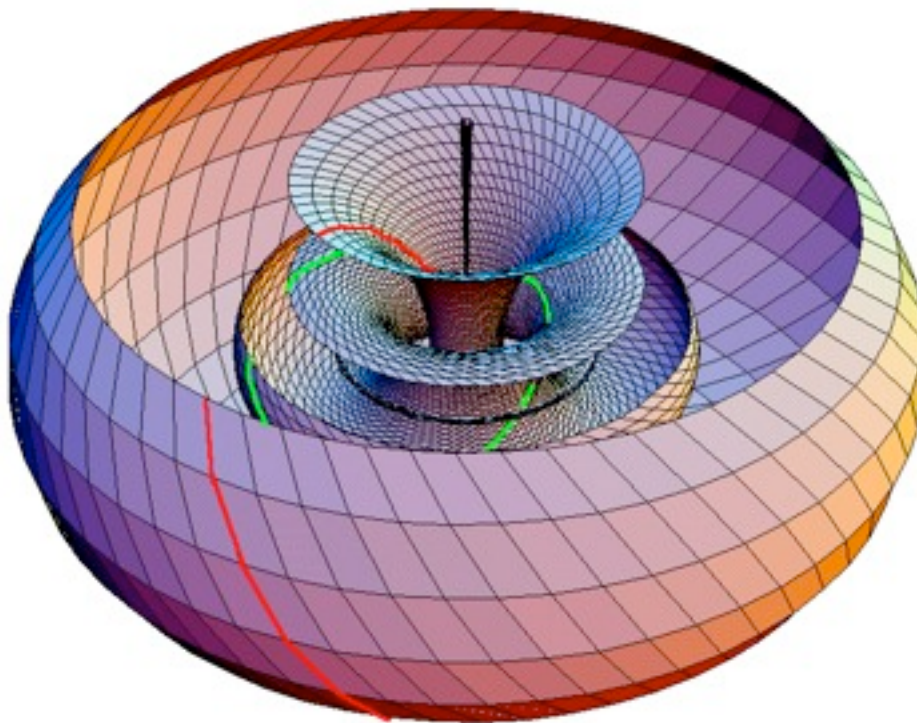
1 on a vertical axis (actually a line or circle through infinity) - 10 vertices

5 on a large intermediate torus - $5 \times 10 = 50$ vertices

5 on a small intermediate torus - $5 \times 10 = 50$ vertices

1 on a circle in a plane perpendicular to the vertical axis - 10 vertices

A nice graphic illustration of this is on the web site of F. G. Marcelis at members.home.nl/fg.marcelis/



I have added rough drawings of:

one of the circles on the large intermediate torus (in red)

(the other 4 would be equally spaced around the torus)

and

one of the circles on the small intermediate torus (in green)

(the other 4 would be equally spaced around the torus).

The 120 {3,3,5} vertices would be equally distributed, 10 per circle, around each of the 12 circles,

so that you might regard each of the circles as a decagon.

The Hopf fibration of $\{3,3,5\}$ is of the 3-sphere S^3 in which $\{3,3,5\}$ lives:

$S^1 \rightarrow S^3 \rightarrow S^2 = CP^1 = SU(2) / U(1) =$ Projective Space of Complex Numbers
Here the base space is S^2 of which the relevant discrete subset is the icosahedron with 12 vertices, one for each of the 12 decagons of the discrete $\{3,3,5\}$ fibration.

There are only two further Hopf fibrations:

One is $S^3 \rightarrow S^7 \rightarrow S^4 = QP = Sp(2) / Spin(4) =$ Projective Space of Quaternions
Sadoc and Mosseri in their book “Geometric Frustration” (Cambridge 2006) said:
“... We now consider quasiperiodic structures derived from the eight-dimensional lattice E_8 ... The network is foliated into successive shells surrounding a vertex. These shells belong to S^7 spheres ... the Hopf fibration of S^7 , with S^3 fibres, ... split[s] the E_8 sites into symmetrically disposed sets of 24 sites in the S^3 fibres ... we then get a shell-by-shell analysis of the four-dimensional structure, which recalls ... the ... algorithm used to generate the Fibonacci chain ... Consider a (hyper)cubic cell in R^8 ... E_8 presents an analogy with the f.c.c. lattice and ... the diamond structure. This cubic cell contains 256 sites.

...

To each of the ten sets of 24 points ... corresponds ... a ... Hopf ... fibre S^3 ...

The ten ... form a cross polytope in R^5 ...

On each fibre, the 24 point form a [24-cell] polytope $\{3,4,3\}$...

each fibre ... generates a four-dimensional sublattice $\{3,3,4,3\}$ of the E_8 lattice.

There are ten equivalent sublattices through the origin,

associated with the ten points on the base S^4 [in R^5]...

The mapping of the [240-vertex 8-dim] Gossett polytope onto ... four-dimensional space ... produces two sets of five $\{3,4,3\}$, each on a different spherical shell S^3 ... surrounding the origin ... each set of five $\{3,4,3\}$ forms a $\{3,3,5\}$ polytope, and one finally gets two concentric $\{3,3,5\}$

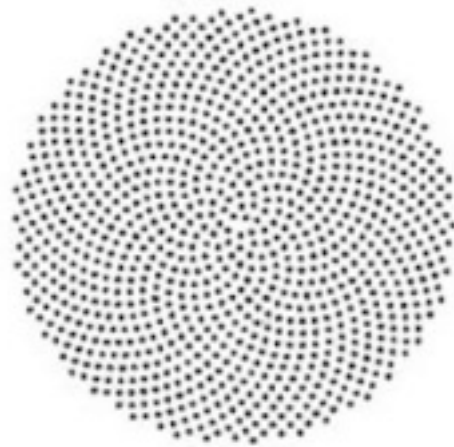
...

[Another] orientation... of the E_8 lattice (with respect to the Hopf fibrations) ... [is based on]... rotation ... with a 2×2 quaternionic matrix ... which acts on pairs of quaternions (points of R^8) ... for each E_8 shell, the points of the base are gathered into horizontal small spheres S^3 ... to generate ... [a]... four-dimensional quasicrystal ... Two characteristic features of the four-dimensional quasicrystal ... First, all shells which contain the same sub-set of points, modulo a scale change, have their radius in one-to-one correspondence with point coordinates on a Fibonacci chain.

Then,

if one takes into account all the shells ... the sequence formed by their square radius also forms a Fibonacci chain. ...”.

Eric A. Lord, Alan L. Mackay, and S. Ranganathan in their book “New Geometries for New Materials” (Cambridge 2006) said: “... in ... the Fibonacci spiral or golden spiral arrangement of points in a plane ... the first n points lie within a circle of radius n , for any n , ...



The Fibonacci spiral to $n = 1000$.

the uniformity of ... distribution ... of the arrangement of points in the Fibonacci spiral ... corresponds to a very efficient packing of identical subunits ... compared to the patterns produced by other angles ...

If ...[the angle]... is rational ... M/N , then the $(n+N)$ th point will lie on the same radius as the n th point ... the distribution ...[for]... π ...



The π spiral to $n = 10,000$. Figure from Navlov (2002)

correspond[s]... to the ... rational approximation $22/7$...”.

The last Hopf fibration is

$S^7 \rightarrow S^{15} \rightarrow S^8 = OP1 = Spin(9)/Spin(8) = \text{Projective Space of Octonions.}$

Each basis element of S^7 corresponds to one of the 7 independent E_8 lattices, each of which has substructure related to $S^3 \rightarrow S^7 \rightarrow S^4$ and to Fibonacci.

S^{15} lives in R^{16} , whose transformation group is $Spin(16)$ of the D_8 Lie Algebra from which E_8 is constructed by

$$\mathbf{248\text{-dim } E_8 = 120\text{-dim adjoint of } D_8 + 128\text{-dim half-spinor of } D_8}$$

D_8 comes from the bivector algebra of the $Cl(16)$ Clifford Algebra, and

due to the 8-periodicity of real Clifford Algebras whereby

$$Cl(8N) = Cl(8) \times \dots (N \text{ times tensor product}) \dots \times Cl(8)$$

$$\mathbf{Cl(16) = Cl(8) \times Cl(8)}$$

Clifford Algebras have dimension 2^N (dimension of N -dim HyperCubes) and the total dimensionality of their subalgebras (or subcubes) is 3^N .

N	2^N	3^N
0		1
1		2 3
2		4 = 2x2 9 = 3x3
3		8 27
4	16 = 4x4	81 = 9x9
5	32	243
6	64 = 8x8	729 = 27x27
7	128	2187
8	256 = 16x16	6561 = 81x81

Plato in his *Timaeus* used 2^N up to 2^8 and 3^N up to 3^5 to get musical intervals such as $256/243$.

AQFT:

Since the E8 classical Lagrangian is Local,
it is necessary to patch together Local Lagrangian Regions
to form a Global Structure describing
a Global E8 Algebraic Quantum Field Theory (AQFT).

Mathematically,
this is done by using Clifford Algebras
(others now using Clifford algebras in related ways include Carlos Castro and David Finkelstein)
to embed E8 into $Cl(16)$
and using a copy of $Cl(16)$ to represent each Local Lagrangian Region.
A Global Structure is then formed
by taking the tensor products of the copies of $Cl(16)$.
Due to Real Clifford Algebra 8-periodicity, $Cl(16) = Cl(8) \times Cl(8)$
and any Real Clifford Algebra, no matter how large,
can be embedded in a tensor product of factors of $Cl(8)$,
and therefore of $Cl(8) \times Cl(8) = Cl(16)$.
Just as the completion of the union of all tensor products
of 2×2 complex Clifford algebra matrices
produces the usual Hyperfinite III von Neumann factor
that describes
creation and annihilation operators on the fermionic Fock space over $C^{(2n)}$
(see John Baez's Week 175),
we can take the completion of the union
of all tensor products of $Cl(16) = Cl(8) \times Cl(8)$
to produce a generalized Hyperfinite III von Neumann factor
that gives a natural Algebraic Quantum Field Theory structure to E8 Physics.

EPR Entanglement:

For an E8 Physics model to be realistic,
it must be consistent with EPR entanglement relations.

Joy Christian in arXiv 0904.4259

“Disproofs of Bell, GHZ, and Hardy Type Theorems
and the Illusion of Entanglement”

said:

“... a [geometrically] correct local-realistic framework ...
provides exact, deterministic, and local underpinnings for
at least the Bell, GHZ-3, GHZ-4, and Hardy states.

...

The alleged non-localities of these states ...
result from misidentified [geometries] of the EPR elements of reality.

...

The correlations are ... the classical correlations
among the points of a 3 or 7-sphere

...

S^3 and S^7 ... are ... parallelizable

...

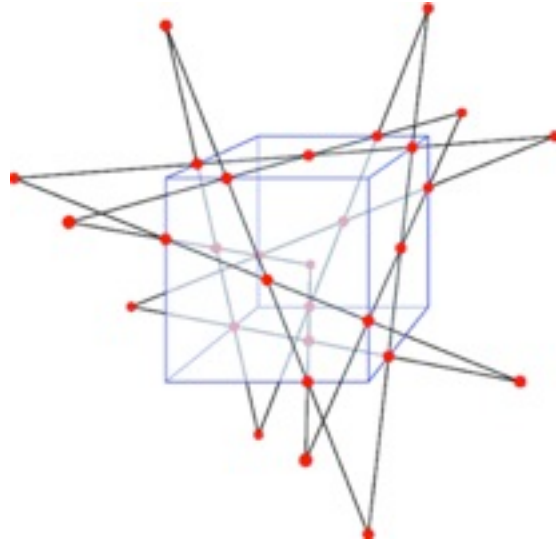
The correlations ... can be seen most transparently
in the elegant language of Clifford algebra ...”.

Since E8 Physics is based on the parallelizable Lie group E8
and related Clifford algebras,

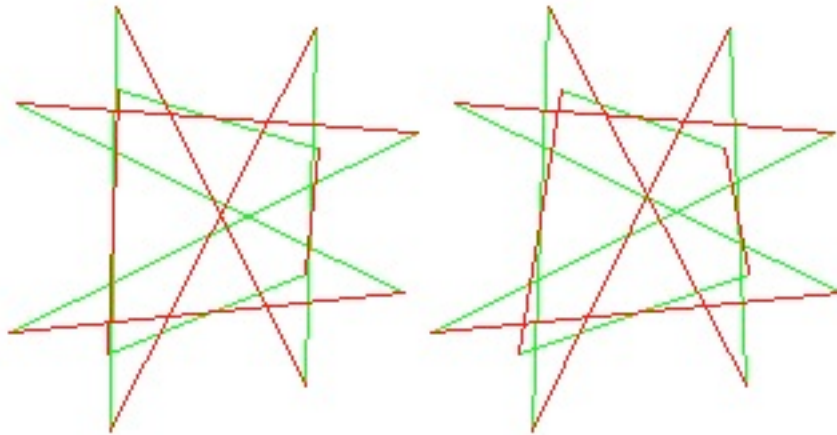
E8 Physics is probably consistent with EPR entanglement
even on the level of its classical Lagrangian structure.

Tetrahelix model of Fundamental Fermions

To use the TetraJJ Nucleus and its Tetrahelix structure to construct a realistic physics model of Fundamental Fermions, consider this Schläfli Double-6 diagram of the 12 Tetrahelices inside the 57 group:

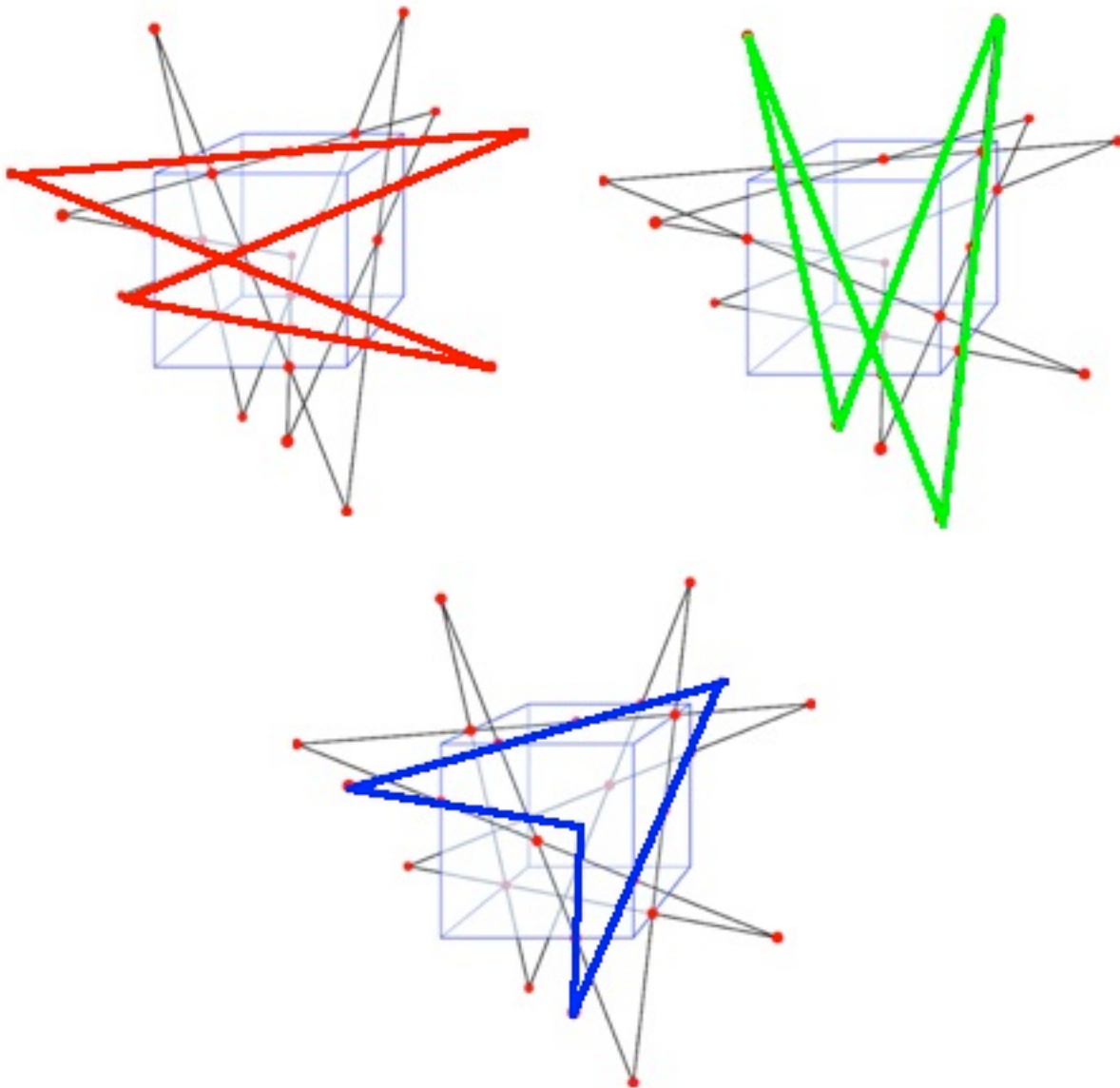


Crossings may be clearer in this stereo image



in which 6 of the Tetrahelix lines have been colored red to indicate their helicity being opposite to that of the 6 remaining as green.

There are three independent groups of 4 Tetrahelices, and I will color them Red, Green, and Blue, and call them by those colors:

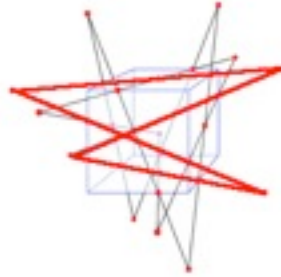


The 57-group Tetrahelices identify the fundamental fermions of physics (that is, electrons, positrons, neutrinos, and quarks) and which fermion any given Large Tetrahedron represents is determined by which of the Tetrahelix subsystems is activated.

For example, consider the fermion particles which are:
Electron, Red Up Quark, Green Up Quark, Blue Up Quark,
Neutrino, Red Down Quark, Green Down Quark, Blue Down Quark

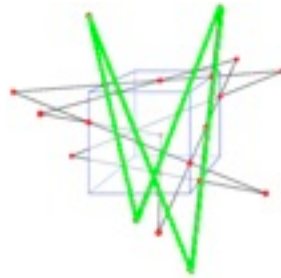
If none of the color groups of Tetrahelix are active, then the fermion is color neutral and almost massless, and is Neutrino with electric charge 0.

If only the Red Tetrahelix group is active,



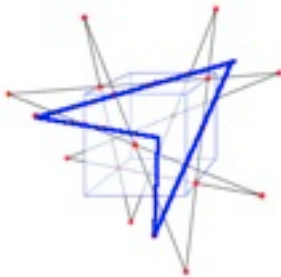
the the fermion is a Red Down Quark with electric charge $-1/3$

If only the Green Tetrahelix group is active,



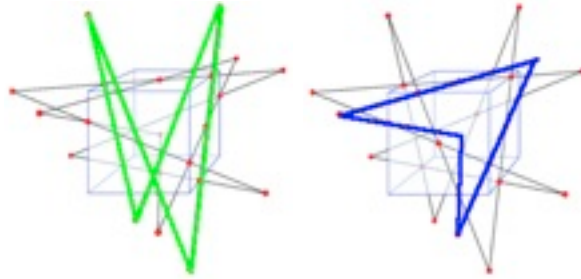
the the fermion is a Green Down Quark with electric charge $-1/3$

If only the Blue Tetrahelix group is active,



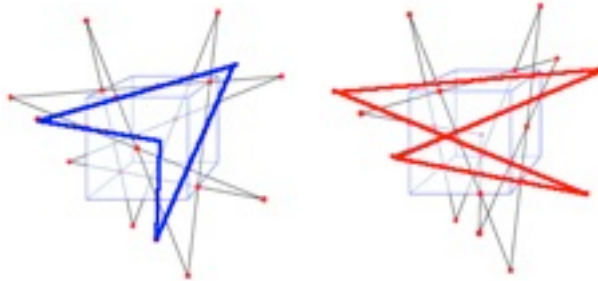
the the fermion is a Blue Down Quark with electric charge $-1/3$

If both the Green and Blue Tetrahelix groups are active,



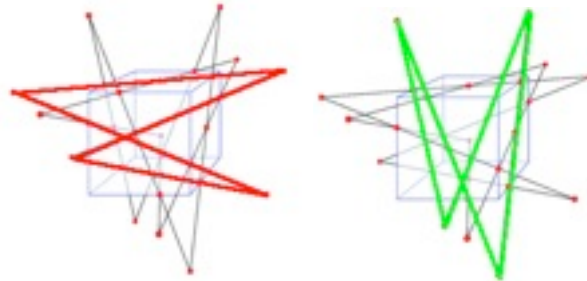
the the fermion is a Red Up Quark with electric charge $+2/3$
The sign changes because of the even number of active Tetrahelix groups,
and the Red color is because it is the complement of Green and Blue.

If both the Blue and Red Tetrahelix groups are active,



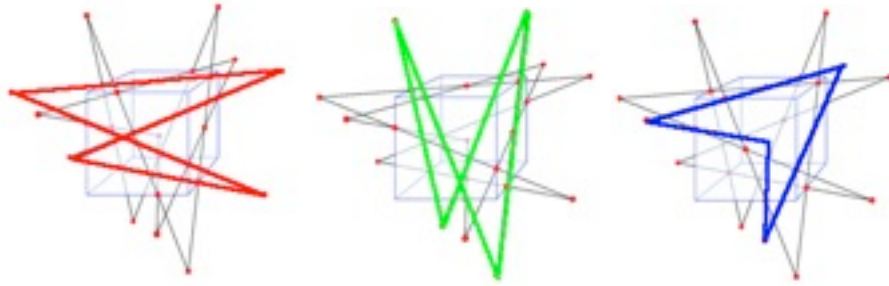
the the fermion is a Green Up Quark with electric charge $+2/3$
The sign changes because of the even number of active Tetrahelix groups,
and the Green color is because it is the complement of Blue and Red.

If both the Red and Green Tetrahelix groups are active,



the the fermion is a Blue Up Quark with electric charge $+2/3$
The sign changes because of the even number of active Tetrahelix groups,
and the Blue color is because it is the complement of Red and Green.

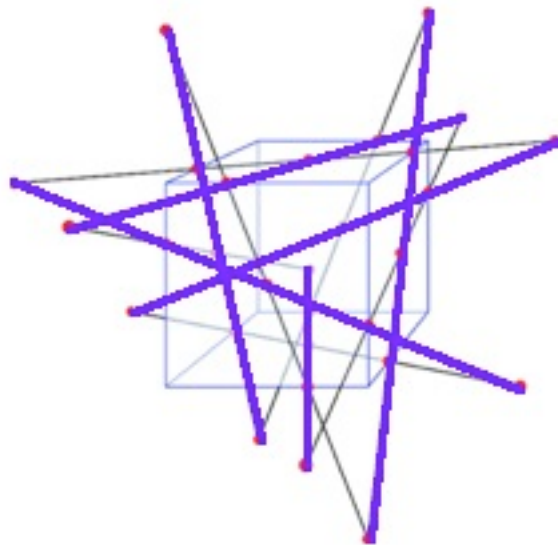
If all three color Tetrahelix groups are active,



then the fermion is also color neutral but has mass, and is Electron with electric charge $-1/3 + -1/3 + -1/3 = -1$

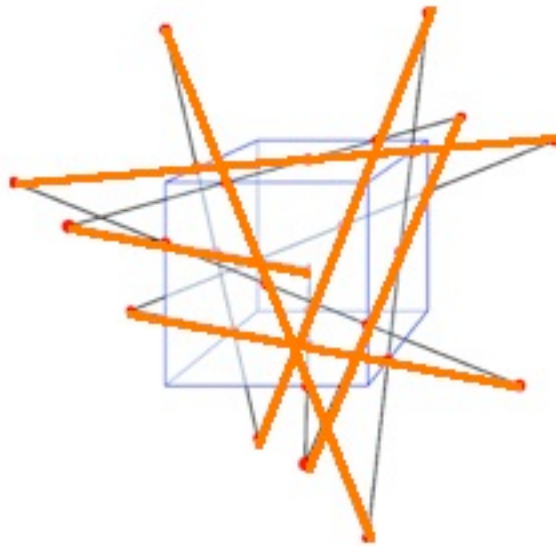
The above classifies all the types of fermions, but it remains to distinguish between particles and antiparticles.

In order to do that, recall that of the 12 Tetrahelix, there are 6 Clockwise and 6 Counter Clockwise, and each of the 3 color sets of 4 have 2 Clockwise and 2 Counter Clockwise, so let the Clockwise represent fermion particles and color them Purple



and

let the Counter Clockwise represent fermion antiparticles and color them Gold



Then, by requiring that any single Large Tetrahedron only activate either the Purple or the Gold sets of Tetrahelix, the Tetrahelix activation structure will determine its nature as a fundamental (first-generation) fermion in a way that is completely consistent with all known physics experimental results, except

that I did not give a way to tell a Neutrino from an AntiNeutrino because they would not have any active Tetrahelix of either helicity. The Neutrino / antiNeutrino helicity might be determined by looking at some residual overall helicity structure of the Large Tetrahedron not part of the Tetrahelix structure.

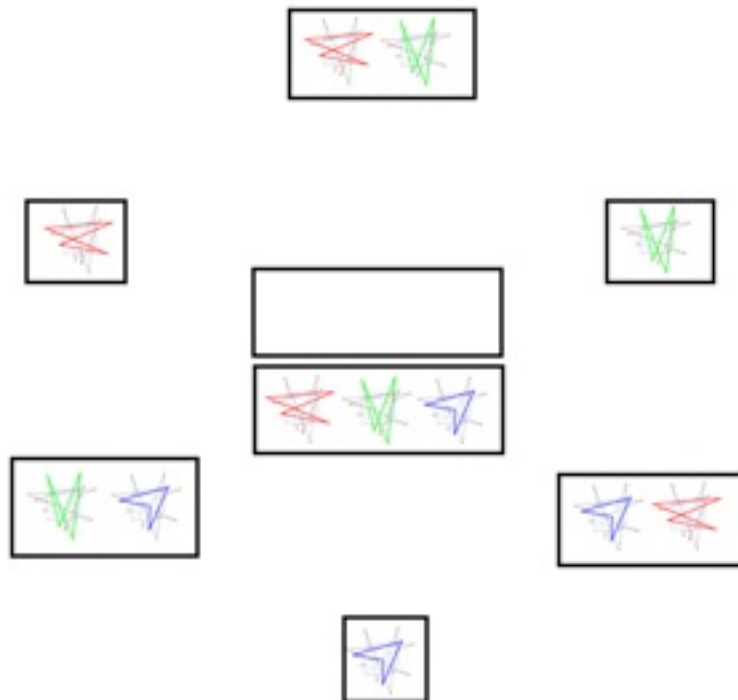
The second and third generation fermions can be built up from pairs or triples of Large Tetrahedra in a natural way.

Geometry of the Four Fundamental Forces

Gauge Bosons can be represented as AntiSymmetric Pairs of Fermion Nearest-Neighbors. The link between the Fermions of the Pair establishes a connection between Gauge Bosons and SpaceTime that enables Gauge Bosons to See, and to interact with, SpaceTime. The CP2 (complex projective 2-space) is a compact Internal Symmetry Space that carries information about the fermion particles that live in the spacetime and the forces that act in the spacetime, among the particles. CP2 is a 4-dim symmetric space that is built from 8-dim color force gauge group SU(3) by dividing out of it a 4-dim electroweak force U(2) so that $CP2 = SU(3) / U(2)$ which has $8-4 = 4$ -dim. Effectively, the CP2 globally has color SU(3) symmetry and locally (by a U(2) at each point of the SU(3)) electroweak U(2), which is often written as $U(2) = SU(2) \times U(1)$ where SU(2) is for the weak force and U(1) is for electromagnetism.

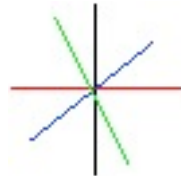
SU(3) gluons:

The 57-tetrahedron TetraJJ Tetrahelix description of the fermion particles can be arranged as:



which is the root vector diagram of the SU(3) Lie group. Since the root vector diagram contains all the information about SU(3), this shows that the 57-tetrahedron TetraJJ contains the SU(3) structure of CP2 which is $CP2 = SU(3) / U(2)$.

Since gluons can carry $\{+r,-r;+g,-g;+b,-b\}$ charge, a gluon can emit three pairs: $\{+r,-r\};\{+g,-g\};\{+b,-b\}$.

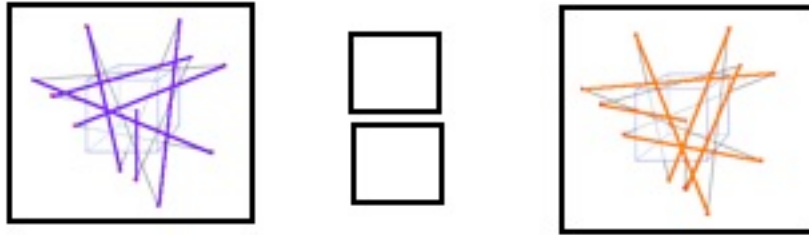


As a gluon can emit three pairs, it can enlarge its path of transitive action in CP2 Internal Symmetry Space to 4 dimensions, which is consistent with SU(3) global transitive action on 4-real-dimensional $CP2 = SU(3) / U(2)$. Therefore, gluon boundary conditions are the same all around the boundary.

The global nature of the color force SU(3) action on CP2 is related to the nature of a gluon as a link with both spacetime and color internal symmetry space characteristics, which requires gluon confinement within protons, pions, and other particles containing them.

U(2) = U(1)xSU(2) and U(1) Photons and SU(2) Weak Bosons:

The U(2) structure of CP2 = SU(3) / U(2) is also contained in the 57-tetrahedron TetraJJ because it has also the structure of:



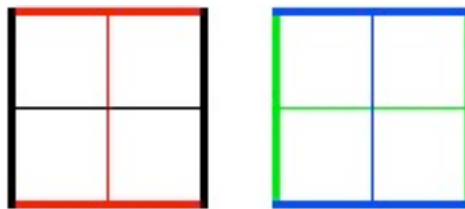
which is the root vector diagram of U(2). The two empty boxes correspond to the chargeless neutral gauge bosons (Weak Z and Photon) similar to the way that the empty box in the SU(3) diagram corresponds to the chargeless neutral Neutrino.

U(1) Photons:

Since all photons have no charge, a photon can only move along its path of transitive action in Internal Symmetry Space.



As a photon cannot emit another photon, it cannot enlarge its path of transitive action in Internal Symmetry Space beyond the 1 dimension of the path of transitive action in Internal Symmetry Space. Therefore, photon boundary conditions form a 4-torus, or four 1-spheres:



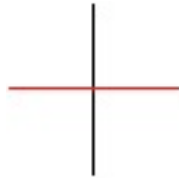
$$U(1) \rightarrow T^4$$

Since $CP^2 = SU(3) / U(2) = SU(3) / SU(2) \times U(1)$
 $U(1)$ has a natural action on a part of CP^2 Internal Symmetry Space.

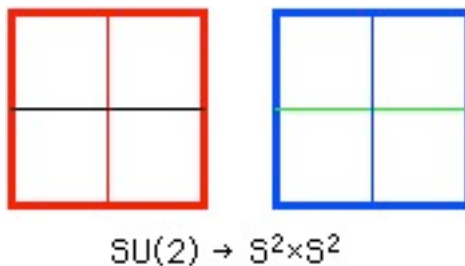
Three more copies of S^1 are necessary to get a 4-dimensional manifold
 $S^1 \times S^1 \times S^1 \times S^1 = T^4$.

SU(2) Weak Bosons:

Since weak bosons can carry $\{+1, -1\}$ charge, a weak boson can emit a $\{+1, -1\}$ pair.



As a weak boson can emit a pair, it can enlarge its path of transitive action in Internal Symmetry Space to 2 dimensions. Therefore, weak boson boundary conditions form two 2-spheres:



Since $CP^n = C^n \cup CP^{(n-1)}$ (where \cup = union, by putting a $CP^{(n-1)}$ at infinity),
 $CP^2 = C^2 \cup C^1 \cup C^0 = C^2 \cup CP^1 = C^2 \cup S^2$.

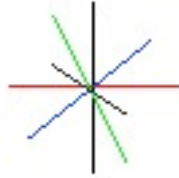
Therefore, CP^2 Internal Symmetry Space contains a 2-sphere S^2 on which $SU(2)$ can act globally, since $SU(2) / U(1) = S^2$.

A second copy of S^2 is necessary to get a 4-dimensional manifold $S^2 \times S^2$.

The mass factor for the weak force has a visualization (arising from e-mail discussion with Dick Andersen). Gauge bosons are visualized as going from a source through a medium to a target. The weak force mass factor is related to the Higgs mechanism. The Higgs scalar field absorbs some of the weak bosons as they go through the medium, thus weakening the weak force and producing the weaker effective weak force that is observed by experiments.

Gravity and gravitons:

Since gravitons can carry $\{+1,-1\};\{+r,-r\};\{+g,-g\};\{+b,-b\}$ charge, a graviton can emit four pairs: $\{+1,-1\};\{+r,-r\};\{+g,-g\};\{+b,-b\}$.



As a graviton can emit at four pairs, its path of transitive action is 4 dimensional. Therefore, graviton boundary conditions are the same all around the boundary. Spin(5), a compact Lie group corresponding to the Spin(2,3) subgroup of Conformal Spin(2,4), acts globally on a compact space of constant curvature, a 4-sphere = $S^4 = \text{Spin}(5) / \text{Spin}(4)$, the Euclidean version of 4-dimensional physical Spacetime (the non-compact Minkowski version on which Spin(2,3) acts being $\text{RP}^1 \times S^3$).

Unlike the other 3 forces that act transitively on the coassociative Internal Symmetry Space, gravity comes from the U(4) subgroup of Spin(8) and therefore acts transitively on the associative physical spacetime.

By the emission of four pairs, a graviton can describe the structure of a 4-dimensional spacetime.



A 4-pair graviton emission is effectively creation of a virtual 1-vertex spacetime Planck mass black hole.

The $(1/M_{\text{Planck}}^2)$ mass factor for gravity has a visualization (arising from e-mail discussion with Dick Andersen). Gauge bosons are visualized as going from a source through a medium to a target. The graviton by itself is long-range and massless, but virtual Planck-mass black holes in spacetime absorb some of the gravitons as they go through the spacetime medium, thus weakening the gravitational force and producing the weaker effective gravitational force that is observed by experiments.

There are two forms of gravity:

1 - gravity directly related to the distribution of matter (call it Einstein gravity) which comes from the Conformal Group and a generalized MacDowell-Mansouri process.

2 - a gravity-like thing related to the Bohm quantum potential (call it Bohm-world-line gravity which comes from interactions among world-lines of particles instead of just particles themselves. Each world-line contains the past and future histories of each particle, so Bohm-world-line gravity involves choosing among possible futures, etc. Since each world-line looks like a string in 4-dim spacetime, Bohm-world-line gravity can be described in terms of Bosonic String Theory. The result is something that acts like gravity but lives in the world of possibilities of the Many-Worlds, and is just what Penrose and Hameroff need to describe the superposition-separation gravity that they use in their models of quantum consciousness. Penrose-Hameroff superposition-separation is described at <http://www.quantumconsciousness.org/penrose-hameroff/consciousevents.html>

A way that the Bohm potential is seen to convert kinetic energy of moving mass in our "matter" universe into potential energy (Bohm potential) in the quantum Many-Worlds is described in a paper that I put on what is now the Cornell arXiv before I got blacklisted, at <http://arxiv.org/abs/quant-ph/9806023>

3-dim Diamond Lattice space

E8 Physics spacetime at high energies has E8 lattice structure which decomposes at lower energies to $M4 \times CP2$ (4+4)-dim Kaluza-Klein with 4-dim Minkowski spacetime which in turn contains 3-dim physical space.

3-dim space has 3-dim Diamond packing/lattice structure which is the same basic vacuum space structure as the Diamond network open packing of Pearce Clusters



with the Geometrical Symmetry of the TetraJJ Nucleus.

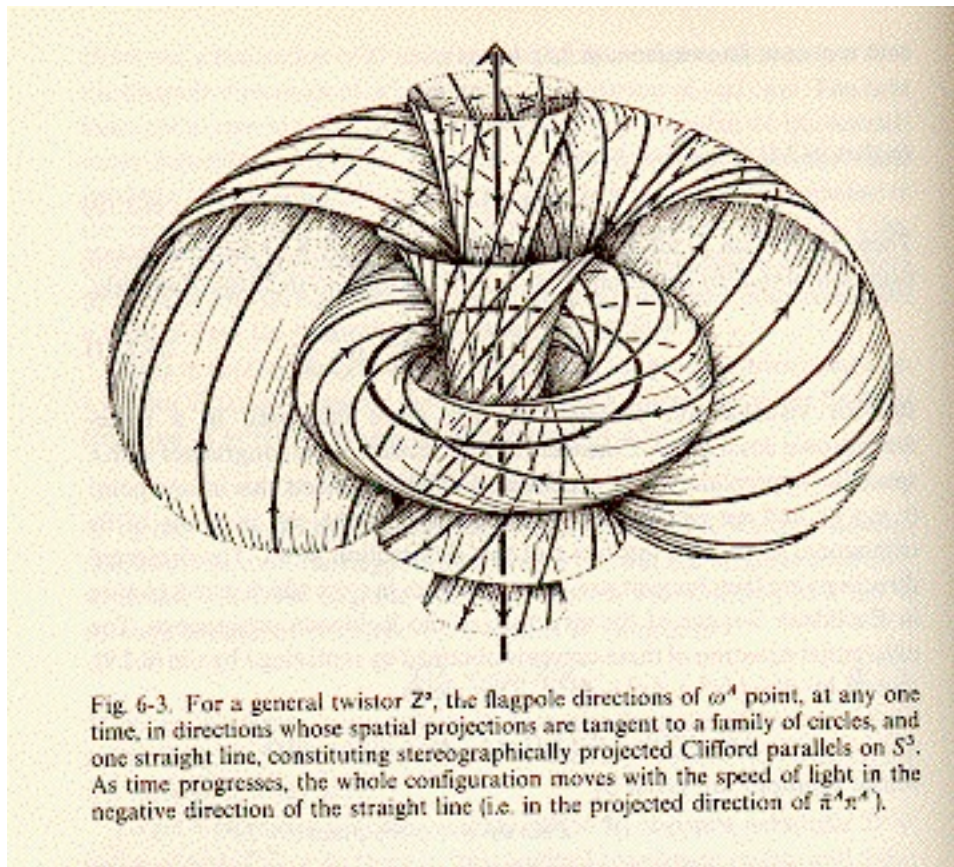
Gravity comes from Conformal Group symmetries of the $M4$.

E8 Physics (like the physics model of Matti Pitkanen) is based on 8-dimensional Kaluza-Klein models with spacetime = $M4 \times CP2$ where:

$M4$ is 4-dimensional Minkowski physical spacetime

$CP2$ is 4-dimensional complex projective plane internal symmetry space.

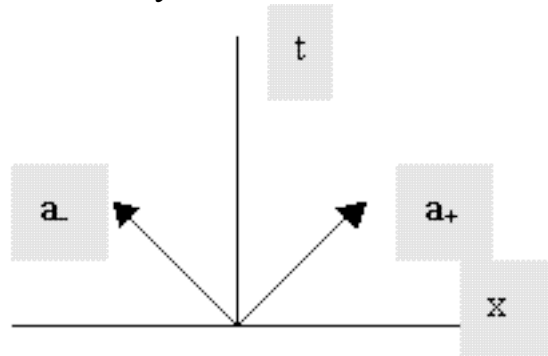
The 3-dim space of compactified M4 is a 3-sphere with Hopf fibration related to Penrose twistors



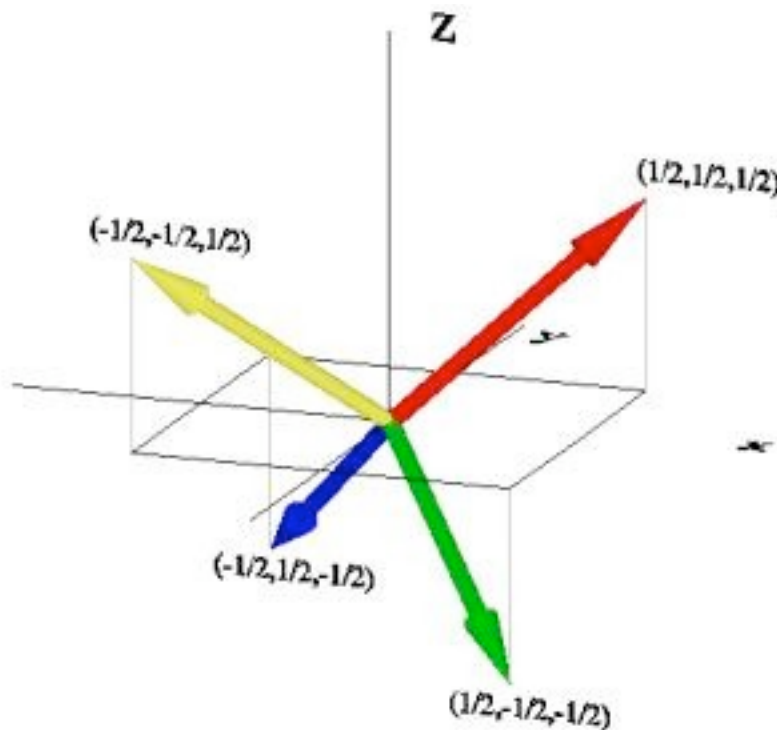
The 3-dimensional space of the 3-sphere and the Diamond Lattice packing is a subspace of a 4-dimensional SpaceTime HyperDiamond Lattice with Feynman Checkerboard Physics, and also of a 8-dimensional SpaceTime E8 Lattices.

4-dim Feynman Checkerboard SpaceTime:

The HyperDiamond Feynman Checkerboard in 1+3 dimensions reproduces the correct Dirac equation. Urs Schreiber has done the work necessary for the proof, after reading the work of George Raetz presented on his web site. A very nice feature of the George Raetz web site is its illustrations, which include an image of a vertex of a 1+1 dimensional Feynman Checkerboard

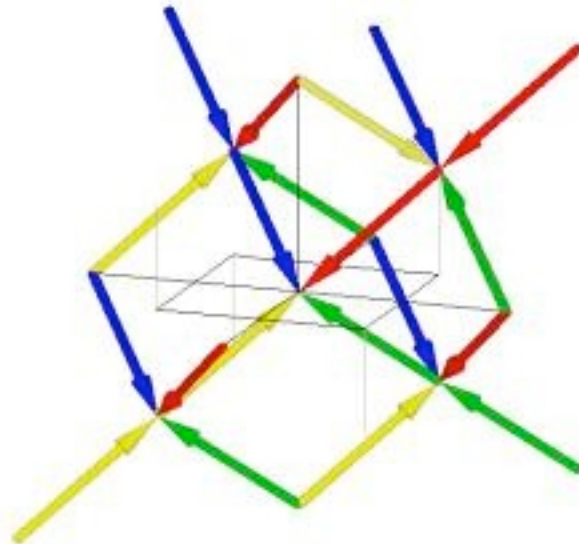


and an image of a projection into three dimensions of a vertex of a 1+3 dimensional Feynman Checkerboard



and

an image of flow contributions to a vertex in a HyperDiamond Random Walk from the four nearest neighbors in its past



Urs Schreiber wrote on the subject: Re: Physically understanding the Dirac equation and 4D in the newsgroup sci.physics.research on 2002-04-03 19:44:31 PST (including an appended forwarded copy of an earlier post) and again on 2002-04-10 19:03:09 PST as found on the web page <http://www-stud.uni-essen.de/~sb0264/spinors-Dirac-checkerboard.html> and the following are excerpts from those posts:

"... I know ... <http://www.innerx.net/personal/tsmith/FynCkb.html> ... and the corresponding lanl paper ...[<http://xxx.lanl.gov/abs/quant-ph/9503015>]... and I know that Tony Smith does give a generalization of Feynman's summing prescription from 1+1 to 1+3 dimensions.

But I have to say that I fail to see that this generalization reproduces the Dirac propagator in 1+3 dimensions, and that I did not find any proof that it does. Actually, I seem to have convinced myself that it does not, but I may of course be quite wrong. I therefore take this opportunity to state my understanding of these matters.

First, I very briefly summarize (my understanding of) Tony Smith's construction: The starting point is the observation that the left $|-\rangle$ and right $|+\rangle$ going states of the 1+1 dim checkerboard model can be labeled by complex numbers

$$|-\rangle \text{ ---} \rightarrow (1 + i)$$

$$|+\rangle \text{ ---} \rightarrow (1 - i)$$

(up to a factor) so that multiplication by the negative imaginary unit swaps components:

$$(-i)(1+i)/2 = (1-i)/2$$

$$(-i)(1-i)/2 = (1+i)/2 .$$

Since the path-sum of the 1+1 dim model reads

$\phi = \text{sum over all possible paths of } (-i \text{ eps } m)^{\text{(number of bends of path)}} = \text{sum over all possible paths of product over all steps of one path of } -i \text{ eps } m \text{ (if change of direction after this step generated by } i) \text{ } 1 \text{ (otherwise)}$

this makes it look very natural to identify the imaginary unit appearing in the sum over paths with the "generator" of kinks in the path. To generalize this to higher dimensions, more square roots of -1 are added, which gives the quaternion algebra in 1+3 dimensions. The two states $|+\rangle$ and $|-\rangle$ from above, which were identified with complex numbers, are now generalized to four states identified with the following quaternions (which can be identified with vectors in M^4 indicating the direction in which a given path is heading at one instant of time):

$$(1 + i + j + k)$$

$$(1 + i - j - k)$$

$$(1 - i + j - k)$$

$$(1 - i - j + k) ,$$

which again constitute a (minimal) left ideal of the algebra (meaning that applying $i, j,$ or k from the left on any linear combination of these four states gives another linear combination of these four states). Hence, now i, j, k are considered as "generators" of kinks in three spatial dimensions and the above summing prescription naturally generalizes to

$\phi = \text{sum over all possible paths of product over all steps of one path of}$
 $-i \text{ eps } m \text{ (if change of direction after this step generated by } i)$
 $-j \text{ eps } m \text{ (if change of direction after this step generated by } j)$
 $-k \text{ eps } m \text{ (if change of direction after this step generated by } k)$
 1 (otherwise)

The physical amplitude is taken to be

$$A * e^{(i \text{ alpha})}$$

where A is the norm of ϕ and α the angle it makes with the x_0 axis.

As I said, this is merely my paraphrase of Tony Smith's proposal as I understand it.

I fully appreciate that the above construction is a nice (very "natural") generalization of the summing prescription of the 1+1 dim checkerboard model.

But if it is to describe real fermions propagating in physical spacetime, this generalized path-sum has to reproduce the propagator obtained from the Dirac equation in 1+3 dimensions, which we know to correctly describe these fermions. Does it do that?

...

Hence I have taken a look at the material [that] ... George Raetz ... present[s] ... titled "The HyperDiamond Random Walk", found at <http://www.pcisys.net/>

~bestwork.1/QRW/the_flow_quaternions.htm , which is mostly new to me.... I am posting this in order to make a suggestion for a more radical modification ... [The]... equation ... $DQ = (iE)Q$... is not covariant. That is because of that quaternion E sitting on the left of the spinor Q in the rhs of [the] equation The Dirac operator D is covariant, but the unit quaternion E on the rhs refers to a specific frame. Under a Lorentz transformation L one finds

$$L DQ = iE LQ = L E' Q \iff DQ = E'Q$$

now with $E' = L^{-1} E L$ instead of E .

This problem disappears when the unit quaternion E is brought to the *right* of the spinor Q .

What we would want is an equation of the form $DQ = Q(iE)$.

In fact, demanding that the spinor Q be an element of the minimal left ideal generated by the primitive projector $P = (1+y_0)(1+E)/4$,

so that $Q = Q' P$,

one sees that $DQ = Q(iE)$ almost looks like the the *Dirac-Lanczos equation*.

(See hep-ph/0112317, equation (5) or ... equation (9.36) [of]... W. Baylis, Clifford (Geometric) Algebras, Birkhaeuser (1996) ...).

To be equivalent to the Dirac-Lanczos equation, and hence to be correct, we need to require that $D = y_0 @0 + y_1 @1 + y_2 @2 + y_3 @3$

instead of ... = $@0 + e_1 @1 + e_2 @2 + e_3 @3$.

All this amounts to sorting out in which particular representation we are actually working here.

In an attempt to address these issues, I now redo the steps presented on http://www.pcisys.net/~bestwork.1/QRW/the_flow_quaternions.htm with some suitable modifications to arrive at the correct Dirac-Lanczos equation (this is supposed to be a suggestion subjected to discussion):

So consider a lattice in Minkowski space generated by a unit cell spanned by the four (Clifford) vectors

$$r = (y_0 + y_1 + y_2 + y_3)/2$$

$$g = (y_0 + y_1 - y_2 - y_3)/2$$

$$b = (y_0 - y_1 + y_2 - y_3)/2$$

$$y = (y_0 - y_1 - y_2 + y_3)/2 .$$

(y_i are the generators of the Dirac algebra $\{y_i, y_j\} = \text{diag}(+1, -1, -1, -1)_{ij}$.)

This is Tony Smith's "hyper diamond".

(Note that I use Clifford vectors instead of quaternions.)

Now consider a "Clifford algebra-weighted" random walk along the edges of this lattice,

which is described by four Clifford valued "amplitudes": K_r, K_g, K_b, K_y and

such that

$$@_r K_r = k (K_g y_2 y_3 + K_b y_3 y_1 + K_y y_1 y_2)$$

$$@_b K_b = k (K_y y_2 y_3 + K_r y_3 y_1 + K_g y_1 y_2)$$

$$@_g K_g = k (K_r y_2 y_3 + K_y y_3 y_1 + K_b y_1 y_2)$$

$$@_y K_y = k (K_b y_2 y_3 + K_g y_3 y_1 + K_r y_1 y_2) .$$

(This is geometrically motivated. The generators on the rhs are those that rotate the unit vectors corresponding to the amplitudes into each other. "k" is some constant.) Note that I multiply the amplitudes from the *right* by the generators of rotation, instead of multiplying them from the left.

Next, assume that this coupled system of differential equations is solved by a spinor Q

$$Q = Q' (1+y_0)(1+iE)/4$$

$$E = (y_2 y_3 + y_3 y_1 + y_1 y_2)/\text{sqrt}(3)$$

with

$$K_r = r Q$$

$$K_g = g Q$$

$$K_b = b Q$$

$$K_y = y Q .$$

This ansatz for solving the above system by means of a single spinor Q is, as I understand it, the central idea.

But note that I have here modified it on the technical side:

Q is explicitly an algebraic Clifford spinor in a definite minimal left ideal,

E squares to -1, not to +1,

and the K_i are obtained from Q by premultiplying with the Clifford basis vectors defined above.

Substituting this ansatz into the above coupled system of differential equations one can form one covariant expression by summing up all four equations:

$$(r @_r + g @_g + b @_b + y @_y) Q = k \text{sqrt}(3) Q E$$

The left hand side is immediate.

To see that the right hand side comes out as indicated simply note that $r + g + b + y = y_0$ and that $Q y_0 = Q$ by construction.

The above equation is the Dirac-Lanzos-Hestenes-Guersey equation, the algebraic version of the equation describing the free relativistic electron.

The left hand side is the flat Dirac operator

$$r \partial_r + g \partial_g + b \partial_b + y \partial_y = \gamma_m \partial_m$$

and

the right hand side, with $k = mc / (\hbar \sqrt{3})$,

is equal to the mass term $i mc / \hbar Q$.

As usual, there are a multitude of ways to rewrite this.

If one wants to emphasize biquaternions then

premultiplying everything with y_0 and

splitting off the projector P on the right of Q to express everything in terms of the,

then also biquaternionic, Q' (compare the definitions given above)

gives Lanczos' version (also used by Baylis and others).

I think this presentation improves a little on that given on George Raetz's web site:

The factor E on the right hand side of the equation is no longer a nuisance but a necessity.

Everything is manifestly covariant (if one recalls that algebraic spinors are manifestly covariant when nothing non-covariant stands on their *left* side).

The role of the quaternionic structure is clarified,

the construction itself does not depend on it.

Also, it is obvious how to generalize to arbitrary dimensions.

In fact, one may easily check that for 1+1 dimensions the above scheme reproduces the Feynman model.

While I enjoy this, there is still some scepticism in order

as long as a central question remains to be clarified:

How much of the Ansatz $K(r,g,b,y) = (r,g,b,y) Q$ is wishful thinking?

For sure,

every Q that solves the system of coupled differential equations that describe the amplitude of the random walk on the hyper diamond lattice

also solves the Dirac equation.

But what about the other way round?

Does every Q that solves the Dirac equation also describe such a random walk. ...".

My proposal to answer the question raised by Urs Schreiber

Does every solution of the Dirac equation also describe a HyperDiamond Feynman Checkerboard random walk?
uses symmetry.

The hyperdiamond random walk transformations include the transformations of the Conformal Group:

- rotations and boosts (to the accuracy of lattice spacing);
- translations (to the accuracy of lattice spacing);
- scale dilatations (to the accuracy of lattice spacing): and
- special conformal transformations (to the accuracy of lattice spacing).

Therefore, to the accuracy of lattice spacing, the hyperdiamond random walks give you all the conformal group Dirac solutions, and since the full symmetry group of the Dirac equation is the conformal group, the answer to the question is "Yes".

Thanks to the work of Urs Schreiber:

The HyperDiamond Feynman Checkerboard in 1+3 dimensions does reproduce the correct Dirac equation.

Here are some references to the conformal symmetry of the Dirac equation: R. S. Krausshar and John Ryan in their paper Some Conformally Flat Spin Manifolds, Dirac Operators and Automorphic Forms at math.AP/022086 say:

"... In this paper we study Clifford and harmonic analysis on some conformal flat spin manifolds. ... manifolds treated here include R^p and $S^1 \times S^{(n-1)}$. Special kinds of Clifford-analytic automorphic forms associated to the different choices of are used to construct Cauchy kernels, Cauchy Integral formulas, Green's kernels and formulas together with Hardy spaces and Plemelj projection operators for L_p spaces of hypersurfaces lying in these manifolds. ... Solutions to the Dirac equation are called Clifford holomorphic functions or monogenic functions. Such functions are covariant under ... conformal or ... Mobius transformations acting over $R^n \cup \{\infty\}$".

Barut and Raczka, in their book *Theory of Group Representations and Applications* (World 1986), say, in section 21.3.E, at pages 616-617:

"... E. The Dynamical Group Interpretation of Wave Equations.

... Example 1. Let $G = O(4,2)$.

Take U to be the 4-dimensional non-unitary representation in which the generators of G are given in terms of the 16 elements of the algebra of Dirac matrices as in exercise 13.6.4.1.

Because $(1/2)L_5 = \gamma_0$ has eigenvalues $n = \pm 1$,

taking the simplest mass relation $mn = K$, we can write

$(m\gamma_0 - K)\Psi(\dot{p}) = 0$, where K is a fixed constant.

Transforming this equation with the Lorentz transformation of parameter E

$\Psi(p) = \exp(i E N) \Psi(\dot{p})$

$N = (1/2) \gamma_0 \gamma_5$

gives

$(\gamma^u p_u - K) \Psi(p) = 0$

which is the Dirac equation ...".

P. A. M. Dirac, in his paper *Wave Equations in Conformal Space*, *Ann. Math.* 37 (1936) 429-442, reprinted in *The Collected Works of P. A. M. Dirac: Volume 1: 1924-1948*, by P. A. M. Dirac (author), Richard Henry Dalitz (editor), Cambridge University Press (1995), at pages 823-836, said:

"... by passing to a four-dimensional conformal space ...

a ... greater symmetry of ... equations of physics ... is shown up, and their invariance under a wider group is demonstrated. ...

The spin wave equation ... seems to be the only simple conformally invariant wave equation involving the spin matrices. ...

This equation is equivalent to the usual wave equation for the electron, except ... [that it is multiplied by] ... the factor $(1 + \alpha_5)$,

which introduces a degeneracy. ...".

8-dim E8 SpaceTime:

In my E8 physics model, for each point of 8-dimensional spacetime physics in the neighborhood of that point is described by E8, which is easily seen to be embedded in the real Clifford algebra $Cl(16)$ which is the tensor product $Cl(8) \times Cl(8)$ of two copies of the real Clifford algebra $Cl(8)$.

By the periodicity of real Clifford algebras,
the tensor product $Cl(16) \times \dots(N \text{ times})\dots \times Cl(16) = Cl(16N)$
so that any real Clifford algebra $Cl(M)$ can, no matter how large is M ,
be embedded in a larger $Cl(16N)$ for some N
and therefore can be represented as
a tensor product $Cl(16) \times \dots(N \text{ times})\dots \times Cl(16)$
and
since E8 is contained in each $Cl(16)$
can be represented as
a tensor product of N copies of E8.

A full Algebraic Quantum Field Theory (AQFT) can be constructed by considering E8 as representing a classical Lagrangian constructed naturally using parts of E8 to represent spacetime, gauge bosons, and fundamental fermion particles and antiparticles.

A full non-local AQFT results from the completion of the union of all such tensor products of E8 and its Lagrangian,
a generalized version of a von Neumann hyperfinite III₁ factor.

The E_7 -group contains the same physics information as E8. Here is how:
fundamental fermion particles - 8 from Tetrahelix structure (see page 23)
fundamental fermion antiparticles - 8 of opposite helicity from particles
Standard Model gauge bosons - from 28 antisymmetric article-antiparticle pairs
of fermions
spacetime - from extending 3-dimensional Diamond space lattice/packing
to 4-dimensional HyperDiamond Feynman Checkerboard lattice
then
adding 4 more HyperDiamond dimensions (corresponding
to internal symmetry space)
to get E8 lattice 8-dimensional spacetime of my E8 physics model
gravity - from 28 generators of rotations/reflections of 8-dimensional spacetime.

Note that with 8-dimensional spacetime each of the 8+8 fundamental fermions has 8 covariant components.

Note also that 8-dimensional spacetime by itself has Octonion structure, and each of the 4-dimensional subspaces (Minkowski spacetime plus Batakis internal symmetry space) has Quaternion structure and the Real-Imaginary distinction between the two 4-dimensional has Complex structure

so all of those together are characterised by $8 \times 4 \times 2 = 64$ dimensions which is the $CxQxO$ (complex x quaternion x octonion) space used by Dixon.

Therefore,

the physical content of each 57-group has

$8 \times 8 = 64$ fermion particle dimensions

$8 \times 8 = 64$ fermion antiparticle dimensions

28 Standard Model gauge group dimensions

64 dimensions to characterize spacetime structures

28 gravity dimensions

for a total of $64+64 + 28+64+28 = 128 + 120 = 248$, the same as E8.

Therefore,

the 57-group physics model has the same information content as E8 physics and

The fundamental physics Algebraic Quantum Field Theory can be constructed, equivalently,

from tensor products of $Cl(16)$

from tensor products of E8 in $Cl(16)$

from tensor products of 57-groups (each having same information as each E8).

Let + denote either $Cl(16)$ or E8 or a 57-group, as they give the same physics.

Begin by considering the Clifford tensor product as a linear chain of +'s.

Consider each + in the linear chain as a node in a linear pregeometry.

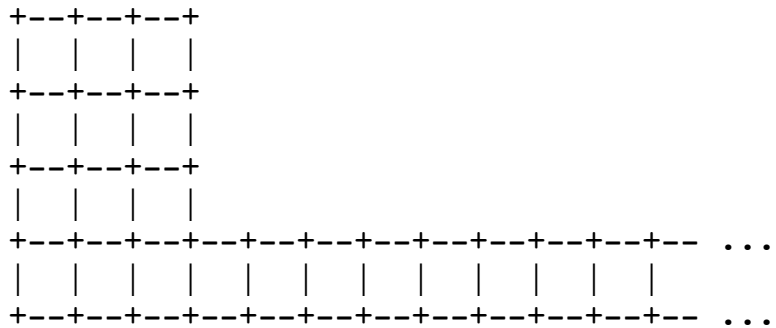
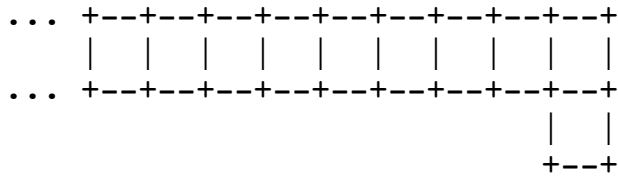
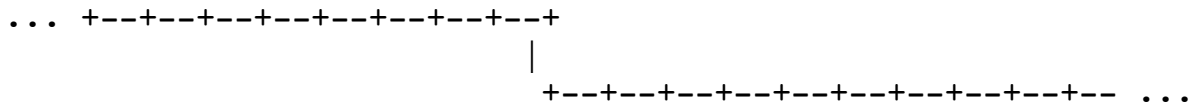
Let the linear pregeometry, like a long line of yarn, "fold" or "weave" it into a higher-dimensional "array" or "tapestry" of Cl's.

Prior to the folding/weaving, each C+node in the linear pregeometry would have 2 nearest neighbors in the chain

... +--+--+--+--+--+--+ ...

that corresponds to the 1-dim lattice of Natural Numbers.

After formation of natural nearest-neighbor-connections among the folded/woven pregeometry nodes, then you might get:



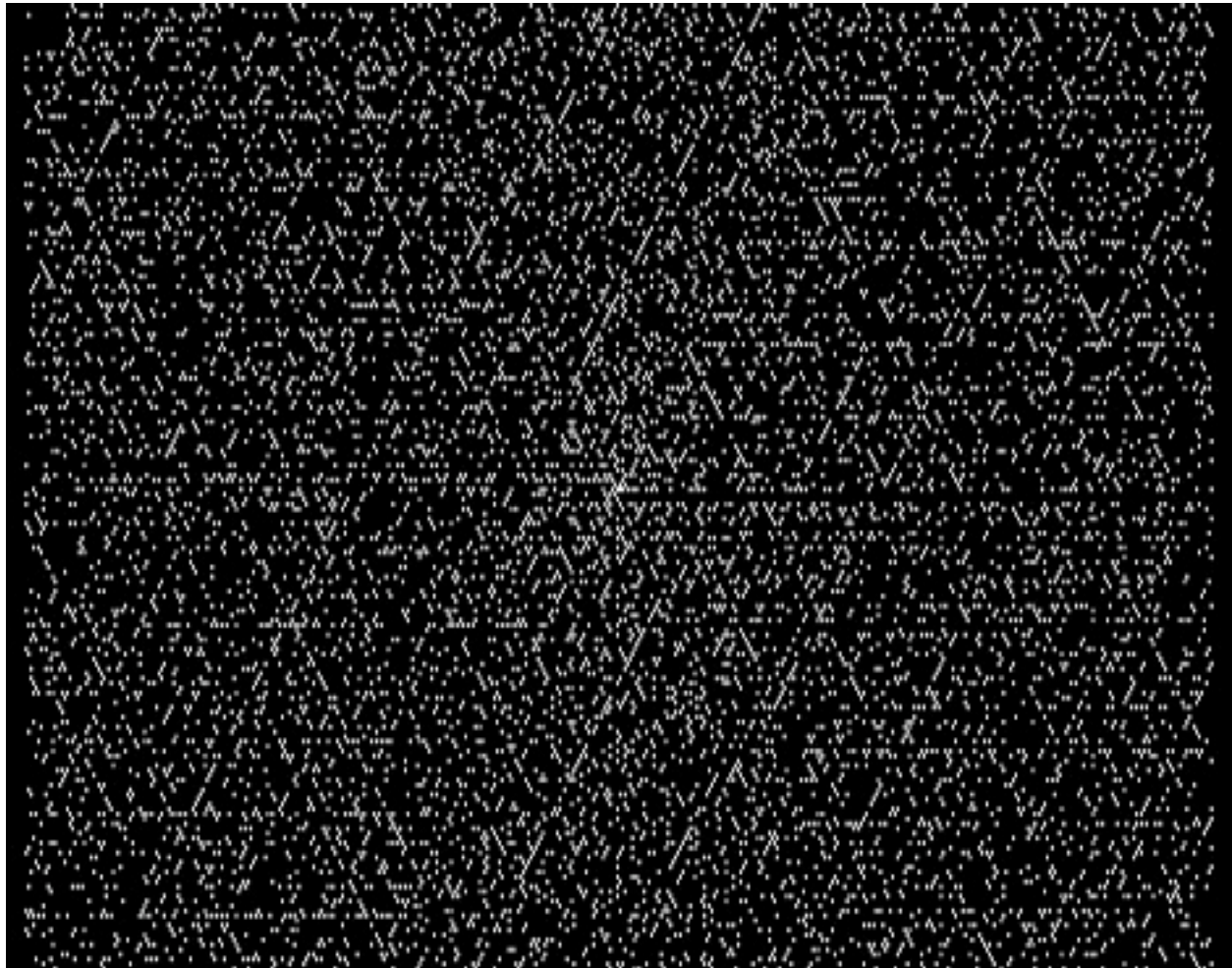
If you continue that pattern of folding/weaving indefinitely in a natural way, you might end up with a 2-dim square lattice that could be taken to be a Feynman Checkerboard in 1+1 = dimensions.

It is interesting that the 2-dimensional weave structure looks a lot like a Ulam spiral. According to an Abarim web page: "... Stanislaw Ulam was attending some boring meeting, and to divert himself somewhat he began to scribble on a piece of paper. ... He put down the number 1 as the bright shining center of a universe of numbers that Big Banged outwardly in a spiral ... Much to his amazement the prime numbers appeared to gravitate towards diagonal lines emanating from the central 1. ...

73	74	75	76	77	78	79	80	81
72	43	44	45	46	47	48	49	50
71	42	21	22	23	24	25	26	51
70	41	20	7	8	9	10	27	52
69	40	19	6	2	11	28	53	
68	39	18	5	4	3	12	29	54
67	38	17	16	15	14	13	30	55
66	37	36	35	34	33	32	31	56
65	64	63	62	61	60	59	58	57

Most of them sat on or in the vicinity of a diagonal, but some obviously didn't. ...".

According to a Pime Number Spiral web page: "... Consider a rectangular grid. We start with the central point and arrange the positive integers in a spiral fashion (anticlockwise) as at right. The prime numbers are then marked ... There is a tendency for the prime numbers to form diagonal lines. This can be seen more clearly in the image below,



which shows a window onto a square array of 640 x 640 numbers, with the primes marked by white pixels. ...".

According to a M. Watkins web page: "... There is currently no explanation for the distinct diagonal lines which appear when the primes are marked out along a particular 'square spiral' path. ...".

Physically, if the 2-dim weave corresponds to 2-dim spacetime, the diagonal lines would correspond to light-cone correlations of points of spacetime.

In dimensions greater than 2, the weaving should produce something like a Moore space-filling curve. According to a web page of V. B. Balayoghan: "... The Hilbert and Moore curves use square cells -- the level n curve has 4^n cells (and hence $4^n - 1$ lines). The Moore curve has the same recursive structure as the Hilbert curve, but ends one cell away from where it started. The Hilbert curve starts and ends at opposite ends of a side of the unit square. ...".

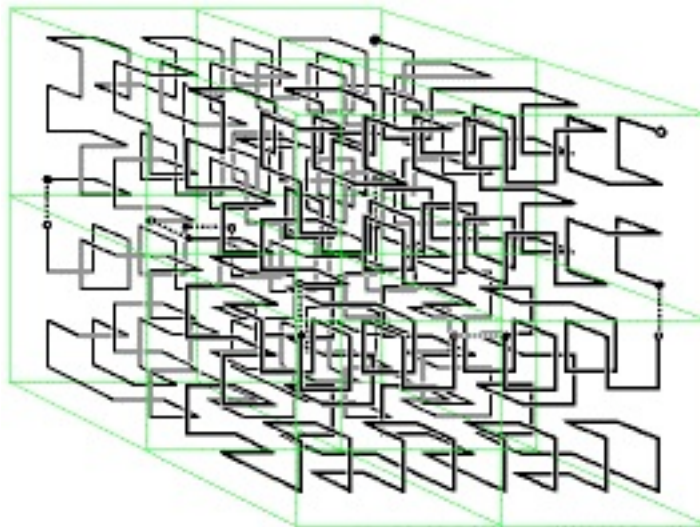
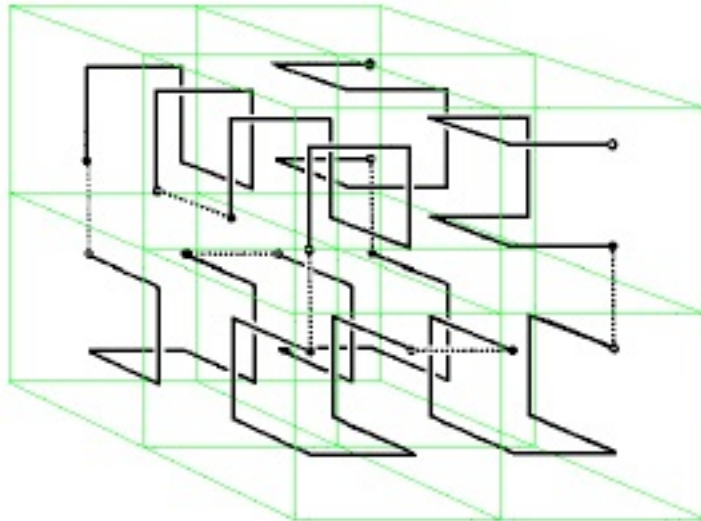
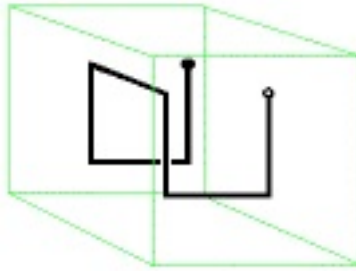
According to a web page by William Gilbert:

"... We exhibit a direct generalization of Hilbert's curve that fills a cube. The first three iterates of this curve are shown. ... In constructing one iterate from the previous one, note that the direction of the curve determines the orientation of the smaller cubes inside the larger one.

The initial stage of this three dimensional curve can be considered as coming from the 3-bit reflected Gray code which traverses the 3-digit binary strings in such a way that each string differs from its predecessor in a single position by the addition or subtraction of 1. The k th iterate could be considered a generalized Gray code on the Cartesian product set $\{0,1,2,\dots,2^{k-1}\}^3$.

The n -bit reflected binary Gray code will describe a path on the edges of an n -dimensional cube that can be used as the initial stage of a Hilbert curve that will fill an n -dimensional cube. ...

[If you look at a 2-dimensional slice of the n -dimensional Moore curve including the time axis and one spatial axis, you see something like a Ulam Spiral and also like a 2-dimensional Feynman checkerboard.] ...



...»

The E8 lattice, or 8-dimensional HyperDiamond lattice, is made up of one hypercubic checkerboard D8 lattice plus another D8 shifted by a glue vector

$(1/2, 1/2, 1/2, 1/2, 1/2, 1/2, 1/2, 1/2)$.

Conway and Sloane, in their book Sphere Packings, Lattices, and Groups (3rd edition, Springer, 1999), in chapter 4, section 7.3, pages 119-120) define a packing $D+n = D_n \cup ([1] + D_n)$ [where the glue vector $[1] = (1/2, \dots, 1/2)$] and say:

"... $D+n$ is a lattice packing if and only if n is even.

$D+3$ is the tetrahedral or diamond packing ... and

$D+4 = Z^4$.

When $n = 8$ this construction is especially important, the lattice $D+8$ being known as E8 ...".

$D+n$ is what David Finkelstein and I named a HyperDiamond lattice (although in odd dimensions it is technically only a packing and not a lattice).

Conway and Sloane also say in chapter 4, section 7.1, page 117) that the lattice D_n is defined only for n greater than or equal to 3.

An E8 HyperDiamond lattice is used to construct the HyperDiamond Feynman Checkerboard model with Planck length lattice spacing.

An 8-dimensional E8 lattice has octonionic structure, but no nearest neighbor light-cone links.

To build an E8 Lattice: Begin with an 8-dimensional spacetime $R^8 = O$, where a basis for O is $\{1, i, j, k, e, ie, je, ke\}$. The vertices of the E8 lattice are of the form

$$(a_0 + a_1e + a_2i + a_3j + a_4ie + a_5ke + a_6k + a_7je)/2,$$

where the a_i may be either all even integers, all odd integers, or four of each (even and odd), with residues mod 2 in the four-integer cases being $(1;0,0,0,1,1,0,1)$ or $(0;1,1,1,0,0,1,0)$ or the same with the last seven cyclically permuted.

E8 forms an integral domain of integral octonions.

An E8 lattice integral domain has 240 units:

$\pm 1, \pm i, \pm j, \pm k, \pm e, \pm ie, \pm je, \pm ke, (\pm 1 \pm ie \pm je \pm ke)/2, (\pm e \pm i \pm j \pm k)/2,$ and the last two with cyclical permutations of $\{i, j, k, e, ie, je, ke\}$ in the order (e, i, j, ie, ke, k, je) .

The cyclical permutation (e, i, j, ie, ke, k, je) preserves the integral domain E8, but is not an automorphism of the octonions since it takes the associative triad $\{i, j, k\}$ into the anti-associative triad $\{j, ie, je\}$.

The cyclical permutation (e, ie, je, i, k, ke, j) is an automorphism of the octonions but takes the E8 integral domain defined above into another of Bruck's cycle of seven integral domains. Denote the integral domain described above as $7E8$, and the other six by $iE8, i = 1, \dots, 6$.

The 240 units of the 7E8 lattice corresponding to the integral domain 7E8 represent the 240 lattice points in the shell at unit distance (also commonly normalized as 2) from the origin (points on the line with iE8, jE8 notation are common points with the iE8 and jE8 lattices):

$\pm 1, \pm i, \pm j, \pm k, \pm e, \pm ie, \pm je, \pm ke,$	
$(\pm 1 \pm ie \pm je \pm ke)/2$	$(\pm e \pm i \pm j \pm k)/2$
$(\pm 1 \pm ke \pm e \pm k)/2$	5E8, 4E8 $(\pm i \pm j \pm ie \pm je)/2$
$(\pm 1 \pm k \pm i \pm je)/2$	$(\pm j \pm ie \pm ke \pm e)/2$
$(\pm 1 \pm je \pm j \pm e)/2$	6E8, 2E8 $(\pm ie \pm ke \pm k \pm i)/2$
$(\pm 1 \pm e \pm ie \pm i)/2$	3E8, 1E8 $(\pm ke \pm k \pm je \pm j)/2$
$(\pm 1 \pm i \pm ke \pm j)/2$	$(\pm k \pm je \pm e \pm ie)/2$
$(\pm 1 \pm j \pm k \pm ie)/2$	$(\pm je \pm e \pm i \pm ke)/2$

The other six integral domains iE8 are:

1E8: $\pm 1, \pm i, \pm j, \pm k, \pm e, \pm ie, \pm je, \pm ke,$	
$(\pm 1 \pm je \pm i \pm j)/2$	$(\pm k \pm e \pm ie \pm ke)/2$
$(\pm 1 \pm j \pm ie \pm ke)/2$	5E8, 6E8 $(\pm i \pm k \pm e \pm je)/2$
$(\pm 1 \pm ke \pm k \pm i)/2$	$(\pm j \pm e \pm ie \pm je)/2$
$(\pm 1 \pm i \pm e \pm ie)/2$	7E8, 3E8 $(\pm j \pm k \pm je \pm ke)/2$
$(\pm 1 \pm ie \pm je \pm k)/2$	2E8, 4E8 $(\pm i \pm j \pm e \pm ke)/2$
$(\pm 1 \pm k \pm j \pm e)/2$	$(\pm i \pm ie \pm je \pm ke)/2$
$(\pm 1 \pm e \pm ke \pm je)/2$	$(\pm i \pm j \pm k \pm ie)/2$

2E8: $\pm 1, \pm i, \pm j, \pm k, \pm e, \pm ie, \pm je, \pm ke,$	
$(\pm 1 \pm i \pm k \pm e)/2$	$(\pm j \pm ie \pm je \pm ke)/2$
$(\pm 1 \pm e \pm je \pm j)/2$	7E8, 6E8 $(\pm i \pm k \pm ie \pm ke)/2$
$(\pm 1 \pm j \pm ke \pm k)/2$	$(\pm i \pm e \pm ie \pm je)/2$
$(\pm 1 \pm k \pm ie \pm je)/2$	1E8, 4E8 $(\pm i \pm j \pm e \pm ie)/2$
$(\pm 1 \pm je \pm i \pm ke)/2$	3E8, 5E8 $(\pm j \pm k \pm e \pm ie)/2$
$(\pm 1 \pm ke \pm e \pm ie)/2$	$(\pm i \pm j \pm k \pm je)/2$
$(\pm 1 \pm ie \pm j \pm i)/2$	$(\pm k \pm e \pm je \pm ke)/2$

3E8: ±1, ±i, ±j, ±k, ±e, ±ie, ±je, ±ke,
 (±1 ±k ±ke ±ie)/2 (±i ±j ±e ±je)/2
 (±1 ±ie ±i ±e)/2 7E8, 1E8 (±j ±k ±je ±ke)/2
 (±1 ±e ±j ±ke)/2 (±i ±k ±ie ±je)/2
 (±1 ±ke ±je ±i)/2 2E8, 5E8 (±j ±k ±e ±ie)/2
 (±1 ±i ±k ±j)/2 4E8, 6E8 (±e ±ie ±je ±ke)/2
 (±1 ±j ±ie ±je)/2 (±i ±k ±e ±ke)/2
 (±1 ±je ±e ±k)/2 (±i ±j ±ie ±ke)/2

4E8: ±1, ±i, ±j, ±k, ±e, ±ie, ±je, ±ke,
 (±1 ±ke ±j ±je)/2 (±i ±k ±e ±ie)/2
 (±1 ±je ±k ±ie)/2 1E8, 2E8 (±i ±j ±e ±ke)/2
 (±1 ±ie ±e ±j)/2 (±i ±k ±je ±ke)/2
 (±1 ±j ±i ±k)/2 3E8, 6E8 (±e ±ie ±je ±ke)/2
 (±1 ±k ±ke ±e)/2 7E8, 5E8 (±i ±j ±ie ±je)/2
 (±1 ±e ±je ±i)/2 (±j ±k ±ie ±ke)/2
 (±1 ±i ±ie ±ke)/2 (±j ±k ±e ±je)/2

5E8: ±1, ±i, ±j, ±k, ±e, ±ie, ±je, ±ke,
 (±1 ±j ±e ±i)/2 (±k ±ie ±je ±ke)/2
 (±1 ±i ±ke ±je)/2 2E8, 3E8 (±j ±k ±e ±ie)/2
 (±1 ±je ±ie ±e)/2 (±i ±j ±k ±ke)/2
 (±1 ±e ±k ±ke)/2 7E8, 4E8 (±i ±j ±ie ±je)/2
 (±1 ±ke ±j ±ie)/2 1E8, 6E8 (±i ±k ±e ±je)/2
 (±1 ±ie ±i ±k)/2 (±j ±e ±je ±ke)/2
 (±1 ±k ±je ±j)/2 (±i ±e ±ie ±ke)/2

6E8: ±1, ±i, ±j, ±k, ±e, ±ie, ±je, ±ke,
 (±1 ±e ±ie ±k)/2 (±i ±j ±je ±ke)/2
 (±1 ±k ±j ±i)/2 3E8, 4E8 (±e ±ie ±je ±ke)/2
 (±1 ±i ±je ±ie)/2 (±j ±k ±e ±ke)/2
 (±1 ±ie ±ke ±j)/2 5E8, 1E8 (±i ±k ±e ±je)/2
 (±1 ±j ±e ±je)/2 7E8, 2E8 (±i ±k ±ie ±ke)/2
 (±1 ±je ±k ±ke)/2 (±i ±j ±e ±ie)/2
 (±1 ±ke ±i ±e)/2 (±j ±k ±ie ±je)/2

The vertices that appear in more than one lattice are:

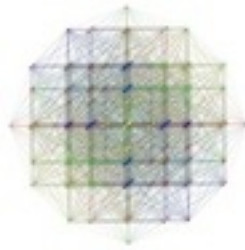
$\pm 1, \pm i, \pm j, \pm k, \pm e, \pm ie, \pm je, \pm ke$ in all of them;
 $(\pm 1 \pm i \pm j \pm k)/2$ and $(\pm e \pm ie \pm je \pm ke)/2$ in $3E8, 4E8, 6E8$;
 $(\pm 1 \pm i \pm e \pm ie)/2$ and $(\pm j \pm k \pm je \pm ke)/2$ in $7E8, 1E8, 3E8$;
 $(\pm 1 \pm j \pm e \pm je)/2$ and $(\pm i \pm k \pm ie \pm ke)/2$ in $7E8, 2E8, 6E8$;
 $(\pm 1 \pm k \pm e \pm ke)/2$ and $(\pm i \pm j \pm ie \pm je)/2$ in $7E8, 4E8, 5E8$;
 $(\pm 1 \pm i \pm j \pm e \pm ie)/2$ and $(\pm j \pm k \pm e \pm ie)/2$ in $2E8, 3E8, 5E8$;
 $(\pm 1 \pm j \pm ie \pm ke)/2$ and $(\pm i \pm k \pm e \pm je)/2$ in $1E8, 5E8, 6E8$;
 $(\pm 1 \pm k \pm ie \pm je)/2$ and $(\pm i \pm j \pm e \pm ke)/2$ in $1E8, 2E8, 4E8$.

The unit vertices in the $E8$ lattices do not include any of the 256 $E8$ light cone vertices, of the form $(\pm 1 \pm i \pm j \pm k \pm e \pm ie \pm je \pm ke)/2$.

They appear in the next layer out from the origin, at radius $\sqrt{2}$, which layer contains in all 2160 vertices.

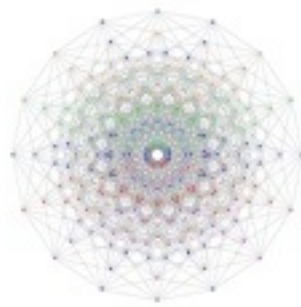
- $2160 = 112 + 256 + 1792 = 112 + (128+128) + 7(128+128)$
- the 112 = root vectors of $D8$
- the $(128+128) = 8$ -cube = two mirror image $D8$ half-spinors related by triality to the 112
- the $7(128+128) = 7$ copies of 8-cube for 7 independent $E8$ lattices, each 8-cube = two mirror image $D8$ half-spinors related by triality to the 112 and thus to the $(128+128)$ and thus to each other.

In the image below,

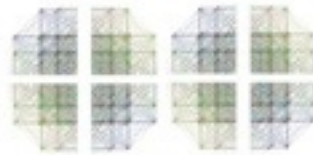


the 240 in the first layer look like

the 112 look like

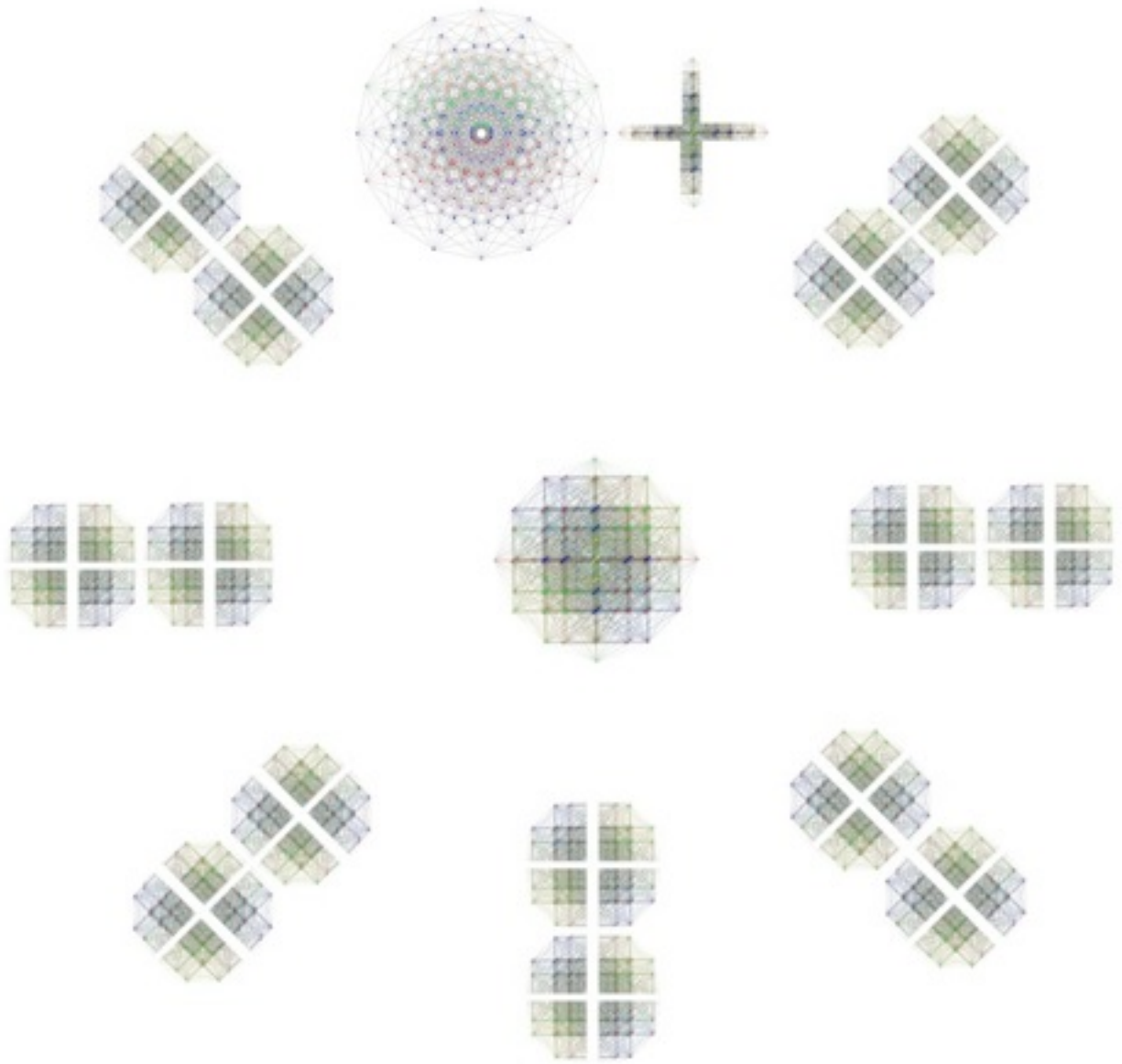


the 256 look like



in the second the 1792 look like

(7 copies of $128+128$).



The real 4_{-21} Witting polytope of the E_8 lattice in R^8 has
 240 vertices;
 6,720 edges;
 60,480 triangular faces;
 241,920 tetrahedra;
 483,840 4-simplexes;
 483,840 5-simplexes 4_{-00} ;
 138,240 + 69,120 6-simplexes 4_{-10} and 4_{-01} ; and
 17,280 7-simplexes 4_{-20} and 2,160 7-cross-polytopes 4_{-11} .

The E8 lattice in R8 has a counterpart in C4, the self-reciprocal honeycomb of Witting polytopes, a lattice of all points whose 4 coordinates are Eisenstein integers with the equivalent congruences

$$u_1 + u_2 + u_3 = u_2 - u_3 + u_4 = 0 \pmod{i \sqrt{3}} \text{ and} \\ u_3 - u_2 = u_1 - u_3 = u_2 - u_1 = u_4 \pmod{i \sqrt{3}}.$$

The self-reciprocal Witting polytope in C4 has

240 vertices,

2,160 edges,

2,160 faces, and

240 cells.

It has 27 edges at each vertex.

Its symmetry group has order $155,520 = 3 \times 51,840$.

It is 6-symmetric, so its central quotient group has order 25,920.

It has 40 diameters orthogonal to which are 40 hyperplanes of symmetry, each of which contains 72 vertices.

It has a van Oss polygon in C2, its section by a plane joining an edge to the center, that is the $3\{4\}3$ in C2, with 24 vertices and 24 edges.

The 24-cell $3\{4\}3$ in R4 has

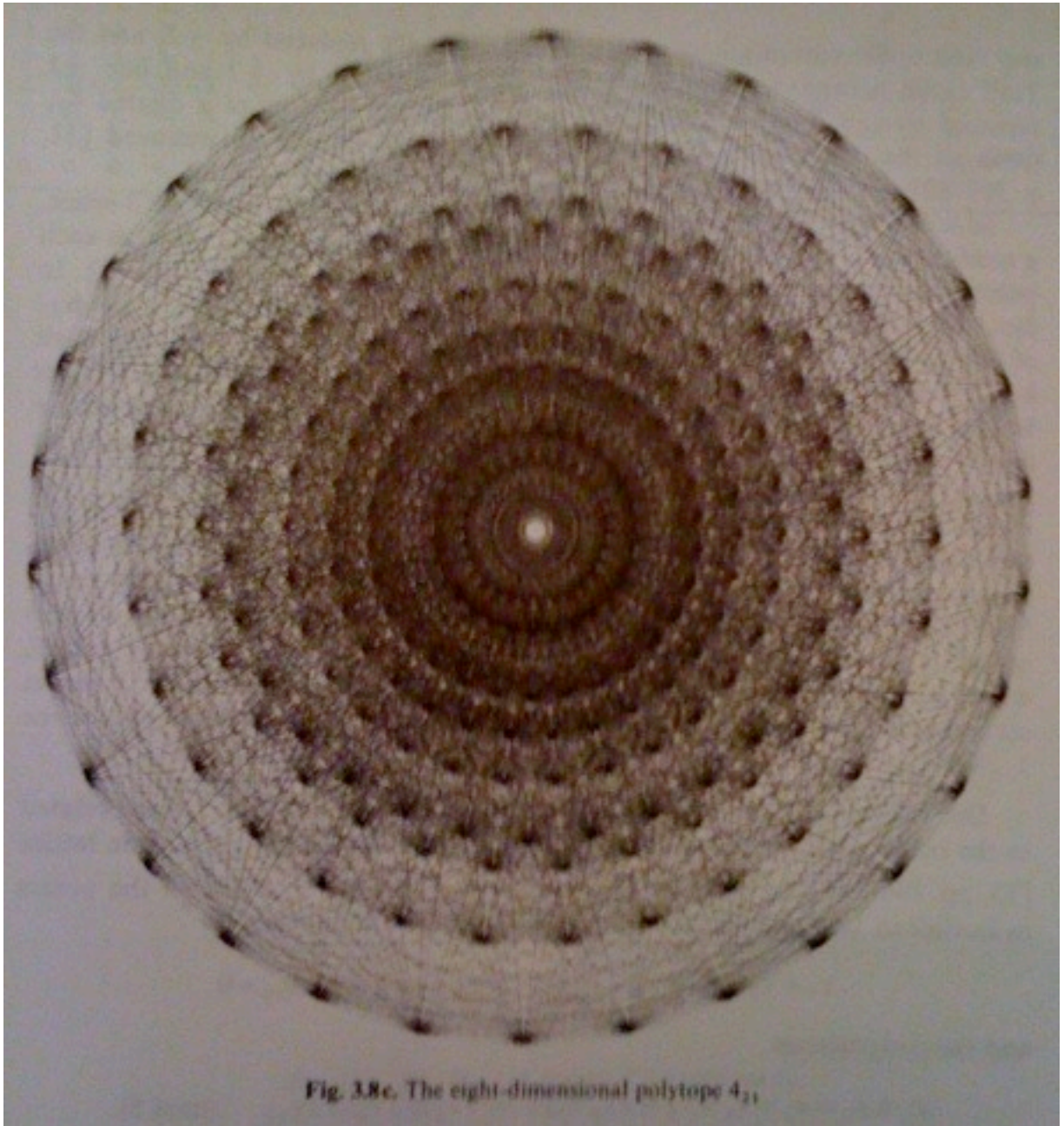
24 vertices,

96 edges,

96 faces, and

24 cells.

The corresponding 8-real-dim real Witting polytope 4_{21} looks like this (from Coxeter's book "Regular Polytopes")



Note that both 4-complex and 8-real have 240 vertices arranged in 8 circles each with 30 vertices, and a lot of lines (so many that it is hard to tell the difference between the two images given their resolution).

However, an important difference is how many lines are at each vertex. Coxeter says in "Complex Regular Polytopes":

"... In ... the Witting polytope ... Regular complex polytope ... $3\{3\}3\{3\}3\{3\}3$... there are 27 edges at each vertex ... the vertex figure is ... $3\{3\}3\{3\}3$... [which has]... 17 vertices, 72 edges, and 27 faces ...

...
 In ... The real counterpart ... 4_{21} ... Each of its 240 vertices belongs to 56 edges (corresponding to the 56 vertices of its 7-dim... vertex figure 3_{21}) ...".

Note that the 27 correspond to the 27 lines on the cubic surface and therefore include the Schläfli Double-6 and

the 56 correspond to the non-central 56 of the E_7 -group. As John Baez said in his review of the book "On Quaternions and Octonions" by John Conway and Derek Smith (): "... E_8 is 248-dimensional ... E_8 is the symmetry group of a 57-dimensional manifold ... when we pack 8-dimensional balls in a [E_8] lattice ... each ball has 240 nearest neighbors, and when we take any one of these neighbors and count the number of others that touch it, we find that there are 56! ... the Freudenthal algebra ... [is]... 56-dimensional ... the smallest non-trivial representation of E_7 ... the dimension of E_7 is 133 ... there is a 5-grading of E_8 ... $248 = 1 + 56 + 1345 + 56 + 1$... there is ... a 3-grading of E_7 ... $133 = 27 + 79 + 27$... the Freudenthal algebra decomposes as ... $56 = 1 + 27 + 27 + 1$...".

As shown by Thomas Larsson, there is a 7-grading of E_8
 $248 = 8 + 28 + 56 + 64 + 56 + 28 + 8$
 with even part $28 + 64 + 28 = 120 = D_8$ adjoint
 and odd part $8 + 56 + 56 + 8 = 128 = D_8$ half-spinor.

Further, 27 is the dimension of the smallest non-trivial representation of E_6 and 248 is the dimension of the smallest non-trivial representation of E_8 .

D4 is the Derivation Group of the 24-dimensional Chevalley Algebra Chev3(O) of 3x3 matrices of the form:

$$\begin{array}{ccc} 0 & S+ & V \\ S+^* & 0 & S- \\ V^* & S-^* & 0 \end{array}$$

where S+, V, and S- are Octonions; and * denotes conjugation.

Note that the full 27-dimensional Jordan Algebra J3(O) has Automorphism Group F4.

The Lie Group E6 is the Automorphism Group of the 56-dimensional Freudenthal Algebra Fr3(O) of 2x2 Zorn-type vector-matrices

$$\begin{array}{cc} a & X \\ Y & b \end{array}$$

where a and b are real numbers and X and Y are elements of the 27-dimensional Jordan algebra J3(O) of 3x3 Hermitian matrices

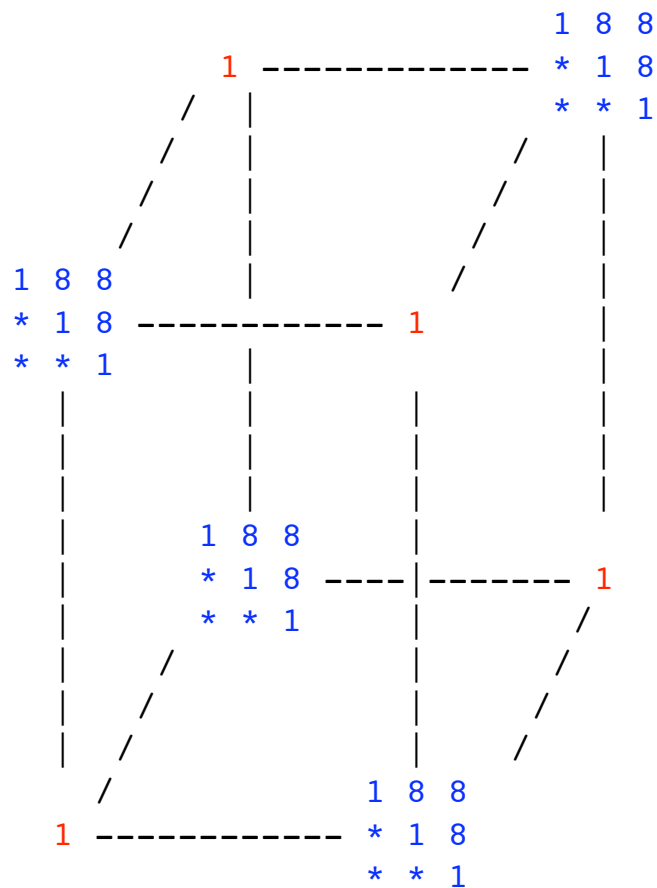
$$\begin{array}{ccc} d & S+ & V \\ S+^* & e & S- \\ V^* & S-^* & f \end{array}$$

where d, e, and f are real numbers; S+, V, and S- are Octonions; and * denotes conjugation.

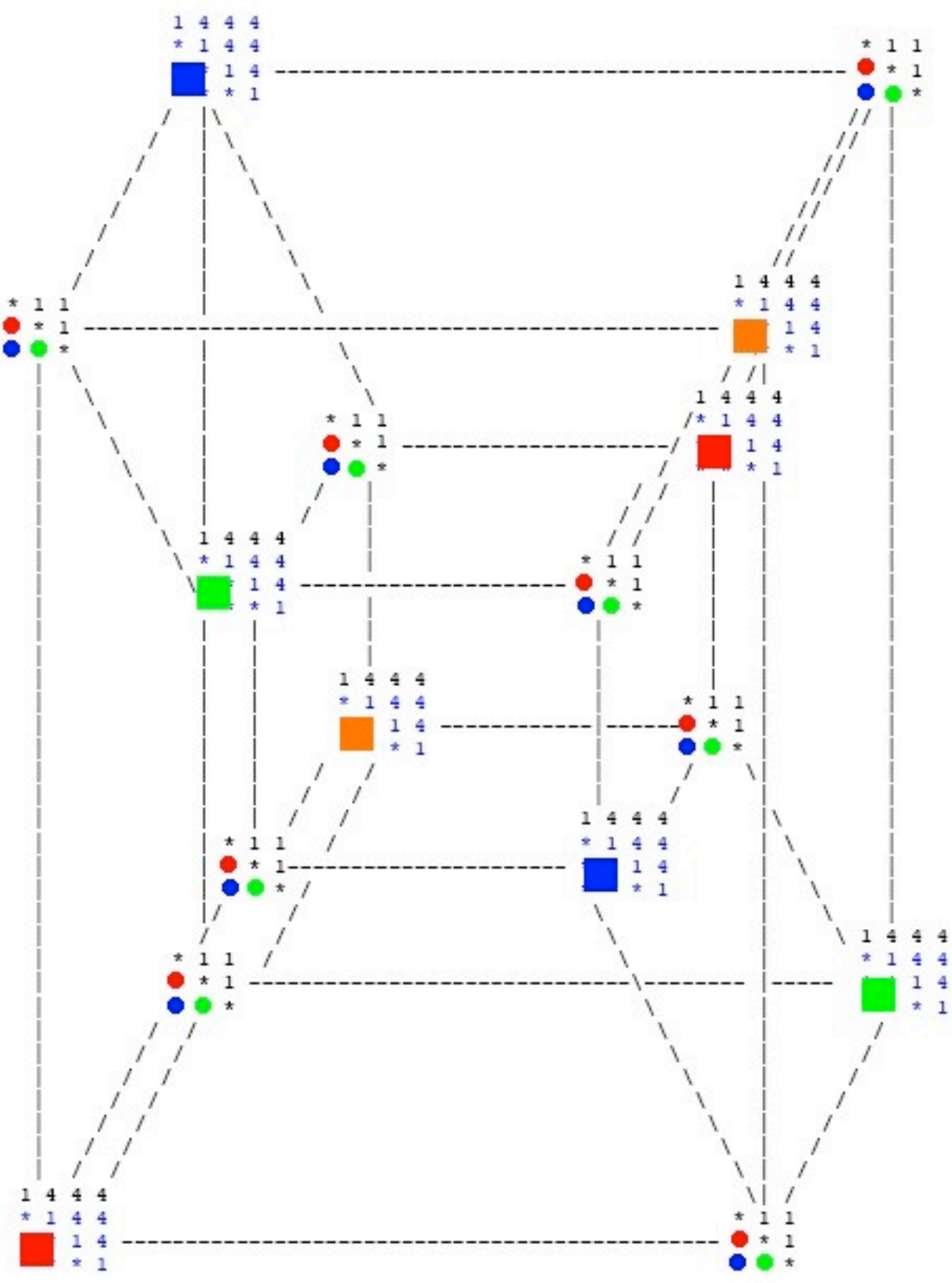
Fr3(O) includes a complexification of J3(O), so that each Half-Spinor Fermion Representation Space has 8 Complex Dimensions and a corresponding Bounded Complex Domain with 8-real-dimensional Shilov Boundary S7 x RP1.

Restriction to the real J3(O) would have produced an Automorphism Group F4 and a real 16-dimensional Spinor space corresponding to OP2 = F4 / B4.

The Lie Group E7 is the Automorphism Group of the 112-dimensional Brown Algebra Br3(O). Unlike Fr3(O), Br3(O) is not a binary algebra, but is a ternary algebra, which leads you to think of 3-dimensional arrays as generalizations of 2-dimensional matrices. When you go to a 3-dim 2x2x2 array for the 112-dim Brown "algebra-like thing" corresponding to E7, you get a picture like this:



When you go to a 4-dim 2x2x2x2 array for E8, you get a 224-dim "thing" that looks like a tesseract but is too small to include the structure of the lowest-dimensional representation of E8, which is 248-dimensional. To see the full structure of 248-dim E8 as a Tesseract Creature follow B. N. Allison and J. R. Faulkner (in A Cayley-Dickson Process for a Class of Structurable Algebras (Trans. AMS 283 (1984) 185-210) they say: "... we obtain a procedure for giving the space Bo of trace zero elements of any ... 28-dimensional degree 4 central simple Jordan algebra B ... the structure of a 27-dimensional exceptional Jordan algebra. ... ") and so use 8 copies of 28-dim J(4,Q) instead of 8 copies of 27-dim J(3,O) and also use 8 copies of a 3-dim thing instead of 8 copies of 1, producing:



The colors indicate the physical interpretation of each vertex of the E8 Tessseract:

Gravity		SpaceTime		Fermion		Fermion
+						
Standard Model				Particles		AntiParticles
gold		blue		red		green
28 + 28	+	(28+28)	+	(28+28)	+	(28+28)
		8	+	8	+	8
(D4 + D4	+	64)	+	(64	+	64)
		120	+	128		
		Cl(16) bivector D8	+	Cl(16) D8 half-spinor		
				E8		

NOTE - NONE of the 8x3 things carry the rank of E8. ALL of the rank 8 of E8 comes from D4 + D4, so the 8x3 does NOT represent 8 copies of SU(2) but rather the 8x3 represents 24-dim Chev(3,O) of which D4 is the Derivation Group.

E8 is the ultimate Exceptional Lie Group, and therefore can be seen as a Unique Parallelizable Structure that can be used to describe realistic physics of Entanglement. Joy Christian in arXiv 0904.4259 "Disproofs of Bell, GHZ, and Hardy Type Theorems and the Illusion of Entanglement" says:

"... a [geometrically] correct local-realistic framework ... provides exact, deterministic, and local underpinnings for at least the Bell, GHZ-3, GHZ-4, and Hardy states. ... The alleged non-localities of these states ... result from misidentified [geometries] of the EPR elements of reality. ...

The correlations are ... the classical correlations among the points of a 3 or 7-sphere ... S3 and S7 ... are ... parallelizable ...

The correlations ... can be seen most transparently in the elegant language of Clifford algebra ...".

Quasicrystals and Tetrahedral Packing

Quasicrystals in 3-dimensional space are 3-dimensional slices of E8 lattices. E8 lattices have binary power-of-2 structures and also involve 3 by 12-structures so that

it is natural that the N=4, N=8, N=12, and N=16 tetrahedral structures would give packings as dense (or maybe a little more) than the quasicrystal ones to which they are probably closely related through their common denominator, the E8 lattices.

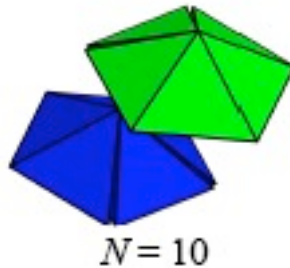
The paper at <http://arxiv.org/abs/1001.0586> said in part:

"... In 1972, Stanislaw Ulam conjectured that spheres would have the lowest maximum packing density of all convex bodies, including tetrahedra ...

That density is ... 0.740480

...

The N = 10 packing consists of two pentagonal dipyramids,



perfect in the sense that four of each set of five tetrahedra are arranged face-to-face ... [giving density] ... 0.829 ... the fifth tetrahedron is oriented in such a way to distribute the (obligatory) gap ... evenly on its two sides.

...

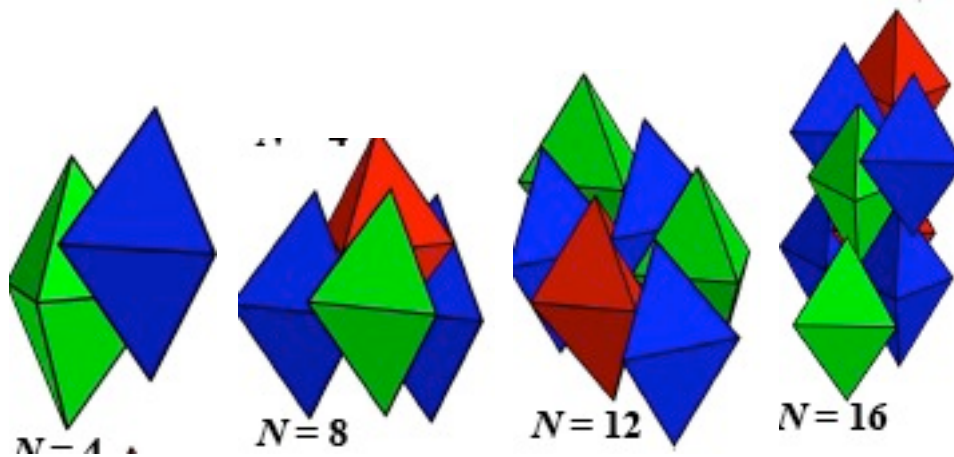
using MC simulations of initially random systems containing up to nearly 22,000 tetrahedra ... an equilibrium fluid of hard tetrahedra spontaneously transforms to a dodecagonal quasicrystal, which can be compressed to ... 0.8324 ...

By numerically constructing and then compressing four unit cells of a periodic quasicrystal approximant with an 82-tetrahedron unit cell, they obtained a packing density as high as ... 0.8503

[see below for more about quasicrystal packing] ...

the densest packing is not the most symmetric one ...

Monte Carlo simulations ... recover the same high packing density ... 0.85634 ... for



small systems containing 4, 8, 12, and 16 tetrahedra. ...".

The quasicrystal case is discussed in more detail in the paper at http://spahn.engin.umich.edu/publications/documents/2009_glotzer_188.pdf which said in part:

"... Tetrahedra do not tile Euclidean space.

However, if extra space is allowed between tetrahedra, or between groups of tetrahedra, dense ordered structures become possible. ...

By compressing a crystalline approximant of the quasicrystal, the highest packing fraction we obtain is ... 0.8503

...

a pentagonal dipyramid is easily built from five tetrahedra if one allows an internal gap of 7.36 degrees.

Two pentagonal dipyramids can share a single tetrahedron to form a nonamer.

Twelve interpenetrating pentagonal dipyramids define an icosahedron with a gap of 1.54 steradians.

...

Pentagonal dipyramids and icosahedra are locally dense, but exhibit non-crystallographic symmetries. ...

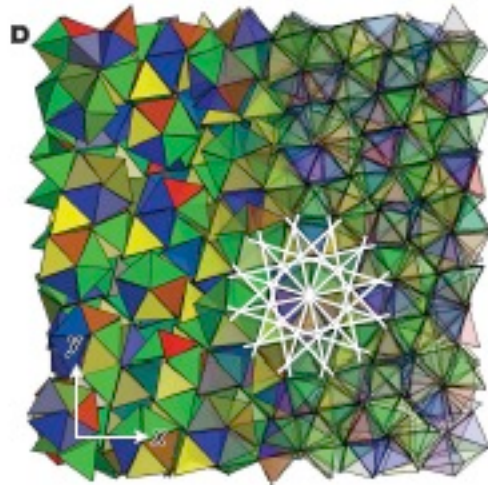
we introduce here a dense, one-dimensional packing given by a linear arrangement of tetrahedra with touching faces known as a tetrahelix, or Bernal spiral.

...

we carry out Monte Carlo simulations ... we equilibrated an initially disordered fluid of 13,824 tetrahedra ... and then we compressed the ordered structure that forms ... this structure is a quasicrystal

...

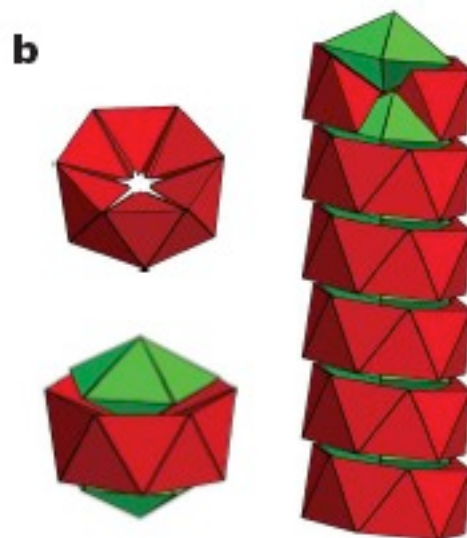
the quasicrystal consists of a periodic stack of corrugated layers w...
The view along the direction of the stacking vector ... reveals ...



Twelve-fold symmetric rings formed by interpenetrating tetrahelices
... throughout the structure

...

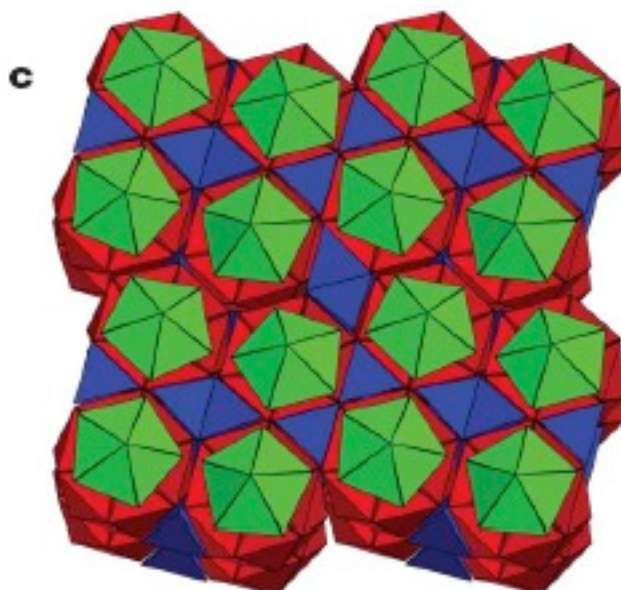
The vertices of the tiling are formed by logs comprised of
rings of twelve tetrahedra,



with neighbouring rings enclosing a pentagonal dipyrmaid

...

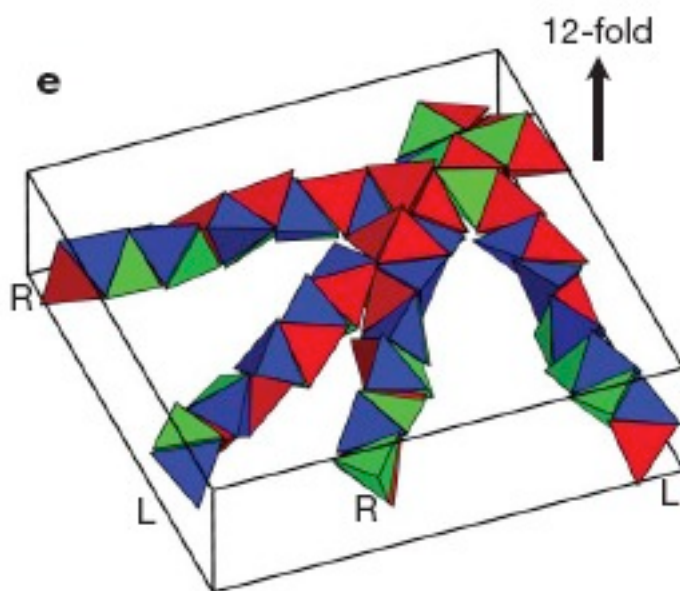
[this shows]... structure ...



approximant to ... quasicrystal tetrahedra

...

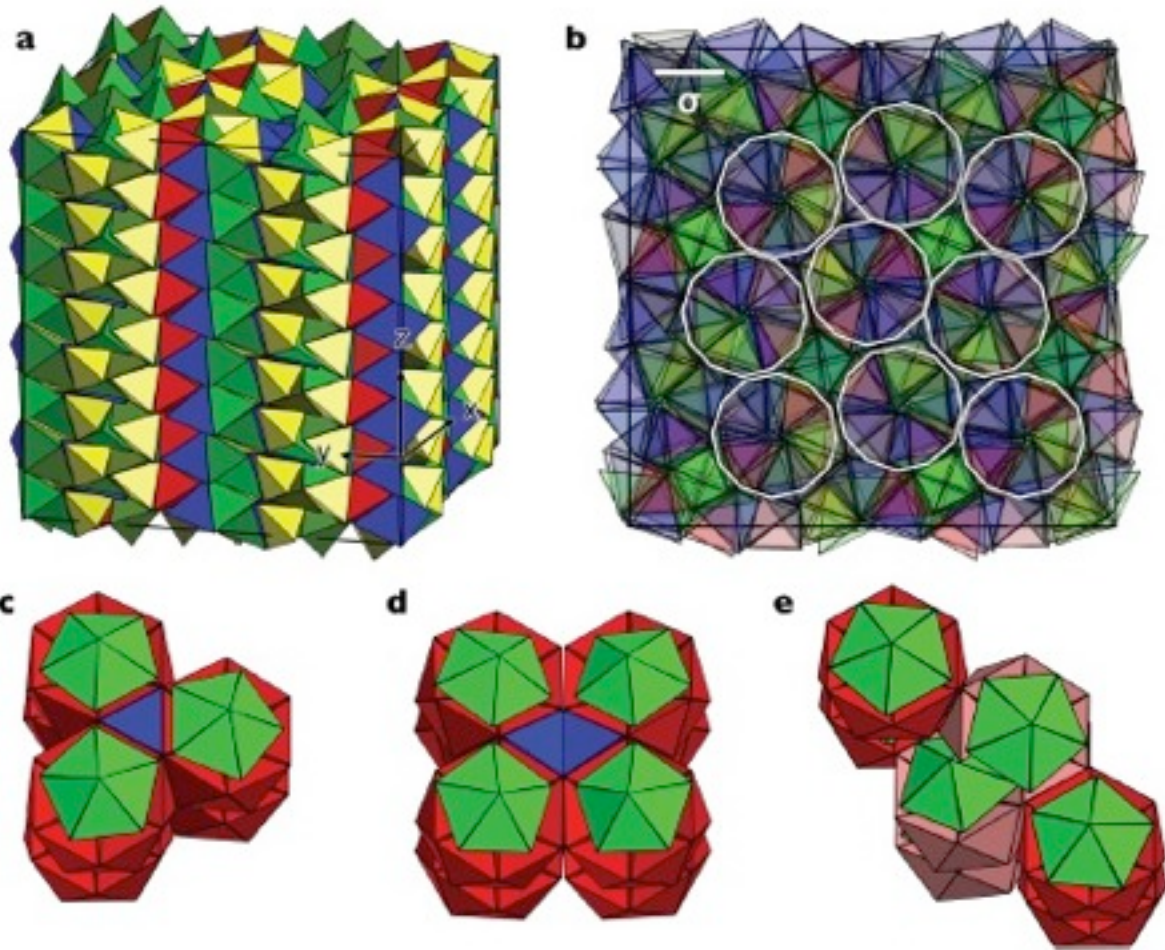
interpenetrating tetrahelices are present throughout ...



Their chirality alternates between left (L) and right (R)
by 30 degree rotations

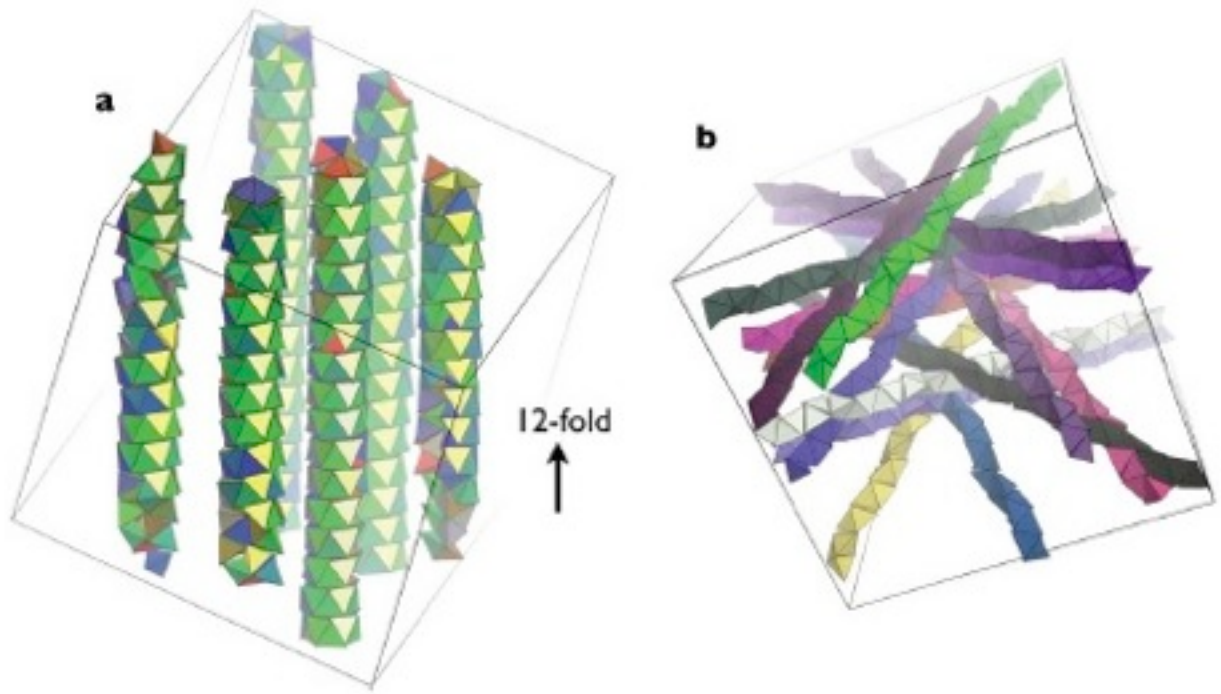
...

[here are]... details of the highest density ... 0.8503 ...
packing of hard tetrahedra observed n this study



...

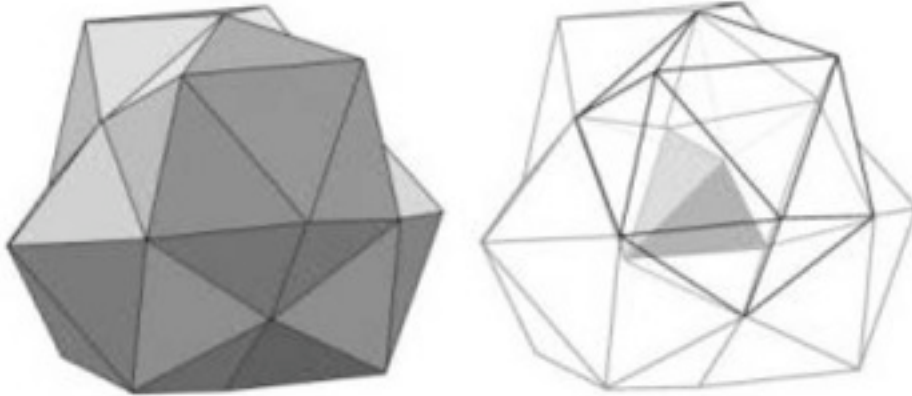
[here are]... One-dimensional building blocks



of ... quasicrystal ...".

TetraJJ Geometry: Nanometer to Planck Casimir-NearField-DarkEnergy

The scale of a TetraJJ Nucleus would determine how close, in 3-dim Space where the fit of component Tetrahedra is not exact, is the spacing between two nearby faces of component Tetrahedra:



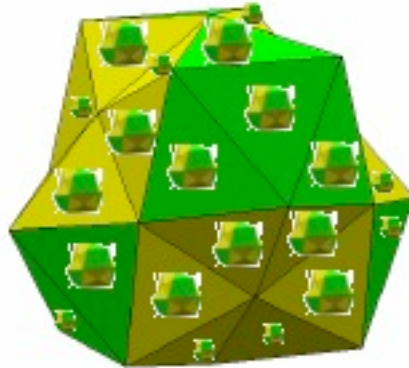
If the spacing is small enough then the Casimir/NearField phenomena might be significant. To evaluate that, consider a TetraJJ Nucleus.

From looking at images, it seems to me that, roughly, the ratios of scale are:

edge of entire 57-group (if it were not truncated)	= 1
edge of each component tetrahedron	= 0.16
gap between two nearby faces of component tetrahedra	= 0.016

To study a wide range of scales, consider that each component tetrahedron is itself made up of a TetraJJ Nucleus of tetrahedra that are smaller by a factor of about 6

which would give you something with 57×57 tetrahedra
(my graphic is crude and incomplete, but I hope it shows the general idea)



Then you can continue the process, each time shrinking by a factor of about 6,
effectively making a fractal solid.

If the Casimir effect becomes important at gap distance nanometer scale,
then
it might become effective after fractal shrinking from 1 cm initial 57-group size
by

$$(0.016 \text{ cm} = 16 \times 10^{-5} \text{ m}) / (10^{-9} \text{ m}) = 160,000$$

Since 7 stages of 6-fold fractal shrinking reduce scale by about 270,000,
consider 6 stages of fractal shrinking.

At that stage, each tetrahedral edge initially 0.16 cm would be
about $1600 \times 10^{-6} \text{ m} / 270,000 = 3 \times 10^{-9} \text{ m} = 6 \text{ nanometers}$
and the gap distance would be about 0.6 nanometers.

Since metals like gold, iron, etc, have atoms
with diameters about $1/3$ of a nanometer,
each tetrahedral edge would have about 18 atoms
and the gap distance would be about the size of 2 atoms.

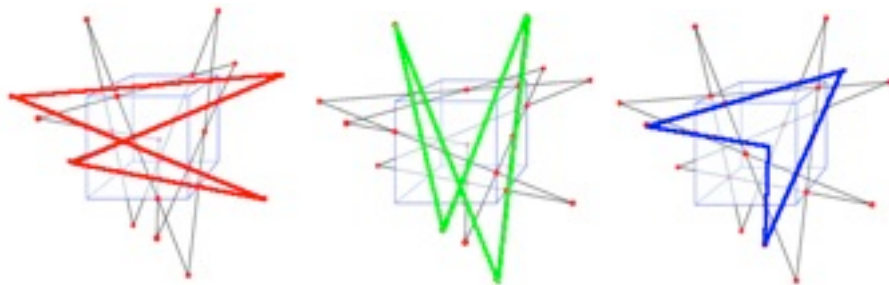
The nanometer scale of atoms is the smallest scale on which manufacturing is practical,
but
it is a much larger scale than that of the fundamental length of a single link in the fundamental SpaceTime Lattice.

Richard Feynman, in his book QED (Princeton 1985, 2006), said “... perhaps the idea that two points can be infinitely close together is wrong ... If we make the minimum possible distance between two points as small as $10^{(-100)}$ centimeters (the smallest distance involved in any experiment today is around $10^{(-16)}$ centimeters) ... inconsistencies arise, such as the total probability of an event add up to slightly more or less than 100%, or we get negative energies ... the effects of gravity ... become important at distances of $10^{(-33)}$ cm. ...”. Feynman’s suggested fundamental distance involving gravity is known as the Planck length, and it is as he said about $10^{(-35)}$ meters or about $10^{(-26)}$ nanometers.

To get from the nanometer scale to the Planck scale by fractal shrinking by a factor of 6 each time would take about 33 levels of shrinking.
Since the Planck length is 33 levels below the nanometer level
while
the nanometer level is only about 7 levels below the centimeter level,
a lot of some sort of aggregation must go on between
the Planck level of fundamental physics
and the nanometer level of atoms.

My guess is that the aggregation works like this for, to use a concrete example, electrons:

The fundamental electron is at the Planck scale represented by a TetraJJ Nucleus with all three color Tetrahelix groups activated



so it is just a very small Planck-size tetrahedron

However, the little electron can move from place to place in the lattice of spacetime, and as Feynman said in describing Quantum Theory, it can and does go every possible way to get from point A to point B, so the little electron accumulates around itself a huge (from the Planck point of view) cloud of virtual-possible particle/antiparticle pairs each of which corresponds to a possible movement of the fundamental electron and the cloud grows up until it gets to the size of the physical electrons that we see in atoms and in our experiments.

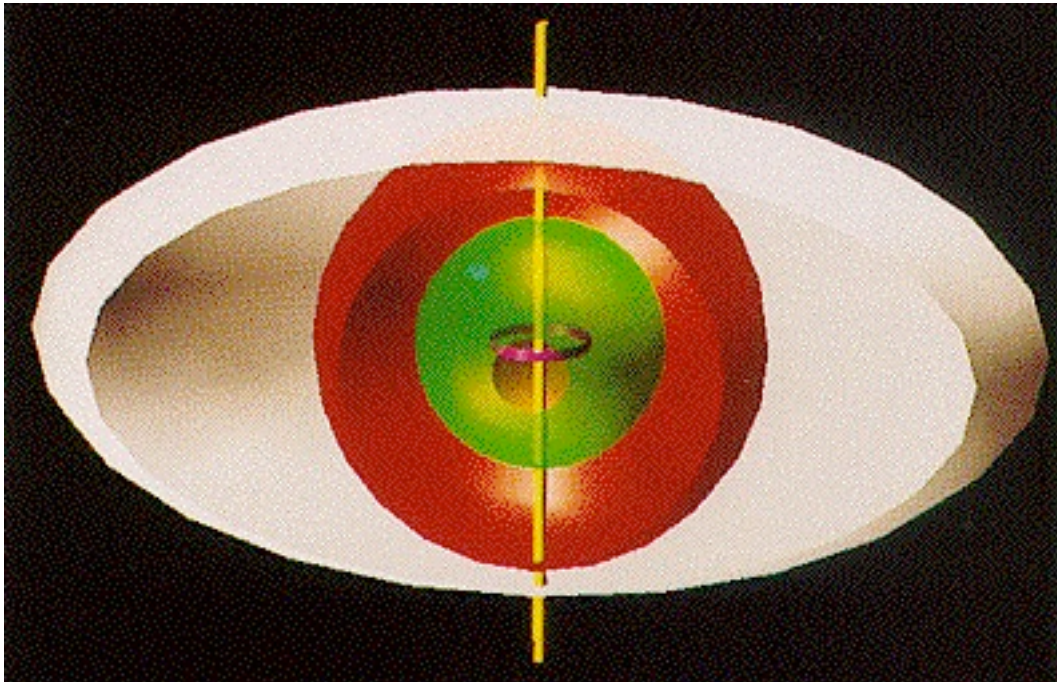
Bert Schroer in hep-th/9908021 describes the formation of the cloud of an electron, saying "... the vacuum structure of [Quantum Field Theory] ... in... a modern [Local Quantum Physics] context suggest that any compactly localized operator applied to the vacuum generates clouds of pairs of particle/antiparticles ... it leads to the impossibility of having a local generation of pure one-particle vectors ..." in any realistic physics model with particle interactions.

The structure of the "clouds of pairs of particle/antiparticles" around a fundamental Planck-scale electron is that of a Kerr-Newman Black Hole, as described by D. Lynden-Bell in astro-ph/0207064 where he says: "... An electromagnetic field ... turns out to be the $G = 0$ limit of the charged rotating Kerr-Newman metrics. These all have gyromagnetic ratio 2, the same as the Dirac electron. ... the quantum electrodynamic charge distribution surrounding the point electron ... giving this high gyromagnetic ratio have charges of both signs rotating at close to the velocity of light. ... internal charges are of opposite signs ... rotate together giving a magnetic dipole with relatively little net charge. ... this is a characteristic of relativistically rotating conductors! ..."

and by D. Ranganathan in gr-qc/0306090 where he says: "... A self consistent solution to Dirac equation in a Kerr Newman space-time with $M^2 > a^2 + Q^2$ is presented for the case when the Dirac particle is the source of the curvature and the electromagnetic field. The solution is localised, continuous everywhere and valid only for a special choice of ... the parameters (m_e , Q , a) appearing in the Dirac equation. ... Such a solution corresponds to a generalisation of the free particle Dirac equation in Minkowski space to include the effects of the curvature produced by the particle. The ordinary free particle solutions of the Dirac equation are completely delocalised; the curvature however, now causes the Dirac wave functions to be localised over a region comparable in dimension to the Compton wavelength of the particle. Note that the wave function still has an enormous spread in comparison to the dimensions of the event or Cauchy horizons of the

particle. ... in the region of the order of the Compton wavelength within which the wave function peaks, the field strengths are so large that virtual pair creation cannot be neglected. The antiparticle thus produced can recombine with the "original" particle at $r = 0$ leaving us to detect the particle now at $r \neq 0$".

Clifford Pickover, in his book "Black Holes - A Traveller's Guide") Wiley 1996), illustrates a black hole



with ergosphere (white),
Outer Event Horizon (red),
Inner Event Horizon (green),
and Ring Singularity (purple).

Quantum Vacuum Phenomena not only describe the world below the nanometer scale of atoms down to the Planck Scale fundamental Fermion elementary particles by showing them to be Kerr-Newman Black Hole clouds, but also describe significant phenomena at and somewhat above the nanometer scale of atoms such as the Casimir Effect and Near Field Phenomena.

As to the Casimir effect, Robert Forward, in his books "Future Magic" (Avon 1988) and "Indistinguishable From Magic" (Baen 1995), says:
"... The Casimir force is a short range attraction between any two objects

caused by ... electromagnetic fluctuations in the vacuum. ... The equations are only valid down to a separation distance proportional to the minimum wavelength at which the plates are still a good conductor or the dielectric constant is not unity. ... The closest separation distance ...[that has been attained is 14 Angstroms]... (about five atoms) with two crossed cylinders of mica. ... the measured force between the two mica cylinders was over ten tons per square meter! ... [To construct a vacuum fluctuation battery, make] ... a wide flat spiral of foil built along the lines of a Slinky toy. ... each turn of the spiral acts against the neighboring turns. The spiral configuration allows substantial compaction of the foil from large spacings to small spacings while maintaining uniform spacing. ... [electric charge could] create an electrostatic repulsion between the plates ... The Casimir force [could] draw the ... leaves together, doing work against the repulsive electric field ...". The "Slinky toy" reference reminds me of the tetrahelix cylinders of a 57-group.

As to Near Field Photon effects, Lukas Novotny and Bert Hecht, in their textbook "Principles of Nano-Optics" (Cambridge 2006), discuss things like Near-Field optical probes with tetrahedral tips and surface plasmons and forces in confined fields etc. They say in their introduction:

"... as we move to smaller and smaller scales, new physical effects become prominent ... in recent years ... new approaches ... overcome ... the diffraction limit (near-field microscopy) ... nanocomposite materials are ... generating increased nonlinearities and collective responses ... surface plasmon waveguides are being implemented for planar optical networks ... photonic bandgap materials ... suppress light propagation in specific frequency windows ...".

The possibility of fabricating nanostructures to interact with Dark Energy has been discussed by Christian Beck, who in hep-th/0207081 talks about

"... deterministic chaotic models of vacuum fluctuations on a small (quantum gravity) scale ..." that seems to connect Mandlbrot fractal ideas with chaotic quantization. He has a more recent paper on that at <http://xxx.lanl.gov/abs/0801.4720> and he has a paper at <http://xxx.lanl.gov/abs/0707.1797> in which he talks about rotating superconductors and Dark Energy which specifically mentions Cooper pair structures. He also discusses Dark Energy at astro-ph/0512327 and astro-ph/0406504. The Josephson Junction experiment mentioned by Christian Beck is by P A Warburton of University College London. who has papers at arxiv/0807.4502 and cond-mat/0303419.

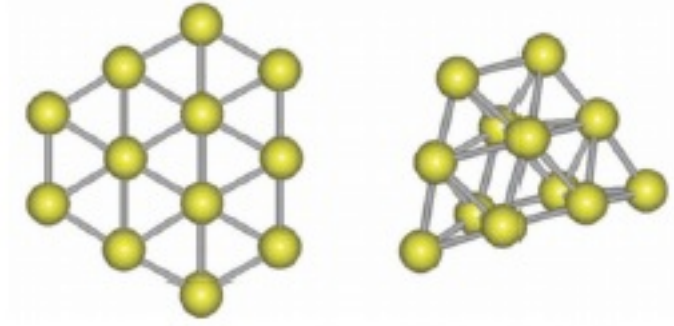
Gold Atom Clusters

Recent experiments with Gold seem to indicate that its fundamental structure is related to the tetrahedron.

According to a 20.05.2008 CSC web article about a Phys. Rev. A paper <http://link.aps.org/abstract/PRA/v77/e053202>

by Johansson, Lechtken, Schooss, Kappes, and Furche:

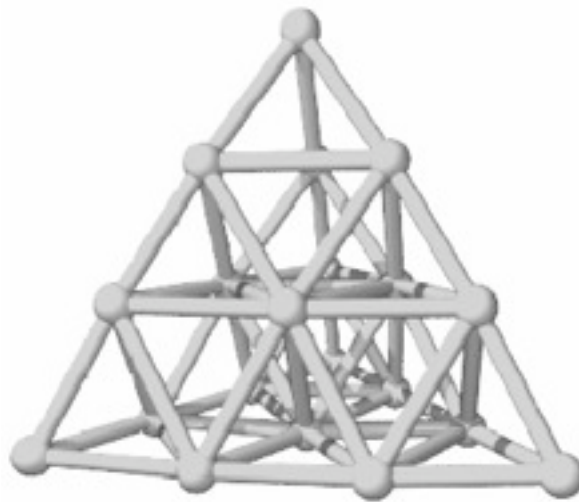
"... transition from a planar [2-dim] to spherical [3-dim] structure



occurs when the number of gold atoms is 12 ...".

Note that in 3-dim the 12 atoms do not form either an icosahedron or a cuboctahedron, but rather form something that looks like part of a tetrahedron.

A 2007 University of Technology Sydney paper by Ford, de Bras, and Cortie entitled Stability of the tetrahedral motif for small gold clusters in the size range 16 to 24 atoms said in part: "... The tetrahedral 20 atom gold cluster



is surprisingly stable, and is believed to be the ground state structure ...".

Cold Fusion and Palladium Atom Clusters

In Palladium cold fusion processes, Ken Shoulders and Steve Shoulders consider micron (1,000 nanometer) size clusters of electrons and how they interact with the Palladium, saying

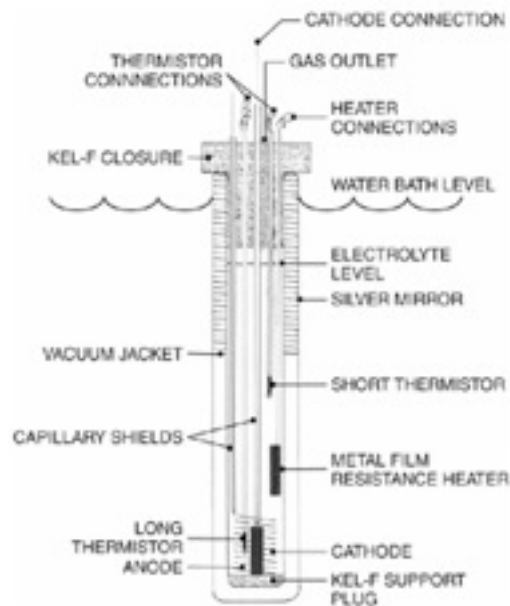
"... The energy ... seems to emanate from cracks formed in the brittle, top layer of Pd. This layer is about 0.1 micrometers [100 nanometers] in thickness ...".

(see <http://www.svn.net/krscfs/nev%20clusters%202.pdf>)

According to a 3/23/2009 EE Times article by R. Colin Johnson:

"... U.S. Navy researchers claimed to have experimentally confirmed cold fusion in a presentation at the American Chemical Society's annual meeting.

"We have compelling evidence that fusion reactions are occurring" at room temperature, said Pamela Mosier-Boss, a scientist with the Space and Naval Warfare Systems Center (San Diego). The results are "the first scientific report of highly energetic neutrons from low-energy nuclear reactions," she added. ...



...

The theoretical underpinnings of cold fusion have yet to be adequately explained. The hypothesis is that when electrolysis is performed on deuterium, molecules are fused into helium, releasing a high-energy neutron. While excess heat has been detected by researchers, no group had yet been able to detect the missing neutrons. Now, the Naval researchers claim that the problem was instrumentation, which was not up to the task of detecting such small numbers of neutrons. To sense such small quantities, Mosier-Boss used a special plastic detector ... Using co-deposition with nickel and gold wire electrodes, which were

inserted into a mixture of palladium chloride and deuterium, the detector was able to capture and track the high-energy neutrons. ... Other presenters at the conference also presented evidence supporting cold fusion, including Antonella De Ninno, a scientist with New Technologies Energy and Environment (Rome), who reported both excess heat and helium gas. "We now have very convincing experimental evidence," De Ninno claimed. Tadahiko Mizuno of Japan's Hokkaido University also reported excess heat generation and gamma-ray emissions.

All three research groups are currently exploring both experimental and theoretical studies in hopes of better understanding the cold fusion process well enough to commercialize it. ...”.

For Palladium, which is the element for which Cold Fusion seems to occur when the Pd is saturated with Deuterium, **small Pd clusters of atoms seem to prefer icosahedral structure**, which may be something that allows a lot of Deuterium to get into the Pd lattice and to interact producing Cold Fusion. **Fuller Tensegrity**



transformations from icosahedra to cuboctahedra (and/ or Jitterbug transformations) might play some role in pushing the Deuterium nuclei close enough for fusion reactions.

In their paper Molecular Dynamics Study of Palladium Clusters: Size Dependent Analysis of Structural Stabilities and Energetics of Pd_n (n less than or equal to 40) via a Lennard-Jones Type Potential in CROATICA CHEMICA ACTA, CCACAA 81 (2) 289-297 (2008) Mustafa Boyukataa and Jadson C. Belchiorb said:

"... Possible stable structures and energetics of palladium clusters, Pd_n ($n = 2-40$), have been investigated by performing molecular-dynamics simulations based on a Lennard-Jones type pair potential. ...

Main observed results are that palladium clusters prefer three-dimensional structures and spherical clusters of medium size appear to have five-fold symmetry.

...

The well-known ground-state structure of 7-atom cluster ...[

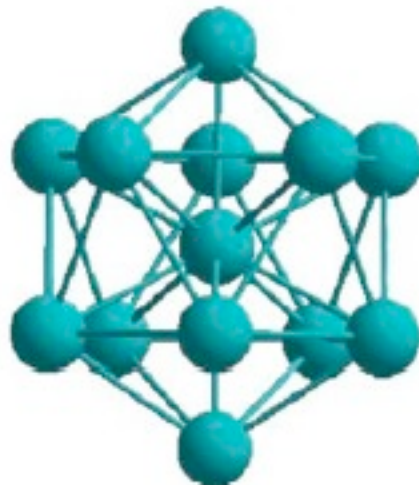


(image from Physical Review B 72 (2005) 115421 by Rogan et al)]...

Pd7 is ... a pentagonal bipyramid

...

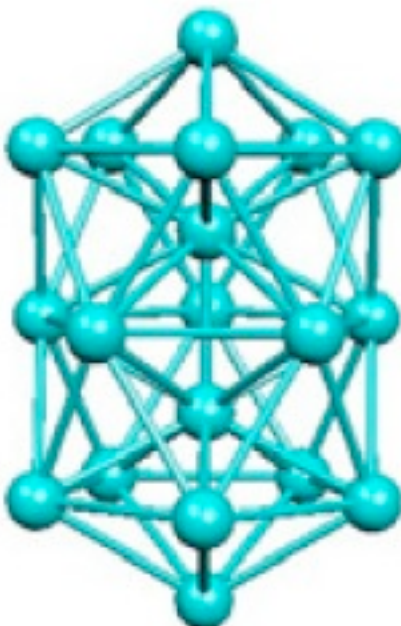
A Five-fold ring is a common backbone leading to a nearly perfect icosahedral form of Pd13. ...[



(image from Physical Review B 72 (2005) 115421 by Rogan et al)]...

In the particular case of Pd13, the icosahedral configuration, a well-known magic structure, is predicted. ...

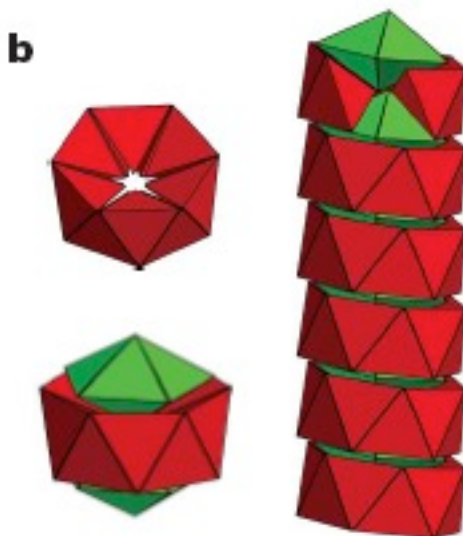
The double icosahedral structure ... is ... found for Pd19 ...[

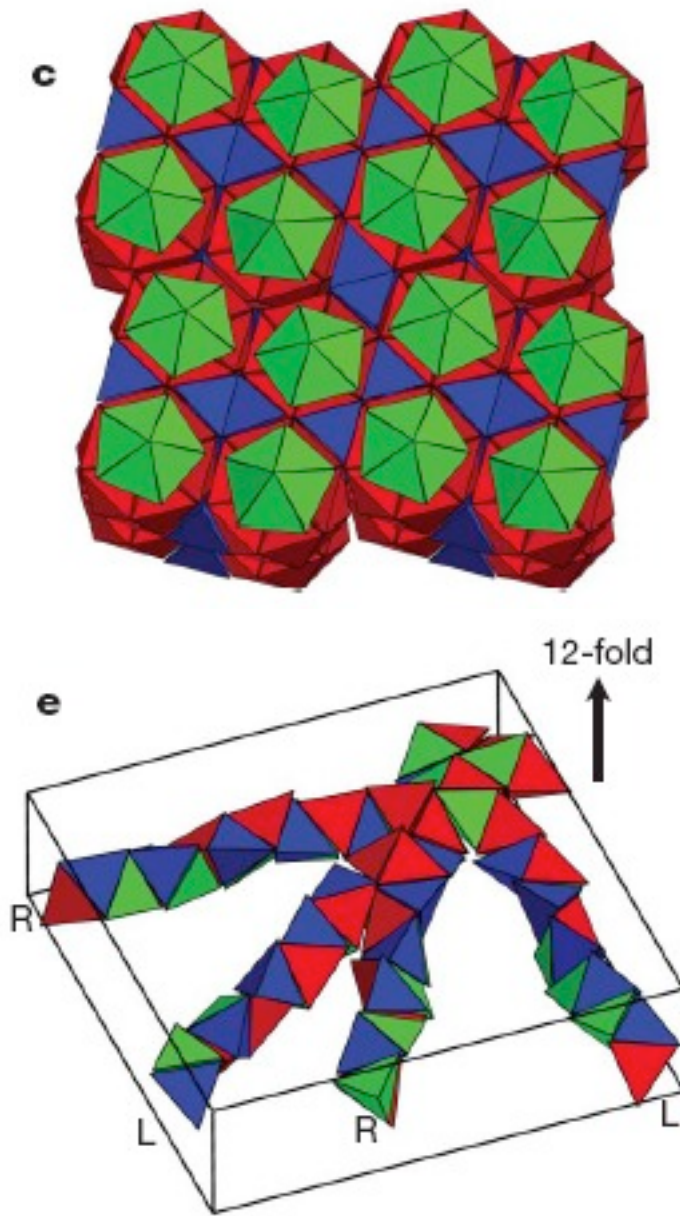


(image from Pnanotechnology 19 (2008) 205701 by Rogan et al)]...

another well-known magic size ... There are 5 hollow sites on the equatorial ring of the Pd19 structure. ...".

It is interesting to compare the Pd19 double icosahedral stack with the multiple icosahedral stack of the QuasiCrystal close-packing of tetrahedra





described in the paper at http://spahn.engin.umich.edu/publications/documents/2009_glotzer_188.pdf which shows double-6 tetrahelix structure.

As to the Fuller Jitterbug phase transition possibility, there is a paper by F. Calvo and A. Carre Structural transitions and stabilization of palladium nanoparticles upon hydrogenation Nanotechnology 17 (2006) 1292–1299 in which they said:

"... we investigate the energetic, thermal and dynamical stability of hydrogenated palladium nanoclusters containing a few hundred atoms.

At zero temperature, icosahedral clusters favour tetrahedral absorption sites, while cubic clusters preferentially absorb at octahedral sites.

...

Our first goal is to explore the relative stability of icosahedral and cubic structures containing an increasing amount of absorbed hydrogen, at zero temperature. For this the optimal geometries are located, and zero-point energy (ZPE) corrections are included.

...

[NOTE THAT ZPE CORRECTIONS ARE TO TAKE INTO ACCOUNT SUCH PHENOMENA AS THE CASIMIR EFFECT ETC AND ARE ACTUALLY NEEDED AND USED]

...

The ... crossover between icosahedral to cubic structures, is found ...[at about]... 270 atoms.

...

Due to the highly statistical character of our investigation, we had to restrict ourselves to specific cluster sizes, built upon the 147-atom Pd cluster.

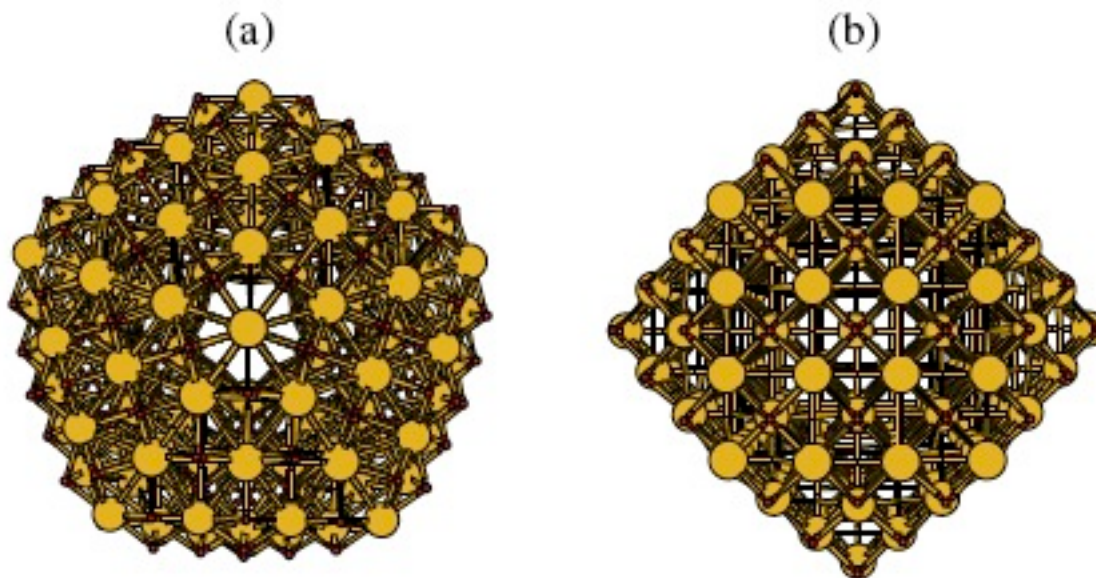


Figure 1. Palladium clusters fully loaded with hydrogen. (a) Pd₁₄₇H₂₀₀, I_h symmetry; (b) Pd₁₄₇H₁₆₄, O_h symmetry.

At this size, the favoured structure in the pure metal is the three-layer icosahedron. ... Several authors ... have emphasized the important influence of quantum delocalization on the stable structure of bulk hydrogenated palladium. ZPE effects have been proposed by Pitt and Gray to explain the observed tetrahedral occupancy of deuterium in palladium ...

In our case, and contrary to the study by Pundt et al on the much larger Pd₂₀₅₇ cluster ... our analysis suggests that increasing the hydrogen content should favour cubic structures over icosahedra. ...

The large icosahedral Pd–H clusters observed by Pundt et al ... could ... be due to a structural transition induced by temperature, rather than hydrogen content only. ...".

Jean-Francois Sadoc and Remy Mosseri in their book “Geometric Frustration” (Cambridge 2006) said: “... The {3,3,5} polytope [600-cell] contains altogether: 120 vertices, 720 edges, 1200 triangular faces, and 600 tetrahedral cells ...

Consider a {3,4,3} polytope [24-cell] which is a regular packing of octahedra on S³ [the 3-sphere in R⁴]. ...

then generate a new polytope ... { 3/4, 3 } ... whose vertices are located at the midpoints of the ... [96] edges ... [of the]... {3,4,3} and is a packing of cubo-octahedra and cubes ...

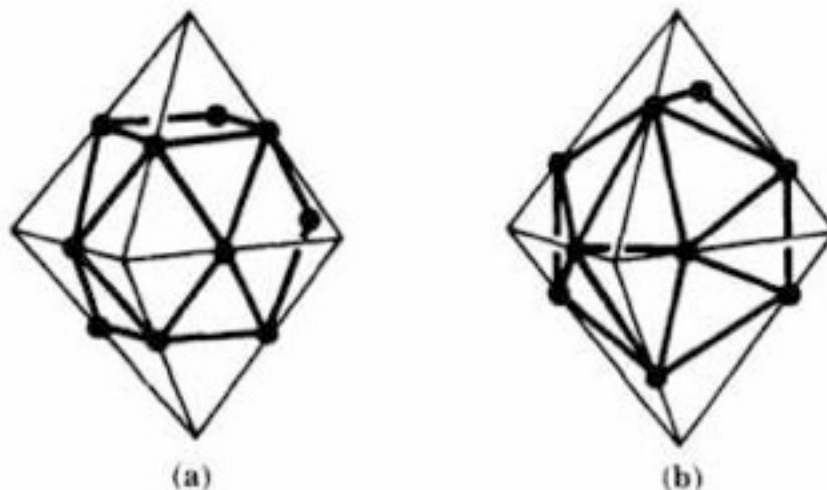


Fig. A6.4. Relation between an octahedron and (a) the cubo-octahedron or (b) the icosahedron.

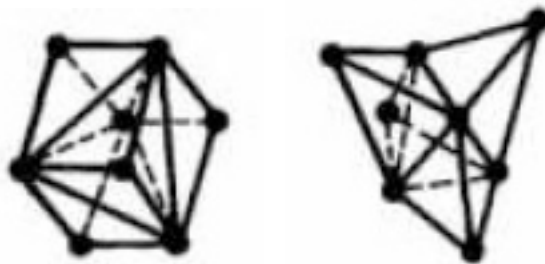
... consider a distorted form of this new polytope which amounts to displacing consistently the [96] new vertices on the [96] edges of the {3,4,3}, away from the mid-edges, but in the ratio $1 / T$ [where $T = (1/2)(1 + \sqrt{5})$] ...

Compare this image from the book “New Geometries for New Materials” (Cambridge 2006) by Eric A. Lord, Alan L. Mackay, and S. Ranganathan:



Figure 4.13 Buckminster Fuller’s ‘jitterbug’ transformation relating the cuboctahedron and the icosahedron.

]... This changes the cubo-octahedra into icosahedra and distorts each cube into five regular tetrahedra ...



... This new polytope, called the snub- $\{3,4,3\}$, contains 96 vertices, and is a packing of 120 tetrahedra and 24 icosahedra. Upon adding 24 new vertices in the centres of the icosahedra, a $\{3,3,5\}$ polytope [600-cell] is obtained. ...”.

In the Pd147 images of icosahedron and cuboctahedron structures, think of a Fuller Jitterbug/Tensegrity transformation between them and how it might push Deuterium nuclei close enough for fusion, and how each fusion reaction might trigger further Jitterbug/Tensegrity transformation of the Pd lattice thus causing a chain reaction.

Pd/Ni Clusters for D/H TSC Jitterbug Fusion

Frank Dodd (Tony) Smith Jr. - 2012

viXra 1209.0007

Clusters of Palladium atoms (also clusters of atoms of Nickel and similar elements) have two basic structures:

Icosahedral and Cuboctahedral

1 - Icosahedon <-> Cuboctahedron Jitterbug Transformation

2 - Pd/Ni clusters with absorbed Deuterium or Hydrogen have two states:

Icosahedral with Tetrahedral absorption sites

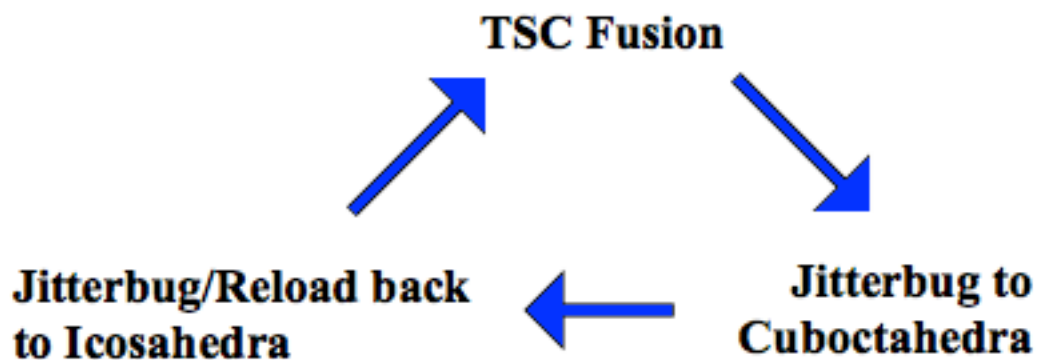
Cuboctahedral with Octahedral absorption sites

3 - Tetrahedral Symmetric Condensation (TSC) in PdD_x produces Fusion.

4 - Icosahedra TSC Fusion Triggers Jitterbug to Cuboctahedra.

5 - Cuboctahedra Jitterbug back to Icosahedra and reload TSC sites.

6 - Repeat the Cycle:



Akito Takahashi has developed a Tetrahedral Symmetric Condensate (TSC) model for fusion $D+D+D+D \rightarrow 8\text{Be}$ and $H+H+H+H \rightarrow 4\text{He}$ in Pd and Ni atomic clusters.

This paper describes the geometry of Pd/Ni atomic clusters and how it enables TSC fusion of D/H within the Pd/Ni clusters.

The basic TSC structure is a half-icosahedron with 10 approximate tetrahedra and approximate octahedron. The tetrahedra and octahedra are approximate because they do not fit together exactly within Pd/Ni atomic clusters because they must be slightly deformed from exactly regular tetrahedra and octahedra in order to fit together in our physical flat 3-dimensional space.

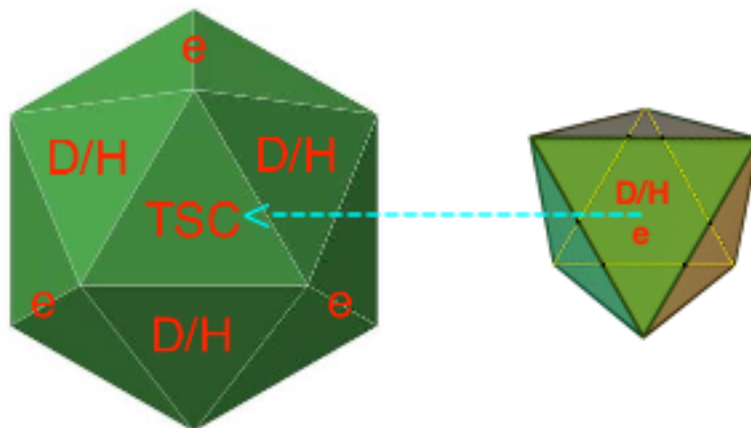
Details of the deformation are being studied by Klee Irwin and his coworkers Fang Fang, Julio Kovacs, and Garrett Sadler. Discussion with them led to the ideas described in this paper.

The vertices of the half-icosahedron and octahedron are positions of Pd/Ni atoms.

As to the half-icosahedron tetrahedral cells (images adapted from Wikipedia):

The central cell marked TSC is the cell in which the TSC fusion reaction takes place at the end of the TSC process. The 3 cells marked D/H initially (at the beginning of the TSC process) contain 3 of the 4 D or 4 H nuclei for TSC fusion.

The 3 pairs of cells marked e contain the electrons for those 3 D/H nuclei.



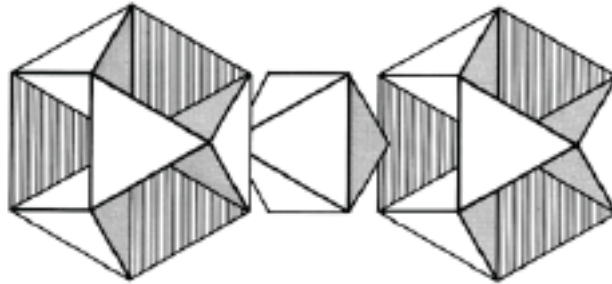
The octahedral cell marked D/H e is located in the atomic cluster directly above the TSC cell such that the TSC top face coincides with the bottom face of the octahedron containing the 4th of the 4 D/H nuclei for TSC fusion and its electron.

In TSC fusion the 4 D/H nuclei, Coulomb-shielded by their electron clouds, condense at the center of the TSC cell where their fusion produces 8 Be / 4 He.

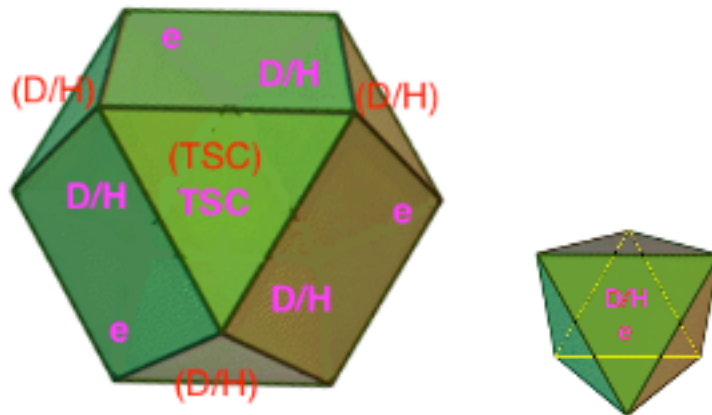
The icosahedral state at the beginning of the TSC process is the stable ground state for the Pd/Ni cluster.

When the TSC fusion energy is released, it drives the Pd/Ni cluster state

by a Jitterbug transformation to an expanded cuboctahedral state.
As Buckminster Fuller showed (Synergetics Macmillan 1975, 1982)



a cuboctahedron is made up of 8 tetrahedral and 6 half-octahedral cells. Since cuboctahedra and octahedra tile flat 3-space, the cells are exactly regular Jitterbug expansions of the approximate tetrahedra and octahedra of the ground-state icosahedral TSC cluster. Note that 2 of the icosahedral tetrahedra correspond by Jitterbug to one of the cuboctahedral half-octahedra. In the image below (adapted from Wikipedia)



The old TSC fusion cell (marked red (TSC)) becomes the new TSC fusion cell (marked magenta TSC) remaining unchanged in its function. Its adjoining 3 half-octahedral cells bring in 3 new D/H fusion fuel nuclei along with their corresponding 3 electrons (marked magenta D/H and e), which 3 electrons spread into empty cells (marked red (D/H)) that initially contained 3 of the D/H nuclei that fuelled the initial TSC fusion reaction. A 4th new D/H fuel nucleus and its electron (marked magenta D/H and e) move into the octahedron sharing a face with the TSC fusion cell.

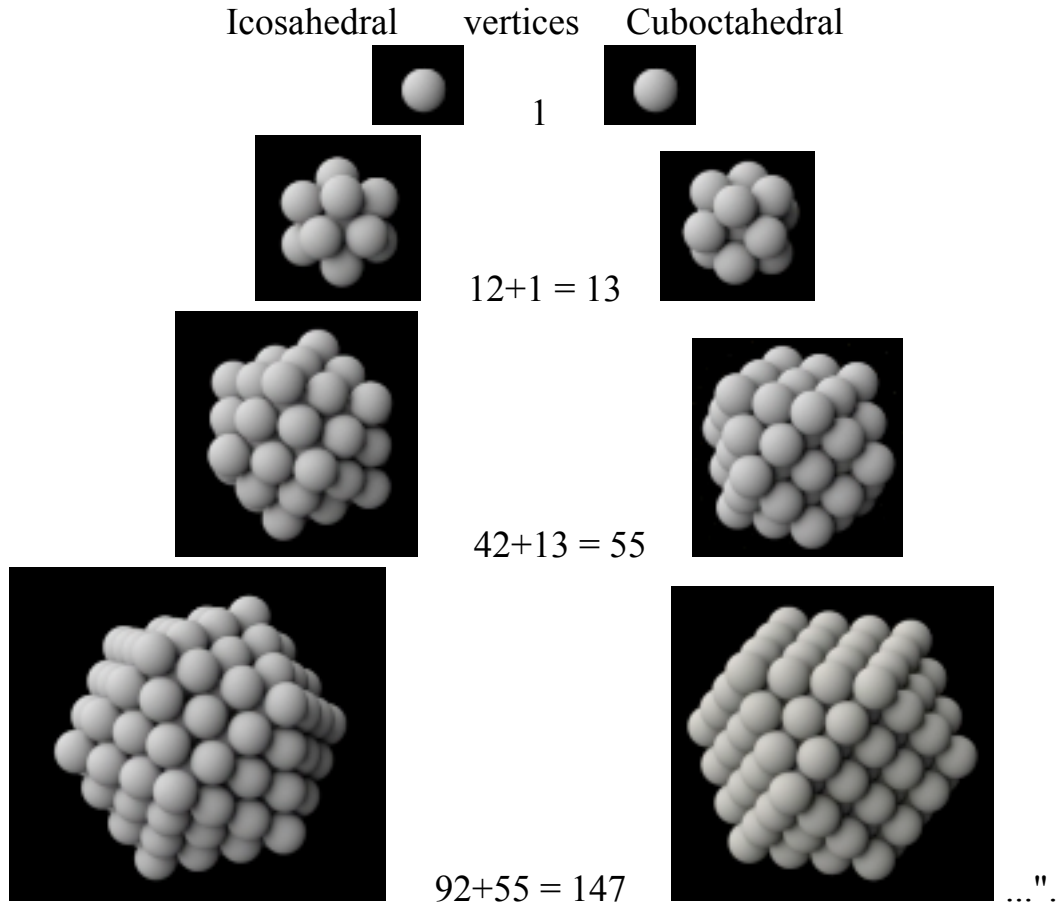
After the energy of the first TSC fusion dissipates, the cluster falls back into the icosahedral ground state for the next round of TSC fusion cycle.

What is the overall structure of the Pd/Ni clusters ?

There are two basic structures that are Jitterbug Transforms of each other:

Icosahedral and Cuboctahedral

From vimeo.com/27662398 by Yan Liang (L2XY2) August 2011: "...



How many TSC fusion sites are in a Pd/Ni cluster ?

A TSC fusion site has (icosahedral phase) a half-icosahedron plus an octahedron.

The 13-atom Pd/Ni cluster has a full icosahedron (two half-icosahedra) but does not have the necessary octahedron and so is not a TSC Fusion Cluster.

The 55-atom Pd/Ni cluster has a full icosahedron (two half-icosahedra) and two octahedra to form 2 TSC fusion sites, so it is a TSC Fusion Cluster of order 2.

The 147-atom Pd/Ni cluster has the 2 TSC fusion sites of the 55-atom TSC cluster plus 12 more half-icosahedra in its outer shells along with octahedra for each, so it is a TSC Fusion Cluster of order 14.

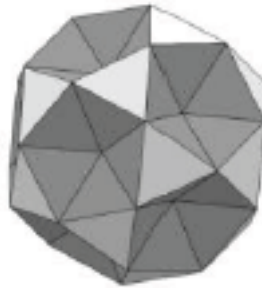
How do the Icosahedral Clusters grow to 147 atoms ?

Eric A. Lord, Alan L. Mackay, and S. Ranganathan say in

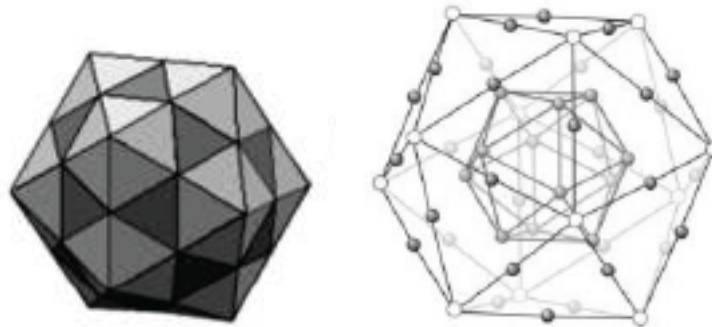
"New Geometries for New Materials" (Cambridge 2006):

"... The Mackay icosahedron is obtained by packing tetrahedra and octahedra around an icosahedron [12 vertices]...

if an octahedron is placed on every face of an icosahedron, the angular gap between neighboring octahedra can be closed by a very small deformation, to bring them into face contact [$12 + 20 \times (6-3)/2 = 42$ vertices]...



... The concave regions of the resulting polyhedron can be filled by five-rings of tetrahedra [$42 + 12 = 54$ vertices]...

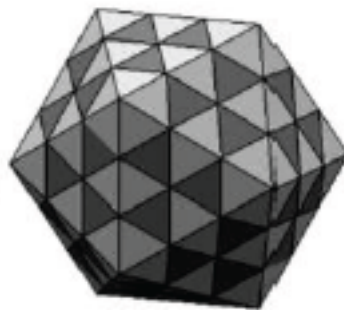


... The 54-atom Mackay cluster ...[triangles: dark = octahedra; light = tetrahedra]...

The process can be continued ...[with octahedra on each of the $12 \times 5 = 60$ outer cell faces of 5-rings thus adding $60 \times (2/2 + 1/3) = 80$ vertices and creating

12 TSC structures similar to half-icosahedra at the 12 vertices of the cluster.

This also creates concave places for 30 pairs of tetrahedra adding no vertices plus 12 tetra-5-rings adding 12 vertices for a total of $54+80+12 = 146$ vertices.



The 146-atom cluster

has $12+2 = 14$ TSC sites]..."

Lord et al use 12, 54, and 146 atoms for Mackay clusters
while Liang uses 13, 55, and 147 atoms.

The difference is whether or not the center vertex is counted, that is,
not so much a real physical difference but a difference in math convention.

What about more than 147 atoms ?

As more layers are added, the deformations of tetrahedra and octahedra accumulate
and eventually destabilize the structures necessary for the TSC fusion process.

The next Mackay cluster beyond 147 atoms has $147+162 = 309$ atoms,
and it is my guess that **147 atoms is optimal for TSC fusion:**

**55 atom clusters have only 2 TSC sites while 147 atom clusters have $2+12 = 14$
and**

309 (and larger) atom clusters may not be sufficiently stable.

Therefore, in a 147-atom Pd/Ni cluster:

each full set of TSC fusion events can consume $14 \times 4 = 56$ D/H nuclei.

How many D/H atoms can live in a 147-atom Pd/Ni cluster ?

F. Calvo and A. Carre say in Nanotechnology 17 (2006) 1292–1299

"Structural transitions and stabilization of palladium nanoparticles upon hydrogenation":

"... Cuboctahedra ...[and]... icosahedra ... contain exactly the same number of
atoms. ... In the case of ... the 147-atom Pd cluster ... the favoured structure in the
pure metal is the three-layer icosahedron.

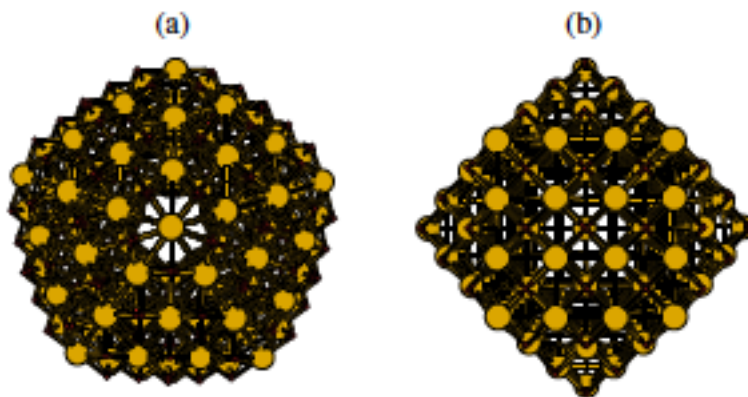


Figure 1. Palladium clusters fully loaded with hydrogen.

(a) $\text{Pd}_{147}\text{H}_{200}$, I_h symmetry; (b) $\text{Pd}_{147}\text{H}_{164}$, O_h symmetry.

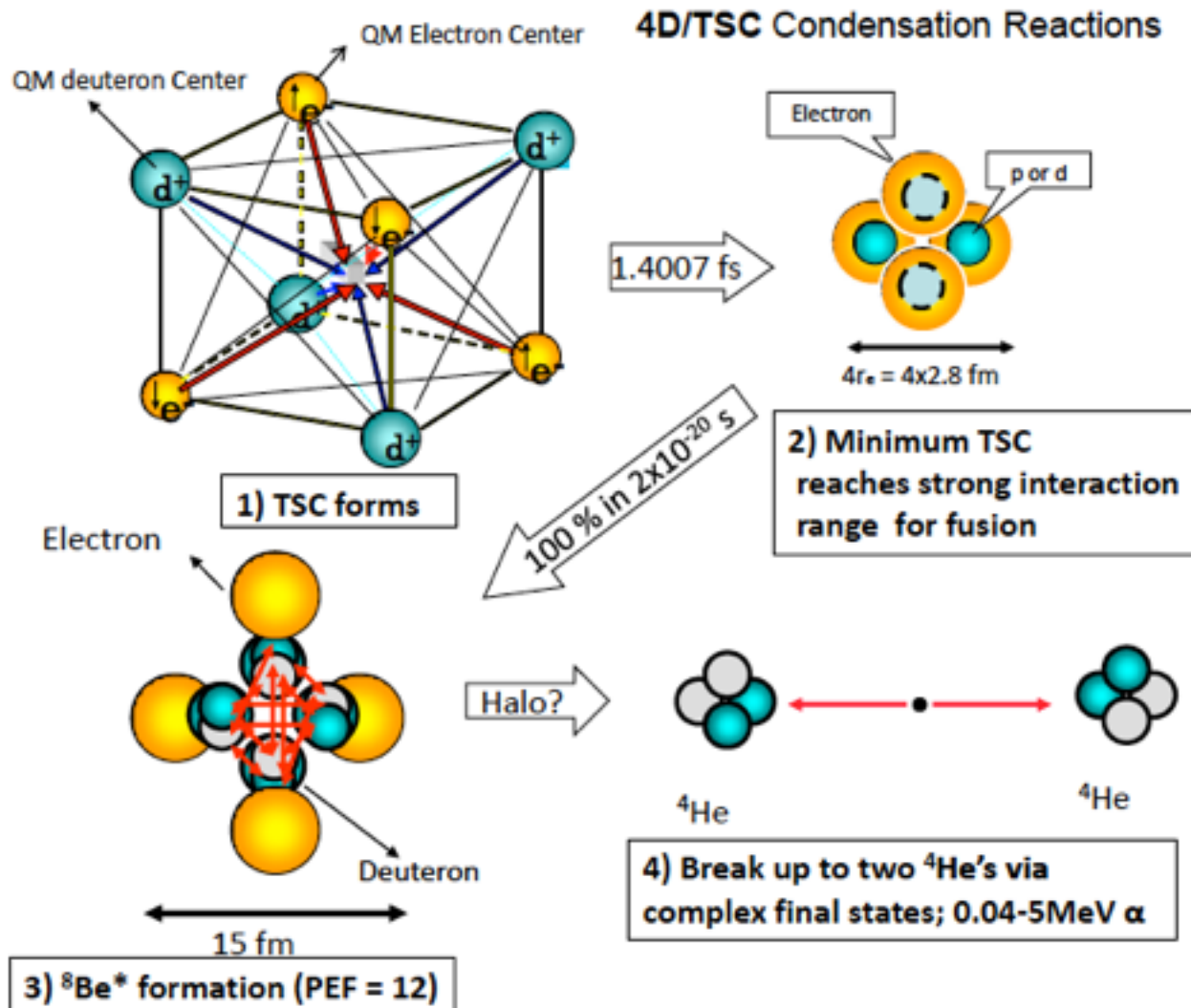
...".

Since the minimum full load for Icosa or Cubocta Pd/Ni 147-atom clusters
is 164 D/H atoms, no more than 3 cycles of full TSC fusion
(each consuming 56 D/H nuclei) can occur without replenishment of D/H from the
surroundings of the clusters (such as immersion of the clusters in D/H gas).

How does TSC Fusion work ?

Akito Takahashi in Physics of Cold Fusion by TSC Theory by Akito Takahashi ICCF17 12-17 August 2012 and J. Condensed Matter Nucl. Sci. 33 (2009) 33-44 and J. Condensed Matter Nucl. Sci. 1 (2007) 129-141 "... proposed ... **deuteron fusion process by ... Tetrahedral Symmetric Condensate (TSC) ...**

Every particle in TSC can make central squeezing motion with same velocity, to keep charge neutrality of total TSC system ... this squeezing motion can be treated as Newtonian mechanics until when four deuterons get into the range (about 5 fm) of strong nuclear interaction. ... TSC starts Newtonian squeezing motion to decrease linearly its size from about 100 pm radius size to ... the minimum size state ... as shown in ... Semi-classical view of squeezing motion of TSC, $\langle e \rangle = (e\downarrow + e\uparrow)/2$ for QM view at four electron centers ...

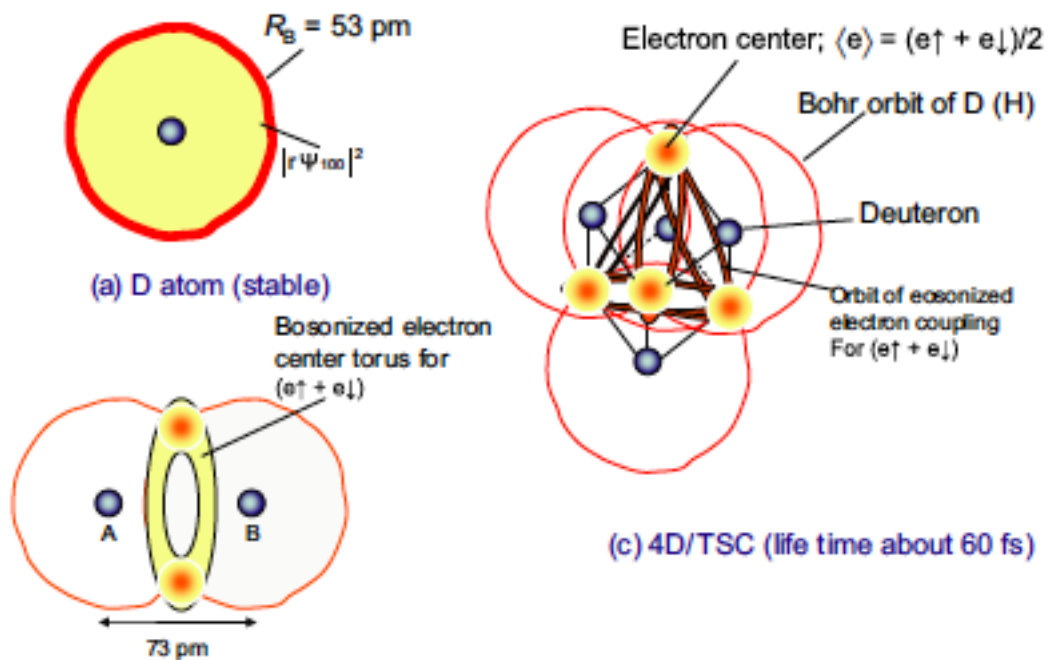


[Note that the TSC process is spontaneous not requiring initial stimulus.]

... Classical squeezing motion ends when four deuterons get into the strong force range (5 fm) and/or when four electrons get to the Pauli's limit (about 5.6 fm for e-e distance). Here for Pauli's limit, we used the classical electron radius of 2.8 fm ... Since the range of strong interaction is comparable to the classical electron diameter (5.6 fm) ... the intermediate nuclear state 8Be^* will be formed just after the minimum size state ...

Immediately at ... 8Be^* formation ... 4d-cluster shrinks to much smaller size (about 2.4 fm radius) of 8Be^* nucleus, and four electrons should go outside due to the Pauli's repulsion for fermions. Shortly in about few fs or less (note; Lifetime of 8Be at ground state is 0.67 fs), 8Be^* will break up into two 4He particles, each of which carries 23.8 MeV kinetic energy ...

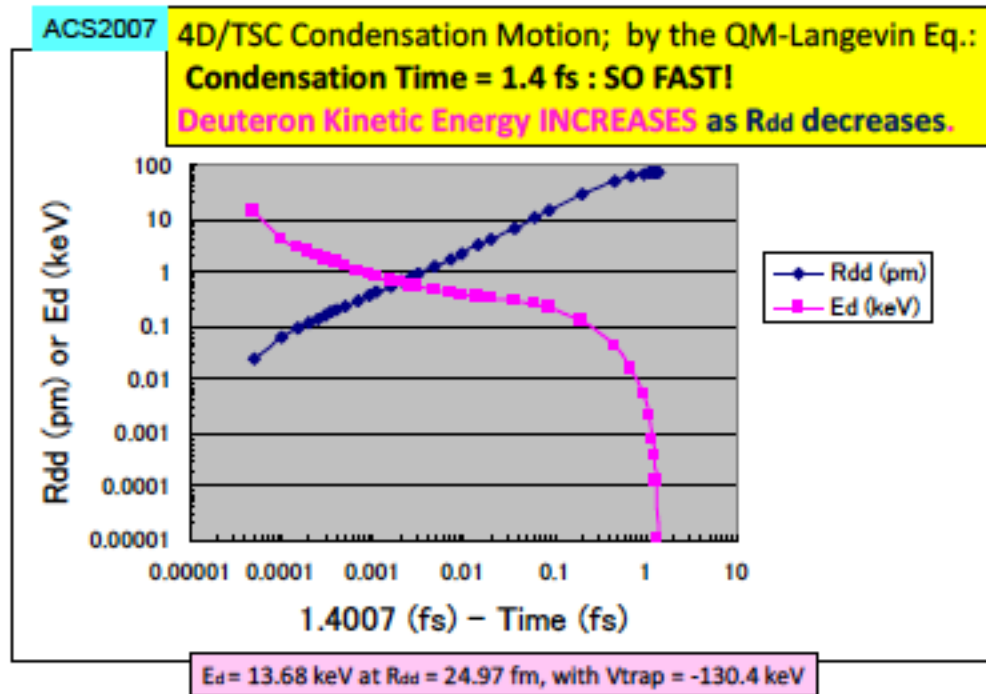
when TSC is just formed ... averaged electron position (electron center of $\langle e \rangle = (e\downarrow + e\uparrow)/2$, Bosonized electron pair ...) ... locates at vertexes of regular cube with tetrahedral combining orbits and outer dilute clouds ...



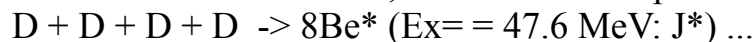
(b) D_2 molecule (stable): $\Psi_{2D} = (2+2\Delta)^{-1/2} [\Psi_{100}(r_{A1}) \Psi_{100}(r_{B2}) + \Psi_{100}(r_{A2}) \Psi_{100}(r_{B1})] X_s(S1, S2)$

... At ... cube ... vertexes ... three Bohr wave functions superpose and electron density is about nine times larger than that of outer dilute cloud. Therefore, the semi-classical treatment of central squeezing motion by Newtonian is approximately fulfilled for "coherent" central averaged momentums for eight particles. ...

As soon as 4D/TSC($t=0$) state with D₂ molecule size ($R_{dd} = 74$ pm) is formed ... the QM-Langevin equation gives numerical solution for time-dependent R_{dd} and mean relative kinetic energy of d-d pair of a face of 6 TSC (d-e-e-d-type) faces, as copied from reference and shown in Fig.10. ...



... The ‘adiabatic’ size of 4D/TSC reaches at a few tens fm size in 1.4 fs, so fast. With adiabatic 4D/TSC size around 20 fm, 4D-fusion takes place by ...



Fusion yield per 4D/TSC generation is calculated by integrating time-dependent fusion rate by the Fermi’s first golden rule ... that was very close to 1.0, namely 100%, during the very small time interval of ca. $2 \times 10^{(-20)}$ s in the final stage of condensation.

Mean relative kinetic energy of neighboring d-d pair of 4D/TSC-minimum is ca. 14 keV, which is accidental resembling value to the hot fusion experimental devices as ITER (DT plasma).

...

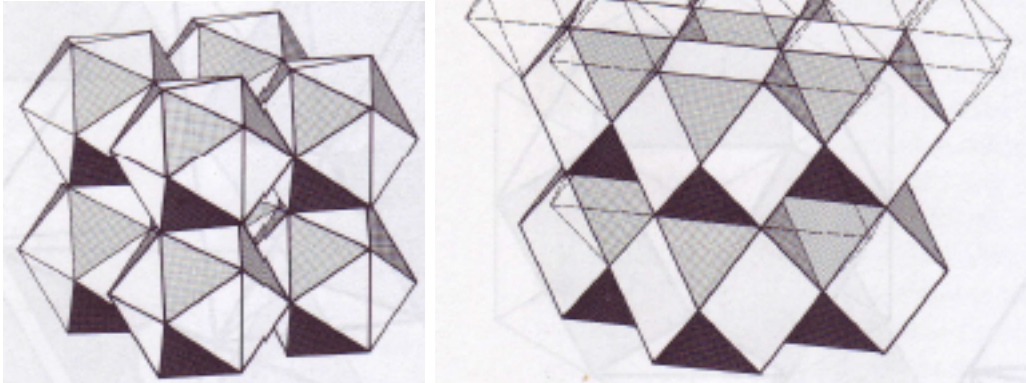
the quantitative study on the **TSC formation probability in D(H)-loaded metal systems is yet to be done** by solving many-body time-dependent problems under organization field of condensed matter. It is challenging work ...".

The answer to that challenge may be

the Icosahedra <-> Cuboctahedra Jitterbug Transformation.

What is the Jitterbug Transformation ?

Icosahedra and Cuboctahedra both have 12 vertices so that it is possible to transform them into each other. Buckminster Fuller called that transformation the Jitterbug



(images from Synergetics by Buckminster Fuller (Macmillan 1975, 1982))

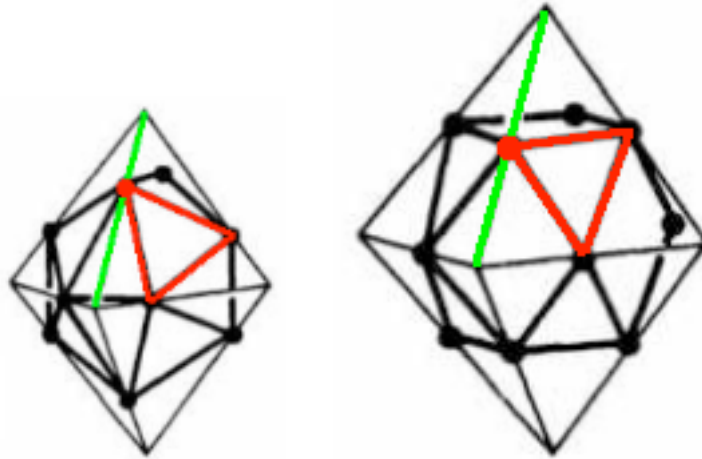
To make Cuboctahedra (unit edge length) from Icosahedra (unit edge length) choose 6 pairs of Icosahedra triangle faces (white in the above images) and lengthen the common edge of each pair by a factor of $\sqrt{2}$. That expansion flattens each of the triangle pairs to produce 6 square faces of the Cuboctahedron. The other Icosahedral $20 - 2 \times 6 = 8$ (shaded) triangle faces are rotated and become the other $14 - 6 = 8$ triangle faces of the Cuboctahedron.

thus increasing the number of faces from $8+6 = 14$ to $8+(6+6) = 20$ while keeping the number of vertices constant at 12.

There are two ways to choose a diagonal of an Icosahedron triangle face pair in the construction, corresponding to the two possible orientations of an Icosahedron.

Choice of diagonal for one Icosahedra triangle face pair forces (by requiring consistency) the choices for all other face pairs of all Icosahedra.

The triangle faces of the Icosahedron/Cuboctahedron are rotated by a Golden Ratio



(images adapted from Geometrical Frustration by Sadoc and Mosseri (Cambridge 2006))

angle defined by
 sliding Icosahedron vertices on the edges of a circumscribing Octahedron
 from points dividing edges into Golden Ratio segments
 to points dividing edges into two equal segments
 so that the Octahedron then circumscribes a Cuboctahedron.
 If the edge lengths of the Icosahedron/Cuboctahedron are kept the same
 then the Octahedron surrounding the Cuboctahedron will be an expansion
 of the Octahedron surrounding the Icosahedron.

Just as in the choice of a Cuboctahedron square diagonal to be compressed,
 there are two ways in which the edge could be divided into Golden Ratio segments,
 corresponding to the two possible orientations of an Icosahedron.

Choice of Golden Ratio segments for one edge forces (by requiring consistency)
 the choices for all other edges.

The volume expansion of the Jitterbug Transformation
 from Icosahedron (unit edge) to Cuboctahedron (unit edge) is:

$$\text{Icosahedron volume} = (5/12) (3 + \text{sqrt}(5)) = 2.18169499$$

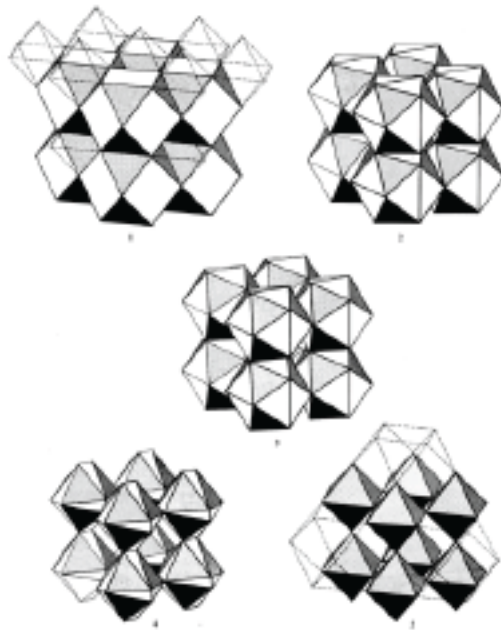
$$\text{Cuboctahedron volume} = (5/3) \text{sqrt}(2) = 2.3570226$$

$$\text{Icosahedron/Cuboctahedron volume ratio} = 0.9256147947$$

$$\text{Cuboctahedron/Icosahedron volume ratio} = 1.0803630254$$

Why do Jitterbug Transformations move D/H among the cluster cells ?

The Jitterbug Transformation proceeds:
from the cuboctahedral state (top left)
to an intermediate state (top right)
to an icosahedral state (center)
to another intermediate state (bottom left)
to a dual cuboctahedral state (bottom right)



(images from Synergetics by Buckminster Fuller (Macmillan 1975, 1982))

and then back up in reverse order to the original cuboctahedral state.

Since the dual cuboctahedral state interchanges octahedra and cuboctahedra with respect to the original cuboctahedral state,

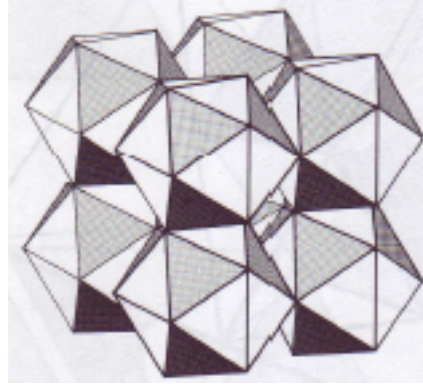
**the D/H fusion fuel nuclei are moved from cell to cell
by the Jitterbug transformations**

thus enabling

reloading of fusion fuel into the TSC fusion cell sites.

Pd/Ni and D/H Fusion from Jitterbug TSC: Mechanical Analogy

(with Colt Series 80 Government 10 mm Delta Elite version of Browning's M1911 semi-auto)



"... The M1911 ... use[s] ... the short recoil ... action ... Cycle ...

1. Ready to fire position. [Slide] is locked to barrel, both are fully forward.

[Icosahedral Pd with D atoms in TSC positions]

2. Upon firing, [slide] and barrel recoil backwards a short distance while locked together. Near the end of the barrel travel, the [slide] and barrel unlock.

[Firing = D-D Fusion]

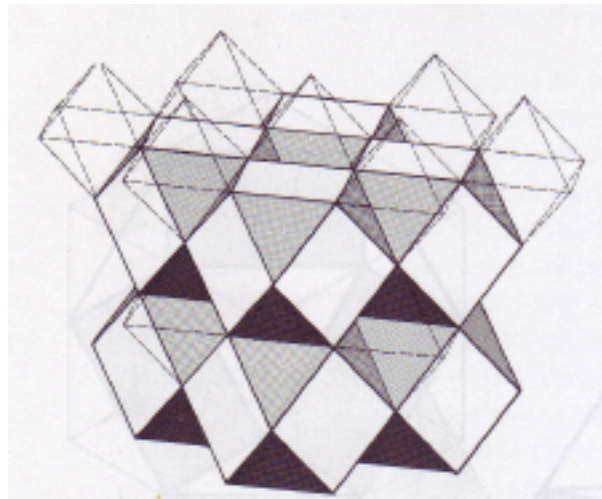
3. The barrel stops, but the unlocked [slide] continues to move to the rear, ejecting the empty shell and compressing the recoil spring.

[Recoil Spring = Icosahedral Stability Phase induces transformation of Cuboctahedra]

4. The [slide] returns forward under spring force, loading a new round into the barrel.

[Loading New Round = Cuboctahedral D atoms moved to Icosahedral TSC positions]

5. [Slide] locks into barrel, and forces barrel to return to battery.



... The very first short-recoil-operated firearm was also the first machine gun, the Maxim gun.

... Vladimirov also used the short recoil principle in the Soviet KPV-14.5 heavy machine gun. ..."

(quote from Wikipedia entries on M1911 pistol and on Recoil operation)

n = number of shells
 N = number of Pd atom vertices
 d = diameter of icosahedral configuration in nm
 C = number of cells in icosahedral phase
 CT = number of tetrahedral cells in icosahedral phase
 CO = number of octahedral cells in icosahedral phase

n N d $C = CT + CO$

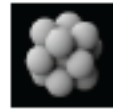
0 1 0.27 $0 = 0 + 0$

icosahedral   cuboctahedral

1 13 0.70 $20 = 20 + 0$



icosahedral



cuboctahedral

2 55 1.13 $100 = 80 + 20$

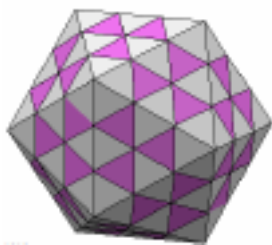


icosa

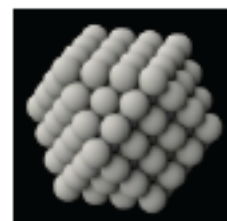
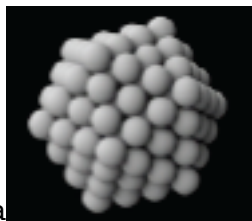


cubo

3 147 1.56 $280 = 200 + 80$



icosa

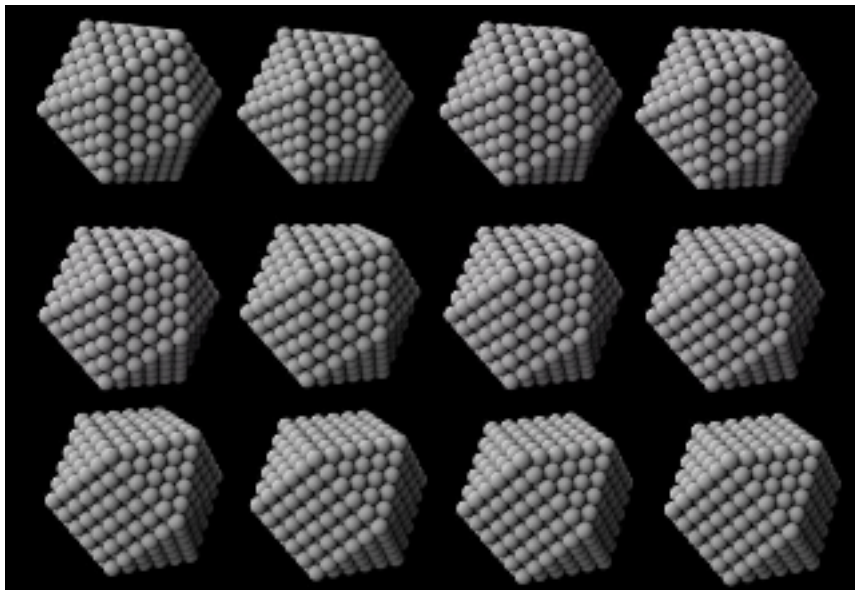


cubo

4 309 2.00 (icosa and cubo images not shown)

n N d(icosahedron)(nm)

5 561 2.44 12 stages of Jitterbug between
icosahedron (top left) and cuboctahedron (bottom right):



At the 5-shell level the Jitterbug transformation is harder to do than at lower levels.

Also, as the shell level and number of atoms increases and the configurations become larger the icosahedral phase becomes less stable.

6 923 2.88

7 1415 3.33

8 2057 3.77

9 2869 4.21

10 3871 4.65

11 5083 5.09

12 6525 5.53

(Images from: Polyhedral Clusters by Lord et al;
Frank and Kasper in Acta Cryst. 11 (1958) 184-190;
Mackay in Acta Cryst. 15 (1962) 1916-1918;
vimeo.com/27662398 by Yan Liang (L2XY2) August 2011.
Data for n, N, and d from Shtaya-Suleiman dissertation Gottingen 2003.)

147-atom Pd clusters have diameter about 1.56 nm according to 2003 Gottingen dissertation of Mohammed A . M. Shtaya-Sulieman at <http://webdoc.sub.gwdg.de/diss/2004/shtaya-suleiman/>

1.5 nm Pd clusters have been produced at Sandia National Laboratories and University of New Mexico Center for Micro-Engineered Materials according to a Journal of Catalysis article "Facile, surfactant-free synthesis of Pd nanoparticles for heterogeneous catalysts" at <http://www.flintbox.com/public/filedownload/2871/2011-038%20Science%20Direct%20Article> by Patrick D. Burton, Timothy J. Boyle, and Abhaya K. Datye.

I would like to see an experiment in which 1.5 nm Pd nanoparticle clusters from Sandia / U. New Mexico are immersed in Deuterium to see whether or not TSC fusion takes place.

Jitterbug Cold Fusion

Fang said in email 18 July 2011:

"... the Phi angle = 60 degree - 2 x the Jitterbug angle, which equals to the angle between the two opposing outer faces of a 20G twist. I was staring at the 20G twist trying to find some clues and suddenly this thought hit me and I immediately verified it. The following is a review of those two angles ...

Green Triangle Edge - length : a
Red Triangle Edge - length : b

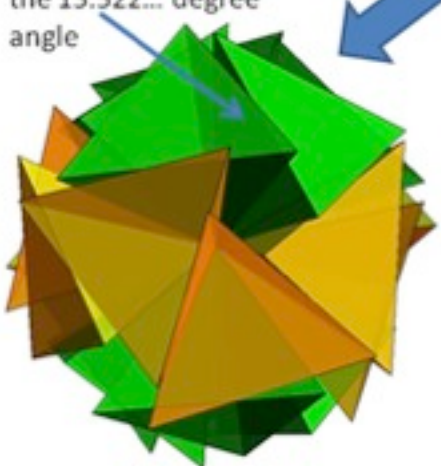
$$\frac{b}{a} = \frac{2\sqrt{2}}{\phi^2}$$

Green: cuboctahedron triangle face
Red: icosahedron triangle face

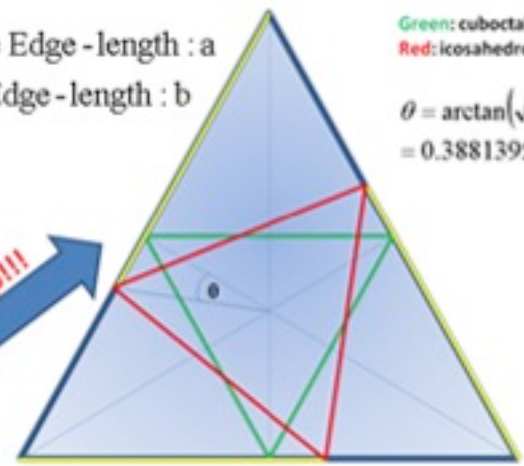
$$\theta = \arctan(\sqrt{3}(2\phi - 3))$$

$$= 0.388139515 = 22.2387561^\circ$$

Notice the relative angle between each touching face pairs is the 15.522... degree angle



Exact same relationship!!!



If we rotate each tetrahedron back to its normal (no splay or twist) position while expanding the edge-length of the outer faces of the tetrahedra (keeping the center of the faces fixed) to form a perfect icosahedron, then the ratio of the icosahedron edge-length to the original tetrahedral edge-length is

$$\frac{2\sqrt{2}}{\phi^2}$$

And the angle rotated here is

$$\arctan(\sqrt{3}(2\phi - 3)) = \arctan(\sqrt{3} / \phi^3) = 22.2387561^\circ$$

...".

Look at the 4 tetrahedra whose exterior faces are marked with red dots:



Their faces are parallel to the 4 of the 8 triangular faces of a cuboctahedron.

If you add the 4 antipodal faces,
you represent all 8 triangular faces of a cuboctahedron.

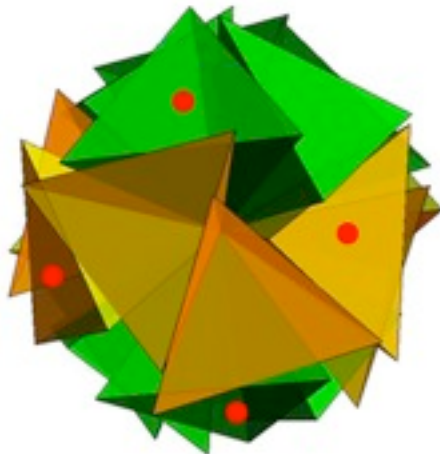
The $20 - 8 = 12$ remaining tetrahedra fall into 2 sets:

One set of 6 represents 6 of the 20 faces of an icosahedron
that is a + jitterbug transformation of the cuboctahedron
and
the other set of 6 represents 6 of the 20 faces of an
icosahedron
that is a - jitterbug transformation of the cuboctahedron.

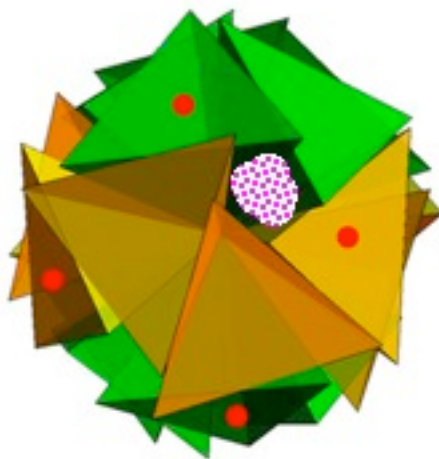
Therefore,
the twisted icosahedron represents through the jitterbug
transformation
both the cuboctahedron
and
the two orientation states of the icosahedron
(choices of how you take the Golden Ratio of octahedron edges).

Start with the twisted icosahedron

It is a very open structure as it contains faces parallel to the 8 triangular faces of a cuboctahedron (the most open state of the jitterbug).

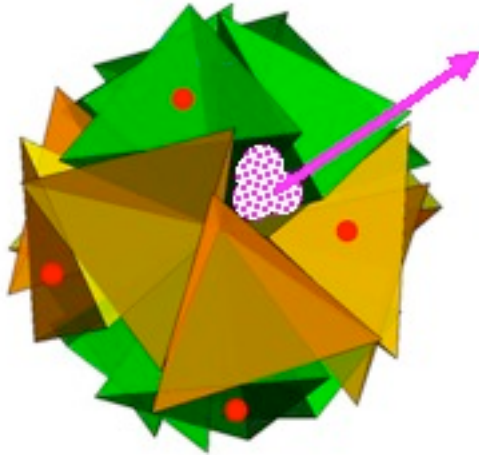


Consider it to represent a cluster of Palladium atoms with a lot of Deuterium (magenta dots) in the spaces between the atoms.

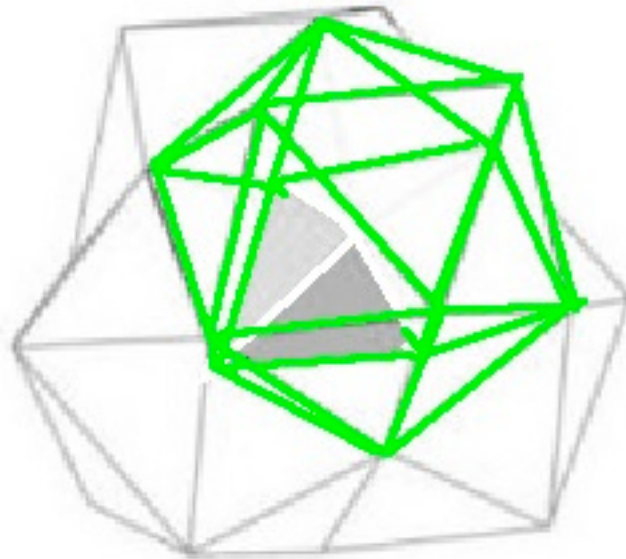


Now close up the icosahedron by untwisting the 20 so that they all fall into the close-as-you-can-get-in-flat-3dim icosahedron configuration and

by doing so
force the deuterium out as jets from each of the 12 pentagon-
cross-section holes.
(only one is shown in the image)

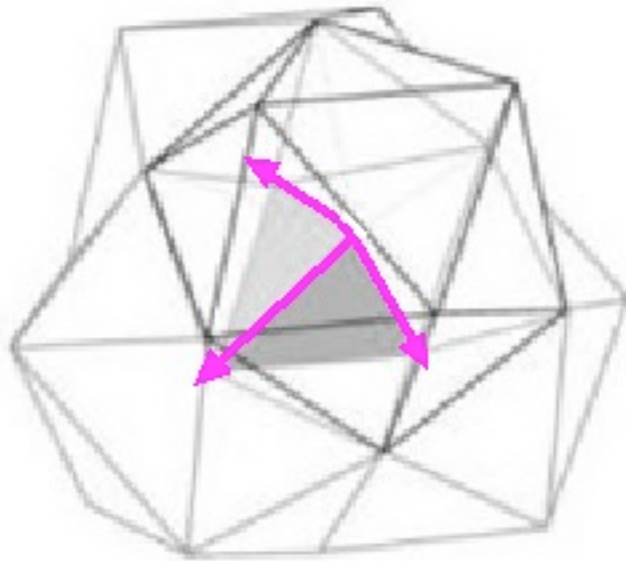


Now consider that the 57-group is the really fundamental
structure
and that the icosahedron we have been playing with is
the icosahedron outlined in green in the 57-group image.

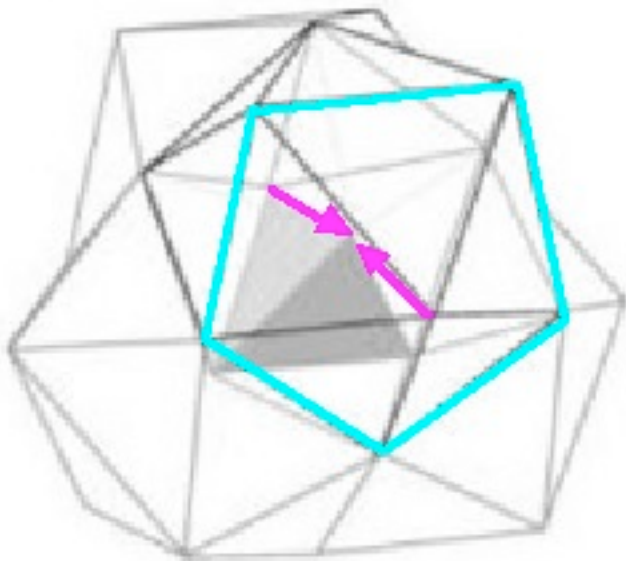


Of the 12 Deuterium jets being forced out of the green
icosahedron in the 57-group

3 (magenta arrows) of the 12 jets go to the INTERIOR of the 57-group



Each of those 3 jets go towards one of the outer 5-group on the outside opposite the green icosahedron. Shown below is one of the 3 jets as it meets a smaller jet from its corresponding outer 5-group (cyan pentagon).

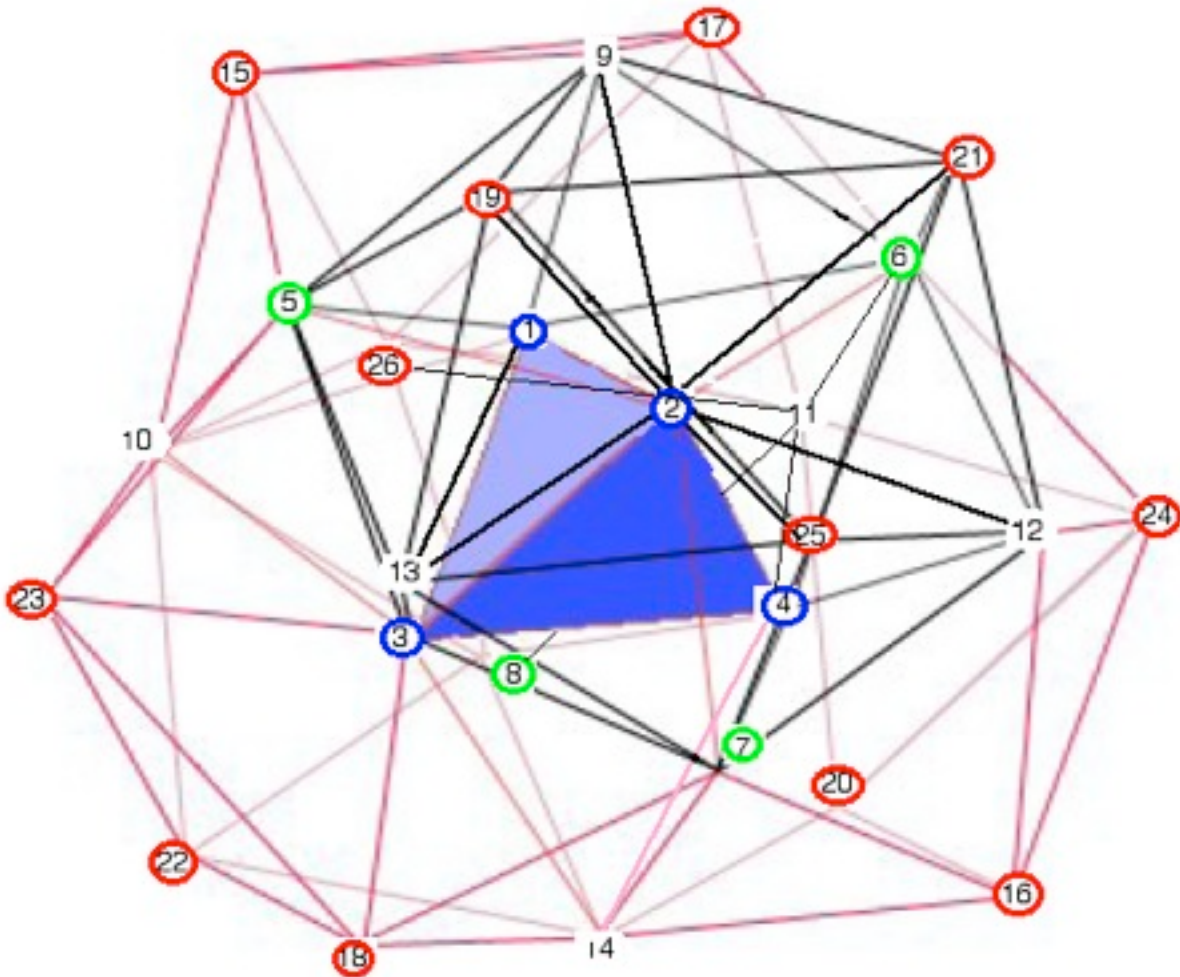


The collision of the jets of Deuterium force some of the Deuterium nuclei close enough to each other to fuse into Helium4 Alpha particles. Thus: **COLD FUSION FROM JITTERBUG TRANSFORMATION.**

57-group Tetrahedra, Faces, Edges and Vertices

Frank Dodd (Tony) Smith, Jr. - 2011 (unless otherwise credited, diagrammatic images are from, or adapted from, works of Lord, Mackay and Ranganathan, or from Wolfram Math World, or from Mathematica models of Garrett Sadler)

The 26 vertices of the 57-group are shown here numbered from the inside out:
1 - 4 (blue) are vertices of the central tetrahedron;
5 - 8 (green) are exterior vertices of the 4 tetrahedra face-joining the center;
9 - 14 (white) are an octahedron of 6 vertices on the outside of the 57-group;
15 - 26 (red) are a cuboctahedron of the outermost 12 vertices on the outside of the 57-group.



This is an effort to look at structures of the 57-group (edges may not be exactly accurate) in terms of vertices that might be shared if gaps were zero, and to compare that with the point of view of looking at edges or faces or tetrahedra that might be shared (or, for tetrahedra, in full contact) if gaps were zero.

If all the 57-group tetrahedra were separate, then there would be:

57 tetrahedra

228 faces = $57 \times 4 = 228$

342 edges = $57 \times 6 = 342$

228 vertices = $57 \times 4 = 228$

If all the tetrahedra were fit together without gaps,
by merging neighboring faces, edges, and vertices,
then there would be:

tetrahedra = 57 = 17 interior + 40 with one exterior face

faces 228 = $(17 \times 4 + 40 \times 3) + 40 = 188 + 40 = 94 \times 2 + 40$

so that there are

94 merged from a full interior pair 2

40 not merged because exterior faces are not paired

for a total, after merger, of 134 faces of which

94 were merged pairs and 40 were not merged at all.

(The 94 merged pairs have $94 \times 3 = 282$ merged vertices,

but this is NOT a full accounting of vertex mergers because

the vertices of the 40 exterior faces have been omitted

as are are mergers of vertices that are not on the same merged face.

A full accounting of all vertices in terms of dodecahedra / partial dodecahedra is
given below.

edges 342 that after merger become 102

as described in detail below.

vertices 228 = $4 \times 20 + 4 \times 10 + 6 \times 8 + 12 \times 5 = 80 + 40 + 48 + 60$

so that there are

4 merged from a full dodecahedral 20

4 merged from a partial dodecahedral 10

6 merged from a partial dodecahedral 8

12 merged from a partial dodecahedral 5

for

a total of $4 + 4 + 6 + 12 = 26$ merged vertices.

Vertices:

Seperately, the 57 tetrahedra of the 57-group have:

57 tetrahedra

228 faces = $57 \times 4 = 228$

342 edges = $57 \times 6 = 342$

228 vertices = $57 \times 4 = 228$

Merged within the 57-group, there are 26 vertices.

Each of the 26 vertices, if the gaps were non-zero, would split into a number of different vertices, one for each tetrahedron sharing that vertex.

For example:

each of the 4 blue vertices of the central tetrahedron would split into 20 vertices, one for each of 20 tetrahedra in an icosahedron;

each of the 4 green vertices would split into 10 vertices;

each of the 6 white vertices would split into 8 vertices;

each of the red $4 \times 3 = 12$ outermost vertices would split into 5 vertices

for

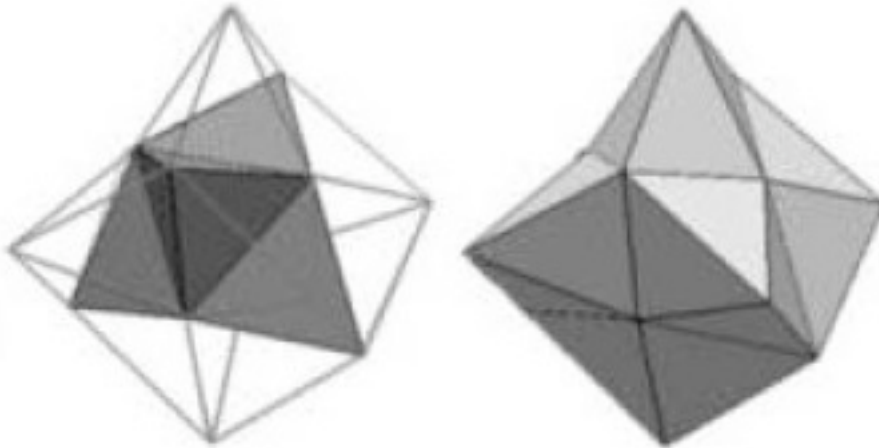
a total of $4 \times 20 + 4 \times 10 + 6 \times 8 + 12 \times 5 = 228$ vertices if all gaps were non-zero.

(Note that if the central 4 vertices were not split (as it is possible in flat space for them to have no gap) then that would reduce their splitting from 20 vertices to 17 so that

the split vertex total would then be $228 - 12 = 216$.

Note also that if all 26 vertices were in a large enough configuration that all 26 were internal and so an interior part of an icosahedron, the split vertex total would then be $26 \times 20 = 520$.)

The $1 + 4 + 12 = 17$ inside tetrahedra (17-group) look like
 (in the illustrations here I am closing all the gaps to zero -
 you can consider that to be done either by deforming some tetrahedra
 or by curving the 3-dim space where they are)

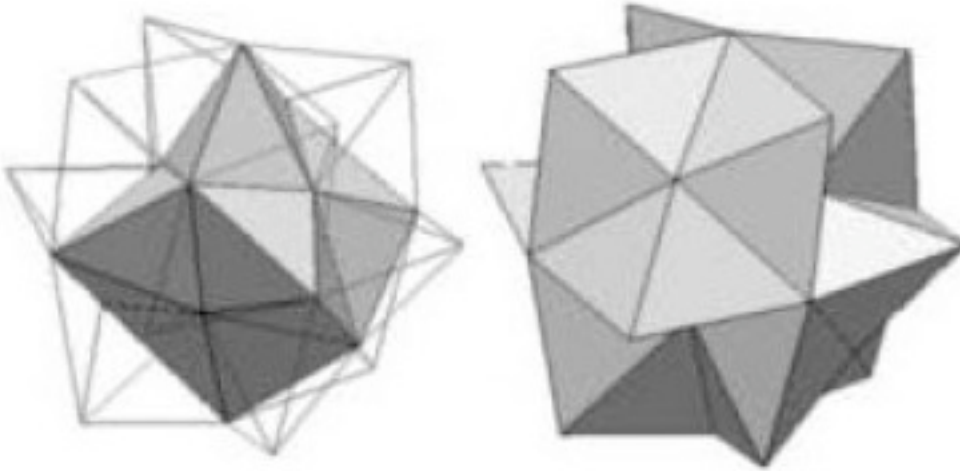


with 17 tetrahedra and (with gaps closed to zero) $4+4+6 = 14$ vertices.

Each of the 4 tetrahedra that share a face with the 1 central tetrahedron
 is
 now sharing its other 3 faces with 3 new tetrahedra
 so that
 its only exterior elements are its 3 edges that
 are not shared with the 1 central tetrahedron.

There are $4 \times 3 = 12$ such exterior edges in the 17-group.
 At each of them you can add 2 new tetrahedra sharing that edge,
 so that
 each of those 12 exterior edges becomes the center axis of a 5-group
 and is under one of 12 new vertices.

That is effectively adding $12 \times 2 = 24$ outside tetrahedra
 and 12 outside vertices to get



$17+24 = 41$ tetrahedra (the 41-group) with $14+12 = 26$ vertices.

NOTE THAT AT THIS STAGE ALL THE 5-GROUPS THAT CONTAIN ONE OF THE 4 TETRAHEDRA AROUND THE CENTRAL TETRAHEDRON ARE COMPLETE

and

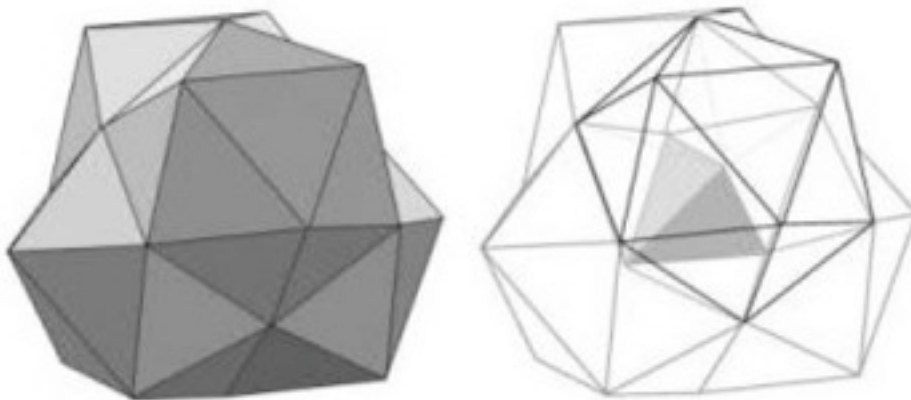
all 26 vertices of the 57-group are present

but

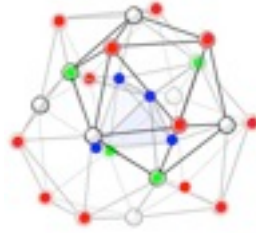
you have to add 16 more tetrahedra

to get the full $16+24 = 40$ exterior tetrahedra of the 57-group.

You can do that WITHOUT adding any more vertices, getting



all 57 tetrahedra and 26 vertices.



The 4 blue vertices are the central tetrahedron.

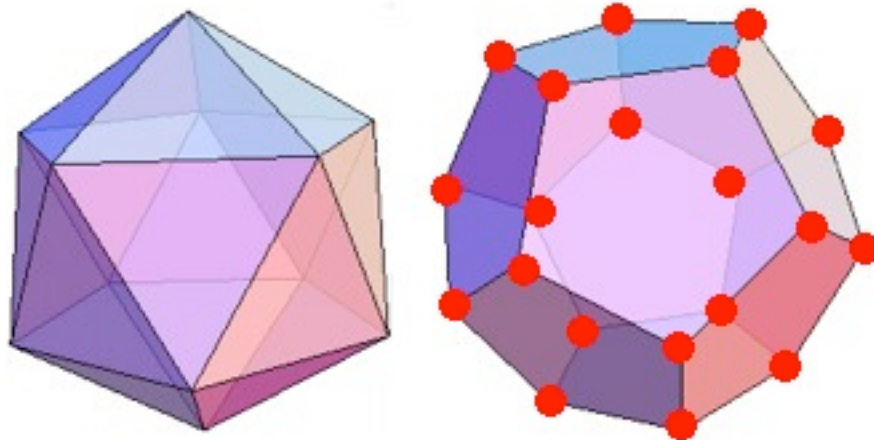
The 4 green vertices are an outer tetrahedron formed by the outer 4 vertices of the 4 tetrahedra that contact the central tetrahedron.

The 6 white vertices are an octahedron formed by the outer 6 vertices of the 12 outer tetrahedra of the $1+4+12 = 17$ -group.

The 12 red vertices are a cuboctahedron formed by the outer $4 \times 3 = 12$ vertices of the 12 outer tetrahedra of the $17+24 = 41$ -group and also are the outermost vertices of the 4 icosahedra that intersect to form the 57-group (3 vertices on each of the outer triangular face of each of the 4 intersecting icosahedra).

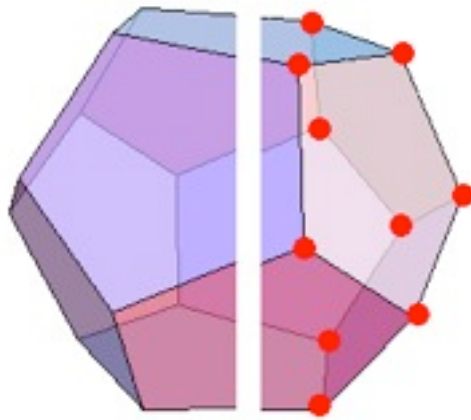
Each of the 26 vertices of the 57-group, if the gaps were non-zero, would split into a number of different vertices, one for each tetrahedron sharing that vertex.

Each of the 4 blue vertices of the central tetrahedron is entirely surrounded by other tetrahedra as part of the maximal subgroups of 20 that form icosahedra. Each of them would split



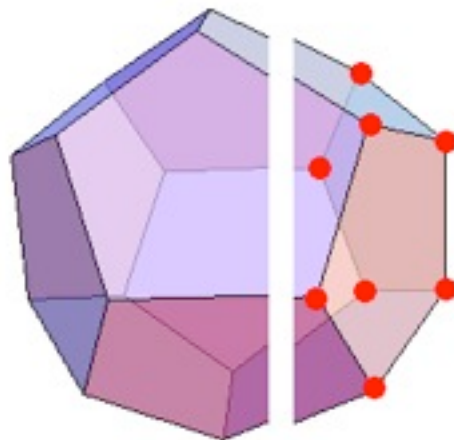
into 20 vertices, one for each of 20 tetrahedra in an icosahedron. Fang Fang has noted that the 20 vertices resulting from the splitting can be seen as the 20 vertices of a dodecahedron with distortion from a regular dodecahedron being a measure of the size of gaps related to the vertex from which the 20 split.

Each of the 4 green vertices would split



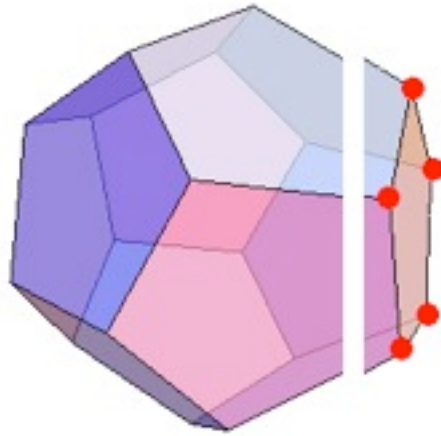
into 10 vertices;

Each of the 6 white vertices would split



into 8 vertices;

Each of the red $4 \times 3 = 12$ outermost vertices, being outermost and only sharing with 4 others of an outside 5-group subset of the 57-group, would split



into 5 vertices

for

a total of $4 \times 20 + 4 \times 10 + 6 \times 8 + 12 \times 5 = 228$ vertices if all gaps were non-zero.

As to how to use dodecahedra-split vertices to do calculations for the 57-group:

1 - There are 26 dodecahedra linked together in the 57-group, so it is more complicated than just seeing how one dodecahedron works, but looking at one dodecahedron is a start.

2 - Since the dodecahedron is the simplest fullerene, known as C₂₀ because the dodecahedron fullerene is made up of 20 carbon atoms, and since fullerenes have been studied theoretically and experimentally a lot in the past couple of decades, here are a few references to papers about C₂₀ fullerene structure:

http://www.maa.org/mathland/mathtrek_9_18_00.html
general article

<http://arxiv.org/abs/chem-ph/9409001>

by Peter R. Taylor, Eric Bylaska, John H. Weare,
and Ryoichi Kawai

"... the smallest fullerene, the dodecahedron C₂₀,
has the lowest energy ...[of]... 20-atom carbon species ...".

<http://digitalcommons.unl.edu/cgi/viewcontent.cgi?article=1019&context=chemzeng>
about calculations of stability

http://www.people.vcu.edu/~qwang/_pdfs/02-PRB-Si20.pdf
about similar Silicon 20-atom structure

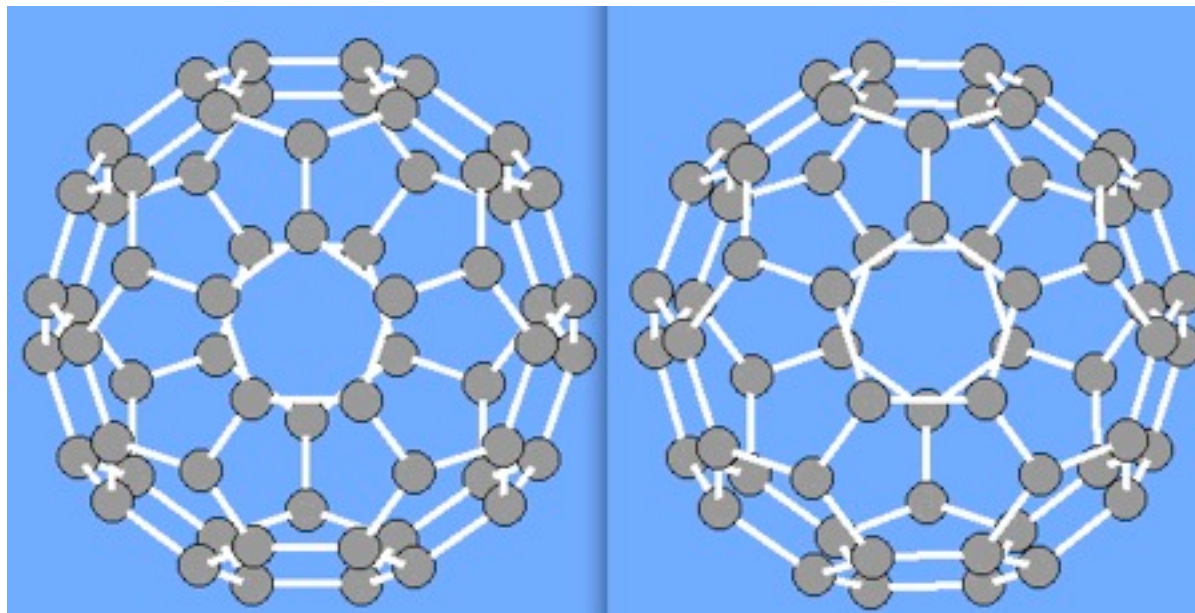
http://www.lsu.edu/departments/flin/papers/C20_extend_model_J_Phys_Cond_Matt19_456206.pdf
about Hubbard model for C20

<http://citeseerx.ist.psu.edu/viewdoc/download?doi=10.1.1.4.5197&rep=rep1&type=pdf>
about resistance distances

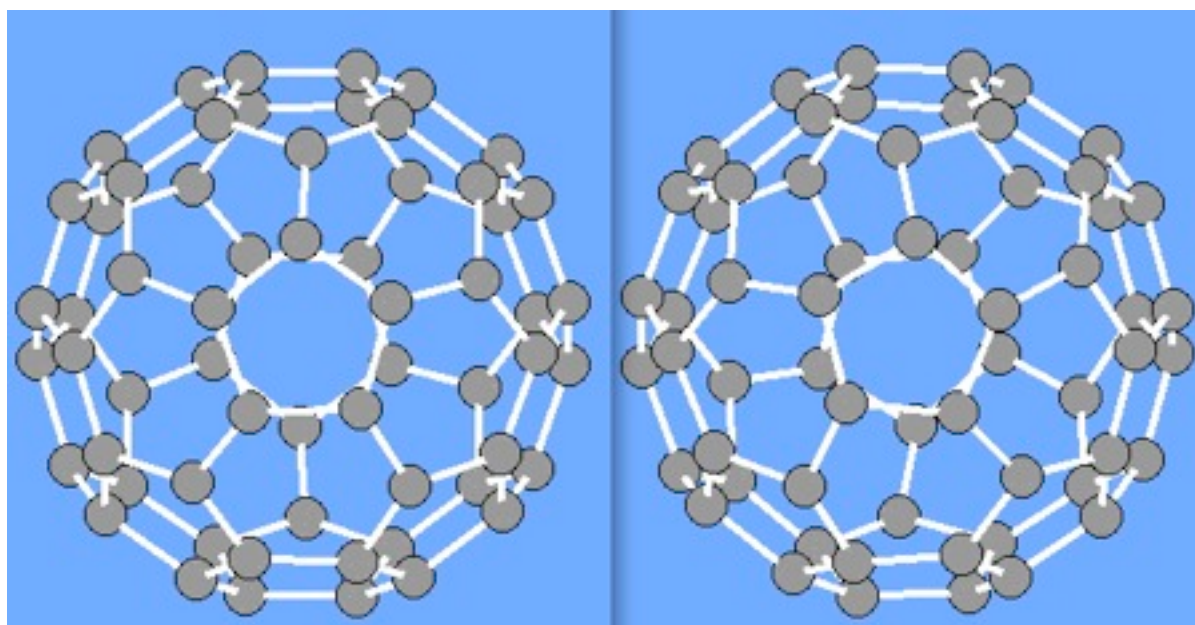
<http://arxiv.org/pdf/0905.2951>
about structural distortion

Also, a friend of mine (Julian Niles) did his Ph.D. thesis on fullerenes. Here are three animated gifs from his thesis about distortions of C60, which may be a bit more complicated than C20 but may be similar enough for you to sort of visualize some aspects of distortions. (you might have to look at the images in a web browser to see the animation)

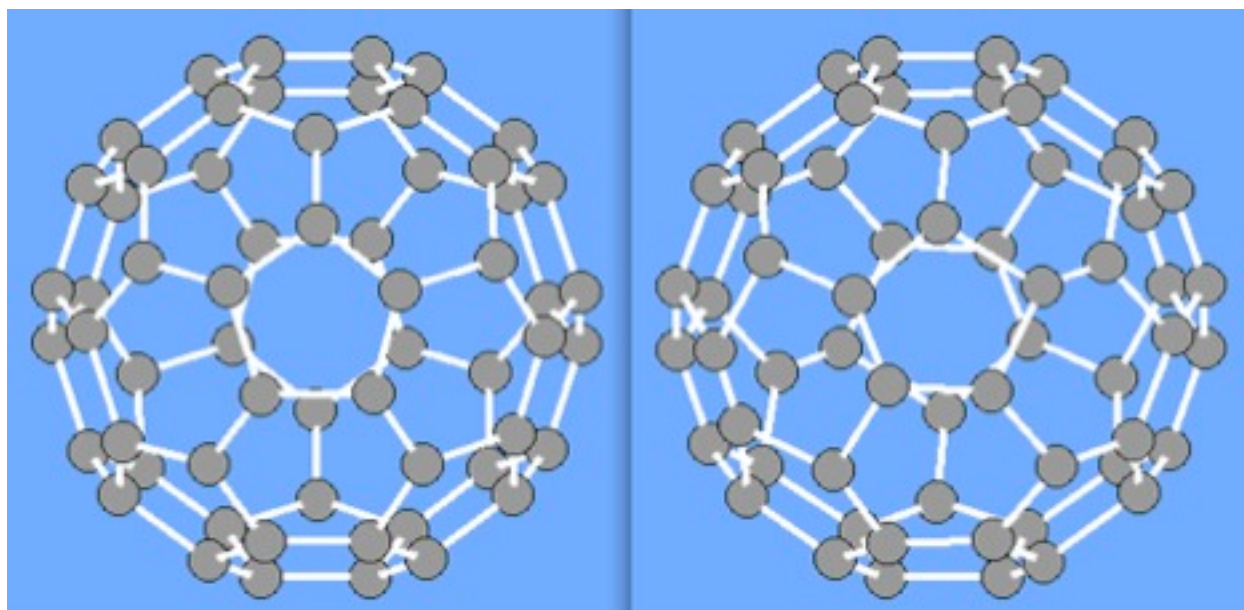
603 C60



976 C60



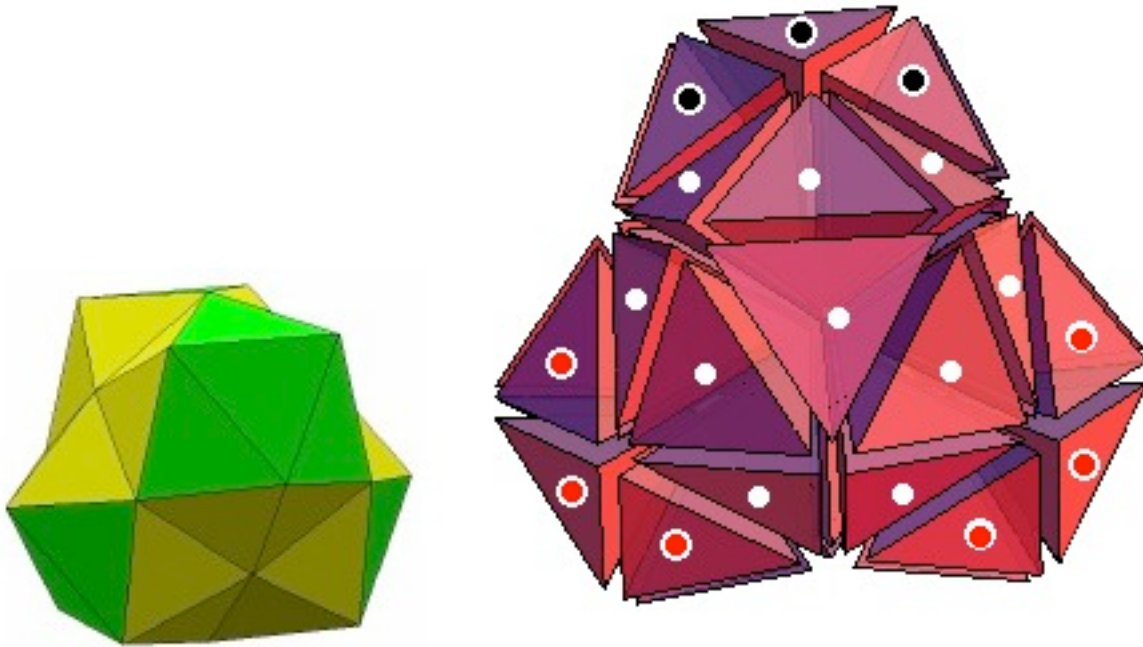
Stretch C60



Edges:

The $57 \times 6 = 342$ edges of the 57 tetrahedra of the 57-group considered separately merge into 102 edges within the 57-group itself.

Pick one of the four icosahedra of the 57-group, whose 20 tetrahedra include the central tetrahedron,



10 tetrahedra have all faces interior to the 57-group.

4 have $4 \times 6 = 24$ edges that are part of sets of 5 shared.

6 have $6 \times 5 = 30$ edges that are part of sets of 5 shared

and

$6 \times 1 = 6$ edges that are part of sets of 3 shared.

The other 10 tetrahedra (white) of that icosahedron have one exterior face

Their $10 \times 3 = 30$ internal edges are part of sets of 5 shared.

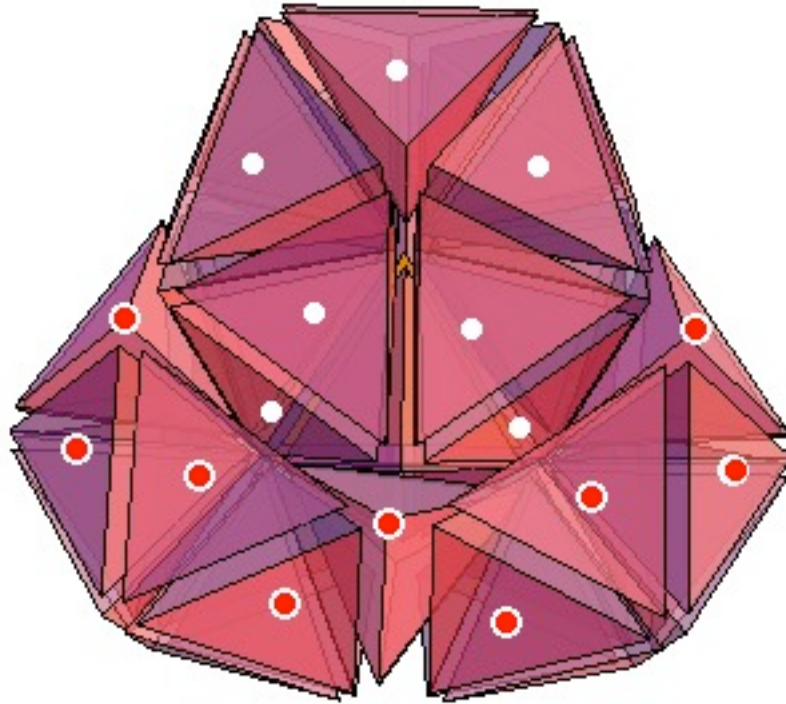
so their 6×5 edges merge to 6 edges.

$6 \times 1 = 6$ of their external edges are part of sets of 3 shared

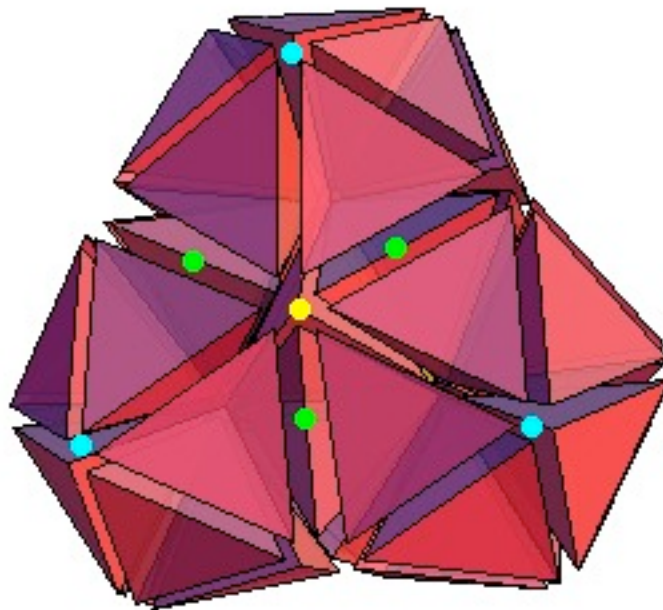
and

$6 \times 2 = 12$ of their external edges are part of sets of 2 shared.

$4 \times 3 = 12$ of their external edges are part of sets of 2 shared.



The remaining $57 - 20 = 37$ tetrahedra do not include the central tetrahedron:



1 tetrahedron (yellow) sharing a face with the central tetrahedron has 6 edges all of which are part of sets of 5 shared;

3 tetrahedra (green) sharing a face with the yellow tetrahedron
 have $3 \times 6 = 18$ edges of which
 $5 + 5 + 5 = 15$ edges are part of sets of 5 shared and
 $1 + 1 + 1 = 3$ edges are part of sets of 3 shared.

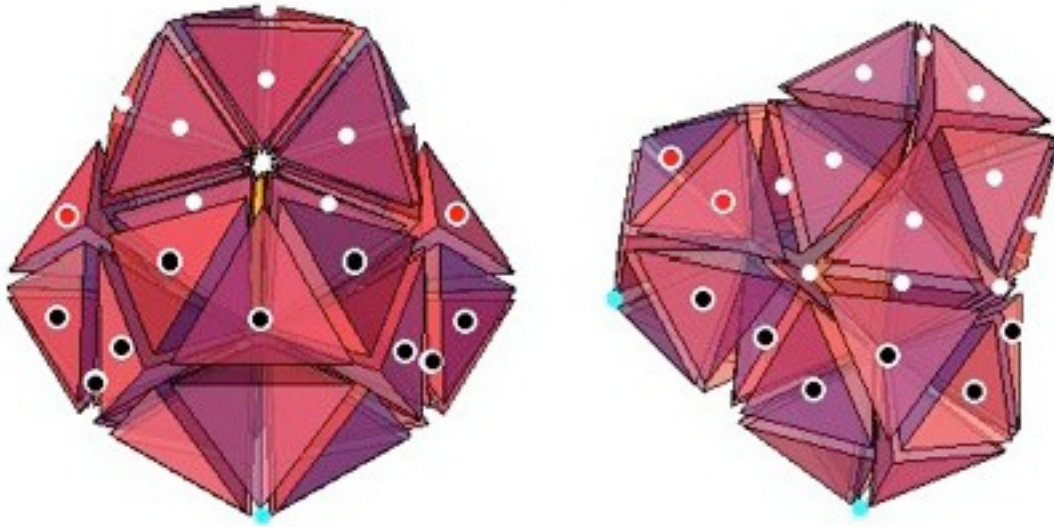
15 = three 5-groups (cyan) each sharing two faces with green tetrahedra
 have $15 \times 6 = 90$ edges of which
 $3 \times (3 + 3 + 3 + 3 + 3) = 45$ edges are part of sets of 5 shared and
 $3 \times (1 + 1) = 6$ edges are part of sets of 3 shared and
 $3 \times (2 + 3 + 3 + 3 + 2) = 39$ edges are part of sets of 2 shared.

18 = two groups of 9:
 one group of 9 (red)
 with a total of $9 \times 6 = 54$ edges of which
 $3 + 3 + 3 + 3 + 5 + 3 + 3 + 3 + 3 = 29$ are part of sets of 5 shared and
 $1 + 1 + 1 + 1 + 1 + 1 + 1 = 7$ are part of a set of 3 shared and
 $2 + 3 + 2 + 2 + 2 + 2 + 3 + 2 = 18$ are part of sets of 2 shared



and

one group of 9 (black)
 with a total of $9 \times 6 = 54$ edges of which
 $3+5+3+3+3+3+3+5+3 = 31$ are part of sets of 5 shared and
 $1+1+1+1+1+1+1+1 = 8$ are part of sets of 3 shared and
 $2+2+2+3+2+2+2 = 15$ are part of sets of 2 shared



so that

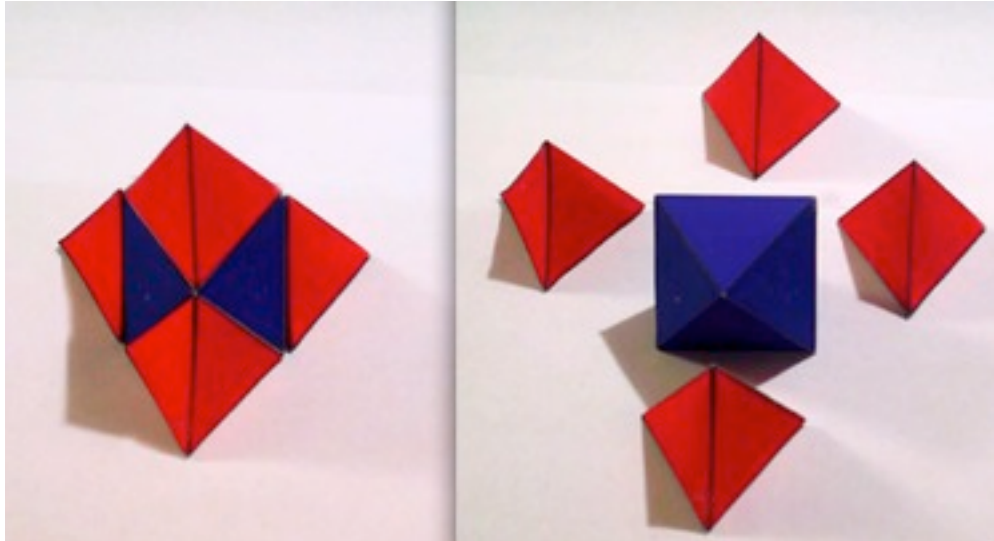
$54+30+6+15+45+29+31 = 210$ are part of sets of 5 and
 $6+6+3+6+7+8 = 36$ are parts of sets of 3 and
 $12+12+39 +18+15 = 96$ are parts of sets of 2.

There are therefore
 210 unmerged edges that are parts of sets of 5 shared
 36 unmerged edges that are part of sets of 3 shared
 96 unmerged edges that are part of sets of 2 shared

Since $210 + 36 + 96 = 342 = 57 \times 6$
 all 342 separate vertices of the 57 tetrahedra of the 57-group are accounted for.

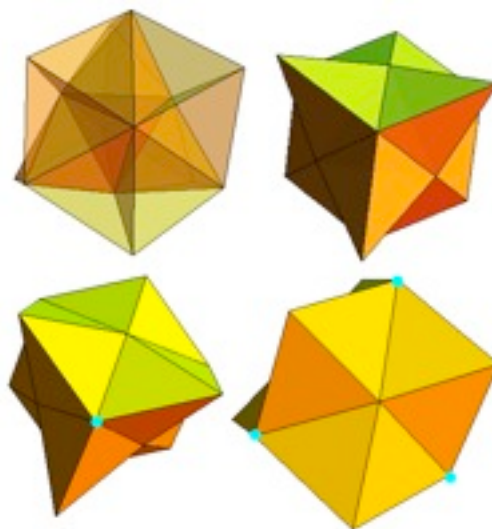
After merger there are $210/5 + 36/3 + 96/2 = 42 + 12 + 48 = 102$ edges.

Note that this shows that the 57-group can be seen from 4 points of view, one for each of the 4 icosahedra that share the central tetrahedron. If the whole 57-group is viewed as having the structure of a very large tetrahedron, then (as Fang has noticed) you can decompose it into



(images from web site at <http://isis.nmsu.edu/~breakingaway/Lessons/cuttingPH/tetrahedra.html>)

4 corner tetrahedra and a central octahedron, with each of the 4 corner tetrahedra corresponding to a 10-group of 10 tetrahedra of one of the 4 icosahedra with an exterior face and the central octahedron corresponding to the 17-group



of interior tetrahedra.

If you want to be a bit more detailed,
you can say that the big tetrahedron should be truncated on all 4 corners,
and that each of the 4 small tetrahedra should be truncated on one corner.

The difference between tetrahedral decomposition point of view
and
the intrinsic structural point of view from which
the interior central 17-group looks more like a tetrahedron than an octahedron
and the 4 corner things look more like 4 half-icosahedra than 4 tetrahedra
is that
the tetrahedral decomposition view shows how the components relate globally to
an overall large tetrahedron structure of the whole 57-group
while
the intrinsic structural view shows the local internal structure of the components.

Both points of view (global and local) are useful.

From the point of view of a chosen icosahedron, the 57-group is made up of:

the icosahedron with 20 tetrahedra marked above with white dots;

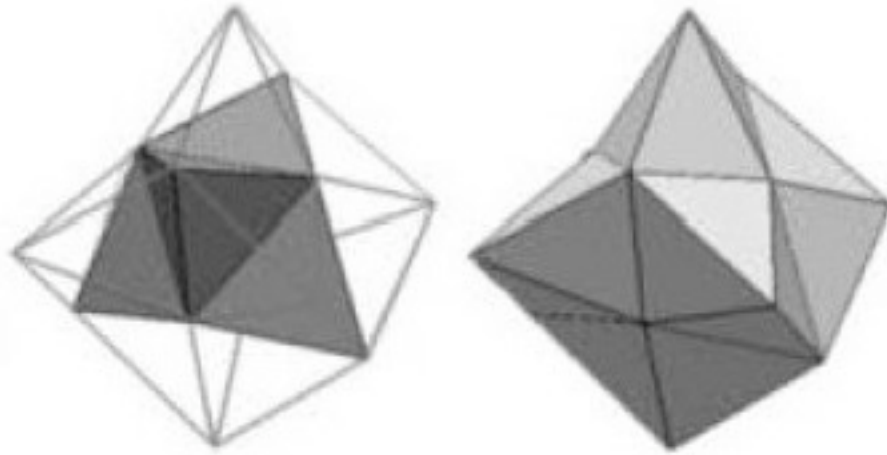
a central cluster of 4 tetrahedra,
one sharing a face with the center tetrahedron (yellow)
and
three (green) sharing a face with the yellow tetrahedron;

3 pentagonal pyramid 5-groups marked above with cyan dots (15 tetrahedra);

a band of 18 face-sharing tetrahedra marked above with red and black dots
forming a ring surrounding the icosahedron and the central cluster of 4 tetrahedra.

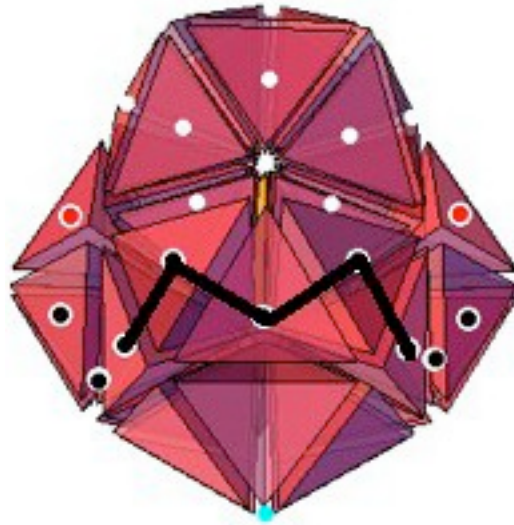
Note that the band of 18 face-sharing tetrahedra consists of:

3 tetrahedra with no external face but do share a face with a green tetrahedron,
and so are part of the central 17 tetrahedra



and

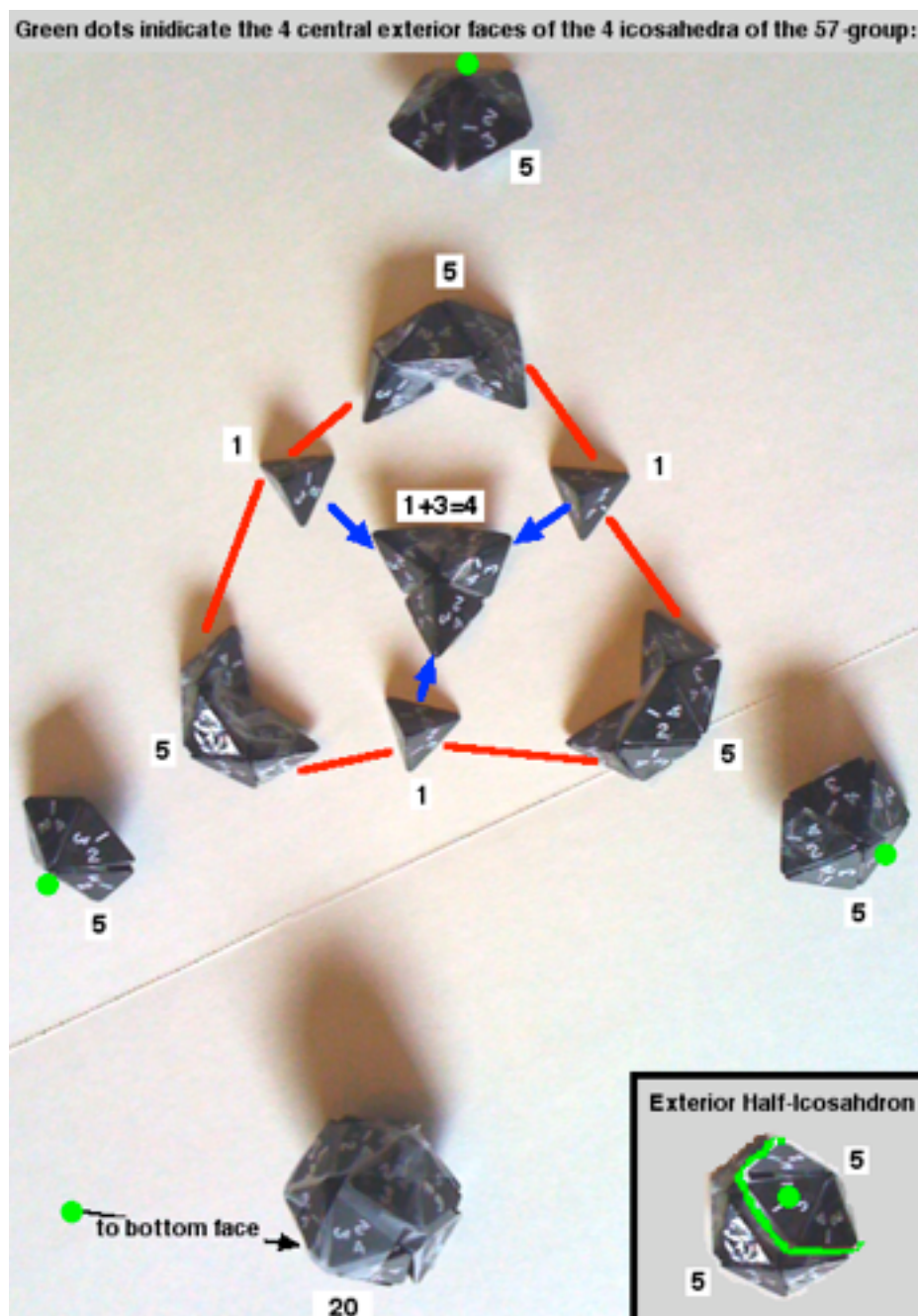
15 tetrahedra that are in 3 chains of 5,
 which 3 chains are separated by the 3 tetrahedra in the central 17.
 Each of those 3 chains of 5, one of which is shown here



linked by a black line,
 corresponds to one of the 3 pentagonal 5-groups outside the chosen icosahedron.

As is clear from the above image, a chain of 5 combines with its 5-group
 to make up half of the 10 equatorial tetrahedra of the icosahedron that
 could be formed within the 57-group by that 5-group.

There are 4 ways you can choose an icosahedron from the 57-group.
When you choose a particular one, you get:



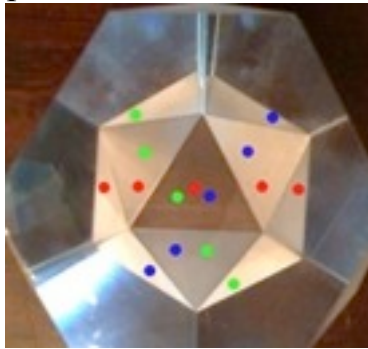
If you set the chosen icosahedron aside,

you can build the rest of the 57-group as follows:

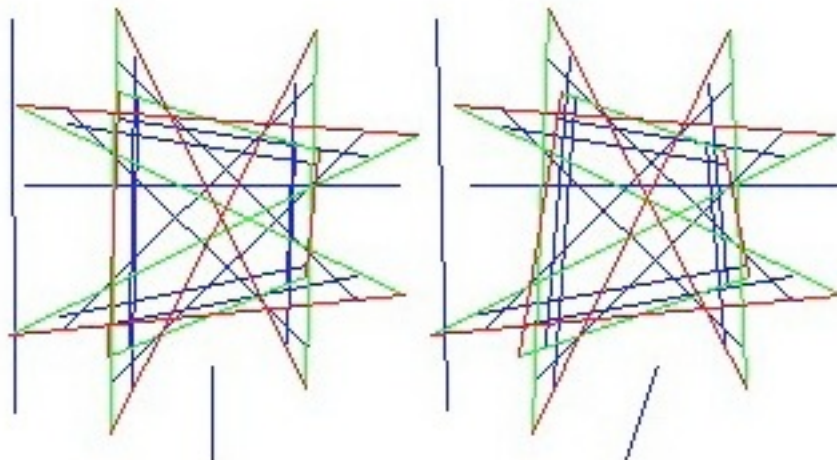
- 1 - Take the 1+3=4 and put it in face contact with the top face of the icosahedron.
- 2 - Take the 3 single 1 and slide them (blue arrows) under the 1+3=4 and over the icosahedron, filling the big gaps there.
- 3 - Take the 3 chain 5 and put them in face contact with the 3 single 1. This makes a face-to-face closed loop chain of 18 tetrahedra that is indicated by red lines.
- 4 - Take the 3 pentagon 5 and put them on top of the structure.

This completes the 57-group.

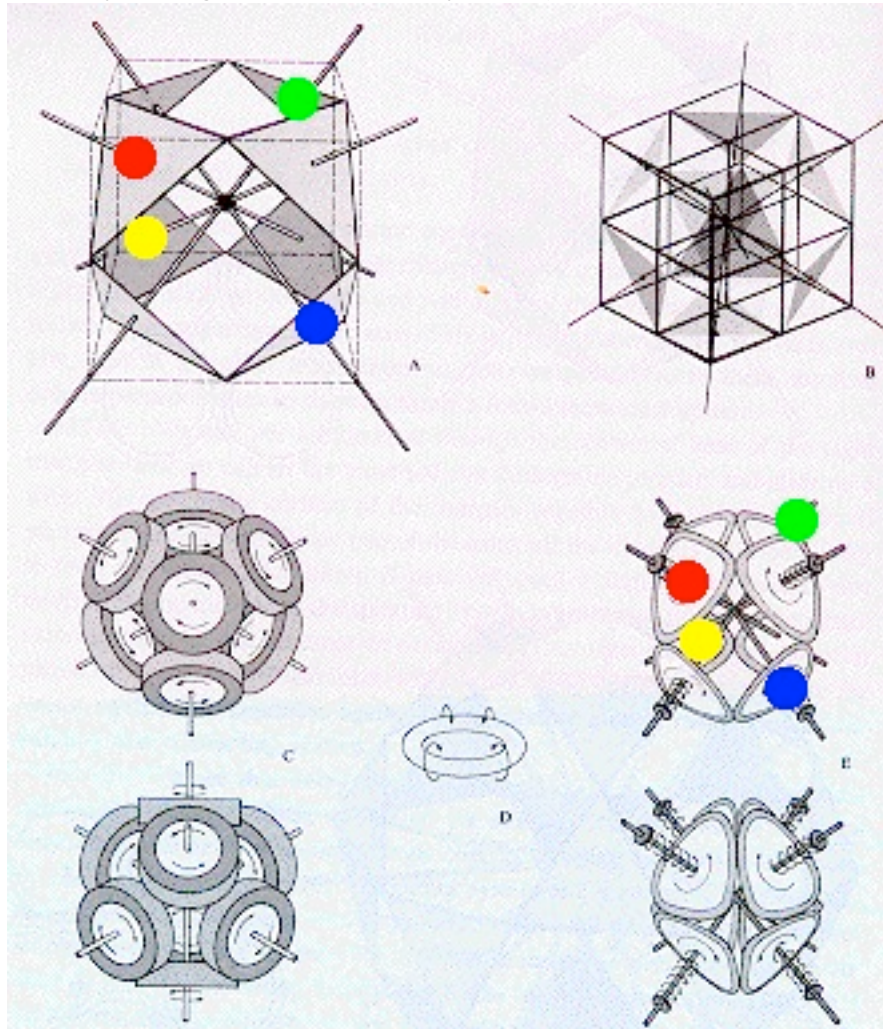
Note that the 3 chain 5 correspond to



the 3 chains of 5 that you see when you look into one of the 4 large faces of a glass truncated tetrahedron, and also to 3 of the 12 lines (the other 9 come from the other 3 ways you could have chosen an icosahedron from the 57-group) in the Schafli Double-6 or the 12 Parallel Pair lines both of which are inside the 27-line Configuration.



Consider the 18-tetra closed loop structures for all 4 of the icosahedra within the 57-group. The configuration of the 4 icosahedra, and therefore of the 4 closed loop 18-chains, is similar to 4 vertices of a tetrahedron, or, equivalently, to 4 alternate vertices out of the 8 vertices of a cube or, equivalently, to 4 alternate triangular faces out of the 8 of a cuboctahedron (indicated below by red, green, blue, and yellow)

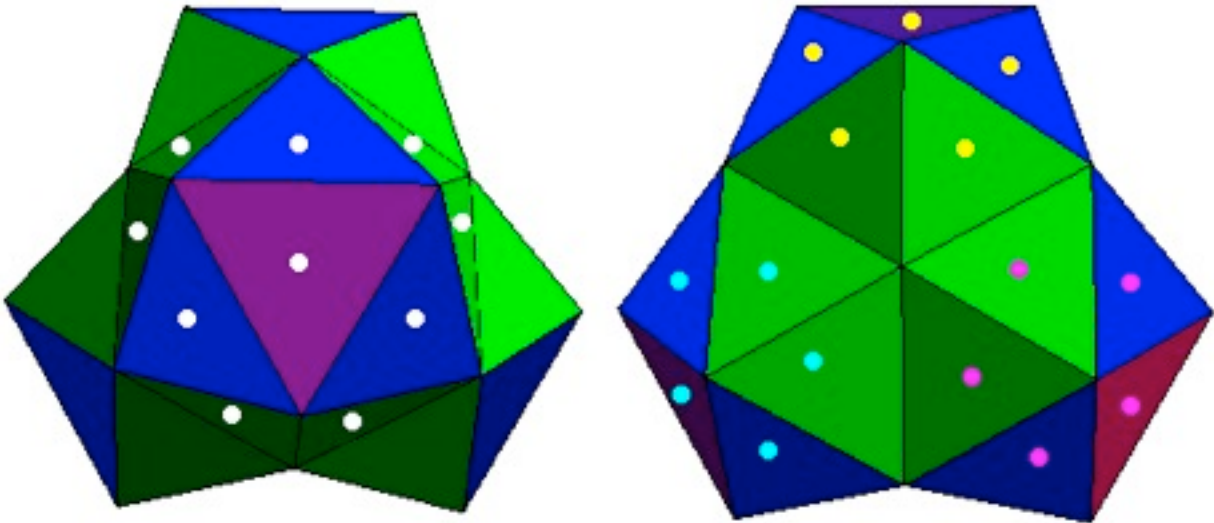


Therefore the 4 closed loop 18-chains describe circulation around each of the 4 axes of the Fuller Vector Equilibrium cuboctahedron and therefore (since the cuboctahedron can be seen as a central figure in the 4-dim 24-cell that is a discrete version of the 3-sphere) to circulation around the 4 axes (t,x,y,z) of spacetime.

Of course, since $18 \times 4 = 72$ is greater than 57, the 4 closed loop 18-chains do share some of their tetrahedra.

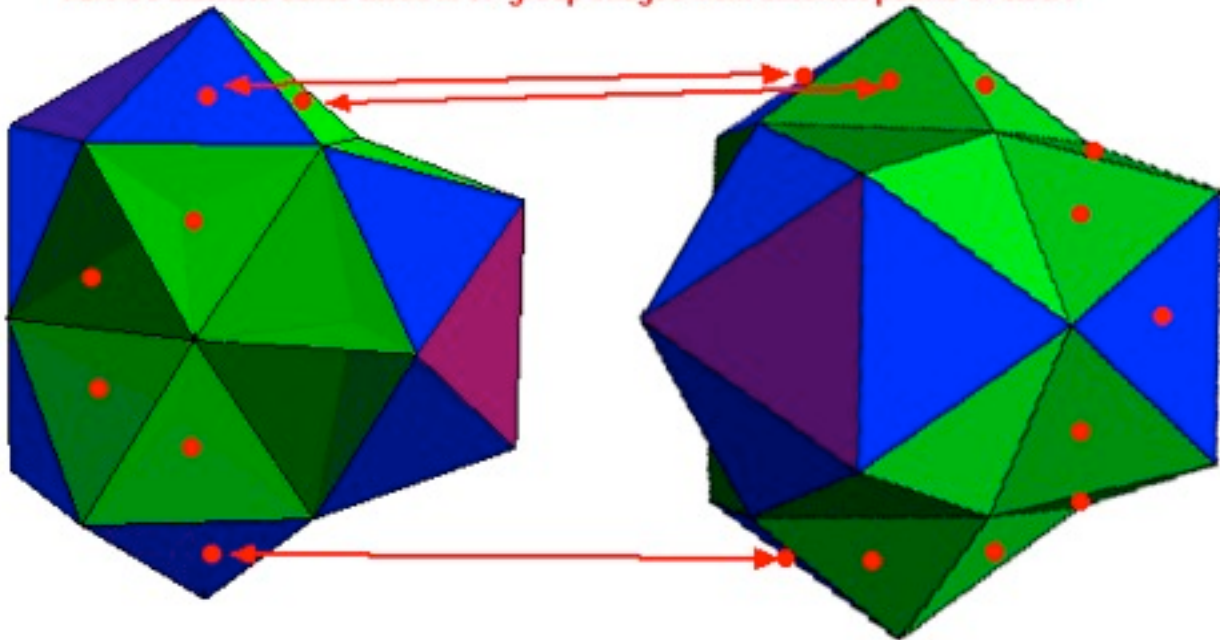
Each closed loop 18-chain contains 15 tetrahedra with an exterior face and 3 interior tetrahedra.

If the 10 exterior faces of the chosen icosahedra are as shown with white dots and the 5 faces of each of the corresponding 3 pentagonal 5-groups are shown with yellow, cyan, and magenta dots in the following two images

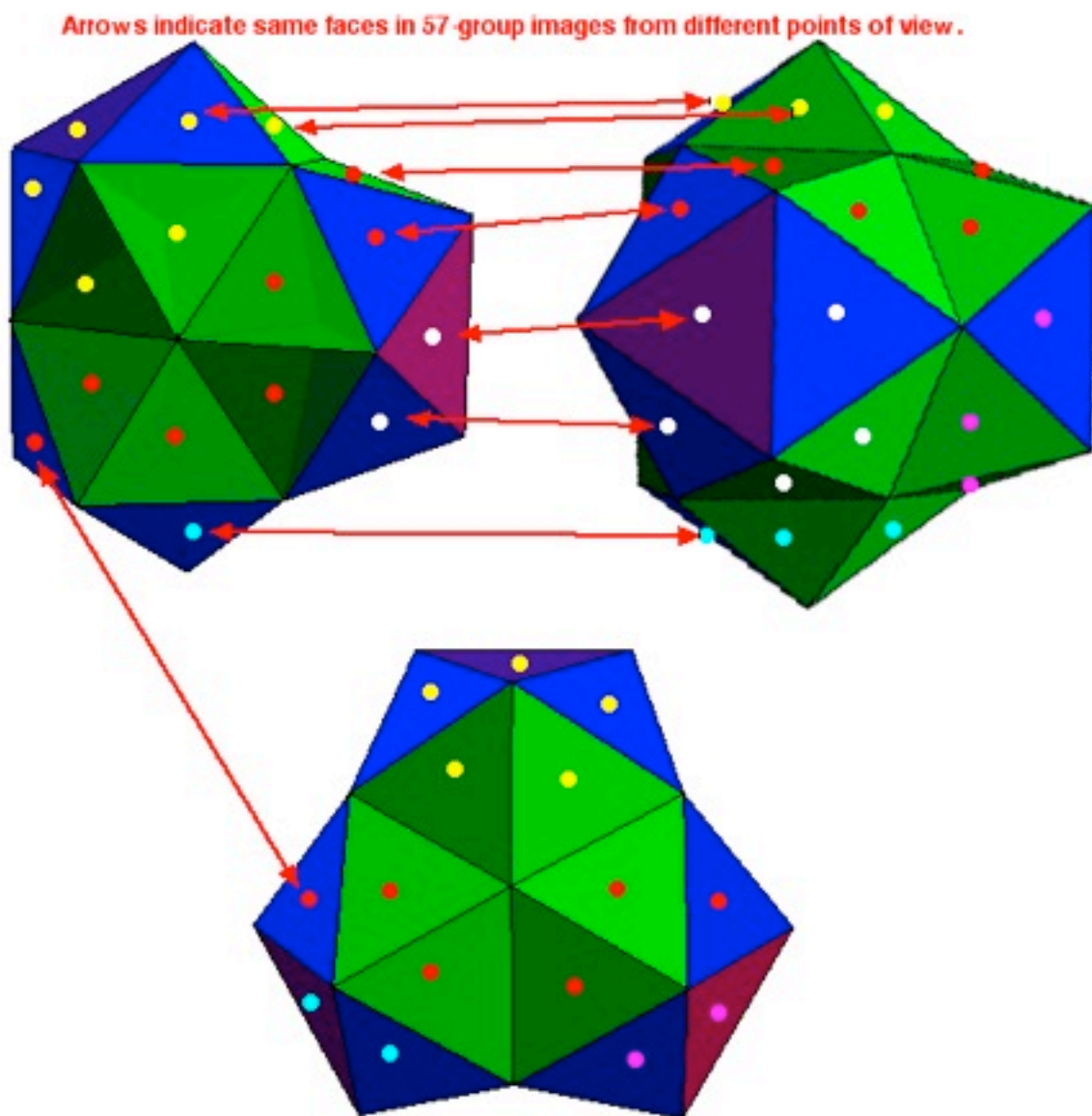


then the remaining $40 - 25 = 15$ exterior faces are the 15 exterior faces of the closed 18-loop which are indicated by red dots in the two images below

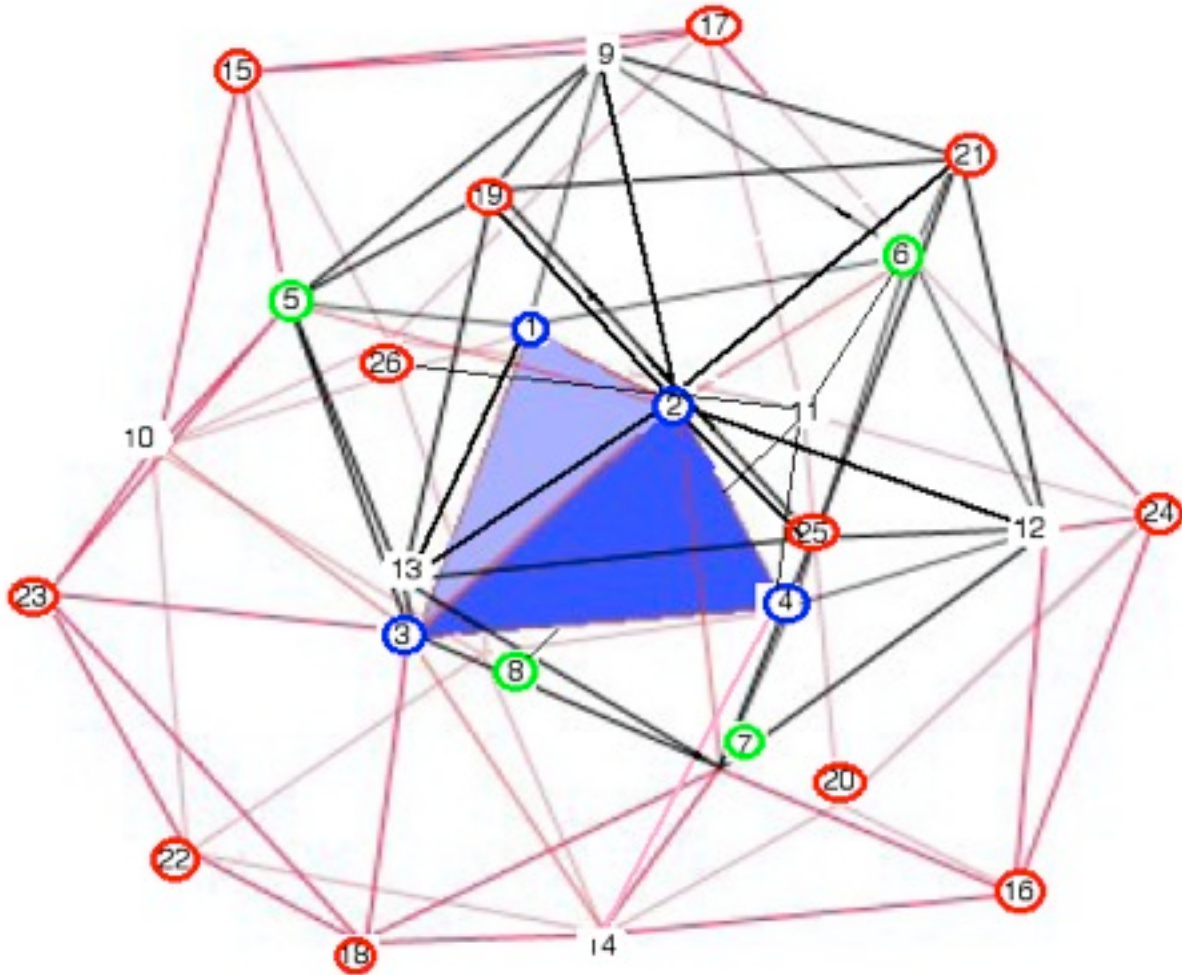
Arrows indicate same faces in 57-group images from different points of view.



Choosing another of the 4 icosahedra, say the one based on the yellow pentagonal 5-group, would give the following 18-group structure:



As to the total count of lines after merger (the image may not show all lines exactly accurately, and any errors are my fault in modifying the image from Lord et al):



The 26 vertices of the 57-group are shown here numbered from the inside out:

1 - 4 (blue) are the 4 vertices of the central tetrahedron.

There are 12 lines from each blue vertex.

5 - 8 (green) are the 4 exterior vertices of the 4 tetrahedra face-joining the center.

There are 9 lines from each green vertex.

9 - 14 (white) are an octahedron of 6 vertices on the outside of the 57-group.

There are 8 lines from each white vertex.

15 - 26 (red) are a cuboctahedron of the outermost 12 vertices on the outside of the 57-group. There are 6 lines from each red vertex.

Since each line connects two vertices, the total number of merged-edge lines should be $(4 \times 12 + 4 \times 9 + 6 \times 8 + 12 \times 6) / 2 = 204 / 2 = 102$ lines.

Faces:

The $228 = 57 \times 4$ faces of the 57 separate tetrahedra of the 57-group merge into 134 faces of the merged 57-group, because:

17 of the 57 tetrahedra are interior to the 57-group and therefore have $17 \times 4 = 68$ faces that are part of facing pairs;

40 of the 57 tetrahedra have 1 exterior face of the 57-group and 3 interior faces so that they have $40 \times 3 = 120$ faces that are part of facing pairs and $40 \times 1 = 40$ faces that are single and not paired to any other face

so that
the $68 + 120 = 188$ paired faces merge to 94 faces
and
the 40 single faces do not merge

resulting in $94 + 40 = 134$ faces in the merged 57-group.

The 94 merged pairs have $94 \times 3 = 282$ merged vertices,
but
this is NOT a full accounting of vertex mergers because

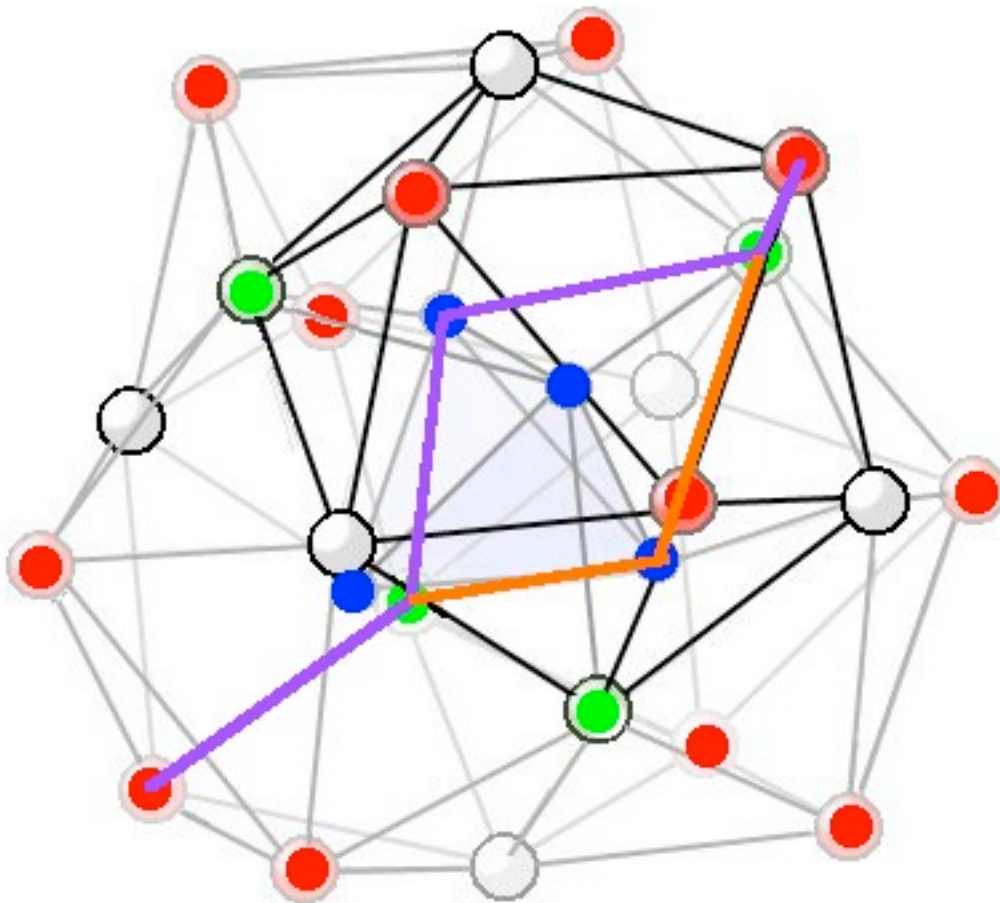
mergers of vertices that are not on the same merged face are omitted
and
mergers of the vertices of the 40 exterior faces are omitted.

Tetrahedra:

The 57 separate tetrahedra do not merge as full tetrahedra, so that after merger the 57-group still has 57 tetrahedra.

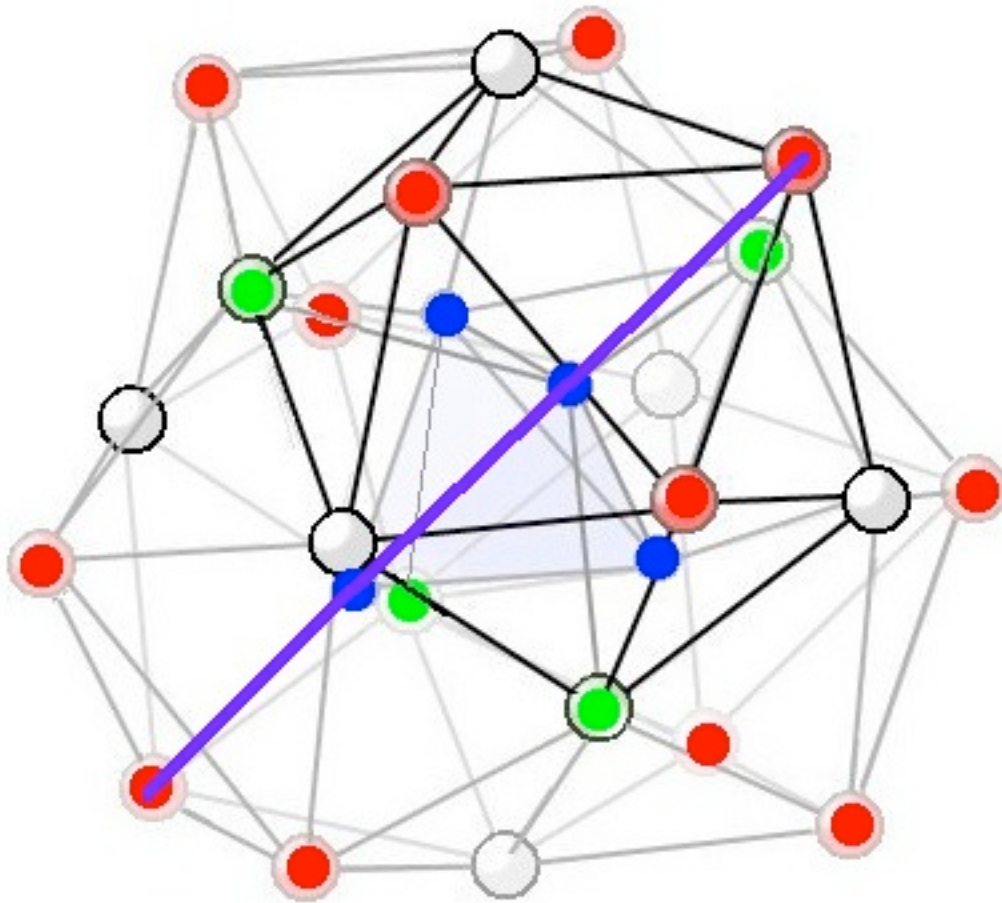
To study paths through the 57-group involving multiple tetrahedra:

1 - Start with this one (out of 6) purple/gold lines (vertex view) between two antipodal exterior cuboctahedron vertices that was the middle right one on my earlier image of 6 things.



It is a purple twisted line of 4 segments (5 vertices) plus (if you change two segments to the gold ones) an oppositely-twisted line. Note that each line involves one blue vertex of the central tetrahedron, so the 2 twisted-line connections use 2 of the 4 blue vertices of the central tetrahedron.

2 - Shorten and straighten (to no twist) the connection path to get



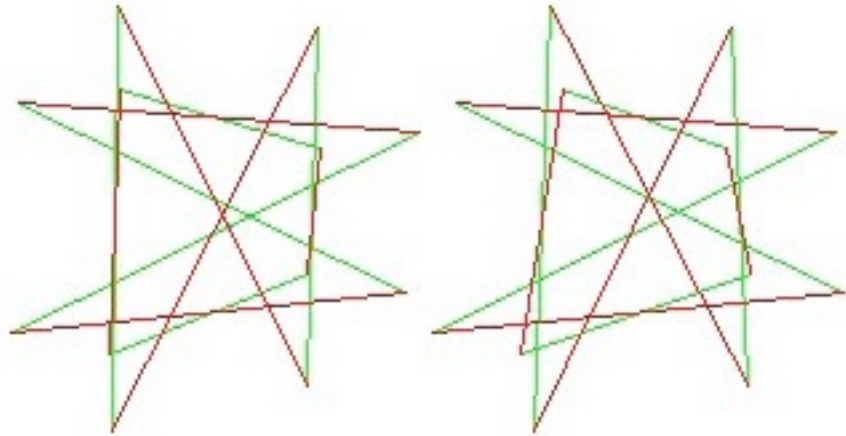
a straight line of 3 purple line segments.

Note that the straight short connection uses the other 2 of the 4 blue vertices of the central tetrahedron.

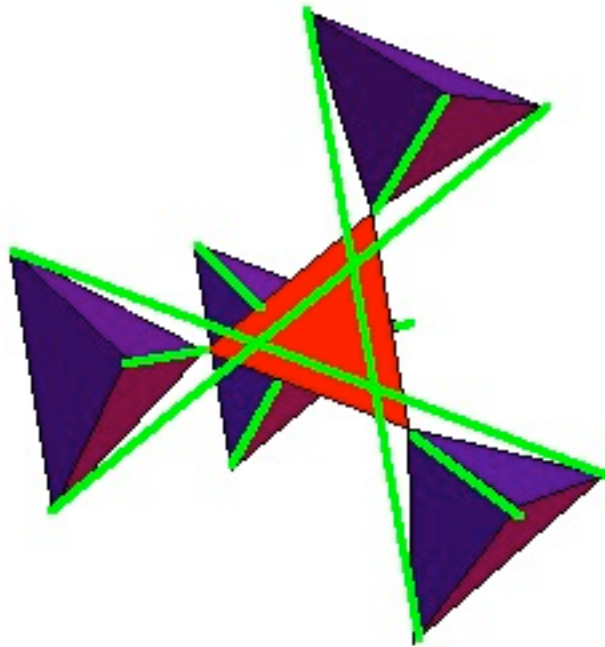
Since there are 6 ways to choose pairs of tetrahedron vertices, one for each of the 6 edges of a the central tetrahedron, there are 5 more ways to do a similar construction corresponding to the $1+5 = 6$ antipodal pairs of the exterior cuboctahedon vertices.

Those 6 lines also correspond to 6 of the lines of the Schlafli Double-6 in particular

to the 6 green lines in this stereo image of the Double-6:

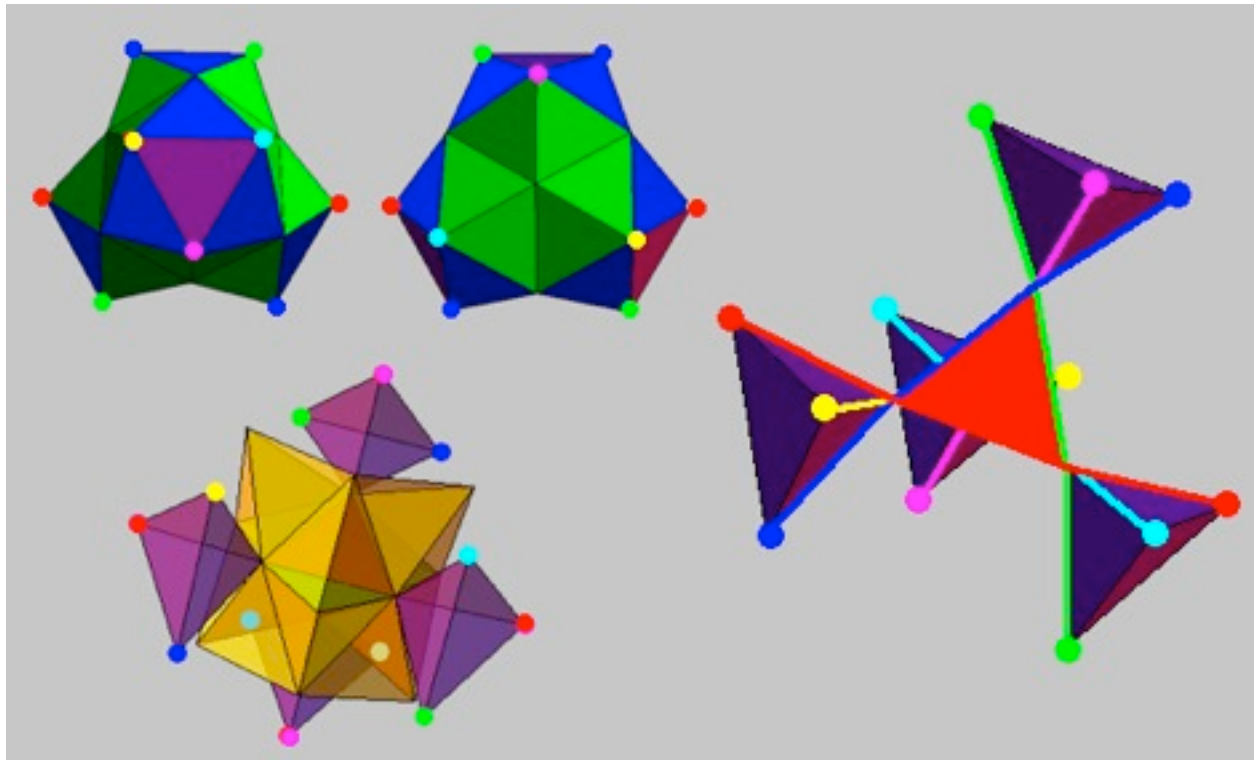


The correspondence is to the 6 green lines shown here in this image



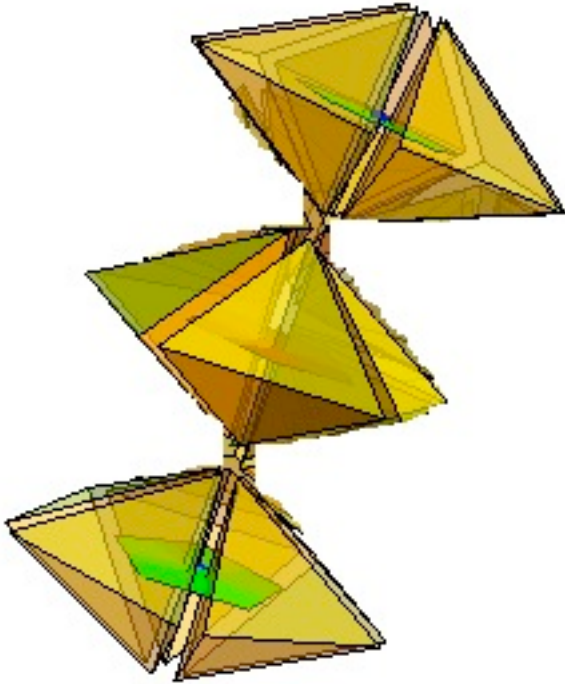
of the central tetrahedron plus the outermost 4 tetrahedra of the 57-group.

Showing the embedding of those $1+4 = 5$ tetrahedra within the 57-group and showing the 6 lines and their external vertices in 6 different colors



indicates that each of the 6 lines determines one of the 6 axes for a helix axial core within the 57-group.

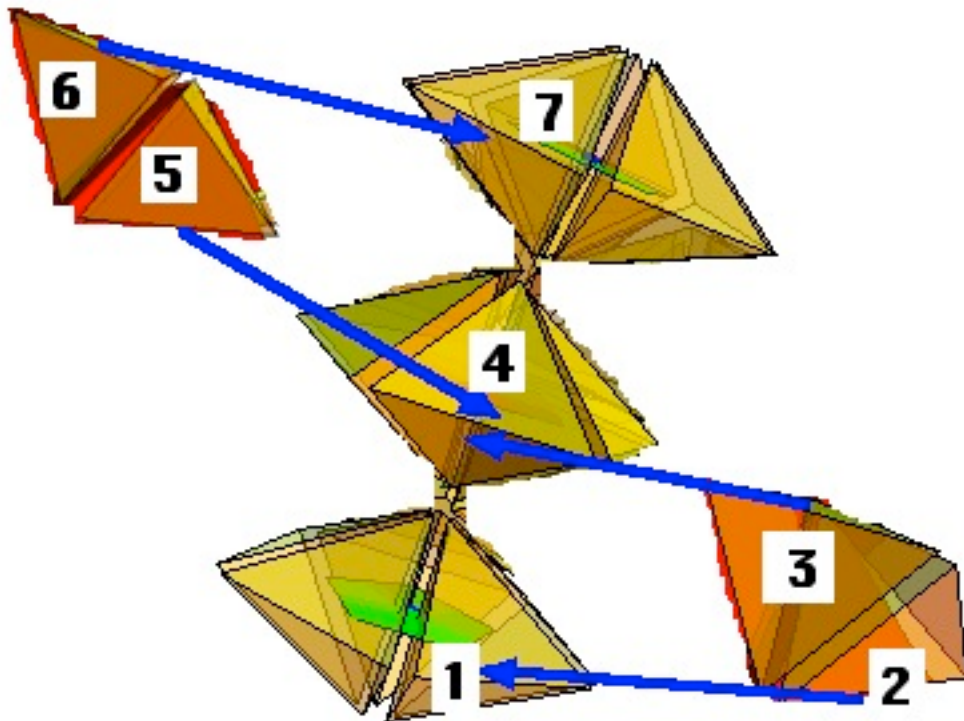
3 - Each of the 3 purple line segments of the straight connection is the axis of a 5-group



which is one of 6 ways you can form the $3 \times 5 = 15$ -tetrahedron axial core of a helix.

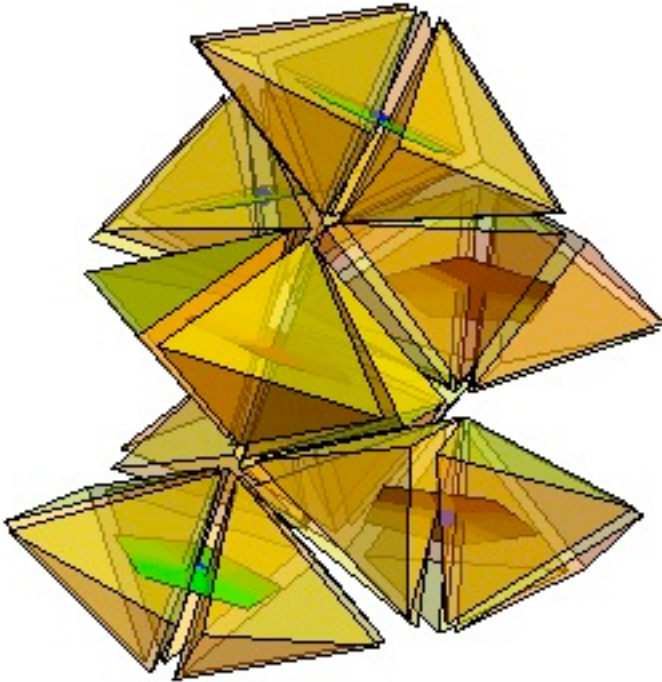
Note that the central 5-group contains the central tetrahedron, and note the rotation of the 5-groups as they go up the axis.

4 - If you want to travel along that axis by face-to-face travel, then you have to add more faces to make the face-to-face connections, and you can do that by adding two pairs of tetrahedra. For example, using a left-handed twist

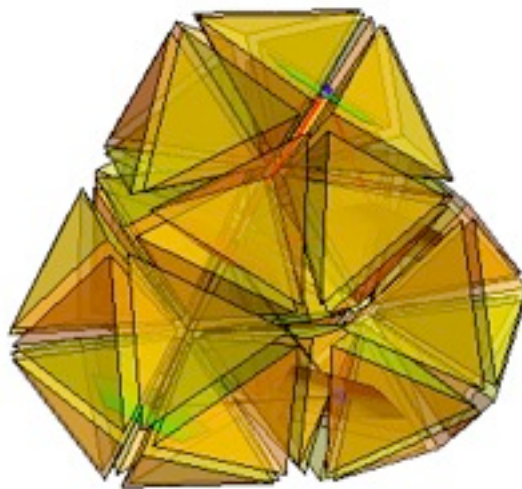


you get a left-twisted helix along the axis made up of 7 tetrahedra. Note that the total rotation from tetrahedron 1 to tetrahedron 7 is only $1/5$ of 360 degrees (that is, it is 72 degrees).

5 - If you want to fill out each of the 4 added tetrahedra into a full 5-group for each, you end up with $15 + 4 \times 5 = 35$ tetrahedra

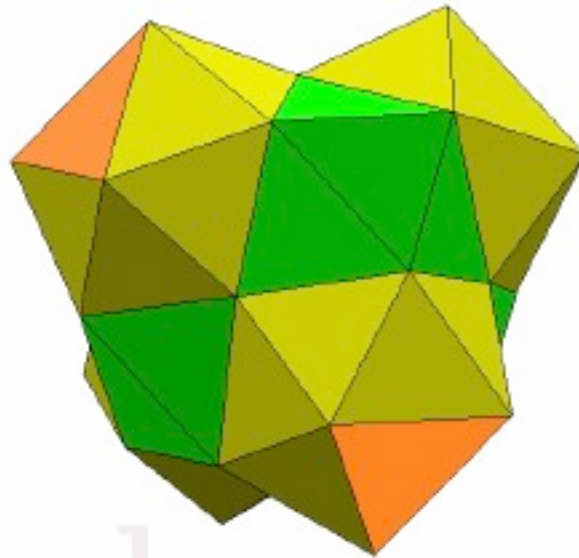


6 - If you want to fill out the 35 tetrahedra into the full 57-group, you add 22 more to get



the 57-group. also known as the gamma-Brass Cluster.

7 - If you add 12 more vertices, and 40 more tetrahedra, you get



the Augmented gamma-Brass Cluster with 38 vertices and 97 tetrahedra.

Note that the 4 outermost (orange in the image) triangular faces correspond to the 4 triangular faces of a Truncated Tetrahedron



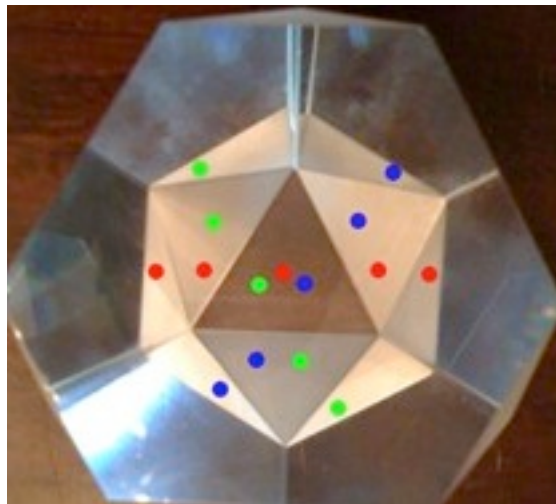
so that the Augmented gamma-Brass Cluster is a tetrahedral-cluster representation of a Truncated Tetrahedron.

8 - If you went inside the Augmented gamma-Brass Cluster Truncated Tetrahedron and looked at one of the triangular face corners you would see



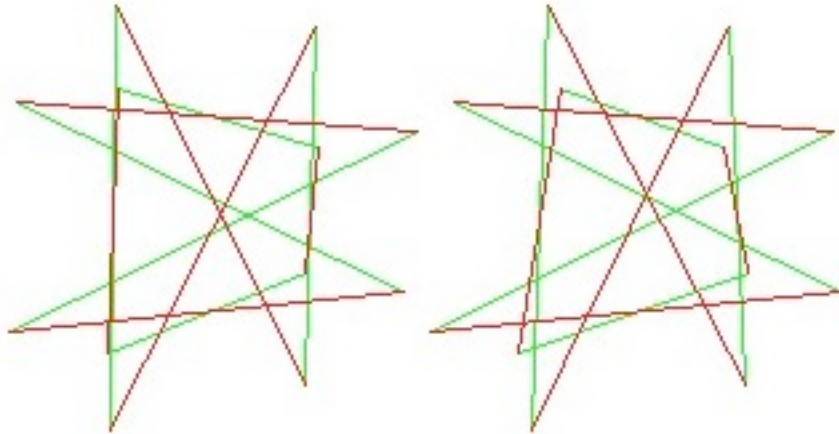
something very much like (except for the slight gaps due to trying to assemble a cluster of tetrahedra in flat 3-dim space) an icosahedron.

9 - If you look into a glass Truncated Tetrahedron

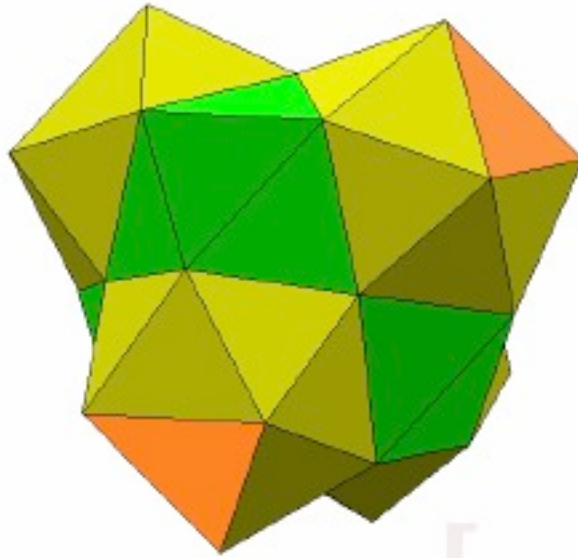


you see 5-chains of faces of half-icosahedra that appear due to reflection. There are 3 chains for each of the 4 truncated faces of the Truncated Tetrahedron. Those $3 \times 4 = 12$ chains correspond to the 12 lines of a Schläfli Double-6.

The Schlafli Double-6



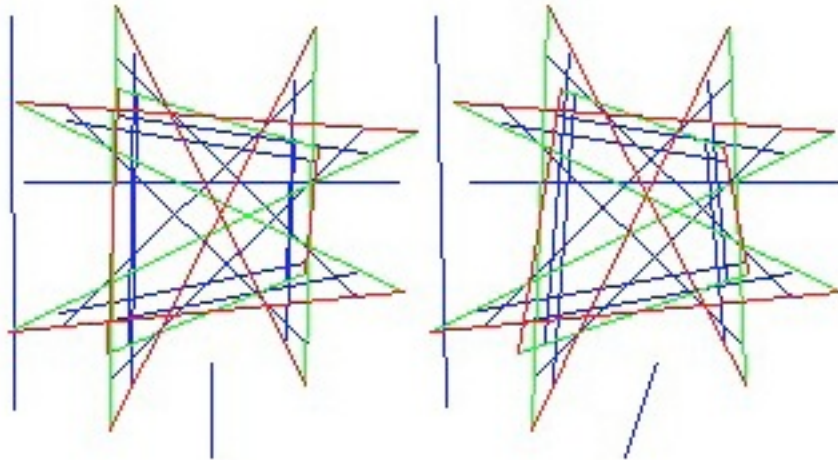
is a configuration of 12 lines whose geometry is similar to that of



a Truncated Tetrahedron and an Augmented gamma-Brass Cluster.

The 12 lines of the Schlafli Double-6 are a subset of the 27 lines of the Configuration of 27 Lines on a General Cubic Surface.

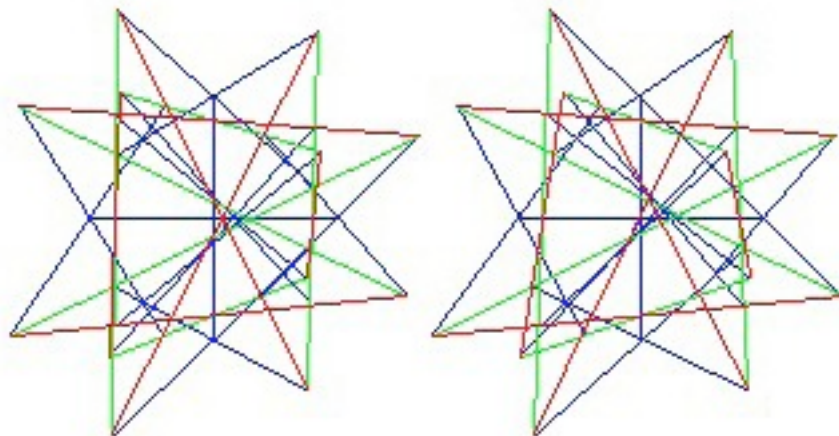
The 27-line General Cubic Surface Configuration



contains, in addition to the 12 lines of the Schläfli Double-6 (red and green), 15 more lines (shown in blue) that are of two types:
3 orthogonal lines (roughly the Cartesian X, Y, Z axes of 3-dim space);
12 lines in 6 Parallel Pairs,
each Parallel Pair being parallel to one of the 6 edges of a tetrahedron.

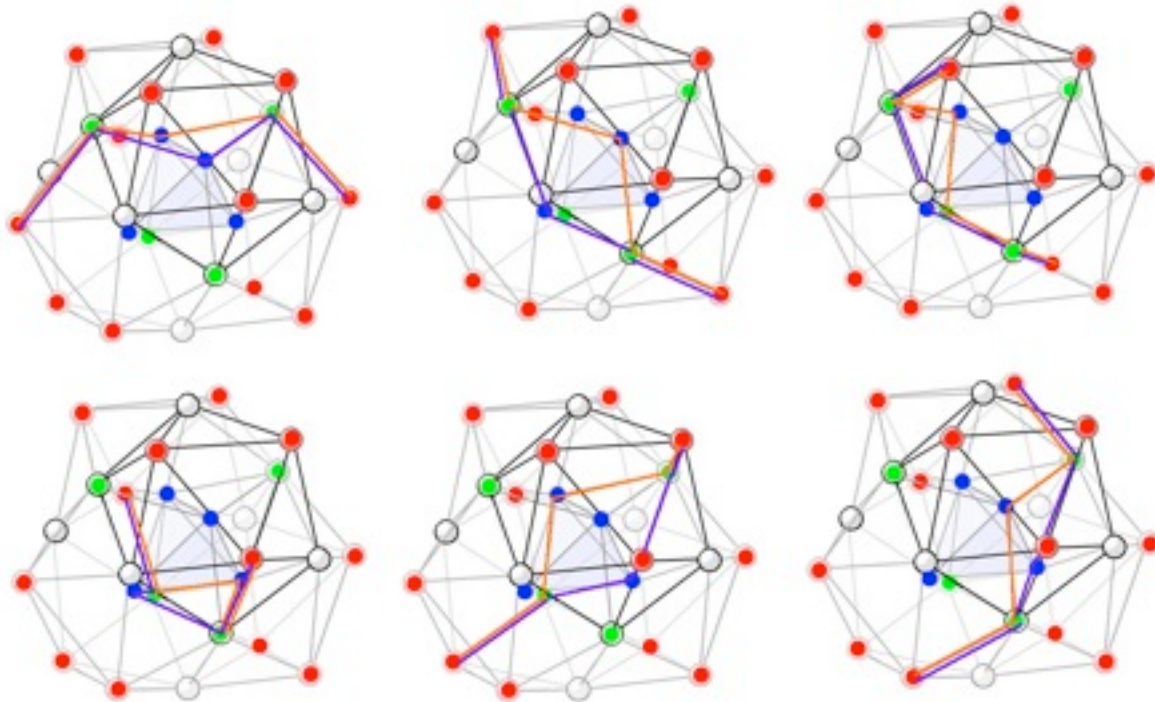
Each of the $12+15 = 27$ lines have 5 points of crossing,
so the configuration has $27 \times 5 = 135$ points.

In case it might help in visualization, here is a stereo image



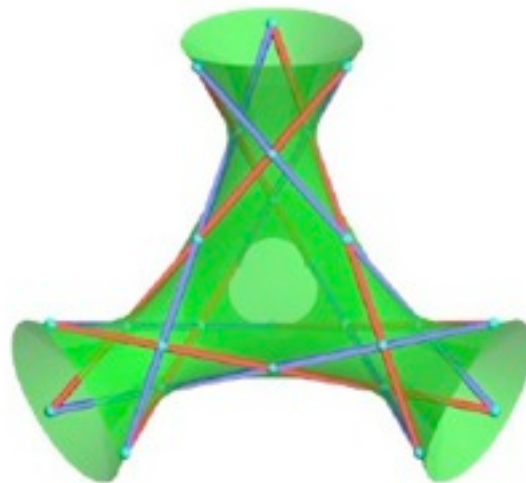
of the dual 27 line 45 point configuration.

Here is how the Double-6 related twelve 5-chains of faces of half-icosahedra that appear due to reflection of truncated faces of the Truncated Tetrahedron correspond to six pairs of 5-chains of vertices of the 57-group gamma-Brass Cluster.



Note that each of the chains connects two antipodal external vertices of the cuboctahedral outermost substructure.

Here is how they correspond to the 12 lines of the Schläfli Double-6 on the General Cubic Surface (image from mathcurve.com by Ferreol and Esculier)



which surface looks like a continuum version of a Truncated Tetrahedron.

Now consider the 12 lines of the 6 Parallel Pair subset of the 27-line General Cubic Surface Configuration



which are shown in yellow (image from mathcurve.com by Ferreol and Esculier).

Note that:

The 12 lines of the Double-6 plus the 12 lines of the Parallel Pairs plus the 3 Orthogonal XYZ Axes Lines of the 27-line Cubic Configuration correspond to the 27-dim Exceptional Jordan Algebra $J(3,O)$ of 3x3 Hermitian Matrices of Octonions

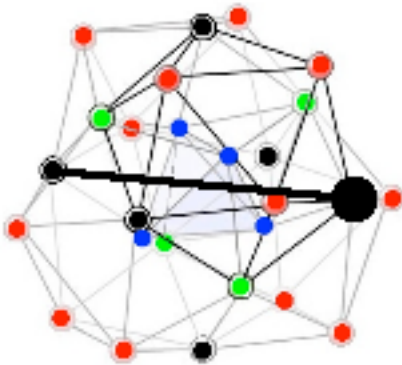
The lattice version of the $J(3,O)$ traceless part of $J(3,O)$ is the 26-dimensional Lorentz Leech lattice $\Lambda_{25,1}$ which is the basis for a realistic 26-dimensional Bosonic String Theory based on E_6 structure and World-Lines as Strings

The Weyl Group of the Lie Algebra E_6 of order $72 \times 6! = 51,840$ is the symmetry group of the 27 line Configuration
(Coxeter, Math. Z. 200 (1988) 3-45).

“... the smallest nontrivial string theory that nature allows ... Bosonic 26-dimensional space-time ... "compactified" on 24 dimensions ... [has as its] ... automorphism group ... the Fischer-Griess Monster M ... of order about 10^{54} ...”

(quote from James Lepowsky in math.QA/0706.4072)

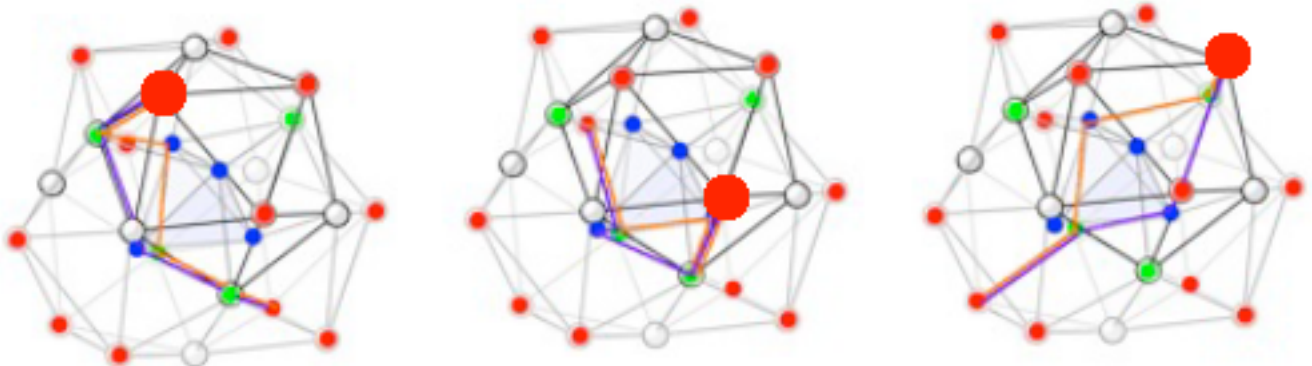
Here is an identification of paths through a 57-group with particles:



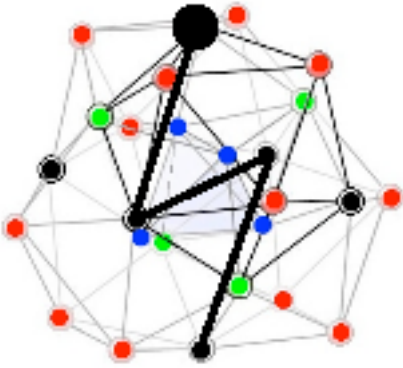
- neutrino - no color charge - no electric charge

2 point path between 2 antipodal points with no intermediate points

3 down quarks - one for each color charge - electric charge -1/3



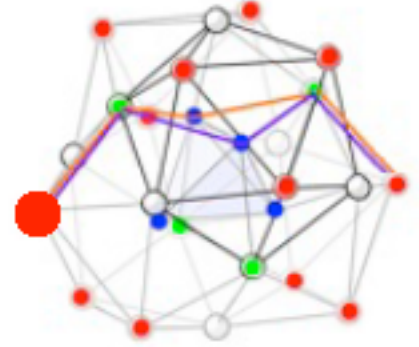
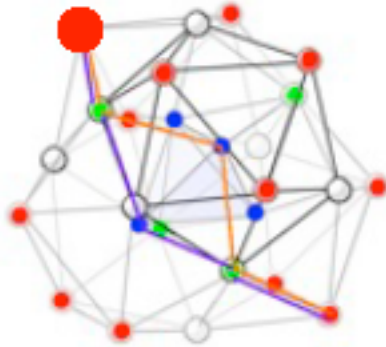
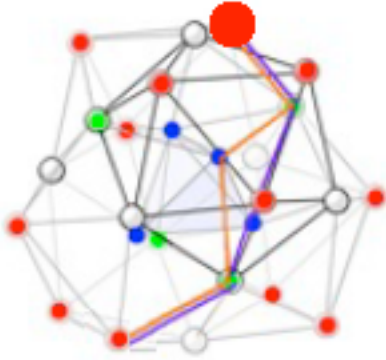
two 5 point paths between 2 antipodal points with 3 intermediate points



electron - no color charge - electric charge -1
 4 point path between 2 antipodal points with 2 intermediate points



3 up quarks - one for each color charge - electric charge +2/3



two 5 point paths between 2 antipodal points with 3 intermediate points

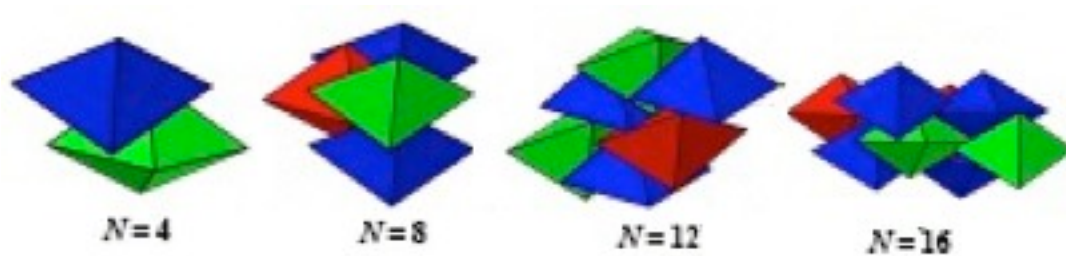
Each path is between a small-ball point and a large-ball point.

Path Flow is from the small-ball point to the large-ball point for Particles.

Path Flow is from the large-ball point to the small-ball point for Antiparticles.

What if you regard each tetrahedron in a QC dense-packing as being a 57G ?

Since a 57G has the overall appearance of a tetrahedron,
make the QC by dense-packing a lot of 57G
using the method of Chen et al in arXiv 1001.0586
in which the 57G (playing the role of tetrahedra) form clusters that look like

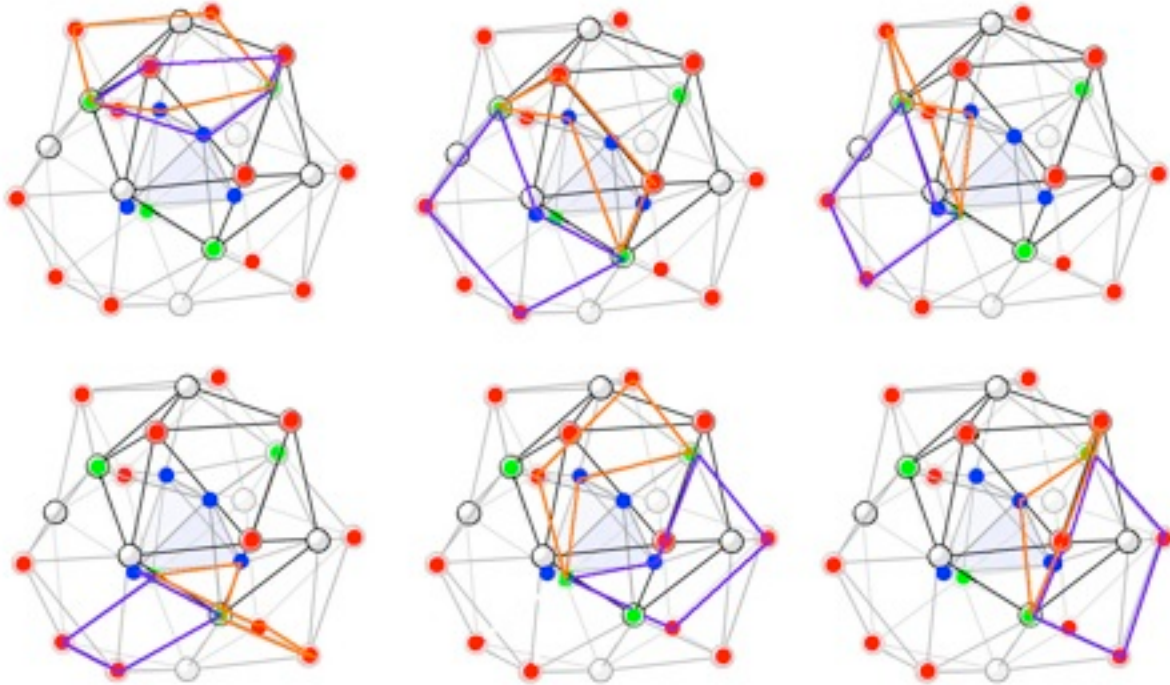


and have the same periodicity as Clifford algebras.

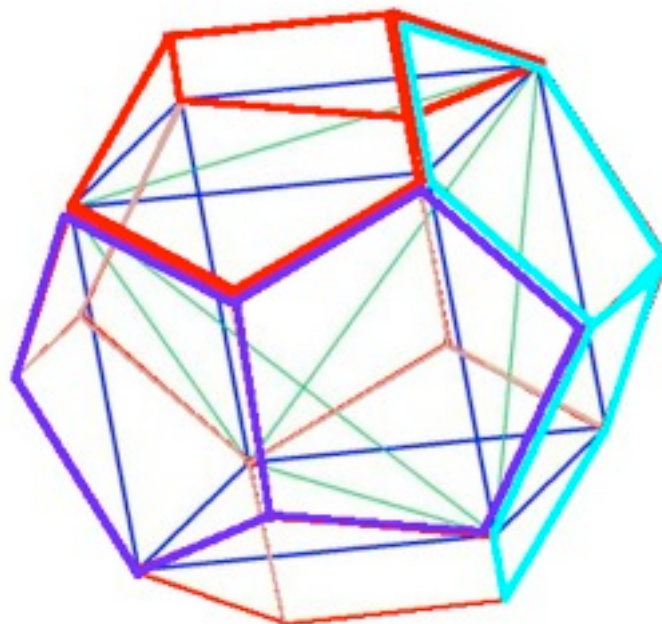
That would give you quantum theory from the Clifford algebras / QC dense packings
and
the fermions of the Standard Model from the paths / Philix in the 57G that
are being packed (playing the role of tetrahedra).

The 12 Double-6 lines are in a sense dual to the 12 Parallel Pair lines.

Here is how the Parallel Pair 12 lines correspond to six pairs of 5-chain-Pentagons of vertices of the 57-group gamma-Brass Cluster.



Note that six pairs of pentagons describe a dodecahedron
(image adapted from www.kjmaclean.com/Geometry/dodecahedron.html):



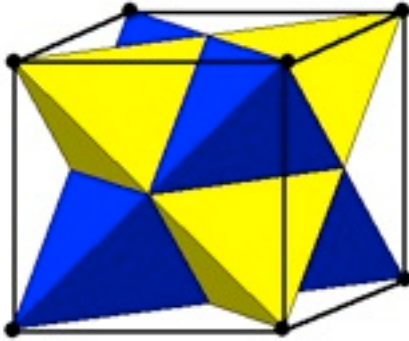
Since a cube sits (5 ways) inside a dodecahedron



(images from wolfram math world and adapted from Steven Dutch web site)

and

a tetrahedron sits (2 ways) inside a cube (image adapted from Steven Dutch web site)



dodecahedral/icosahedral Golden Ratio $\sqrt{5}$ symmetry
 includes cubic/octahedral/cuboctahedral $\sqrt{3}$ symmetry
 which includes tetrahedral $\sqrt{2}$ symmetry.

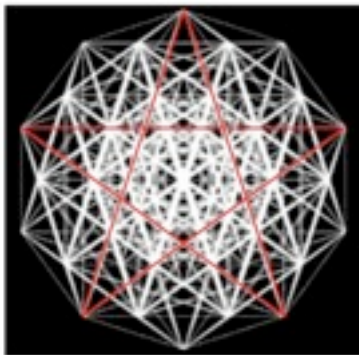
Those symmetries based on 5 and 3 and 2 (and so also 10 and 6 and 4)
 can also be seen in the 600-cell and the E8 root vectors.

In the case of the 600-cell, two Golden Ratio copies of which make up
 the 240 root vectors of E8, the 120 vertices can be seen in terms of
 the Clifford-Hopf fibration of the 3-sphere $S^1 \rightarrow S^3 \rightarrow S^2$

(S^1 = circle or line, S^3 = 3-sphere, S^2 = 2-sphere base of fibration)

in three different ways (See the book "Geometrical Frustration" by Sadoc and Mosseri):

Ten-fold Screw Axis: (image from Bathsheba Grossman E8 glass)



10 on a vertical axis

5 sets of 10 on 5 circles on an large intermediate torus

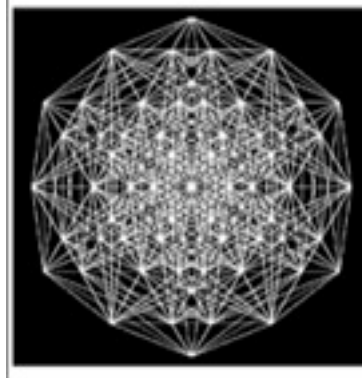
5 sets of 10 on 5 circles on a small intermediate torus

10 on a circle in a plane perpendicular to the vertical axis.

There are $1+5+5+1 = 12$ Ten-fold Screw Axis fibres,

corresponding to the vertices of an icosahedron in the base 2-sphere

Six-fold Screw Axis: (image from Bathsheba Grossman E8 glass)

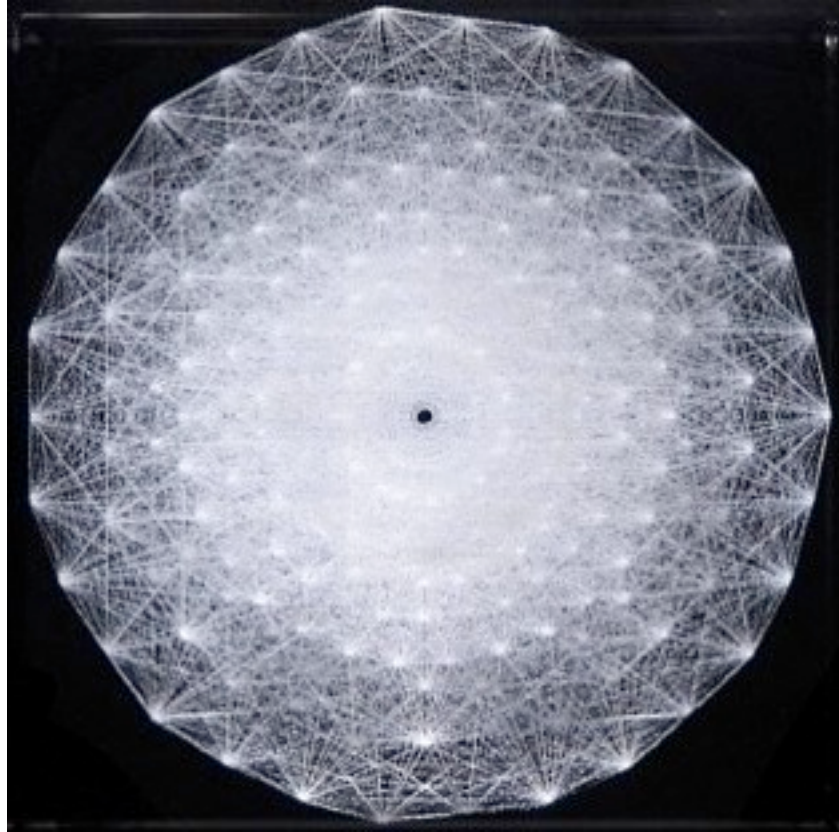


20 sets of 6 on 20 circles. There are 20 Six-fold Screw Axis fibres, corresponding to the vertices of a dodecahedron in the base 2-sphere

Four-fold Screw Axis: (image from Bathsheba Grossman E8 glass)



30 sets of 4 on 30 circles. There are 30 Four-fold Screw Axis fibres, corresponding to the vertices of an icosidodecahedron in the base 2-sphere. The vertices as a ball with 8 layers of 30 vertices each, which $8 \times 30 = 240$ vertices correspond to two copies of the 30 sets of 4, which can be thought of as the 8 circles of 30 that are often used for graphic pictures of the 240 E8 root vectors.



E8 lives inside Cl(16) as Adjoint D3 + Conjugate Spinor D8

**Cl(16) x ...(N times tensor product)... x Cl(16)
by 8-periodicity is Cl(16N)**

**Completion of Union of All Cl(16) Tensor Products
gives
hyperfinite II1 factor Algebraic Quantum Field Theory**

Water and Tetrahedra

Frank Dodd (Tony) Smith, Jr. - 2011

Water as Cellular Automata

Water Self-Replicating Structures

Water as Tetrahedral Fluid

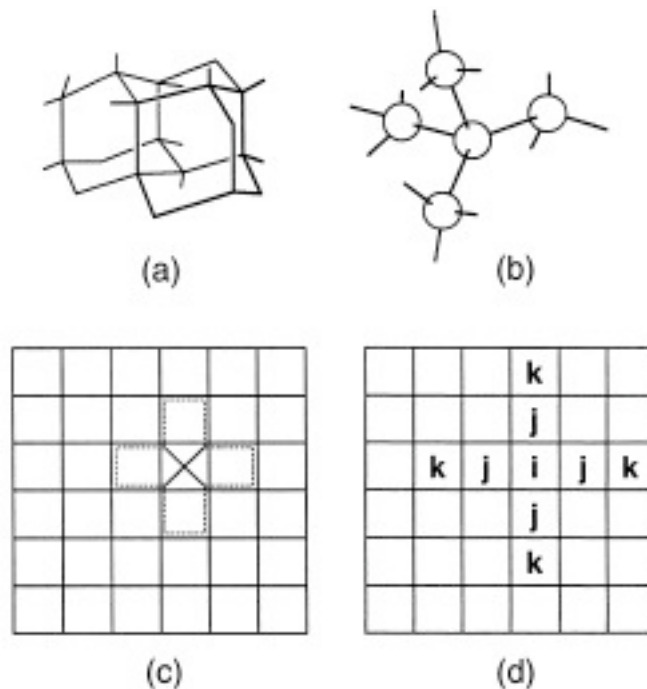
Water as Tetrahedral Quasicrystal

Water as Tetrahedral Dimers

Water Planet (Earth) and 57-group of Tetrahedra

Water as Cellular Automata

Kier, Cheng, and Testa in *Future Generation Computer Systems* 16 (1999) 273-289 say: "... Cellular automata are dynamical computational systems that are discrete in space, time and state and whose behavior is specified completely by rules governing local relationships. ... Our model is composed of a grid of spaces called cells on the surface of a torus to remove boundary conditions. Each cell i has four tessellated neighbors, j , and four extended neighbors, k , in what is called an extended von Neumann neighborhood ... The ... DOS ... programs, collectively called *Ding Hao*, are in the process of being transferred to a Windows operating system. ...



... The configurations achieved after many iterations reach a collective organization ... What we observe and record from the cellular automata simulations are emergent attributes of a complex system ...

A ... model of water is that of an extended network of hydrogen-bonded molecules that lack a single, identifiable, long-lived structure. The hydrogen bonds continually form and break producing a constantly changing mosaic when viewed at the molecular system level. This model lends itself to simulation using dynamic methods such as cellular automata ... using rules governing the joining and breaking of water-designated cells. ...

Two parameters were adopted in our model to govern the probabilities of water particles moving in the grid. ... The grid was the surface of a torus to eliminate boundary conditions. ...

The breaking probability, PB, is the probability for a molecule at i to break away from another at j when there is exactly one occupied j cell ... The value for PB lies in the closed unit interval.

The second parameter, J, describes the movement of a molecular particle at i toward or away from the particle at a k cell in the extended von Neumann neighborhood ... when the intermediate j cell is vacant. J is a positive real number. When J = 1, it indicates that the particle, i, has the same probability of movement toward or away as for the case when k is empty. When J > 1, it indicates that i has a greater probability of movement toward an occupied cell, k than when k is empty. When J < 1, it indicates that i has a lower probability of such movement. ...

Our studies on water have shown a relationship between PB and J expressed as:

$$\log J(W) = -1.50 PB(W) + 0.60$$

...

The study also produced an approximate relationship between the breaking probability of two joined cells PB(W), and the fraction of free water particles associated with a particular temperature ... This observation translates into a relationship between a numerical value of the probability rule and the water temperature $PB(W) = 0.01 T$ (degrees C). ...

From the dynamics simulating water, several attributes are recorded.

f0 fraction of cells not bound to other cells;

f1 fraction of cells bound to only one other cell;

f2 fraction of cells bound to two other cells;

f3 fraction of cells bound to three other cells;

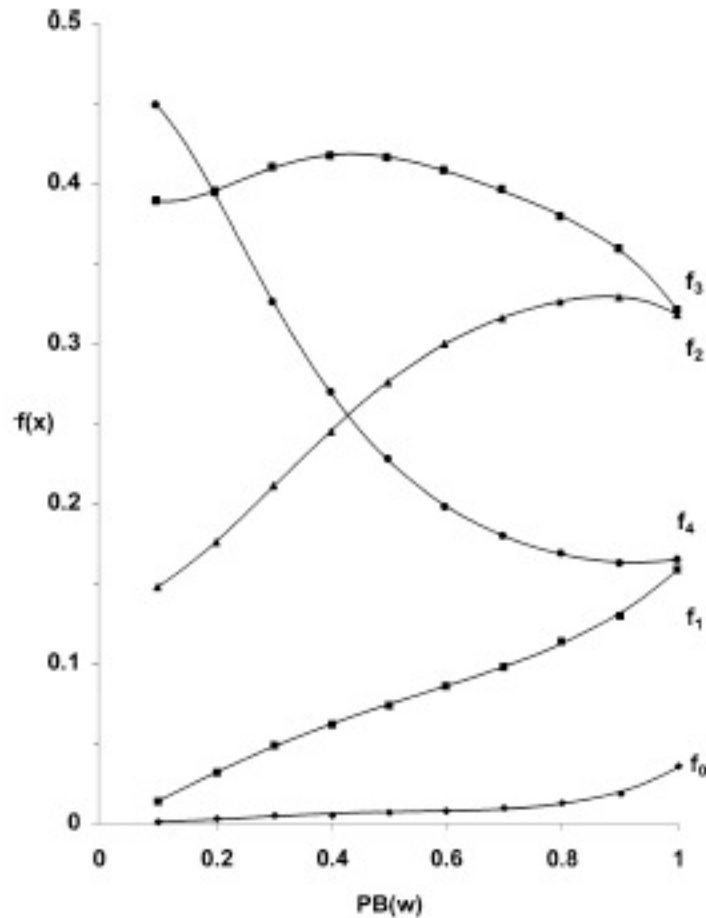
f4 fraction of cells bound to four other cells;

fH free hydrogen fraction = 1/2 of fraction of unbound cell faces;

NHB number of hydrogen bonds per water cell = count of joined faces per cell.

... These attributes characterize the particular configuration associated with a set of PB and J rules. ...

A profile of water cells, described by the fraction of each bonding type, f0–f4, for each temperature, is shown ...



... a set of equations relating several physical properties of water to attributes from the cellular automata simulations are shown ...

Water properties related to cellular automata attributes

Property	Equation	r^2 correlation
Vapor pressure	$\log P_v$ (mm Hg)=13.77 ($f_0 + f_1$) + 0.795	0.987
Dielectric consta	$\epsilon = -224f_1 + 86.9$	0.989
Viscosity	η (cP)=3.165 $f_4 - 0.187$	0.989
Ionization	$-\log K_w = -20.94f_H + 16.43$	0.999
Surface tension	γ (dyn/cm)=16.07 $N_{HB} + 22.35$	0.970
Compressibility	κ ($\times 10^6$ /Bar) = -53.82 $f_3 + 66.66$	0.953

... These correlations between simulated water attributes and various physical properties indicate that the water model we have created with cellular automata has significant validity. ...”.

Kier, Seybold, and Cheng have written a textbook “Modeling Chemical Systems Using Cellular Automata” (Springer 2005) on the subject.

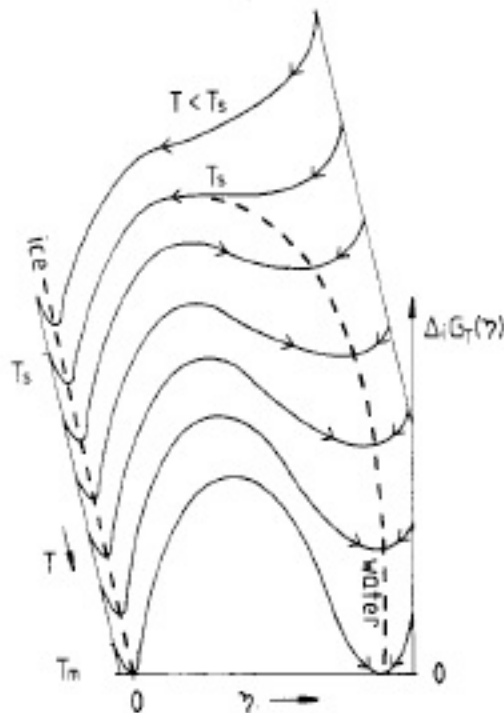
Water Self-Replicating Structures

Robin J. Speedy in J. Phys. Chem 88 (1984) 3364-3373 says:

“... pentagonal rings of hydrogen-bonded water molecules ... have the qualities of (a) self-replication and (b) association with cavities

...

Water differs from other liquids in that when it is cooled below 0 degrees C thermodynamic properties show increasing fluctuations about their average values, with possible divergences at $T_s = -46$ degrees C. It is as though the valley on the free energy surface ...

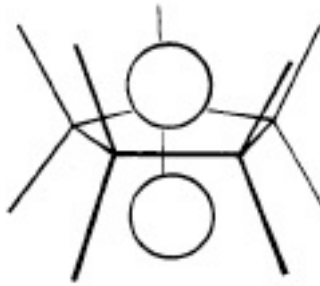


... whose minimum determines the properties supercooled water, becomes shallow and broad (with respect to some structural order parameter ...), allowing the system to sample an increasingly diverse range of structures, and eventually flattens out completely so that the valley comes to an end at T_s

in cold water each molecule is hydrogen bonded to three or four neighbors which tend to be tetrahedrally disposed and that, at any instant, the structure can be viewed as a single connected three-dimensional ... tetrahedral ... network.

To account for the anomalies it is then logically sufficient to suppose that there are, in the network, some particular structures which are (a) self-replicating and (b) associated with cavities. ...

pentagonal rings of hydrogen-bonded water molecules are self-replicating, in the sense that the presence of a pentagon biases adjacent regions of the network in favor of reproductions of itself and that each pentagon is probably associated with a pair of cavities ...



... A pair of dodecahedra, for example, can stabilize each other by sharing a pentagonal face and therefore tend to cluster together.

...

Given the enhanced probability of one pentagon adjacent to a solute, the self-replicating propensity of the pentagon implies an enhanced probability of more pentagons in the region extending perhaps several pentagon diameters away from the solute. Therefore, the “influence” of a solute on the solvent need not be localized to its immediate solvation shell, or even to that region of the solvent that lies within the range of direct interactions, but can be spread diffusely over an extended region. ...”.

Water as Tetrahedral Fluid

Kolafa and Nezbeda in *Molecular Physics* 84 (1995) 421-434 say:

“... Despite the fact that there are no attractive forces acting between hard tetrahedrons, their shape induces, at high densities, a structure which resembles the structure of liquid water ...

Hard tetrahedrons ... HTH ... exhibit an extreme non-sphericity and their specific way of packing ... in ... a fluid of regular hard tetrahedrons ... gives rise to ... the structure of water ... with ... pentagonal formations of tetrahedrons from 'selfreplicating structures' ...

Liquid water is known to exhibit a number of anomalies, which result from a well-developed hydrogen-bond network with a more or less regular tetrahedral symmetry. ... a purely geometrical theory due to Speedy, based on pentagonal (and higher) formations of hydrogen-bonded molecules, seems to be the 'deepest' ... insight into the structure of the hydrogen-bond network and hence to explain the anomalous properties of water qualitatively ...

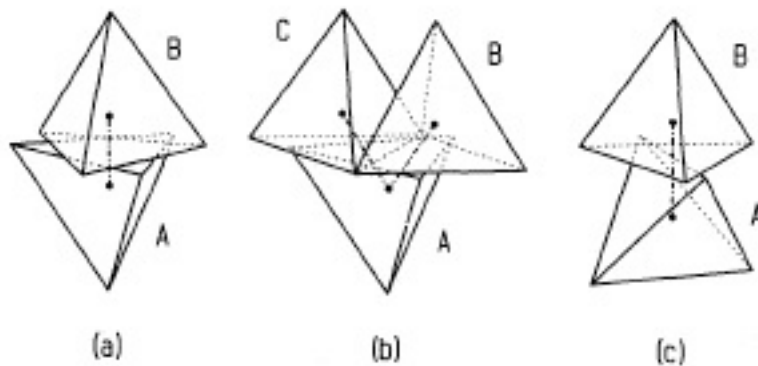
For the HTH fluid the functions of main interest are the centre-to-centre ... and vertex-to-vertex ... correlation functions. ...

The concept of an irregular distorted but locally tetrahedral network of hydrogen bonds (HBs) has become a standard tool for describing properties and anomalies of

liquid water. This view has been supported by molecular simulations using different potential models and has allowed the study of phenomena such as polygons (cycles) in the HB network or the occurrence of various polyhedrons.

...

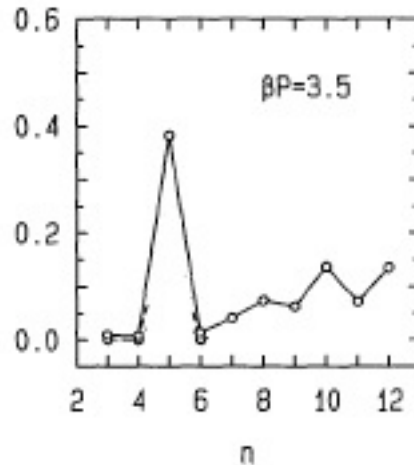
- (1) There is a high probability that an arbitrarily selected molecule has four neighbours which are tetrahedrally arranged.
- (2) The hydrogen-bond network is fully connected (percolated). Two-, three-, and four-bonded molecules are the most probable.
- (3) The conformation of a hydrogen bonded pair of molecules is more likely to be staggered ... than eclipsed ...
- (4) Of all bridgeless (non-short-circuited) polygons made from hydrogen-bonded molecules, pentagons and hexagons are the most probable, although neither longer polygons are negligible.
- (5) Pentagonal rings of bonded molecules form *self-replicating structures*, i.e., it is more probable to find a pentagon in the vicinity of another pentagon than at a random place. A similar (but weaker) phenomenon occurs for hexagons.
- (6) Water at low temperatures (supercooled water) contains bulky polyhedrons with pentagonal and hexagonal faces. These polyhedrons are bound by their faces in an irregular way. ...



...

The shortest centre-to-centre distance ... (a) ... face-to-face ...
 For ... (b) ... two tetrahedrons ... form a double hydrogen bond with ... a third ...
 for ... (c) ... it is not possible to decide ... which ... face ...is 'bonded' ...

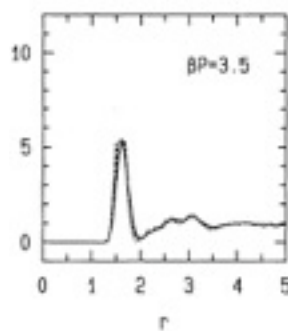
with increasing density/pressure the specific way of packing of the HTHs begins to dominate ... for the highest density ... $\beta P = 3.5$... the centre-to-centre correlation function ... becomes water-like ... Concentrations of ... bridgeless polygons ... are shown ... for ... hydrogen bond ... distance... 1.7 ...



... A sharp peak at $n = 5$ is observed ... The value for $n = 8$... reflect[s] ... two pentagons sharing one edge ...

The polygon structure of the HTH may be compared with the structure of water, where both pentagons and hexagons are present in approximately equal numbers ... this difference between water and hard tetrahedrons can be explained by the tendency of a pair of bonded water molecules to be in a staggered conformation, whereas a pair of face-to-face tetrahedrons prefers an eclipsed conformation. ...

Since the role of pentagons in the HTH fluid is even more pronounced than in water, we ... calculated the pentagon-pentagon correlation function ...



... We can thus conclude that pentagonal rings in the HTH fluid form 'self-replicating structures': when we consider any edge (pair of 'hydrogen bonded' tetrahedrons) of a pentagon, the eclipsed conformation of these two tetrahedrons makes it easier for the other three tetrahedrons to form an additional pentagon containing this edge ...".

Water as Quasicrystal

Haji-Akbari¹, Engel, Keys, Zheng, Petschek, Palffy-Muhoray, and Glotzer in arXiv 1012.5138 say:

“... a fluid of hard tetrahedra undergoes a first-order phase transition to a dodecagonal quasicrystal, which can be compressed to a packing fraction of $\phi = 0.8324$.

By compressing a crystalline approximant of the quasicrystal, the highest packing fraction we obtain is $\phi = 0.8503$.

If quasicrystal formation is suppressed, the system remains disordered, jams, and compresses to $\phi = 0.7858$.

Jamming and crystallization are both preceded by an entropy-driven transition from a simple fluid of independent tetrahedra to a complex fluid characterized by tetrahedra arranged in densely packed local motifs that form a percolating network at the transition. ...

Aside from studies of packing, hard tetrahedra have been used to model the structure of water.

...

In hard particle systems, the potential energy of two particles is considered infinite if they interpenetrate and zero otherwise. ... hard particles can maximize entropy by ordering ... In the limit of infinite pressure, an arrangement with maximum packing fraction is stable because it minimizes specific volume and Gibbs free energy. One of the simplest shapes for which the packing problem is still unsolved is the regular tetrahedron.

Tetrahedra do not tile Euclidean space. However, if extra space is allowed between tetrahedra, or between groups of tetrahedra, dense ordered structures become possible. Imagine building a dense cluster, one tetrahedron at a time. As shown ... tetrahedral dice are stuck together with modelling putty ...



... a pentagonal dipyramid (PD) is easily built from five tetrahedra if one allows an internal gap of 7.36° .



Two PDs can share a single tetrahedron to form a nonamer.

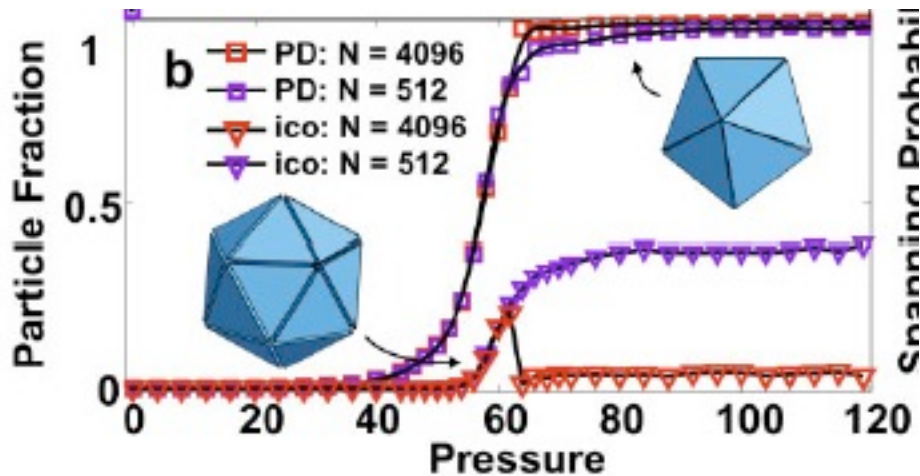


Twelve interpenetrating PDs define an icosahedron with a gap of 1.54 steradians. ...



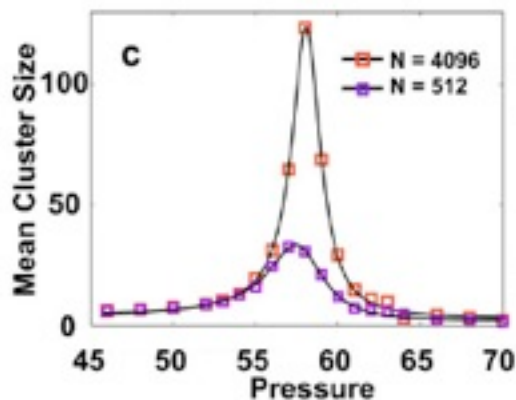
... a dense, one-dimensional packing given by a linear arrangement of tetrahedra with touching faces [is] known as a tetrahelix, or Bernal spiral ... The tetrahelix maximizes packing density in one dimension. ...

To obtain dense packings of hard regular tetrahedra, we carry out Monte-Carlo (MC) simulations ... of a small system with 512 tetrahedra and a large system with 4096 tetrahedra. ... The large system undergoes a first order transition on compression of the fluid phase and forms a quasicrystal. ...



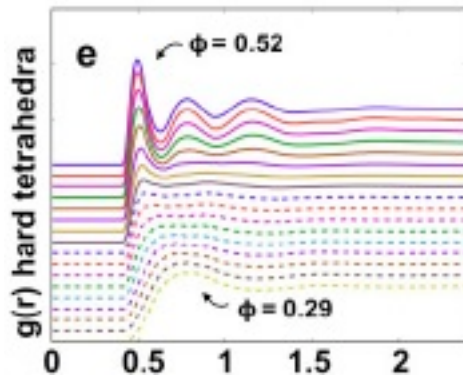
... We see that the fraction of tetrahedra belonging to at least one PD increases well before jamming or crystallization.

With increasing pressure, interpenetrating PDs form icosahedra and finally merge into a percolating PD network as the fraction of tetrahedral in PD approaches unity. ...[The figure shows]... Mean cluster size of interpenetrating PDs ...[and]... suggests a percolation transition of the PD network ... at $P^*p = 58 \pm 2$, prior to both jamming and crystallization. We do not observe tetrahedratic liquid crystal phases ...



... For the large system, the fraction of tetrahedra in icosahedra suddenly drops at $P^* = 62$ when crystallization occurs. Comparison with the glass shows that many fewer icosahedra remain in the quasicrystal. ...

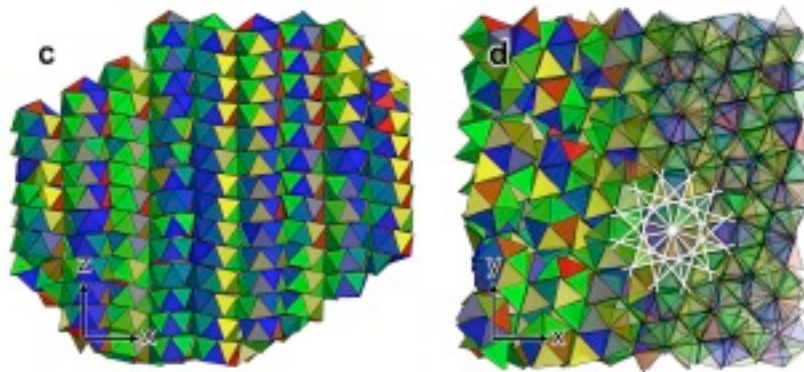
Structural changes of the fluid are revealed by the unusual behaviour of its radial distribution function $g(r)$, as shown ...



... We find that the first peak near $r = 0.75\sigma$ disappears upon compression at low pressure, only to reappear for higher pressure, splitting into two peaks at $r = 0.55\sigma$ and $r = 0.80\sigma$. The positions of these peaks are characteristic of face-to-face and edge-to-edge arrangements, respectively, within a single PD.

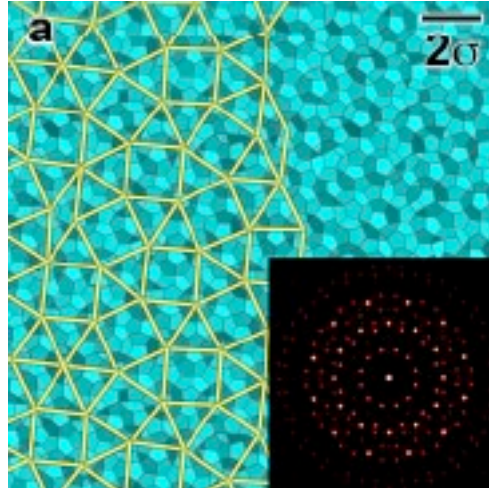
...

The spontaneous formation of a quasicrystal from the fluid is remarkable ...

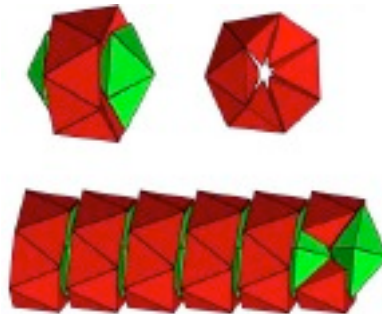


... it can be seen that the quasicrystal consists of a periodic stack of corrugated layers with spacing 0.93σ . The view along the direction of the stacking vector reveals details of the structure within the layers. Twelve-fold symmetric rings formed by interpenetrating tetrahelices exist throughout the structure. The helix chirality is switched by 30° rotations ...

The structure of the quasicrystal can be understood more easily by examining the dual representation constructed by connecting the centres of mass of neighbouring tetrahedra. In the dual representation, PDs are represented by pentagons. The mapping is applied to a layer of an 8000 particle quasicrystal ...

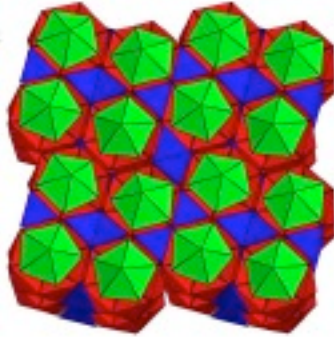


... Recurring motifs are rings of twelve tetrahedra that are stacked periodically to form “logs”...

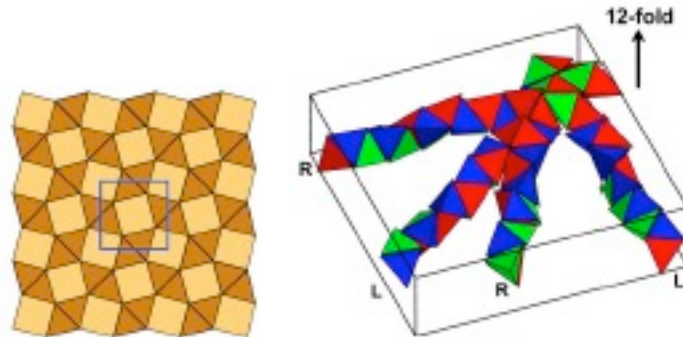


... the symmetry axes of the logs arrange into a non-repeating pattern of squares and triangles (tile edge length 1.83σ) – an observation that we confirm in systems with 13824 and 21952 particles ... The diffraction pattern obtained by positioning scatterers at the centres of tetrahedra shows rings of Bragg peaks, indicating the presence of long-range order with twelve-fold symmetry not compatible with periodicity. Perfect quasicrystals are aperiodic while extending to infinity; they therefore cannot be realized in experiments or simulations, which are, by necessity, finite. The observed tilings and diffraction patterns with twelve-fold symmetry are sufficient in practice for the identification of our self-assembled structures as dodecagonal quasicrystals. ...

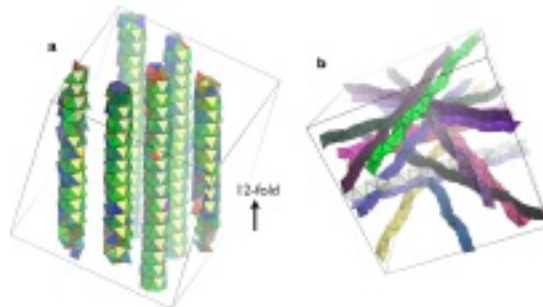
Quasicrystal approximants are periodic crystals with local tiling structure identical to that in the quasicrystal. Since they are closely related, and they are often observed in experiments, we consider them as candidates for dense packings. The dodecagonal approximant with the smallest unit cell (space group) has 82 tetrahedra ...



... and corresponds to one of the Archimedean tilings. At each vertex we see the logs of twelve-member rings (shown in red) capped by single PDs (green). The logs pack well into squares and triangles with additional, intermediary tetrahedra (blue). The vertex configuration of the tiling is ...

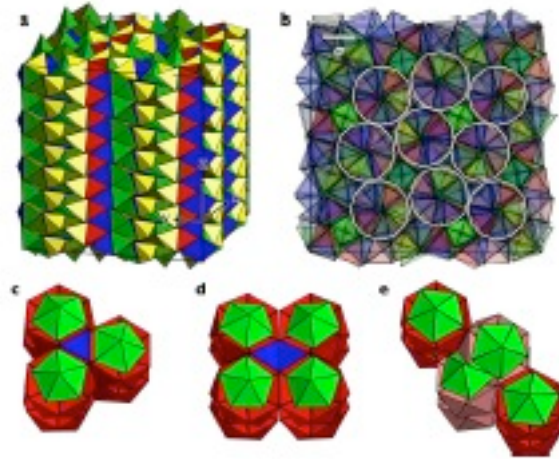


... Interpenetrating tetrahelices can also be seen in the approximant ... [and in] the dodecagonal quasicrystal ...



... Tetrahelices containing more than 48 tetrahedra ... in the $N = 13824$ system ... projected along the twelve-fold axis ... are limited to twelve directions. ... The chirality ... is switched every 30 degrees. ...

“Building” and numerically compressing a unit cell of this ideal structure achieves a packing fraction of $\phi = 0.8479$. If we compress a $2 \times 2 \times 2$ unit cell, the packing fraction marginally increases to $\phi = 0.8503$...



... For ease of viewing, the $2 \times 2 \times 2$ cell has been periodically continued into a $2 \times 2 \times 8$ cell. ... In the translucent image, the twelvefold logs can be identified. The logs arrange into triangle (c) and square (d) tiles with 9.5 and 22 tetrahedra, respectively. ...

Why should square-triangle tilings be preferred for dense packings of tetrahedra?

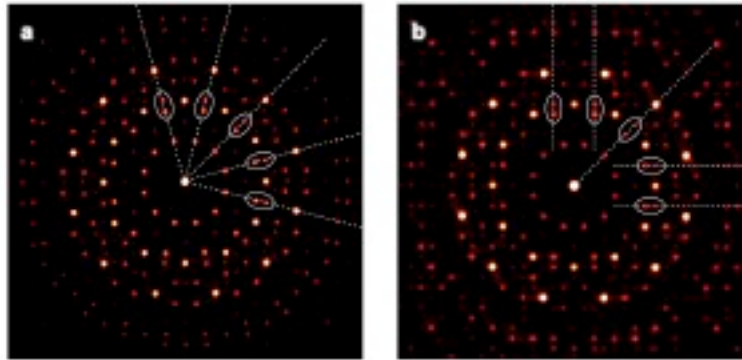
First, we compare the packing fraction of the square tile (22 tetrahedra) to that of the triangle tile (9.5 tetrahedra).

Their ratio $\phi_{\text{Triangle}} / \phi_{\text{Square}} = 19 / 11\sqrt{3} \approx 0.9972$ is nearly unity, which suggests that tetrahedra pack equally well in both tiles.

Second, we note that rings comprising the logs are tilted ... and the layers of the structure are corrugated ... This is a direct consequence of the face-to-face packing of tetrahedra where neighbouring logs kiss. As a result, the square tile has a negative Gaussian curvature while the triangle tile has a positive one.

Alternating the two tiles produces a net zero curvature in the layers, as observed in the quasicrystal and its approximant. ...

Bragg peaks have perfect twelve-fold symmetry in the dodecagonal quasicrystal (a), the symmetry is broken to four-fold symmetry in the approximant (b). ...



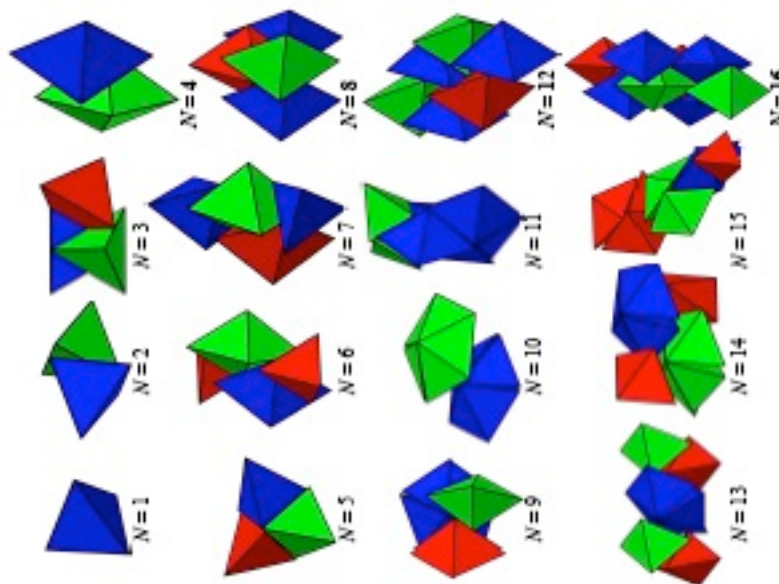
... As indicated by white dashed lines and ellipsoids, weak Bragg peaks of the approximant are shifted slightly from their positions in the quasicrystal.

...
the local structure of the ... approximant, the dodecagonal quasicrystal and the disordered glass ... are ... only subtly different, and more sensitive measures of local order, as ... Fraction of tetrahedra participating in pentagonal dipyrramids ... and icosahedra ... are required. The crucial step during crystallization is the transformation of the percolating PD network into layers, and the elimination of icosahedra. ...”.

Water as Dimers

Chen, Engel, and Glotzer in arXiv 1001.0586 say:

“... We present the densest known packing of regular tetrahedra with density $\Phi = 4000 / 4671 = 0.856347 \dots$



#Tetra N	Maximum Density		Success Rate	Motifs, Structural Description
	Numerical, ϕ^2	Analytical, ϕ		
1	0.367346	18/49	100%	1 monomer [11]
2	0.719486	ϕ_2	100%	2 monomers, transitive [22]
3	0.666665	2/3	21%	3 monomers, three-fold symmetric
4	0.856347	4000/4671	80%	2 dimers (positive + negative)
5	0.748096	ϕ_5	22%	1 pentamer, asymmetric
6	0.764058	ϕ_6	11%	2 dimers + 2 monomers
7	0.749304	3500/4671	15%	2 × 2 dimers minus 1 monomer
8	0.856347	4000/4671	44%	2 × 2 dimers, identical to $N = 4$
9	0.766081		—	1 pentagonal dipyramid + 2 dimers
10	0.829282	ϕ_{10}	2%	2 pentagonal dipyramids
11	0.794604		—	1 nonamer + 2 monomers
12	0.856347	4000/4671	3%	3 × 2 dimers, identical to $N = 4$
13	0.788728		4%	1 pentagonal dipyramid + 4 dimers
14	0.816834		3%	2 pentagonal dipyramids + 2 dimers
15	0.788693		—	Disordered, non-optimal
16	0.856342	4000/4671	< 1%	4 × 2 dimers, identical to $N = 4$
⋮	⋮			⋮
8 × 82	0.850267			Quasicrystal approximant [21]

... The dimer structures are remarkable in the relative simplicity of the 4-tetrahedron unit cell as compared to the 82-tetrahedron unit cell of the quasicrystal approximant, whose density is only slightly less than that of the densest dimer packing. The dodecagonal quasicrystal is the only ordered phase observed to form from random initial configurations of large collections of tetrahedra at moderate densities. It is thus interesting to note that for some certain values of N , when the small systems do not form the dimer lattice packing, they instead prefer clusters (motifs) present in the quasicrystal and its approximant, predominantly pentagonal dipyramids. This suggests that the two types of packings

- the dimer crystal and the quasicrystal/approximant - may compete, raising interesting questions about the relative stability of the two very different structures at finite pressure. ...”.




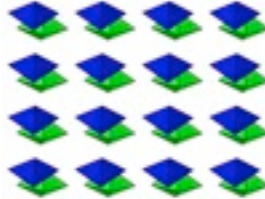
If you regard a Tetrahedron as a pair of Binary Dipoles then the high (0.85+) density configurations have the same **8-periodicity property as the Real Clifford Algebras**:


#Binary Dipoles M	Maximum Density		Success Rate	Motifs, Structural Description
	Numerical, $\hat{\phi}$	Analytical, ϕ		
2	0.367346	18/49	100%	1 monomer [11]
4	0.719486	ϕ_2	100%	2 monomers, transitive [22]
6	0.666665	2/3	21%	3 monomers, three-fold symmetric
8	0.856347	4000/4671	80%	2 dimers (positive + negative)
10	0.748096	ϕ_5	22%	1 pentamer, asymmetric
12	0.764058	ϕ_6	11%	2 dimers + 2 monomers
14	0.749304	3500/4671	15%	2 × 2 dimers minus 1 monomer
16	0.856347	4000/4671	44%	2 × 2 dimers, identical to $N = 4$
18	0.766081		—	1 pentagonal dipyrmaid + 2 dimers
20	0.829282	ϕ_{10}	2%	2 pentagonal dipyrmaids
22	0.794604		—	1 nonamer + 2 monomers
24	0.856347	4000/4671	3%	3 × 2 dimers, identical to $N = 4$
26	0.788728		4%	1 pentagonal dipyrmaid + 4 dimers
28	0.816834		3%	2 pentagonal dipyrmaids + 2 dimers
30	0.788693		—	Disordered, non-optimal
32	0.856342	4000/4671	< 1%	4 × 2 dimers, identical to $N = 4$
⋮	⋮			⋮
164x8	0.850267			Quasicrystal approximant [21]

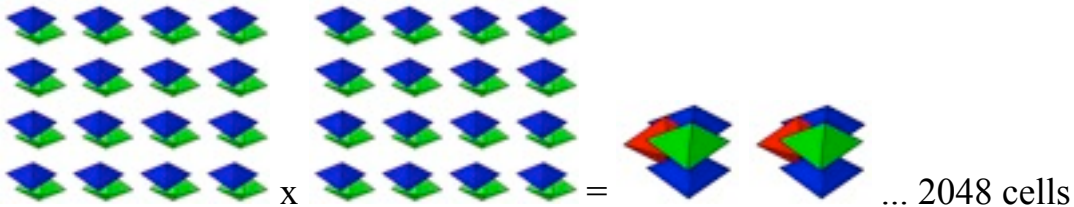
which is consistent with regarding the 4 vertices of a Tetrahedron as the 4 elements of the Cl(2) Real Clifford Algebra, isomorphic to the Quaternions, with graded structure 1+2+1, and so 4 tetrahedra as Cl(4x2) = Cl(8).

From that point of view, **the true Quasicrystal would correspond to a generalized Hyperfinite III von Neumann factor that gives a natural Algebraic Quantum Field Theory structure to E8 Physics.**

The 4-tetrahedra 2-dimer  corresponding to $Cl(8)$ has 16 vertices in each basic cell. It takes 16 of those cells to get enough vertices to represent the $256 = 16 \times 16$ elements of $Cl(8)$:



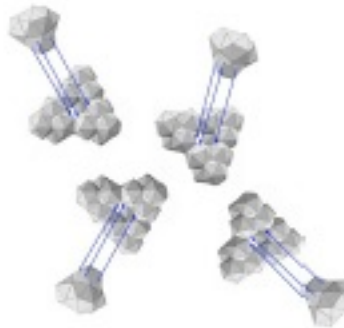
The 8-tetrahedra 4-dimer  corresponding to $C(8) \times Cl(8) = Cl(16)$ has 32 vertices in each basic cell. It takes 2048 of those cells to get enough vertices to represent the $65536 = 32 \times 2048 = 256 \times 256$ elements of $Cl(16)$:



The $8 \times 2048 = 16384$ tetrahedra whose 65536 vertices represent $Cl(16)$ form a dense (85.63 %) packing of flat 3-dim space.



A much less dense diamond lattice  in flat 3-dim space can be formed from Pearce clusters. Combining Pearce structures with four 57-groups



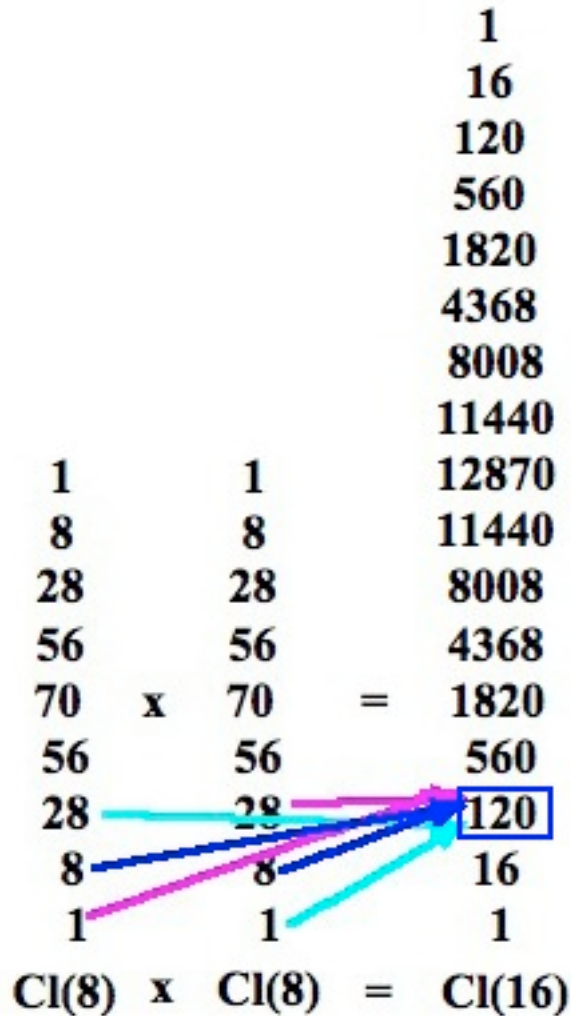
gives a 240-polytope made up of two 600-cells that describe the E_8 Lie algebra which has 248 elements, 240 of which are root vectors.

What part of the very dense 65536-dim $Cl(16)$ forms the very thin diamond lattice with 248-dim E_8 whose symmetry describes a realistic physics model?

As shown by graded structure, 248-dim E8 is made up of
the bivector 120 of Cl(16)

plus

a 128 Cl(16) half-spinor $8 \times 8 = 64 + 8 \times 8 = 64$

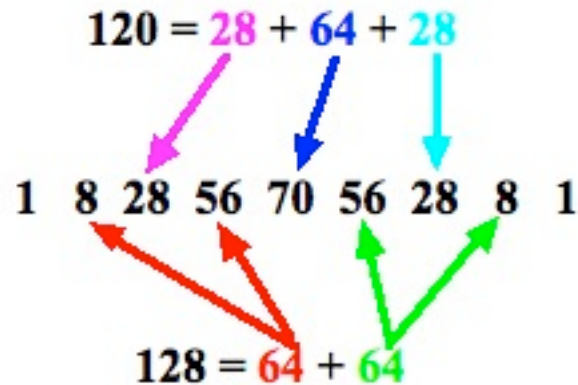


Spinors:

$$(8s+8c) \times (8s+8c) = \boxed{8s \times 8s} + \boxed{8c \times 8c} + 8s \times 8c + 8c \times 8s$$

so that only 120+128 = 248 of the 65536 elements of Cl(16) are used for E8.

In fact, $120+128 = 248$ -dim E8 can fit inside only one copy of 256-dim Cl(8)



where the 1 scalar, 6 of 70 middle elements, and 1 pseudoscalar are not used and where the physical interpretation of the structure is naturally realistic (E8 fermions in Cl(8) odd part, E8 bosons + spacetime in Cl(8) even part).

The E8 grading $8\ 28\ 56\ 64\ 56\ 28\ 8$ can be seen as

$$\begin{array}{ccccccc}
 & & & 63 & & & \\
 8 & 28 & 56 & 1 & 56 & 28 & 8
 \end{array}$$

which as shown by

Rutwig Campoamor-Stursberg in Acta Physica Polonica B 41 (2010) 53-77 can be contracted to $SL(8) + H_{92}$

where

$SL(8) = 63$ of $64 = 8 \times 8$ Position/Momentum combinations of 8-dim spacetime

H92 = Heisenberg Algebra with
gauge boson creation/annihilation operators in the even part $28 + 1 + 28$
and
fermion creation/annihilation operators in the odd part $8+56 + 56+8$

From the Clifford Algebra point of view:

The loose E8 structure sits inside less than 1 / 256 of the dense packing of $256 \times 256 = 65536$ -element Cl(16).

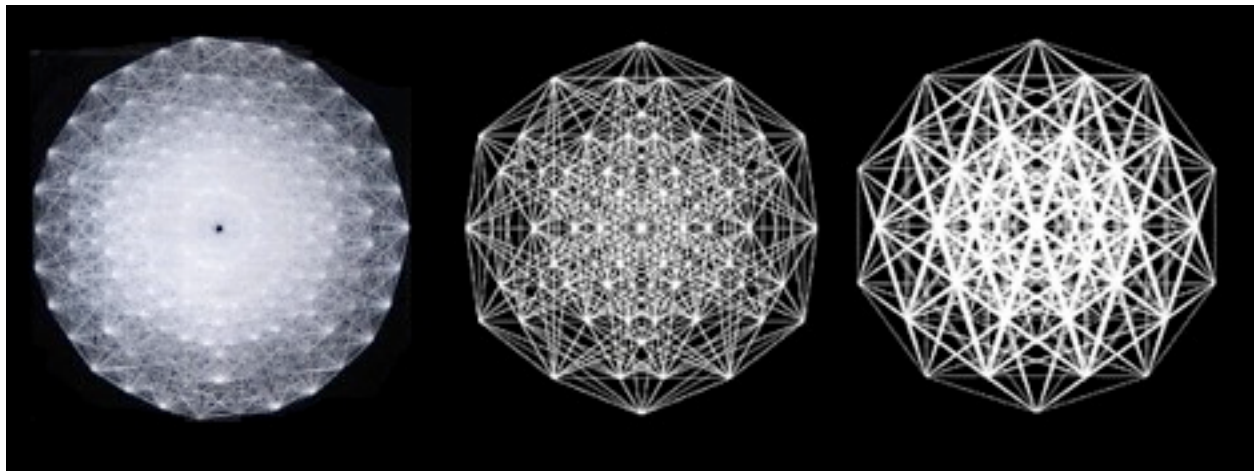
What is the physical interpretation of all that “extra” space ?

Since 4-dim HyperDiamond and 3-dim Diamond and 2-dim Feynman Checkerboard and 1-dim Line Segment lattices can be seen as sublattices or projections of the 8-dim E8 lattice structure and

since Quasicrystals in 4 and 3 and 2 and 1 dimension can be seen as irrational slices through the 8-dim E8 lattice structure, especially by slicing by the most irrational number, the Golden Ratio, thus producing Fibonacci Quasicrystal structure

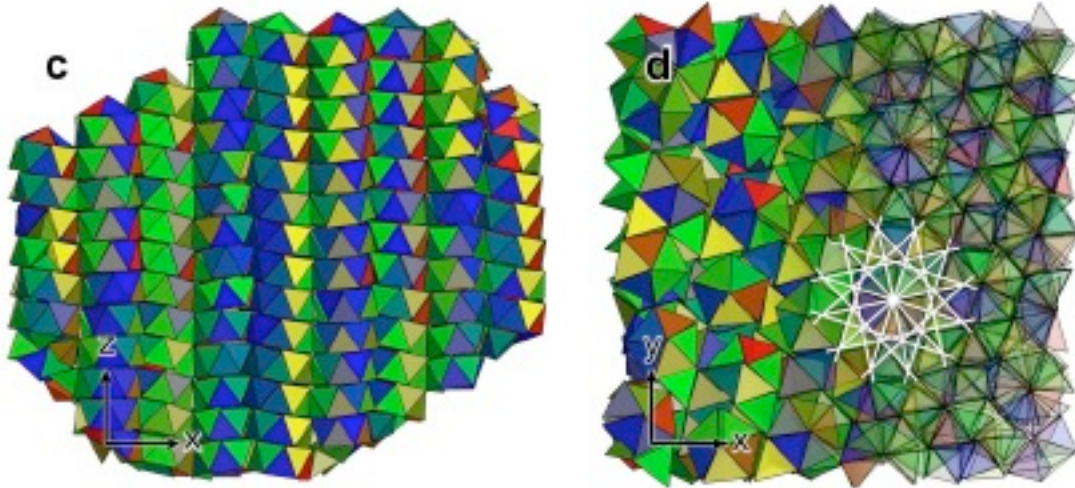
the physical interpretation of the vast “extra” space covered by dense Tetra/Quasicrystal Packing but not covered by loose Diamond Lattice Structure will be discussed here in terms of E8 Lattice Structure.

Although the 240 root vectors of **E8 symmetry** are often shown with 30-fold symmetry as in the left image below from Bathsbeba Grossman’s web site



E8 can also be seen to have **12-fold** (center) and 10-fold (right) symmetries as can be seen by rotating Bathsbeba Grossman’s 3-dim glass E8 sculptures.

Such **12-fold symmetry is also characteristic of Tetra/Quasicrystal Packing** as discussed by Haji-Akbari¹, Engel, Keys, Zheng, Petschek, Palffy-Muhoray, and Glotzer in arXiv 1012.5138 where they describe “... A quasicrystal with packing fraction $\phi = 0.8324$ obtained by first equilibrating an initially disordered fluid of 13824 hard tetrahedra using Monte Carlo simulation and subsequent numerical compression ...” and say “... The images show ... opaque and translucent views of two rotated narrow slices (c)-(d). The white overlay in (d) shows the distinctive twelve-fold symmetry of the dodecagonal quasicrystal. ...”



... Corrugated layers with normals along z are apparent in (c). The colouring of tetrahedra is based on orientation. ... By compressing a crystalline approximant of the quasicrystal, the highest packing fraction we obtain is $\phi = 0.8503$ Aside from studies of packing, **hard tetrahedra have been used to model the structure of water. ...**”.

Just as water is the medium in which the structures of life live in Earth’s oceans,
the dense tetrahedra of Tetra/Quasicrystal Packing
are the active vacuum/medium
necessary for
Quantum Phenomena in the thin Lattice of E8 HyperDiamond Physics.

As Schroer said in hep-th/9908021, in any interacting system “... **any compactly localized operator applied to the vacuum generates clouds of pairs of particle/antiparticles ...**”.

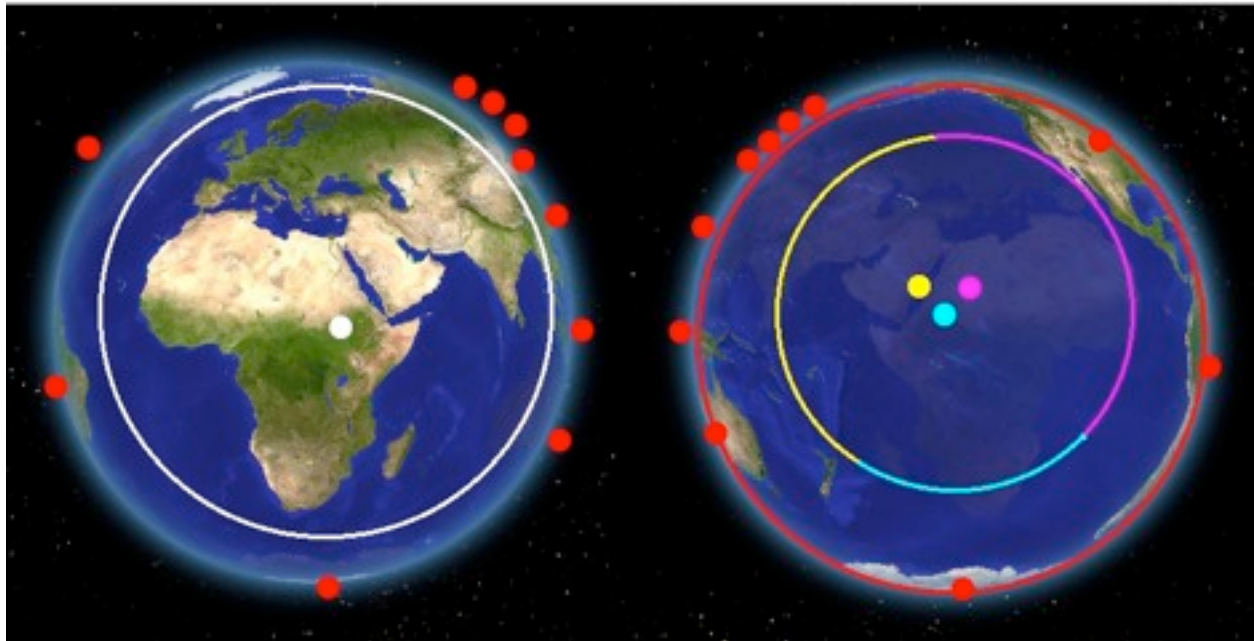
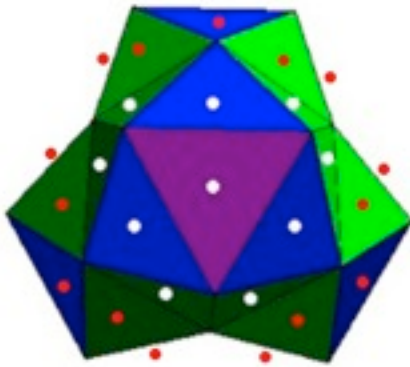
The source of those clouds of pairs of particle/antiparticles is the active vacuum/medium of the dense Tetra/Quasicrystal Packing in which lives the thin Lattice of E8 HyperDiamond Physics.

Earth as a 57-group

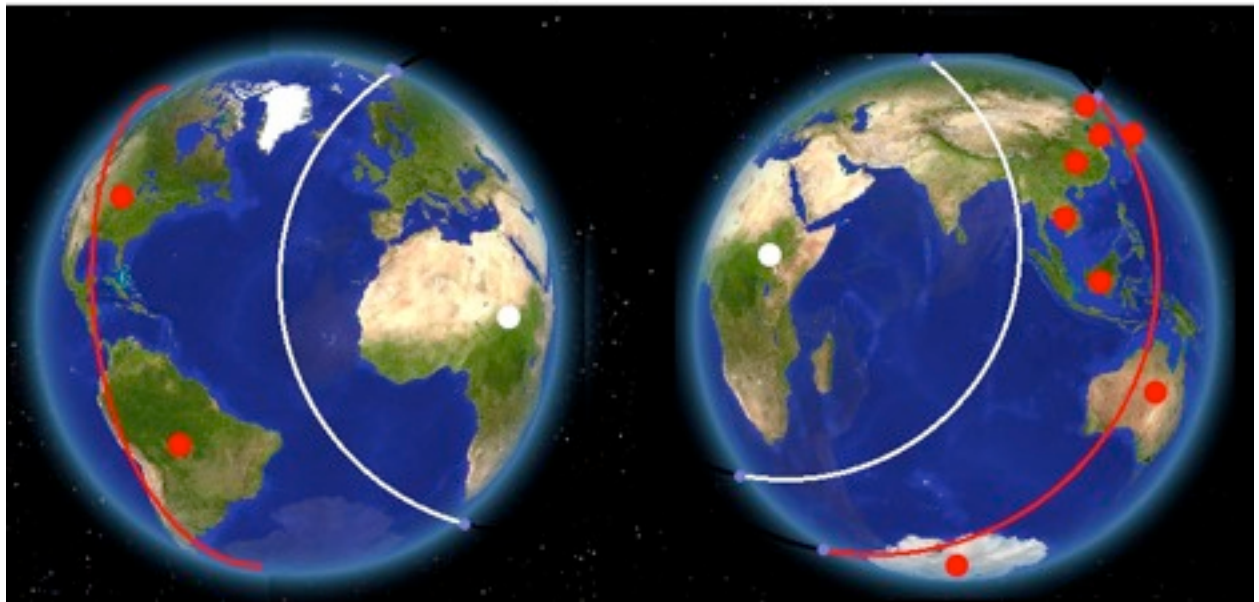
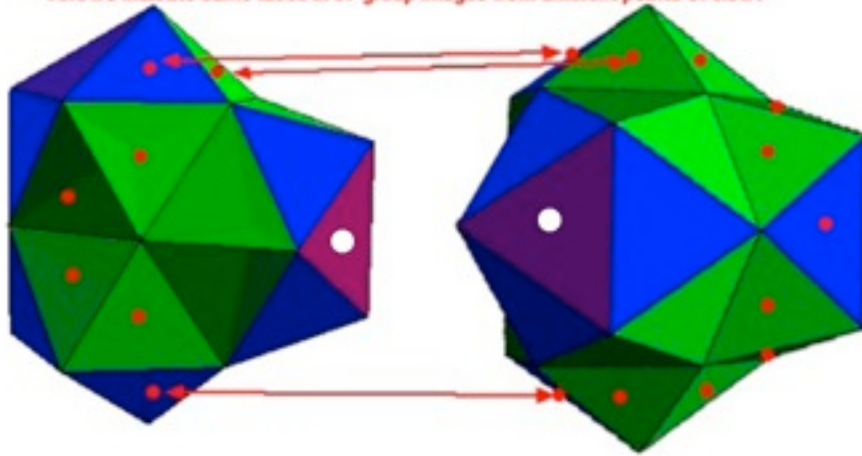
Frank Dodd (Tony) Smith, Jr. - 2011

If you think of the chosen icosahedron as Africa, Europe, and West Asia (including India) and the opposite 3 pentagonal 5-groups as the Pacific Ocean and the 15 exterior faces of the 18-cycle as North and South America, Antarctica, Australia, Indonesia, Vietnam, China, Korea, Japan and Siberia then

you see that the Earth has the structure of the 57-group with Africa-Europe-West Asia as the Icosahedron chosen from the 4 icosahedra.



Arrows indicate same faces in 57 group images from different points of view.



To describe tetrahedral packing gaps of the 57-group in detail, use dodecahedra at each unsplit vertex where 20 tetrahedra come together (using partial dodecahedra at relatively outer vertices) at each of the 26 vertices of the 57-group and then distort the dodecahedra to account for the gaps of 3-dim flat space.

For the case of a pentagonal 5-group the gaps are pairs of vertices instead of dodecahedra, and since pairs of points determine lines, you can compare the lengths of the 5 gap lines of the 5-group.

A simple comparison would be between the cases:
4 of the gap lines zero, all of the gap into one gap line and
all 5 gap lines of equal length, the gap spread evenly.

Then you can calculate the total gap volume, and since the 5 tetrahedra all have the same volume, the total volume of the 5-group is 5 x tetrahedron volume plus total gap volume.

The configuration with the smallest total gap volume should be the most dense.

As the following image of diagrams and calculations shows the most dense configuration is with all the gap into one gap line.

Note that the diagram text mentions volume calculation, when I actually only calculated the area of a cross-section of the volume, but the relative comparison result may still be the same.

As Fang said "... the gap volume for the five-group case ...[is]... (if we assume the tetrahedral edge length is 1)

$$\frac{1}{8} \sin[2\pi - 5\text{ArcCos}[1/3]] = 11 \sqrt{2}/972,$$

thus the ratio

to the tetrahedral volume ($\sqrt{2}/12$) is 11:81.

image from Conway and Torquato PNAS 103 (2006) 10612-10617

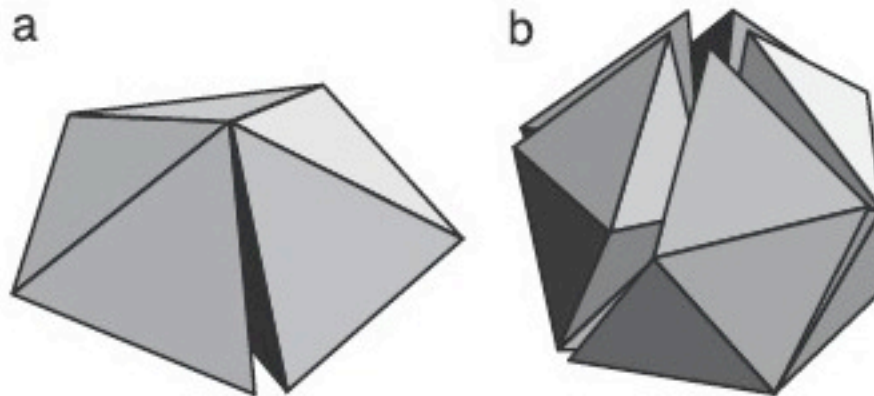
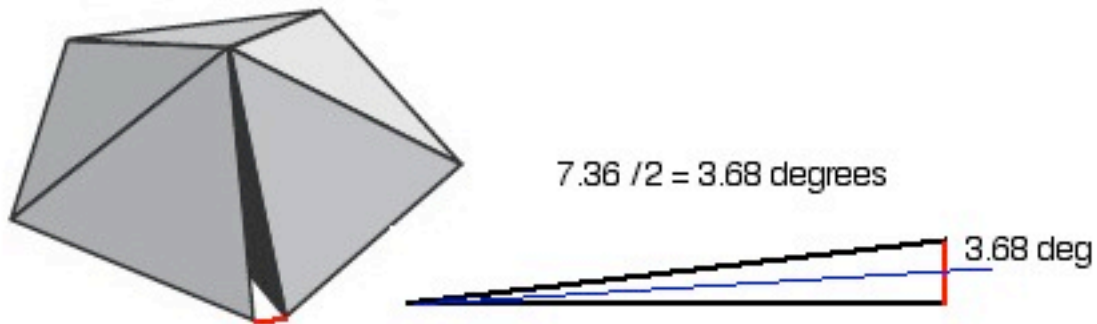


Fig. 1. Certain arrangements of tetrahedra. (a) Five regular tetrahedra about a shared edge. The angle of the gap is 7.36° . (b) Twenty regular tetrahedra about a shared vertex. The gaps amount to 1.54 steradians.



$$\cos(3.68) = 0.99793808$$

$$\sin(3.68) = 0.064183966$$

$$\text{Gap Volume with unit radius} = (2 \times ((1/2) \times \cos(3.68) \times \sin(3.68)))$$

Gap Volume with unit radius and even distribution of gaps =

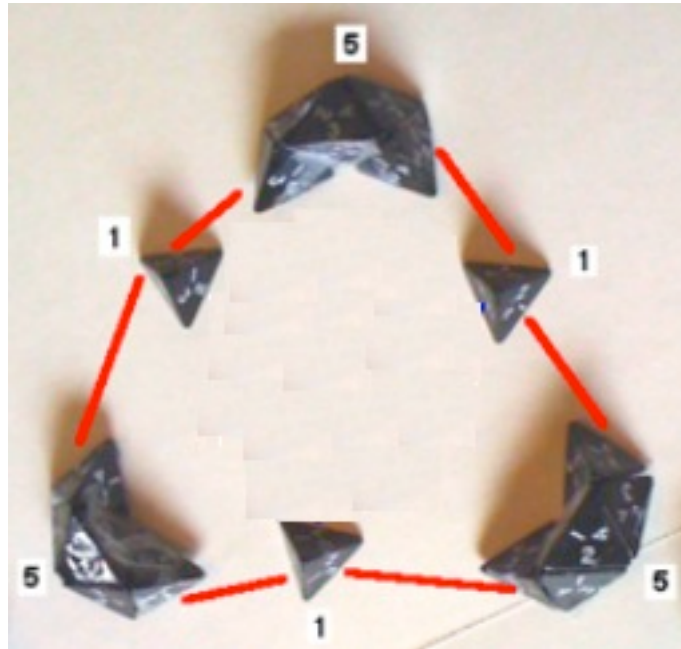
$$= (2 \times ((1/2) \times \cos(3.68) \times \sin(3.68))) \times 5$$

$$\cos(0.736) = 0.99991750$$

$$(7.36 / 5) / 2 = 0.736 \text{ degrees}$$

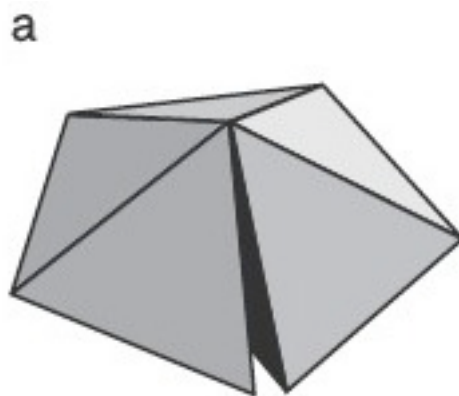
$$\sin(0.736) \times 5 = 0.064226350$$

The most interesting dynamic structure is of the 57-group, rather than smaller or larger clusters and the key to 57-group dynamic structure is its 18-tetrahedron ring structure

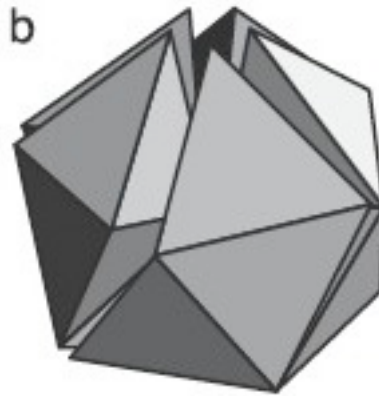


with 3 groups of 5 tetrahedra that fit exactly face-to-face connected by 3 junction tetrahedra that contain the gap angles.

Consider these clusters of tetrahedra:



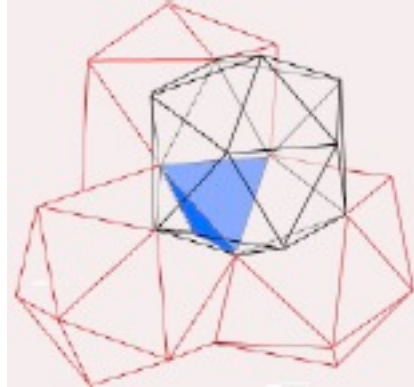
pentagonal 5-group - maximal density if gap-angle concentrated in one gap
(see calculations above)



icosahedron 20-group - maximal density may be if gap concentrated at one vertex (with some other vertices necessarily having partial gaps)
(I have not yet done the calculations)



57-group - 4 icosahedra interpenetrating each other - maximal density might NOT be with all 4 icosahedra in the icosahedral maximal density state, because the 4 icosahedra interpenetrate and it may be that putting one icosahedron in maximal state might block others from being put in maximal state. Also, the 57-group has 4 ring structures of 18 tetrahedra, one for each of the 4 interpenetrating icosahedra, so that gaps in the rings should be taken into account. In short, the 57-group has more interesting internal structure than either the smaller groups within it or the larger groups beyond it.

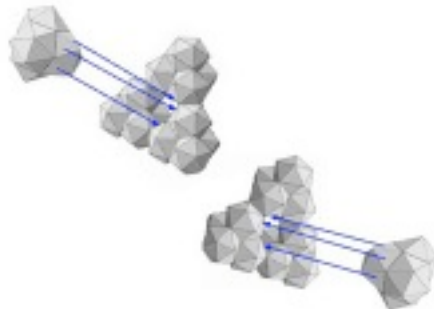


Pearce 81-group - 4 icosahedra plus 1 center tetrahedron each of whose faces are shared with 1 face of 1 of the 4 icosahedra - maximal density may be each of the 4 icosahedra in the icosahedral maximal density state



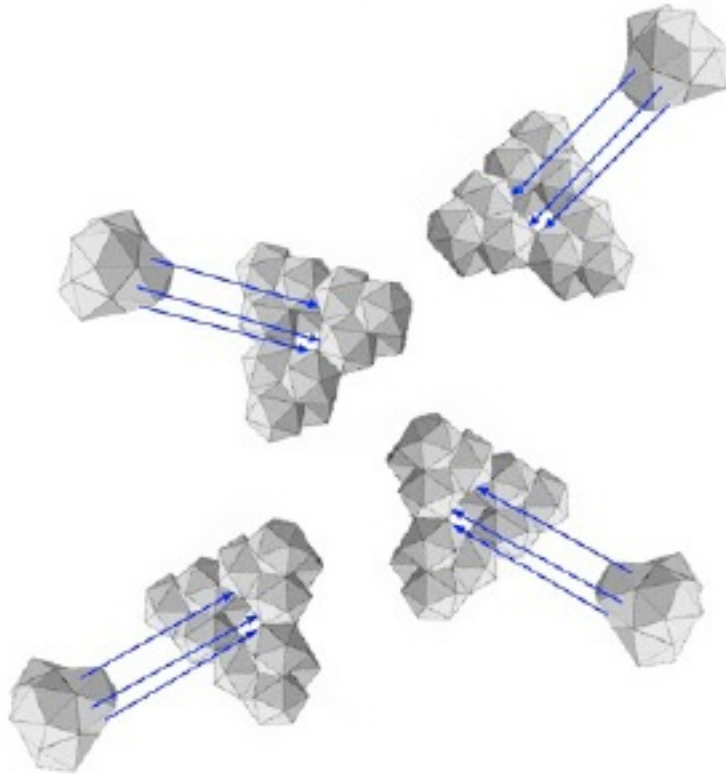
Diamond lattice network basis cluster of 4 Pearce 81-groups - maximal density may be each of the 4 icosahedra in the icosahedral maximal volume state.

Note that the 600-cell structure with 120 vertices contains two 57-groups as its dynamic keystones



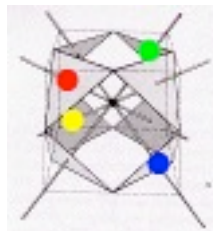
as described on pages 26-28 of my 150 page paper at <http://tony5m17h.net/TetraJJDECF.pdf> and

the 240 Polytope with 240 vertices and $600+600 = 1200$ cells contains four 57-groups as its dynamic keystones



as described on page 33 of my 150 page paper at <http://www.valdostamuseum.org/hamsmith/TetraJJDECF.pdf>

Note that setting a 57-group as a dynamic keystone chooses one of the four icosahedra, so all four dynamic keystone 57-groups are needed to produce four 18-tetrahedra rings corresponding to the four axes of the Fuller Vector Equilibrium



cuboctahedron and therefore (since the cuboctahedron can be seen as a central figure in the 4-dim 24-cell that is a discrete version of the 3-sphere) to circulation around the 4 axes (t,x,y,z) of spacetime.